Libro de RESÚMENES

IV ENCUENTRO OCEANOGRAFÍA FÍSICA ESPAÑOLA

EOF 2016

Universidad de Alicante
20-22 Julio de 2016

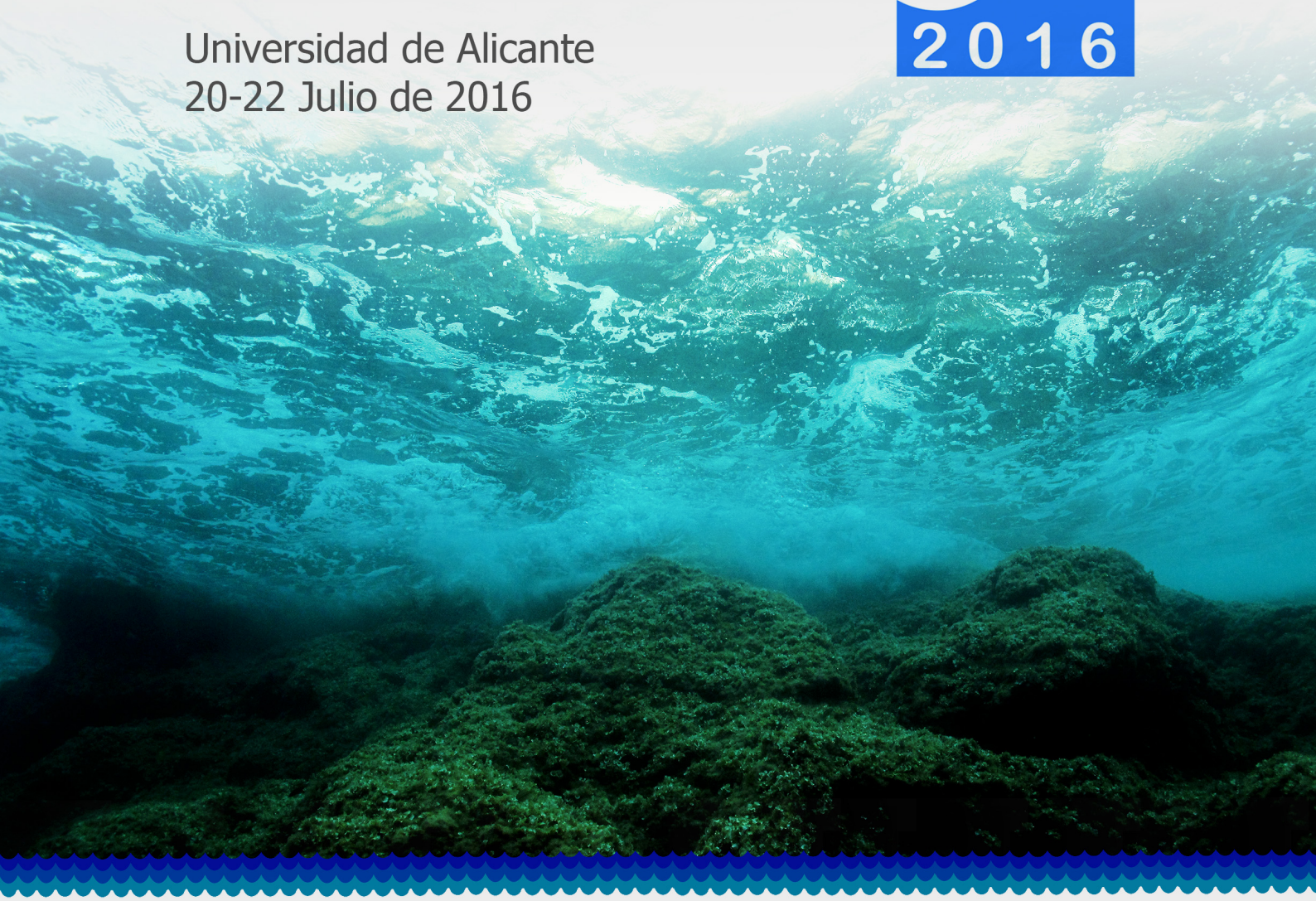

Universitat d'Alacant
Universidad de Alicante

UNIVERSIDAD DE LAS PALMAS DE GRAN CANARIA

UCA Universidad de Cádiz

UNIVERSITAT DE BARCELONA

Universidad Católica de Valencia San Vicente Mártir

UNIVERSIDADE DE VIGO

IV Encuentro Oceanografía Física Española

Alicante (España), 20-22 Julio 2016

Esta publicación debe citarse como:

VALLE C, AGUILAR J, ALVAREZ E, ARECHAVALA P, ASENSIO L, CABRERA R, CORBÍ H, DE-LA-OSSA JA, DEL-PILAR Y, FERNÁNDEZ V, FERNÁNDEZ Y, FERRERO LM, FORCADA A, GIMÉNEZ F, GONZÁLEZ JM, HERNÁNDEZ A, IZQUIERDO D, MANCHO AM, MARCO C, MARTÍNEZ E, MOLINA S, PELEGRÍ JL, RAMOS A, ROSÓN G, RUBIO E, SÁNCHEZ A, SÁNCHEZ JL, SÁNCHEZ P, SANZ C, TOLEDO K, ZUBCOFF JJ (Ed.). 2016. Libro de Resúmenes. IV Encuentro Oceanografía Física Española. Universidad de Alicante, Alicante. 143 pp. ISBN: 978-84-16724-17-8.

Edita:	Universidad de Alicante Departamento de Ciencias del Mar y Biología Aplicada
ISBN:	978-84-16724-17-8
Diseño de portada:	Luis M. Ferrero
Imagén de portada:	Maite Vázquez
Maquetación:	Luis M. Ferrero, Pablo Arechavala, Reme Cabrera

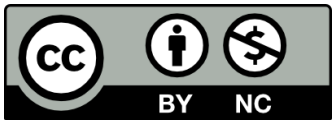

Comité organizador

Agustín Sánchez Arcilla, Universitat Politècnica de Catalunya
Alonso Hernández Guerra, Universidad de Las Palmas de Gran Canaria
Enrique Álvarez Fanjul, Puertos del Estado
Gabriel Rosón, Universidad de Vigo
Josep L. Pelegrí, Institut de Ciències del Mar, CSIC
Sergio Molina, Universidad de Alicante

Comité organizador local

Aitor Forcada, Universidad de Alicante
Alfonso Ramos, Universidad de Alicante
Candela Marco, Universidad de Alicante
Carlos Sanz, Universidad de Alicante
Carlos Valle, Universidad de Alicante
David Izquierdo, Universidad de Alicante
Elena Martínez, Universidad de Alicante
Esther Rubio, Universidad de Alicante
Francisca Giménez, Universidad de Alicante
Hugo Corbí, Universidad de Alicante
Javier Aguilar, Universidad de Alicante
José Antonio de la Ossa, Universidad de Alicante
José Jacobo Zubcoff, Universidad de Alicante
José Luis Sánchez, Universidad de Alicante
José Miguel González, Universidad de Alicante
Kilian Toledo, Universidad de Alicante
Leticia Asensio, Universidad de Alicante
Luis M. Ferrero Vicente, Universidad de Alicante
Pablo Arechavala, Universidad de Alicante
Pablo Sánchez, Universidad de Alicante
Reme Cabrera, Universidad de Cádiz
Victoria Fernández, Universidad de Alicante

Yoana Del Pilar, Universidad de Alicante

Yolanda Fernández, Universidad de Alicante

Comité científico

Agustín Sánchez Arcilla, Universitat Politècnica de Catalunya

Alfredo Izquierdo, Universidad de Cádiz

Alicia Lavín, Instituto Español de Oceanografía, Madrid

Alonso Hernández Guerra, Universidad de Las Palmas de Gran Canaria

Amanda Pascual, Institut Mediterrani d'Estudis Avançats, UIB-CSIC, Mallorca

Ana María Mancho, Instituto de Ciencias Matemáticas, CSIC

Angel Rodríguez Santana, Universidad de Las Palmas de Gran Canaria

Antonio Martínez Marrero, Universidad de Las Palmas de Gran Canaria

Belén Rodríguez de Fonseca, Universidad Complutense de Madrid

Carlos Souto Torres, Universidad de Vigo

César González Pola, Instituto Español de Oceanografía, Gijón

Damià Gomis, Institut Mediterrani d'Estudis Avançats, UIB-CSIC, Mallorca

Des Barton, Instituto de Investigaciones Mariñas, CSIC

Emili Garcia Ladona, Institut de Ciències del Mar, CSIC

Enrique Álvarez Fanjul, Puertos del Estado

Eugenio Fraile, Instituto Español de Oceanografía, Tenerife

Gabriel Rosón, Universidad de Vigo

Jesús García Lafuente, Universidad de Málaga

Josep L. Pelegrí, Institut de Ciències del Mar, CSIC

Luis Ferrer, AZTI-Tecnalia

Manuel Espino, Universitat Politècnica de Catalunya

Manuel Vargas, Instituto Español de Oceanografía, Málaga

Marisa Montoya, Universidad Complutense de Madrid

Miguel Gil Coto, Instituto de Investigaciones Mariñas, CSIC

Pablo Sangrà, Universidad de Las Palmas de Gran Canaria

Pedro Vélez, Instituto Español de Oceanografía, Tenerife

Ramiro Varelo, Universidad de Vigo

Ricardo Sánchez Leal, Instituto Español de Oceanografía, Cádiz

Sergio Molina, Universidad de Alicante

Instituciones organizadoras:

Universidad de Alicante

Universitat de Barcelona

Universidad de Cadiz

Universidad Católica de Valencia San Vicente Mártir

Universidad de Las Palmas de Gran Canaria

Universidad de Vigo

AUTOR / Área temática / Tipo de comunicación ..... # Página

Dominant Modes of Variability of the Sea Surface Height in the North Atlantic Subtropical Gyre from Altimetry Data

Isa Alba[1], Irene Laiz[2], Alonso Hernández-Guerra[1]

[1] Instituto Universitario de Oceanografía y Cambio Global (IOCAG-ULPGC), Universidad de Las Palmas de Gran Canaria
[2] Departamento de Física Aplicada, Universidad de Cádiz

ABSTRACT

A temporal and spatial Empirical Orthogonal Function (EOF) analysis has been performed on monthly máximum sea surface height (SSH) satellite data over twenty-two years (January 1993-December 2014) to examine the SSH patterns of variability of the North Atlantic Subtropical Gyre (NASG). Data was downloaded from the Archiving, Validation, and Interpretation of Satellite Oceanographic data (AVISO) remote sensing service (http://www.aviso.oceanobs.com/). EOFs separate the gridded data into distinct orthogonal modes which concentrate the variance into a set of orthogonal spatial maps and time series. The EOF method allows to observe where and when the sea level variations occur in each mode. The subtropical gyre in the North Atlantic includes a recirculation regime toward the equator in the eastern basin and a large transport in the western basin.

SAMOA: la oceanografía operacional al servicio de las Autoridades Portuarias

Enrique Alvarez Fanjul[1], Marcos García Sotillo[1], Begoña Pérez Gómez[1], José María García Valdecasas[1], Susana Pérez Rubio[1], Álvaro Rodríguez Dapena[1], Isabel Martínez Marco[2], Yolanda Luna[2], Elena Padorno[2], Gabriel Díaz Hernandez[3], Javier López Lara[3], Raúl Medina[3], Manel Grifoll[4], Manuel Espino[4], Marc Mestres[4], Laura Rafols[4], Agustín Sánchez Arcilla[4]

[1] Puertos del Estado
[2] AEMET
[3] IH-Cantabria
[4] LIM-UPC

RESUMEN

El proyecto SAMOA es un conjunto de desarrollos que servirán para dar servicio a las Autoridades Portuarias y potenciar el sistema de oceanografía operacional de Puertos del Estado. Se implementarán operativamente 10 modelos atmosféricos de alta resolución, 10 modelos de oleaje y 8 modelos de circulación, y se desplegarán 13 nuevas estaciones meteorológicas y 3 GPS, asociados estos últimos a los mareógrafos ya existentes. Adicionalmente, se desarrollarán una serie de herramientas de valor añadido, como modelos de vertidos, que servirán para potenciar el uso de los resultados.

INTRODUCCIÓN

Aproximadamente un 85% del total de importaciones y un 60% de las exportaciones españolas, medidas en términos de toneladas, se canalizan a través de los puertos, dato que habla por sí mismo del papel vital que juegan en la economía nacional. Así, a través las 28 Autoridades Portuarias que configuran el Sistema Portuario de Titularidad Estatal transitaron durante el pasado ejercicio 2015 un total de 30 millones de pasajeros y 502 millones de toneladas.

Los puertos están inmersos en un medio físico dinámico, sometidos a los rigores de las variables océano-meteorológicas esenciales, como el viento, el oleaje y el nivel del mar. Estas condicionan de manera determinante a los puertos, desde el diseño a la operatividad, pasando por la fase constructiva.

A fin de suministrar a los puertos la información necesaria para la toma de decisiones en dicho entorno, Puertos del Estado ha desarrollado y mantenido en las últimas décadas sistemas de monitorización (boyas, mareógrafos, correntímetros), caracterización climática (retro-análisis), y predicción numérica (oleaje, nivel del mar, corrientes) que permiten dar respuesta a muchas de las necesidades de los puertos, así como de otros sectores socio-económicos. Sin embargo, estos sistemas adolecen en numerosas ocasiones de la resolución espacial que es necesaria para abordar los problemas concretos derivados de la actividad portuaria, tales como la agitación en el interior de las dársenas y su impacto en los buques, la operatividad de las grúas, la seguridad en el acceso a través de las bocanas, etc…

Con objeto de dar respuesta concreta a estas necesidades, y potenciar la evolución y el uso del sistema ya existente, nace la iniciativa SAMOA (Sistema de Apoyo Meteorológico y Oceanográfico a las Autoridades Portuarias), cofinanciado por Puertos del Estado y las Autoridades Portuarias, y basado en los resultados del proyecto SAMPA, en el cual se ha implementado un sistema de oceanografía de alta resolución en la zona del Estrecho de Gibraltar y la Bahía de Algeciras.

MATERIAL Y MÉTODOS

Técnicamente, SAMOA consiste en la mejora y extensión, al conjunto del Sistema Portuario de Titularidad Estatal, de los productos desarrollados en el proyecto SAMPA. Un total de 18 Autoridades Portuarias y 25 Puertos se beneficiarán de estos nuevos sistemas.

Se desarrollarán y se implementarán operativamente 10 modelos atmosféricos de alta resolución (1 Km de resolución, basados en Harmonie), 10 modelos de oleaje (5 m., modelo de pendiente suave) y 8 modelos de circulación (40 m., ROMS), y se implementarán 13 nuevas estaciones meteorológicas y 3 GPS, asociados estos últimos a los mareógrafos ya existentes.

Los modelos numéricos estarán dinámicamente anidados a modelos operativos de escala regional: predicción de oleaje de Puertos del Estado, sistema Copernicus de circulación

marina (IBI-MFC) y predicción atmosférica de AEMET. Una vez los sistemas entren en su fase operativa, se gestionarán desde el sistema 24/7 de Puertos del Estado.
A fin de dar un mayor valor añadido a todos los productos generados, se integrarán en un visualizador que será puesto a disposición de los puertos. Además, existirá un sistema de alertas vía e-mail y SMS, plenamente configurable por los usuarios en las AA.PP. Igualmente, se desarrollarán modelos de seguimiento de vertidos y de contaminantes atmosféricos, que utilizarán como entrada las salidas de los modelos numéricos que están siendo desarrollados

RESULTADOS Y DISCUSIÓN

Los resultados de SAMOA tendrán múltiples aplicaciones para los puertos: operación de las infraestructuras, ayudas a la navegación, lucha contra derrames, control de la calidad del agua y del aire, etc... Una vez finalizada su implantación, SAMOA constituirá el núcleo de un moderno sistema de información océano-meteorológica que permitirá tomar decisiones basadas en el conocimiento en el quehacer diario del puerto, tal y como ocurre ahora mismo en el Puerto del Algeciras con los resultados de SAMPA
El proyecto se encuentra ahora en mitad de su etapa de desarrollo, ya estando disponibles multitud de validaciones de los desarrollos y encontrándose en fase pre-operativa una buena parte de los modelos y software de valor añadido. Estos se expondrán en la ponencia a presentar.

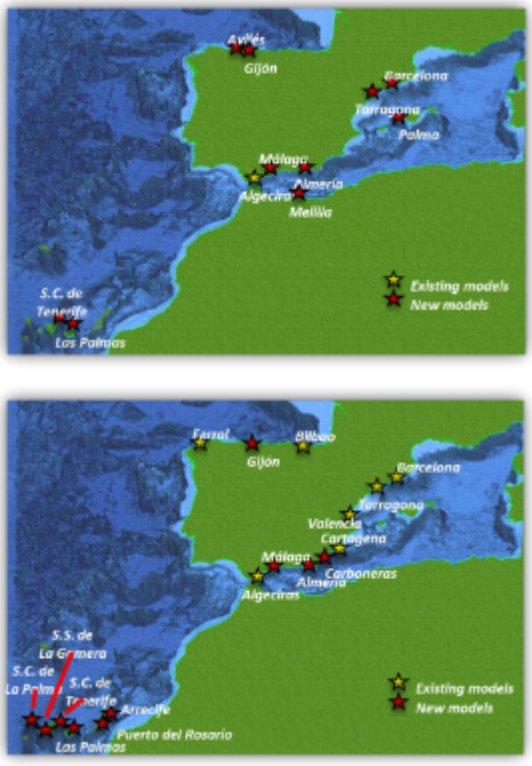

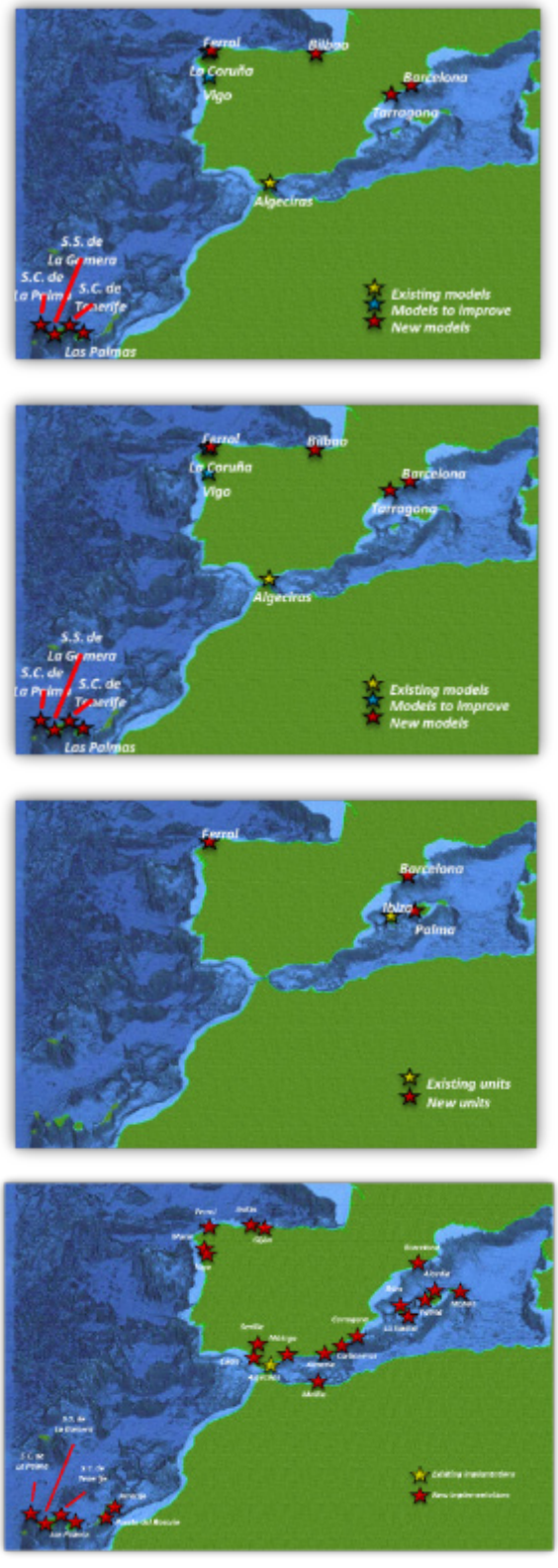

Fig. 1. Desarrollos de SAMOA. De Arriba abajo: modelos atmosféricos de alta resolución, modelos de agitación portuaria, modelos de circulación, nuevas estaciones meteorológicas, estaciones GPS y software de visualización y alerta

Jordi Font, oceanógrafo físico

Joaquim Ballabrera, Mikhail Emelianov, Carolina Gabarró, Emili García-Ladona, Antonio García-Olivares, Josep L. Pelegrí, Jaume Piera, Marcos Portabella, Jordi Salat, Carine Simon, Antonio Turiel, Álvaro Viudez, y todos los miembros del Departamento de Oceanografía Física y Tecnológica del Instituto de Ciencias del Mar

Departament d'Oceanografia Física i Tecnològica, Institut de Ciències del Mar, CSIC, Barcelona

RESUMEN

Tras finalizar en 1973 la licenciatura en Física, Jordi Font Ferré obtiene una beca del entonces Instituto de Investigaciones Pesqueras, hoy en día el Institut de Ciències del Mar. En 1977 su beca termina y, convertido en profesor de secundaria de Matemáticas, continua trabajando en temas oceanográficos y participando en campañas de forma voluntaria. En 1983 inicia una tesis doctoral sobre la Oceanografía Física del Mar Catalán, que culmina en 1986, el mismo año en que obtiene una plaza permanente de científico con el perfil de Oceanografía Física, la primera plaza en este ámbito dentro del Consejo Superior de Investigaciones Científicas. A lo largo de 40 años de carrera profesional, Jordi ha realizado contribuciones muy significativas en temas muy diversos, relacionados con la circulación oceánica, la oceanografía física del Mar Mediterráneo, la dinámica de mesoescala y el estudio del océano a partir de sensores remotos. Durante las dos últimas décadas, con el apoyo de diversos proyectos del Plan Nacional de Ciencia y Tecnología de España y la Agencia Espacial Europea, Jordi lideró la parte oceánica de la misión espacial Soil Moisture Ocean Salinity (SMOS), encaminada a la medición remota de la salinidad superficial de los océanos. Jordi ha sido un factor fundamental para el crecimiento y madurez de la oceanografía física en el Institut de Ciències del Mar – que actualmente cuenta con 12 investigadores permanentes que lideran un grupo de más de 40 técnicos y jóvenes investigadores integrados en el Departamento de Oceanografía Física y Tecnológica – y ha contribuido en gran medida al progreso de esta disciplina en España y el arco mediterráneo. Jordi participó en los comités ejecutivos de numerosos programas y, entre el 2004 y 2010, presidió el Comité de Física y Clima del Océano de la Comisión Internacional para la Exploración Científica del Mar Mediterráneo. A lo largo de toda su trayectoria, Jordi combinó su buen hacer científico con una extraordinaria capacidad de coordinación de grandes grupos de trabajo, marcada siempre por un carácter franco y generoso. En el año 2011, la Generalitat de Catalunya reconoció su trayectoria otorgándole el Premi Nacional de les Arts en la categoría de pensamiento y cultura científica. El proyecto SMOS fue también reconocido por la ciudad de Barcelona (Premio Cristòfol Juandó), la Sociedad IEEE de Geociencias y Sensores Remotos, y la Agencia Espacial Europea. En el momento de su jubilación, en enero de 2016, Jordi había publicado más de 300 trabajos, alrededor de una tercera parte en revistas del SCI, con un índice global de impacto h=32. La mayor parte de sus publicaciones pueden obtenerse en http://oce.icm.csic.es/es/colecciones y su CV se encuentra en http://oce.icm.csic.es/ca/jfont.

A comparison of the CMEMS Iberia–Biscay–Ireland (IBI) forecasted and reanalyzed ocean products

R. Aznar[(1)], M.G. Sotillo[(1)], S. Cailleau[(2)], P. Lorente[(1)], B. Levier[(2)], A. Amo-Baladrón[(1)], G. Reffray[(2)], E. Álvarez-Fanjul[(1)]

[1] Puertos del Estado, Avenida del Partenón 10, 28042, Madrid, Spain
[2] Mercator Ocean, 8–10 Rue Hermès, 31520 Ramonville Saint-Agne, France

ABSTRACT

The goal of this study was to intercompare, along an overlapping 9-month period between April and December 2011, the ocean physical daily forecast and 10-year (2002–2012) reanalysis products provided by the Iberia–Biscay–Ireland Monitoring and Forecasting Center (IBI-MFC), in the framework of the Copernicus Marine Environment Monitoring Service (CMEMS). These two products differ in the use of an observational data assimilation scheme in the reanalysis and in their spatial resolution. Both modeled solutions are compared against several observational data sources at regional and local scale. The forecast and reanalysis show realistic patterns in the area of study at regional scale. Nevertheless, at finer scales the results reveal better performances of the 1/12° reanalysis over open waters and the 1/36° forecast in areas away from the coastline. The comparison shows that the data assimilation scheme may improve the performance in coastal areas, but presents limited effects in complex coastal regions. Spatial resolution seems to play a key role in these areas, especially around the Iberian Peninsula, where the higher resolution forecast brings in general better results than the coarser resolution reanalysis. The study suggests that the observational data assimilation represents a crucial step towards improving the performance of regional modeled solutions, as long as the spatial resolution is kept at fine-enough meshes in order to prevent higher uncertainties in coastal and shelf areas.

INTRODUCTION

The near real-time operational monitoring and forecasting of the marine environment are essential to understand the ocean dynamics and support high-stakes decision-making for coastal management, preventing natural anthropogenic hazards. The combined use of observing networks with regional operational ocean forecasting systems and reanalyses with increased spatial resolution [1] emerge as useful predictive tools for economic and societal concerns.

Both the ocean operational forecasting and the production of ocean reanalysis are currently undergoing a major impulse thanks to the Copernicus Marine Environment Monitoring Service (CMEMS), the European Program for the establishment of a European capacity for Earth Observation, which is fully operational from May 2015 (http://marine.copernicus.eu).

The service covers the European seas by defining six different areas. Among them, the Iberia–Biscay–Ireland Monitoring and Forecasting Center (IBI-MFC) of Puertos del Estado (PdE) provides two kinds of modeling products at regional scale [2][3]: one operational forecast product updated on a daily basis since April 2011 [4] and a recently achieved physical 10 year (2002–2012) reanalysis [5] freely available through CMEMS website.

Both IBI forecast and reanalysis systems supply model solutions for the same region, but differ in terms of spatial resolution and the use of an assimilation scheme of observational data in the latter. Thus, the main goal of the present study is to intercompare both products for a 9 month period (April–December 2011) of concurrent ocean estimations, evaluating quantitatively their performance against observational data. This study is especially meaningful since it assesses the two model products delivered to users by IBI-MFC on a continuous basis.

METHODOLOGY

The IBI-MFC operational ocean forecast and reanalysis products (IBIop and IBIre, respectively) were generated by means of two different eddy-permitting NEMO baroclinic ocean model versions, configured ad-hoc for covering the IBI area. In both cases, NEMO solves the 3D primitive equations on an Arakawa-C grid. As for IBIop, a NEMO version was used at a 1/36° horizontal resolution (~2 km) and into 50 vertical z-levels, whereas the 2.3 version was applied at 1/12° and 75 vertical levels for IBIre.

Atmospheric fields are provided by the ECMWF operational Integrated Forecast System (IFS) for IBIop and the ERA-interim reanalysis products for IBIre, whereas open boundary conditions are given by the CMEMS ocean

global eddy resolving operational forecast system and global reanalysis for IBIop and IBIre, respectively. Additionally, lateral boundary conditions are implemented for 33 rivers from several sources.

IBIop takes every week initial conditions 14 days in the past from 3D analyzed outputs provided by the global forecast system, while for IBIre, they are given by the global reanalysis to start at rest the simulation.

RESULTS AND DISCUSSION

Similarities but also disparities have been obtained between the IBIop forecast and IBIre reanalysis solutions from April to December 2011. Both simulated products have been compared with observational data: first at regional scale against remote sensing data, then at local scale with in situ high-frequency data from mooring and finally at deeper layers.

The IBIop and IBIre SST statistics vs. CMEMS L4 OSTIA data emphasize that IBIop performs better than IBIre near the coasts, essentially around the Iberian Peninsula (Fig. 1).

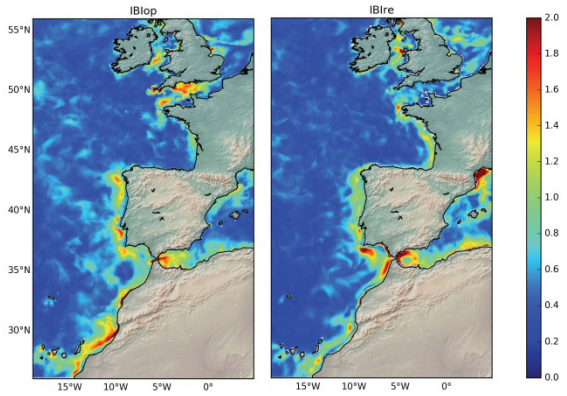

Fig. 1: Summer (JJA) 2011 SST RMSE of IBIop (left) and IBIre (right) vs. OSTIA (°C).

The higher spatial resolution arises as an important factor in areas like the Iberian coastal regions, characterized by complex slope bathymetry and coastline, where spatial structures are more easily replicated in the 1/36º IBI forecast, as shown by the comparison against PdE mooring buoys measurements (Fig. 2). The results also highlight the coarse resolution and data assimilation constraints in coastal regions, where observational data are scarce, as evidenced by the poorer 1/12º IBIre performance in these regions. On the other hand, the analysis of surface spatial fields reveals an improvement of IBIre over IBIop in open waters, possibly due to the observational data assimilation scheme used in IBIre.

At deeper layers, both IBI modeled products represent realistic Mediterranean Outflow Water patterns, thanks to the data assimilation scheme in IBIre and the spinup technique used in IBIop, even though they present very large net water transport values in the Strait of Gibraltar.

This study is a first attempt to assess the performance of the IBI-MFC ocean physical daily forecast and reanalysis products, currently available to all users through the CMEMS catalog (http://marine.copernicus.eu).

The study suggests that the observational data assimilation represents a crucial step towards improving the performance of regional modeled solutions, as long as it does not go together with a decrease in spatial resolution linked with uncertainties in shelf and coastal regions.

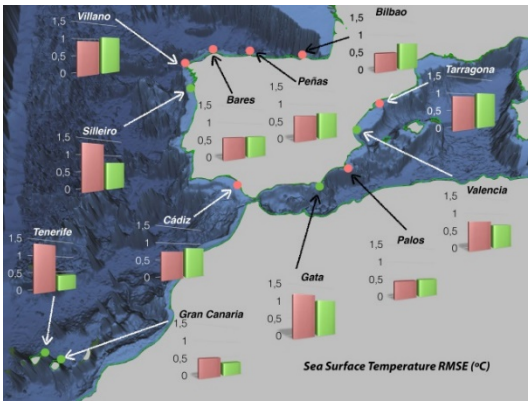

Fig. 2: RMSE histograms of IBIop (red) and IBIre (green) vs. observational SST (in °C) at PdE buoys locations. Locations are colored according to the product with best RMSE performance. Period: April–December 2011.

A loss of spatial resolution may limit the benefits of data assimilation and worsen the reanalysis solution in regions such as the Iberian Peninsula coastal areas. It is therefore crucial to apply data assimilation at fine-enough meshes, particularly in intricate coastal sectors.

These results therefore support, in the framework of the Copernicus Marine service, the IBI-MFC decision to insert observational data assimilation in a new high resolution (1/36°) NEMO operational model version to be released next year.

REFERENCES

1 - Adani, M., Dobricic, S., Pinardi, N., 2011. Quality assessment of a 1985–2007 Mediterranean Sea Analysis. *J. Atmos. Ocean. Technol*. 28: 569–589.

2 - Sotillo, M.G., Cailleau, S., Lorente, P., Levier, B., Aznar, R., Reffray, G., Amo-Baladrón, A., Chanut, J., Benkiran, M., Álvarez Fanjul, E., 2015. The MyOcean IBI Ocean forecast and reanalysis systems: operational products and roadmap to the future Copernicus Service. *J. Oper. Oceanogr*. 1–17 http://dx.doi.org/10.1080/1755876X.2015.1014663.

3 - Aznar R., Sotillo M.G., Cailleau S., Lorente P., Levier B., Amo-Baladrón A., Reffray G., Álvarez-Fanjul E., 2016. Strengths and weaknesses of the CMEMS forecasted and reanalyzed solutions for the Iberia–Biscay–Ireland (IBI) waters. *Journal of Marine Systems*. 159: 1-14. http://dx.doi.org/10.1016/j.jmarsys.2016.02.007.

4 - Cailleau, S., Chanut, J., Levier, B.,Maraldi, C., Reffray, G., 2010. The new regional generation of Mercator Ocean system in the Iberian Biscay Irish (IBI) area. *Mercator Ocean Q. Newsl*. 39: 5–15.

5 - Levier, B., Benkiran, M., Reffray, G., Sotillo, M.G., 2014. IBIRYS: a Regional High Resolution Reanalysis (Physical and Biogeochemical) over the European North East Shelf. *Vol. 2014. EGU.*

Anatomy of a subtropical mode water eddy

Bàrbara Barceló-Llull[1], Pablo Sangrà[1], Enric Pallàs-Sanz[2], Eric D. Barton[3], Sheila N. Estrada-Allis[2], Antonio Martínez-Marrero[1], Borja Aguiar-González[4], Diana Grisolía[1], Carmen Gordo[1], Ángel Rodríguez-Santana[1] Ángeles Marrero-Díaz[1], Javier Arístegui[1]

[1] Universidad de Las Palmas de Gran Canaria, ULPGC, Gran Canaria, Spain
[2] Departamento de Oceanografía Física, CICESE, Ensenada, México
[3] IIM, CSIC, Vigo, Spain
[4] NIOZ Royal Netherlands Institute for Sea Research, Department of Ocean Systems Sciences and Utrecht University, P.O. Box 59, 1790 AB Den Burg, Texel, the Netherlands

ABSTRACT

An interdisciplinary survey of a subtropical mode water eddy was conducted within the Canary Eddy Corridor in September 2014. The anatomy of the eddy is investigated with near submesoscale fine resolution 2D data and coarser resolution 3D data. The eddy was 4 months old, at least 500 m deep and 40 km in radius. It may be viewed as propagating negative anomaly of potential vorticity (PV). We observe two cores of low PV: one in the subsurface layers centered at 90 m and another broader core located between 175 m and the maximum sampled depth of the 3D data (325 m). The subsurface core is where the maximum values of normalized relative vorticity, Ro=0.6, and azimuthal velocity, U=0.5 m s^{-1}, are reached, and is defined as the eddy dynamical core. The dynamical core, 30 km in radius, is in solid body rotation with period of 4 days. Content of kinetic energy (KE) exceeds available potential energy (APE), KE/APE=1.58. Inferred available heat and salt content anomalies are 2.9×10^{18} J and 14.3×10^{10} kg, respectively. Vertical velocity (w) is estimated from 3D density and horizontal velocity fields through a generalized omega equation. Although complex, the inferred w field shows a basically dipolar structure. At the eddy center w is zero and maximum absolute values are located at the eddy periphery (6 m day^{-1}). Coinciding with the occurrence of the w cells a noticeable enhancement of phytoplankton biomass is observed at the eddy periphery.

Observación de procesos físicos de submesoescala y escala fina con métodos acústicos: últimos avances en Oceanografía Sísmica

Berta Biescas[1], Valentí Sallarès[2], Jhon F. Mojica[2] & Daniel Danigno[2]

[1] Istituto di Scienze Marine, ISMAR-CNR, Bologna, Italia.
[2] Institut de Ciències del Mar, ICM-CSIC, Barcelona, España

RESUMEN

La oceanografía sísmica tiene como objetivo el estudio de los procesos físicos en el océano a partir del método acústico de sísmica de reflexión multicanal (MCS). El método de exploración acústica permite la observación de estructuras termohalinas de mesoescala, submesoescala y escala fina, así como la interacción entre ellas y con el fondo marino. El grupo de investigación de oceanografía sísmica del Institut de Ciències del Mar de Barcelona lleva trabajando en esta temática durante 10 años, siendo unos de los grupos pioneros a nivel internacional. En este trabajo explicamos los avances conseguidos en los últimos 5 años, principalmente en tres sublíneas: la inversión de datos de reflectividad para conseguir mapas de temperatura y salinidad; el estudio de cascada de energía a partir del análisis espectral de los desplazamientos verticales registrados en los reflectores acústicos; y la optimización de la tecnología de MCS para la exploración oceanográfica.

INTRODUCCIÓN

La oceanografía sísmica (OS) se basa en el método de sísmica de reflexión multicanal, el cual detecta la estructura interna del océano con resoluciones del orden de 10 m en ambas dimensiones, vertical y lateral. Principalmente presenta dos grandes potenciales, por una parte permite explorar toda la columna de agua hasta el fondo marino, sin límite en la profundidad, y a lo largo de secciones laterales de cientos de kilómetros, cubriendo un amplio rango de escalas dinámicas. Por otra parte, al abarcar toda la columna de agua, nos permite observar la física del océano profundo, que es actualmente una de las zonas menos exploradas de nuestro planeta debido a las dificultades tecnológicas que conlleva. La oceanografía sísmica ha mostrado durante estos últimos 10 años que puede cubrir un vacío observacional existente con la tecnología marina convencional. La mayoría de estudios oceanográficos obtenidos con esta técnica han sido realizados a partir de datos de oportunidad, adquiridos en campañas geofísicas para estudio del subsuelo marino. El hecho de poder reaprovechar los datos antiguos de geofísica marina nos proporciona un incalculable banco de datos a nivel histórico y global en todos los océanos. El objetivo del presente trabajo es presentar un resumen de las aportaciones más reclevantes en los útlimos 5 años, hechas por el equipo de investigación de OS del Institut de Ciències del Mar.

MÉTODO ACÚSTICO

El método de la sísmica de reflexión multicanal (MCS) utiliza una tecnología que consiste en una fuente acústica que es arrastrada por un barco y un streamer de hidrófonos que es arrastrado a continuación de la fuente. Habitualmente, la fuente acústica consiste en un cañón de presión de aire que se dispara a intervalos regulares durante la adquisición de datos. Las ondas acústicas se propagan en el medio acuático y son reflejadas en contrastes de impedancia acústica (Z=densidad·velocidad del sonido). Las ondas reflejadas son registradas en superficie, en el streamer de hidrófonos y las reflexiones sísmicas son procesadas hasta obtener imágenes 2D como la que se muestra en la Fig. 1, donde los máximos blancos y negros representan los máximos de reflectividad, correspondientes a máximos de gradiente vertical termohalino de signo positivo o negativo.

RESULTADOS

El esfuerzo realizado en inversión de datos de reflectividad ha sido esencial para el avance de la oceanografía sísmica. La inversión nos permite calcular los parámetros del medio, en este caso temperatura (T) y salinidad (S), a partir de las características de las ondas que se propagan por ellos. Posteriormente, a partir de T y S, podemos derivar otras propiedades como la densidad potencial, velocidad del sonido, etc. El grupo de investigación del Institut de Ciències del Mar (ICM) ha trabajado principalmente en dos métodos de inversión: un método basado en la deconvolución de la onda y el

método llamado inversión de onda completa (en inglés conocido como full waveform inversion, FWI).

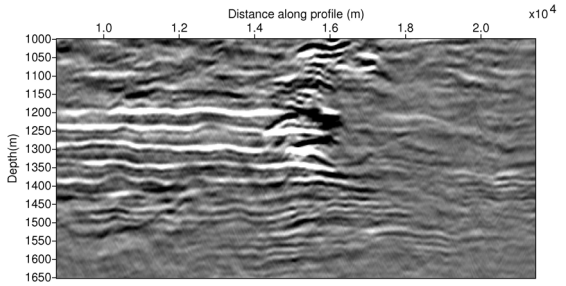

Figura 1. Imágen acústica de la interacción de un remolino y una estructura en escalera, Golfo de Cádiz, NE Océano Atlántico (Biescas et al 2010).

El método basado en la deconvolución, no es un método fundamentado en la teoría de inversión como tal, si no que consiste en el cálculo de perfiles de impedancia acústica a partir de la sumación de dos componentes: i) alta frecuencia calculada a partir de la integración de perfiles de reflectividad acústica; y ii) baja frecuencia calculada a partir de sondas oceanográficas. Una vez calculada la impedancia acústica, se derivan con un método iterativo de convergencia, los pares de T y S que mejor se ajustan a ese valor de impedancia acústica y cumplen las propiedades T-S de la zona. Este método fue aplicado a datos reales en el Golfo de Cádiz, en el trabajo de Biescas et al 2014, obteniendo errores de 0.1 y 0.09 para la temperatura y la salinidad respectivamente. El trabajo realizado en el método de inversión de onda completa ha sido un trabajo metodológico, en el cual se ha desarrollado el código de inversión y las estrategias de cálculo para datos sintéticos (kernels de inversión, secuencia de frecuencias, modelo inicial, propagación directa, etc.), presentado en los trabajos de Kormann et al 2009 y Bornstein et al 2012. . El último trabajo presentado en esta temática fue el de Danigno et al 2016, que desarrolla un código propio y lo aplica a datos reales obteniendo errores de 0.18ºC y 0.08 para temperatura y salinidad respectivamente (Fig.2).

Los resultados del principal estudio sobre cascada energética realizado por nuestro grupo, están en proceso de publicación en el trabajo Sallarès et al 2016. Este estudio ha consistido en la caracterización de los procesos energéticos que afectan la termoclina del Mar de Alborán, a partir de datos acústicos de MCS de alta resolución. Estos las isopicnas y analizar su espectro. La comparación de los espectros resultantes con espectros característicos de procesos energéticos oceánicos, muestra la existencia de ondas internas a escalas mayores de los 100 m, procesos turbulentos a escalas menores de 30 m y un marcado proceso transicional en escalas entre 30 m y 100 m, datos permiten cuantificar los desplazamientos verticales de atribuido a inestabilidades de vórtice laminar que ha sido observado por primera vez en este contexto oceanográfico. Este resultado evindecía la importancia de tener un sistema de observación adecuado que abarque un amplio rango de escalas laterales y nos permita hacer unas observaciones completas de todos los procesos dinámicos involucrados y las interacciones entre ellos.

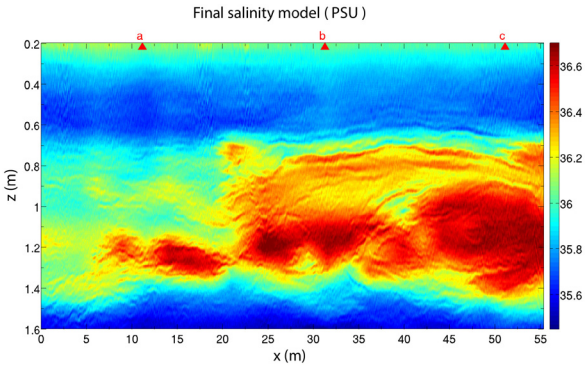

Figura 2. Sección de salinidad invertida a partir de datos MCS en el Golfo de Cádiz, NE Océano Atlántico (Danigno et al 2016).

Paralelamente, el equipo del ICM ha hecho un esfuerzo importante en la definición de los requisitos tecnológicos para un sistema de MCS optimizado para la exploración oceanográfica. Los detalles técnicos de la fuente acústica (ondícula, pico de presión, contenido frecuencial) y el diseño del streamer (espaciado de canales, longitud) fueron publicados en el trabajo de Biescas et al 2015. Los resultados de este estudio cumplen con dos objetivos principales: el sistema propuesto minimiza el pico de presión respecto a las fuente utilizadas en MCS convencional, con el objetivo de minimizar el impacto en el ecosistema marino; y se propone un sistema más portable y ligero que el de MCS convencional, con el fin de que pueda ser instalado en cualquier buque oceanográfico.

AGRADECIMIENTOS

Los trabajos presentados se han podido realizar gracias a los proyectos POSEIDON (Ref: CTM2010-25169), APOGEO (Ref: CTM2011-16001-E/MAR), OCEANSEIS (FP7-PEOPLE-2010-IOF-271936) y SEISMARE (FP7-PEOPLE-2012-COFUND-600407) financiados por la UE.

REFERENCIAS

1- Biescas et al 2010. Seismic imaging of staircase layers below the Mediterranean Undercurrent, 2010. Deep Sea Research.
3- Biescas et al 2014. Recovery of temperature, salinity and potential density from ocean reflectivity., 2014. JGROceans.
4- Koprmann et al 2009. Synthetic modelling of acoustic propagation applied to seismic oceanography experiments, 2009. GRL.
5- Borsntein et al 2013. Direct temperature and salinity acoustic full waveform inversion, 2013. GRLs.

6- Danigno et al 2016. Fine-scale thermohaline ocean structure retrieved with 2D Pre-stack full-waveform inversion of multichannel seismic data:. JGROceans.

Registro de procesos de afloramiento en el borde costero del Umbral de Camarinal

Marina Bolado-Penagos[1], Juan Jesús Gomiz-Pascual[2], Iria Sala[1], Águeda Vázquez[2] & Miguel Bruno[3]

[1] Facultad de Ciencias del Mar y Ambientales, Universidad de Cádiz, Campus de Puerto Real, 11510 Cádiz.
[2] Escuela Superior de Ingeniería, Universidad de Cádiz, Campus de Puerto Real, 11510 Cádiz.
[3] Centro Andaluz de Ciencia y Tecnología Marinas, Universidad de Cádiz, Campus de Puerto Real, 11510 Cádiz.

RESUMEN

El presente estudio muestra el análisis detallado de las mediciones que fueron realizadas en el marco del proyecto MEGAN (Mesoscale and submesoscale processes in the Strait of Gibraltar) para una estación fija en las proximidades del umbral de Camarinal. El análisis se basó en varios lanzamientos de CTD, registro de medidas de termosalinógrafo y perfilador de corrientes acústico (ADCP) instalado en el barco. La estación fue realizada en condiciones de mareas vivas donde la presencia de las ondas internas de gran amplitud que se generan en el umbral de Camarinal es más probable. Las mediciones de CTD cubrieron la totalidad de un ciclo de marea, abarcando la fase de corriente hacia el Atlántico, hasta la fase de corriente hacia el Mediterráneo, lo que ha permitido estudiar el comportamiento de la interfaz que separa las masas de agua atlántica y mediterránea (AMI). Durante el ciclo de marea analizado se observa el afloramiento de aguas de la interfaz en el borde costero cuando la corriente se dirige hacia el Atlántico. Además, se encuentran máximos de fluorescencia próximos a superficie, cuando la corriente se dirige hacia el Mediterráneo, que podrían ser debidos a la llegada de aguas costeras a la zona de estudio, con mayor concentración de fitoplancton, desde la zona de Trafalgar y que son eventualmente retenidos por la formación de un vórtice ciclónico costero localizado entre Punta Paloma y Tarifa.

INTRODUCCIÓN

El Estrecho de Gibraltar constituye la única unión entre las cuencas Mediterránea y Atlántica. Este se encuentra condicionado por la batimetría, siendo Camarinal el principal de sus umbrales, que actúa como cuello de botella entre las masas de agua que se dan a ambos lados del Estrecho. El régimen hidrodinámico del Estrecho se corresponde con un flujo estacionario bicapa al que se superponen otros flujos de distinta escala espacio-temporal.

El mayor precursor de mezcla interfacial en el sistema bicapa del Estrecho es la presencia de ondas internas de gran amplitud y corto periodo. Estas son generadas por la interacción del flujo estratificado con la topografía del umbral de Camarinal, siendo visible su presencia por la rugosidad que provocan en la superficie del mar [1].

En presencia de un flujo de marea hacia el Atlántico intenso (~1 m/s), las ondas internas quedarán arrestadas en el Umbral [2], siendo el tiempo que las mismas queden retenidas función de la intensidad del flujo. Una vez se debilita (~0.5 m/s), las ondas son liberadas hacia el Mediterráneo.

Las ondas internas podrían inducir además la succión de aguas ricas en clorofila desde los márgenes costeros hacia el centro del canal. Evidencias de que se trata de un área de acumulación han sido descritas en trabajos previos a partir de imágenes de satélite de clorofila [3], análisis de la distribución de zooplancton a lo largo de los frentes de onda o simulaciones hidrodinámicas. Dicha acumulación será posteriormente transportada hacía Alborán, cuando la corriente de marea se dirige hacia el Mediterráneo.

Con el fin de estudiar la dinámica de los afloramientos de las aguas de la interfaz debidos a la generación de estas ondas internas, se realizó una estación fija, a una profundidad inferior a 40 metros, en las inmediaciones del umbral de Camarinal.

MATERIAL Y MÉTODOS

Las observaciones recogidas en este estudio fueron realizadas en el desarrollo de la campaña a bordo del B.O. Sarmiento de Gamboa en septiembre de 2015. En condiciones de mareas vivas, cuando es esperada la generación de ondas internas sobre el umbral de Camarinal, se realizó una estación fija en las inmediaciones del mismo (36º3’18.02’’N, 5º45’14.64’’W), en la cual se tomaron durante 24 horas medidas a bordo del buque.

En dicho punto se dieron siete estaciones CTD (CTD Sea-Bird SEACAT). Las estaciones han permitido cubrir la casi

totalidad de un ciclo de marea (Fig. 1), dándose la primera al comienzo de la fase de marea saliente (sentido Atlántico), y la última de ellas tras el máximo de marea entrante (sentido Mediterráneo). Los datos brutos obtenidos a partir de los CTD tienen una resolución vertical aproximadamente de 1 cm, siendo posteriormente filtrados a intervalos de un metro. Temperatura, salinidad y fluorescencia superficial se obtuvieron mediante el termosalinógrafo Sea-Bird SEACAT SBE 21 instalado en el buque. Los registros de corrientes fueron adquiridos a partir del perfilador de corrientes por efecto doppler DopplerTeledyne RD Instruments ADCP OceanSurveyor 75 KHz. Estos últimos fueron tomados en intervalos de 1 minuto con el fin obtener la suficiente resolución espacio temporal que permitiese captar en detalle los posibles cambios que pudieran darse en los perfiles de velocidad inducidos por los fenómenos que tienen lugar en la zona de estudio.

RESULTADOS Y DISCUSIÓN

Las siete estaciones de CTD realizadas muestran un incremento de fluorescencia conforme se desarrolla el ciclo de marea. Dicho aumento se produce en superficie, siendo las ultimas estaciones las que presentan mayor magnitud. Los tres primeros perfiles de CTD coinciden con la fase de corriente de marea hacia el Atlántico, flujo dirigido hacia el oeste, donde se muestra la presencia de aguas de origen mediterráneo (mayor salinidad y menor temperatura). Según la predicción para la intensidad de la corriente, en el instante en el que se realizó el segundo y tercer lanzamiento, la onda interna se encontraría arrestada en el Umbral. La columna de agua aparece mezclada, sin presencia de gradiente vertical, pudiendo haber sido inundada por aguas que proceden de la interfaz.

Al invertirse el sentido del flujo, dirigiéndose ahora hacia el Mediterráneo, la columna de agua aparece estratificada. Valores superiores de temperatura superficial están acompañados de mayores valores de fluorescencia, también en superficie. Estos resultados, registrados por CTD, coinciden con los obtenidos por el sistema de registro continuo de variables superficiales instalado en el buque.

El aumento de fluorescencia en superficie cuando el flujo se encuentra dirigido hacia el este podría ser debido al aporte de las aguas ricas en clorofila que viene del borde costero de Trafalgar, zona muy productiva de forma permanente. Los vientos imperantes en el momento de la realización de la estación eran del este, lo que podría ayudar a la retención de aguas ricas en nutrientes en el borde costero. El aumento de clorofila en el área con vientos de levante se ha constatado con imágenes de satélite en trabajos anteriores, donde se observa como la clorofila puede llegar a descolgarse en la zona de Trafalgar.

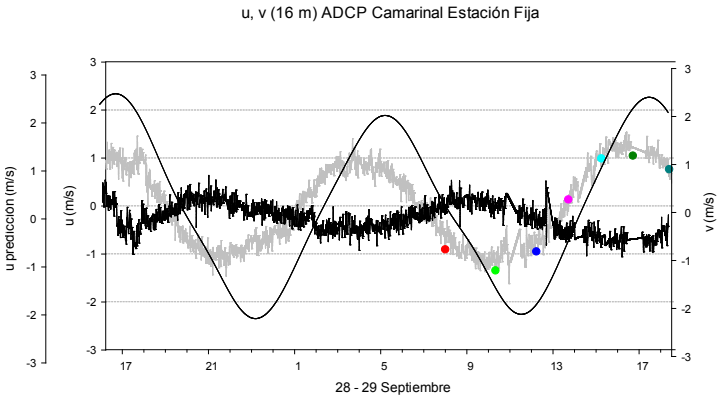

Fig. 1. Registro mediciones ADCP (u, gris; v, negro). En línea continua se presenta la predicción de la corriente en el Umbral (45 m). Los puntos de colores hacen referencia a cada lanzamiento de CTD que fue realizado en la estación.

AGRADECIMIENTOS

Este trabajo se integra en el proyecto CTM2013-49048-C2-1-R, CTM2013 49048-C2-2-R financiado por el Ministerio de Economía y Competitividad de España.

REFERENCIAS

1 - Bruno M, Alonso JJ, Cózar A, Vidal J, Ruiz-Cañavate A, Echevarría F, Ruiz J, 2002. The boiling wáter phenomena at Camarinal sill, the strait of Gibraltar. *Deep. Res. Part II*, 49:4097-4113.

2 - Vázquez A, Bruno M, Izquierdo A, Macías D, Ruiz-Cañavate A, 2008. Meteorologically forced subinertial flows and internal wave generation at the main Sill of the Strait of Gibraltar, *Deep. Res. Part I*, 55:1277-1283.

3 - Vázquez A, Flecha S, Bruno M, Macías D, Navarro G, 2009. Internal waves and short-scale distribution patterns of chlorophyll in the Strait of Gibraltar and Alborán Sea. *Geophys. Res. Lett*., 36, L23601

Spatial and temporal variability of Nutrients in the Ría de Vigo

Águeda Cabrero[1], Elena Tel[2], Gonzalo González-Nuevo[1]

[1] Instituto Español de Oceanografía (IEO). Centro Oceanográfico de Vigo
[2] Instituto Español de Oceanografía (IEO). Servicios Centrales.

ABSTRACT

The Ría of Vigo (Galicia, NW Spain) is an estuary located in the northern boundary (42–43°N) of the eastern North Atlantic upwelling system. Since 1994, the Instituto Español de Oceanografía (IEO), as part of RADIALES program, has been monitoring, in a monthly basis, a hydrographic standard section composed of 4 oceanographic stations located in the inner, medium and outer part of the ría. In addition to hydrographic profiles, biogeochemical and plankton samples have been collected. The average values of the main nutrients in the study area and its inter- and intra-annual variability in relation with the oceanographic features are represented in order to establish reference and range values for the different seasons.

INTRODUCCIÓN

La costa oeste de Galicia (NO de España), donde se encuentra situada la Ría de Vigo, es el límite norte del sistema de afloramiento costero provocado por el viento, que se extiende a lo largo del margen este del Atlántico, desde 10 a 44 ºN. A las latitudes en las que se desarrolla este estudio, los vientos de plataforma siguen un patrón estacional ligado a la climatología de gran escala del Atlántico Nordeste. Durante la primavera-verano, predominan los vientos del Norte favorables al afloramiento mientras que en otoño-invierno prevalecen los vientos del Sur favorables al hundimiento [1].

Los vientos de componente norte fuerzan un transporte de Ekman en la capa superior, retirando un volumen significativo de agua que es reemplazado por agua oceánica subsuperficial mas fría y rica en nutrientes, Agua Central del Atlántico Nordeste (ACNAE) [2]. Existen dos ramas de esta agua, una más ligera, cálida y salada de origen subtropical (ACNAEst) y otra más fría y menos salada que tiene un origen subpolar (ACNAEsp). Ambas afloran sobre la plataforma y en las Rías Bajas, dependiendo del periodo del año y de la intensidad y dirección de los vientos costeros.

Durante el periodo de hundimiento, el agua superficial se apila contra la costa para posteriormente hundirse. A la vez se desarrolla una corriente de agua templada, salina y con menor contenido en nutrientes sobre el talud que va hacia el polo. La Corriente Ibérica hacia el Polo (IPC) [3], confina el agua costera sobre la plataforma, impidiendo los intercambios plataforma-océano. Otro fenómeno de gran interés son las plumas de agua dulce, llamadas plumas flotantes del Oeste Ibérico (WIBP) [4], localizadas sobre la plataforma y originadas por la escorrentía continental. Sin embargo, dentro de este esquema general, la mayor variabilidad del forzamiento atmosférico tiene lugar en forma de eventos, lo que se traduce en una compleja variabilidad a corta escala temporal [5].

Las rías interactúan fuertemente con la circulación de afloramiento/hundimiento en la plataforma y con los procesos biogeoquímicos [6]. La circulación en la Ría de Vigo es típicamente en dos capas, una de entrada de agua oceánica más densa por el fondo y otra de salida de agua menos salina y densa por superficie.

El programa RADIALES lleva recogiendo datos del Radial de Vigo desde 1994, monitorizando con frecuencia mensual el estado del medio marino y del plancton. Entre las medidas sistemáticas se recogen perfiles de CTD, concentraciones de nutrientes inorgánicos, de oxígeno disuelto y abundancia, biomasa y diversidad de bacterias, asi como muestras de fito y zooplancton. Recientemente, se han incorporado también medidas del sistema del carbono como son el pH y la alcalinidad. Los datos obtenidos en estas series se emplean regularmente en el asesoramiento a diversas organizaciones y administraciones nacionales e internacionales, como el Consejo Internacional de Exploración del Mar (ICES). Desde 2014 se han ido incorporando paulatinamente a iniciativas como European Marine Data and Observations Network (EMODNET) o el International Group for Marine Ecological Time Series (IGMETS).

MATERIAL Y MÉTODOS

La sección oceanográfica de la Ría de Vigo está formada por 4 estaciones situadas en la parte interna, media y externa de la ría. En cada estación se realiza un perfil vertical de temperatura, salinidad, fluorescencia y PAR (radiación fotosintéticamente activa) usando un CTD SBE25. Además se realizan pescas de fito- y zooplancton y se toman muestras de agua a distintas profundidades para el

análisis de nutrientes (nitrato, nitrito, amonio, fosfato y silicato). La serie completa de datos ha sido validada localmente y sometida a un exhaustivo control de calidad para detectar errores, picos y anomalías en el cierre de botellas. Este control incluye la incorporación de "flags" de calidad de acuerdo con los criterios establecidos internacionalmente [7] en el marco de los proyectos europeos SeaDataNet y EMODNET-Química que proporcionan información añadida sobre la fiabilidad de los datos. Una vez validados se han incorporado a través del Centro de Datos del IEO a la infraestructura paneuropea SeaDataNet desde la cual son accesibles.

RESULTADOS Y DISCUSIÓN

A partir del conjunto validado de datos (1994-2010) se han determinado los perfiles promedio de cada variable para cada estación. Estos perfiles tipo se están utilizando como referencia para el control de calidad de datos de muestreos posteriores, incluyendo la detección y marcado de anomalías. La longitud y frecuencia de la serie de datos permite estudiar la distribución espacio-temporal de los nutrientes, así como su comparación con las condiciones oceanográficas de cada época del año. A modo de ejemplo se muestran las variaciones entre enero y julio en las concentraciones de nutrientes a lo largo de la sección (Fig. 1). La ACNAE gana nutrientes mineralizados a medida que avanza la estación de afloramiento debido a un intenso proceso de remineralización en la plataforma [8]. Esto puede ser observado si se compara la variación mensual de las secciones verticales medias a lo largo del periodo de afloramiento. Del mismo modo la entrada principal de nutrientes debida al aporte fluvial durante los meses de invierno también puede ser identificada así como las diferencias entre la parte interna y externa de la Ría.

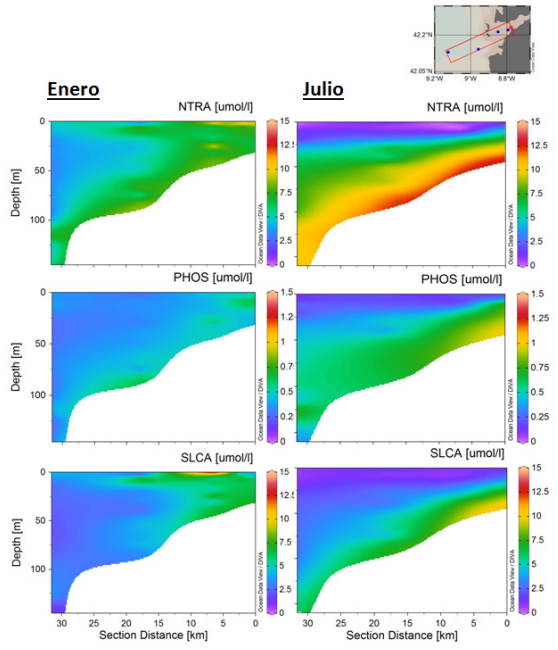

Fig. 1. Sección vertical de las concentraciones de nitrato, fosfato y silicato en Enero y Julio.

El estudio de la evolución temporal de la concentración de los diferentes nutrientes (Fig. 2), permite identificar periodos con menor aporte de nutrientes en la zona, lo cual se puede relacionar con variaciones en la biomasa y de composición de las distintas comunidades planctónicas con posibles consecuencias en niveles tróficos superiores.

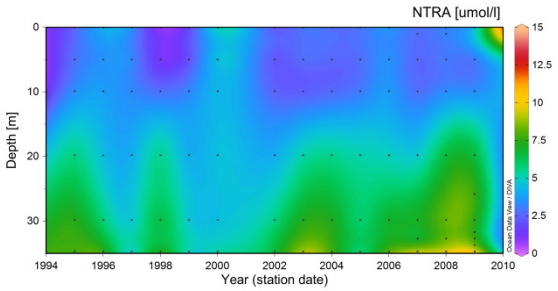

Fig. 2. Variación anual de los valores medios de la concentración de nitratos en la estación central de la Ría.

AGRADECIMIENTOS

Este trabajo puede hacerse gracias a la labor de los investigadores Ana Miranda y Gerardo Casas, que junto a la tripulación del B/O J.M. Navaz mensualmente realizan el radial de Vigo. Este trabajo ha sido parcialmente financiado por los proyectos europeos SeaDataNetII (FP7/2007-2013/283607), EMODnet (DGMARE/2012/10/ Lot 4 Chemistry/SI2.656742)

REFERENCIAS

1 - Wooster WS, Bakun A & McLain DR, 1976. Seasonal upwelling cycle along eastern boundary of North Atlantic. J. Mar. Res. 34: 131–141.

2 - Fraga F, 1981. Upwelling off the Galician coast, Northwest Spain. Coastal Upwelling Series. 1: 176–182.

3 - Frouin R, Fiúza AFG, Ambar I, Boyd TJ, 1990. Observations of a poleward surface current off the coast of Portugal and Spain during winter. J. Geophys. Res. 95(C1): 679-691.

4 - Peliz A, Rosa TL, Santos AMP, Pissarra JL, 2002. Fronts, jets, and counter-flows in the Western Iberian upwelling system. J. Mar. Syst. 35: 61-77.

5 - Torres R, Barton ED, Miller P & Fanjul E, 2003. Spatial patterns of wind and sea surface temperature in the Galician upwelling region. J. Geophys. Res. 108(C4), 3130.

6 - Arístegui J, Barton ED, Álvarez-Salgado XA, Santos AMP, Figueiras FG, Kifani S, Hernández-León S, Mason E, Machú E, Demarcq H, 2009. Sub-regional ecosystem variability in the Canary Current upwelling. Progr. Oceanogr. 83: 83–48.

7 - SeaDataNet Data Quality Control Procedures v2.0. 2010. http://www.seadatanet.org/content/download/18414/119624/file/SeaDataNet_QC_procedures_V2_%28May_2010%29.pdf

8 - Álvarez–Salgado XA, Castro CG, Pérez FF, Fraga F, 1997. Nutrient mineralization patterns in shelf waters of the Western Iberian upwelling. Cont. Shelf Res. 17: 1247–1270.

Biscay AGL. An observatory for state of the art operational oceanography at IEO. Derived products, sensor networks and future developments

Daniel Cano[1], César González-Pola[2], Raquel Somavilla[2] , Elena Tel[3], Carmen Rodriguez[1], Manuel Ruiz Villarreal[4] & Alicia Lavín[1]

[1] Instituto Español de Oceanografía. Centro Oceanográfico de Santander
[2] Instituto Español de Oceanografía. Centro Oceanográfico de Gijón
[3] Instituto Español de Oceanografía. Servicios Centrales. Madrid
[4] Instituto Español de Oceanografía. Centro Oceanográfico de Coruña

ABSTRACT

Since 1991, shelf and slope waters of the Southern Bay of Biscay are regularly sampled in a monthly hydrographical section north of Santander. From 2003, a deep hydrological standard section was included and on June 2007, an ocean-meteorological buoy was moored at the end of Santander Section (www.boya_agl.st.ieo.es). All of three are part of IEOOS (IEO Observing System). Biscay AGL is one observatory for the EU FixO[3] project.

Biscay AGL is more than the combination of the AGL Buoy and the hydrographical samplings. This observatory produces not only time series of several parameters at different time resolutions but also derived products, both in real and in delayed time. Derived products from this buoy include annual cycles as well as anomalies of physical and biogeochemical magnitudes like air-sea heat fluxes, salinity and water temperatures, sub inertial currents, surface chlorophyll Different products are derived from in-situ measurements at the AGL buoy like estimates of the mixed layer depth, wind and currents roses and wave intensity diagrams.

Many sensor networks have been deployed to monitor marine environment, and more will follow in the future. Due to the large number of sensor manufacturers, integrating diverse sensors into observation systems is not straightforward. By defining standardized service interfaces (like those based on OGC standards) it is possible to enable access to sensor networks and archived sensor data that can be discovered and accessed using standard protocols and application programming interfaces and therefore to comply with the requirements of the INSPIRE directive. Future developments include the deployment of a full sensor network as well as adding new devices to the Biscay AGL tool in order to achieve a deeper knowledge of the ocean.

INTRODUCTION

Since 1991, shelf and slope waters of the Southern Bay of Biscay are regularly sampled in a monthly hydrographical line north of Santander to a maximum depth of 1000m, as part of the IEO Radiales project [1].

From 2003, a deep hydrological standard sections (part of the VACLAN project) is occupied twice a year extending the Santander section 90 miles offshore. Measurements include CTDO2, nutrients and currents from vessel-mounted ADCP and LADCP. The database in the area hold by IEO is complemented with a current meters line moored in 2003 at 43º48'N, 3º 47'W sampling temperature, salinity and currents at the core of Central, Mediterranean and Labrador Sea water.

On June 2007, an ocean-meteorological Buoy [2] was moored at the Santander Section, 22 miles north of Santander at about 2850m depth, to complete the ocean information with the ocean-atmosphere interaction. The Santander section and AGL Buoy data highlight that heat and salt show a quite different behaviour in terms of their balance in the upper layers of the Bay of Biscay. All of three are part of IEOOS [3]. Biscay AGL is one observatory for the EU FixO3 project [4].

The combination of both resources lead to a powerful tool, Biscay AGL, which is more than the combination of the AGL Buoy and the hydrographical samplings. This tool produces not only time series of several parameters at different time resolutions but also derived products, both real time and delayed time. Products derived from this buoy include but not only annual cycles of multiple variables as well as anomalous values, both seasonal and

prompt. Also more particular ones such as air-sea heat fluxes, salinity and water temperatures anomalies, sub inertial currents series, chlorophyll surface series, estimate of the mixed layer depth and wind and currents roses.

Many sensor networks have been deployed to monitor Earth's environment, and more will follow in the future. Environmental sensors have improved continuously by becoming smaller, cheaper, and more intelligent. Due to the large number of sensor manufacturers and differing accompanying protocols, integrating diverse sensors into observation systems is not straightforward. By defining standardized service interfaces, a sensor web based on SWE (Sensor Web Enablement) services hides the heterogeneity of an underlying sensor network, its communication details and various hardware components, from the applications built on top of it. By these services it is possible to enable access to sensor networks and archived sensor data that can be discovered and accessed using standard protocols and application programming interfaces. Through this abstraction from sensor details, their usage in applications is facilitated.

DATASERIES AND DERIVED PRODUCTS

Data acquired by Biscay AGL observatory may be displayed as time series in the usual manner. Another way to use this data is to elaborate derived products which provide direct information. Two types of products are provided by Biscay AGL, real time and delayed time. In Fig. 1 an example is shown. Top plot shows the real time SST anomaly and bottom plot shows delayed time air-sea heat flux since 2007 to March 2016.

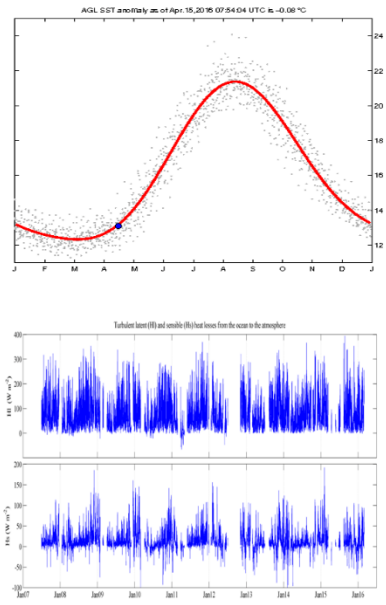

Fig. 1 Real time SST anomaly and delayed time air-sea heat flux

SENSOR NETWORKS

Sensor Web infrastructures are setup to access real-time data observed by sensors. Thereby, sensors range from simple weather stations over satellites to complex 'virtual' sensors such as simulations. The Sensor Web also provides means to task and control such sensors, as well as to retrieve events and alerts triggered through sensors.

All those functionalities of the Sensor Web are provided in an interoperable way - meaning that services implement standardized interfaces developed by the Open Geospatial Consortium (OGC) [5] and its Sensor Web Enablement (SWE) initiative [6].
The main adopted OGC standards in the SWE network include:

- **Observations & Measurements (O&M)** –The general models and XML encodings for observations and measurements.
- **PUCK Protocol Standard** – Defines a protocol to retrieve a SensorML description, sensor "driver" code, and other information from the device itself, thus enabling automatic sensor installation, configuration and operation.
- **Sensor Model Language (SensorML)** – Standard models and XML Schema for describing the processes within sensor and observation processing systems.
- **Sensor Observation Service (SOS)** – Open interface for a web service to obtain observations and sensor and platform descriptions from one or more sensors.
- **Sensor Planning Service (SPS)** – An open interface for a web service by which a client can 1) determine the feasibility of collecting data from one or more sensors or models and 2) submit collection requests.
- **SWE Common Data Model** – Defines low-level data models for exchanging sensor related data between nodes of the OGC® Sensor Web Enablement (SWE) framework.
- **SWE Service Model** -– Defines data types for common use across OGC Sensor Web Enablement (SWE) services. Five of these packages define operation request and response types.

REFERENCES

1 - Radiales Project Web Page
2 - Augusto González de Linares Buoy Web Page
3 -Tel, E., Balbin, R., Cabanas, J.-M., Garcia, M.-J., Garcia-Martinez, M. C., Gonzalez-Pola, C., Lavin, A., Lopez-Jurado, J.-L., Rodriguez, C., Ruiz-Villarreal, M., Sánchez-Leal, R. F., Vargas-Yáñez, M., and Vélez-Belchí, P.: IEOOS: the Spanish Institute of Oceanography Observing System, Ocean Sci., 12, 345-353, doi:10.5194/os-12-345-2016, 2016.
4 – FixO^3 observatories
5 – Open Geospatial Consortium

6 – Sensor Web Enablement initiative

Characteristics of Agulhas Rings

María Casanova-Masjoan, Pablo Sangrà, Antonio Martínez, Diana Grisolía & Alonso Hernández-Guerra

Instituto de Oceanografía y Cambio Global, IOCAG, Universidad de Las Palmas de Gran Canaria, ULPGC, Spain

ABSTRACT

The formation of Agulhas Rings in the Agulhas retroflection is the main source for the entry of Indian water into the Atlantic. The objective of this work is to characterize a Agulhas Ring and its dynamics. Methods used for this purpose consist in vertical sections and θ-S diagrams from CTD and Niskin bottles samples during the MOC-Austral survey in March 2010. Furthermore, wavelet and dynamic analysis of the ring from remote sensing imagery and NOAA drifters are used to study its dynamics. CTD data was collected in a longitudinal section that crossed a core of a ring during the survey. Drifters were also launched in the core ring during the survey. Altimetry data was processed and analysed from the ring formation to the end of the survey to estimate the ring lifetime. Data showed that the ring diameter is 260 km and 800 m depth. The ring rotation is clockwise and with a period of 8 days. Ring cores have greater salinity and temperature than the water around. It is also found that the drifters trajectories out of the ring travel near the African coast to the North.

Mejora de la representación de afloramientos costeros en un CGCM mediante la corrección de sesgos globales

Antonio Castaño-Tierno[1], Teresa Losada[1], Elsa Mohino[1], Belén Rodríguez-Fonseca[1,2] & C.R. Mechoso[3]

[1] Departamento de Física de la Tierra, Astronomía y Astrofísica I, Geofísica y Meteorología. UCM, Av. Complutense s/n, 28040 Madrid (Spain)
[2] Instituto de Geociencias (CSIC-UCM), Facultad de CC. Físicas, Plaza de Ciencias 1, 28040 Madrid (Spain).
[3] University of California Los Ángeles, California (USA)

RESUMEN

Los modelos acoplados de atmósfera-océano son una herramienta muy útil, ampliamente utilizada en el estudio de la variabilidad y el cambio climático. Sin embargo, dichos modelos tienen importantes sesgos, especialmente en las regiones tropicales. En este trabajo realizamos un experimento de sensibilidad mediante a) una simulación de veinticinco años del modelo atmosférico global UCLA v.7.1-SsiB, acoplado al modelo de océano del MIT (UCLA-MIT) y b) una simulación del mismo modelo en la que hemos introducido una reducción artificial de la radiación solar entre 30S y 60S, donde se sabe que la cantidad de nubes que simula el modelo es insuficiente. De esta forma estudiamos cómo afectaría una incidencia de radiación más realista a cuencas remotas, en particular al Atlántico tropical. Se comprueba que los sesgos mejoran, incluyendo zonas de gran importancia económica como las regiones de afloramiento costero. Además, se muestra cómo los errores del modelo pueden reducirse y la variabilidad cambiar gracias a la estrategia conocida como *anomaly coupling*. Esta consiste en modificar la rutina de acoplado del modelo de forma que la única información que se transmite entre el océano y la atmósfera (y viceversa) son las anomalías respecto a la climatología. De esta forma se puede evaluar qué fracción del sesgo del modelo se debe a errores en la climatología y cuál se debe a una representación imperfecta de la variabilidad.

INTRODUCCIÓN

Los afloramientos costeros de agua fría y rica en nutrientes tienen una gran importancia económica y ecológica [1], ya que la existencia de múltiples ecosistemas muy ricos en pesca depende de ellos. Los cuatro principales se encuentran al este de los océanos, en latitudes subtropicales: el de la Corriente de Humboldt, California, Canarias y Benguela. Su correcta representación en los modelos de circulación general es de gran importancia para estudiar su posible evolución futura. Dichos modelos tienen importantes sesgos en todo el globo [2], que se acentúan en estas regiones, debido a una conjunción de factores [3].

En este trabajo se aplican dos correcciones diferentes al modelo de circulación general UCLA-MIT y se estudia cómo mejora la representación de los sesgos oceánicos (temperatura de la superficie del mar (SST) y ascensos de agua de capas más profundas) y atmosféricos (vientos zonal y meridional y presión en superficie).

La primera corrección consiste en reducir la radiación solar incidente en el océano Sur (toda la banda entre 30S y 60S), ya que la mala representación de las nubes en esa región parece ser uno de los principales factores que influyen en la mala simulación de los movimientos de la zona de convergencia intertropical (ITCZ), que a su vez influye en los sesgos de las regiones subtropicales [4, 5].

La segunda corrección pretende evaluar el sesgo en todo el globo mediante la técnica conocida como *anomaly coupling* [6], consistente en acoplar solo las anomalías de la componente oceánica y atmosférica del modelo, y no la salida completa de cada modelo. De esta forma pretendemos reducir los sesgos, además de estudiar qué parte del error de los modelos se debe a la variabilidad simulada y qué parte es un sesgo sistemático.

MATERIAL Y MÉTODOS

Para la primera parte del trabajo se han realizado dos simulaciones de cincuenta años con el modelo acoplado UCLA-MIT. En ambas se han elegido los veinticinco últimos años para llevar a cabo este trabajo. Una simulación (ctl) es la simulación de control, mientras que en la otra (cosz) se ha realizado una reducción de la radiación solar incidente en la región entre 30S y 60S. Se

ha estudiado el sesgo de la simulación, además del ciclo estacional de la SST en las cuatro principales zonas de afloramientos costeros (California, Humboldt, Canarias y Benguela), poniendo especial énfasis en las situadas en el océano Atlántico.

Para la segunda parte se han realizado dos simulaciones largas (160 años de simulación no acoplada y 100 años de simulación acoplada) para preparar una simulación de cincuenta años con anomaly coupling en todo el globo.

RESULTADOS Y DISCUSIÓN

Los sesgos de temperatura en las zonas de upwelling mejoran [7] (se muestra la región de Benguela, Fig. 1) al mejorar la representación de los sesgos en todo el globo, pero también debido al reforzamiento de las altas presiones subtropicales (Fig. 2), que a su vez hacen que los vientos sean más realistas en las zonas de upwelling.

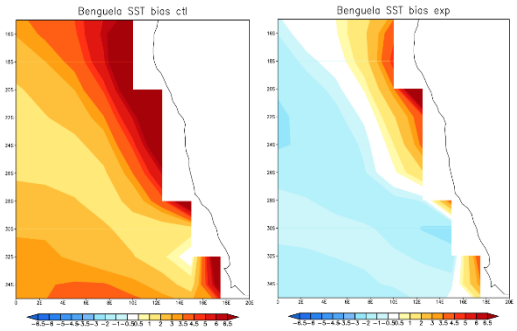

Fig. 1. Sesgo de SST del modelo UCLA en la región de Benguela para control (izq.) y experimento cosz (der.).

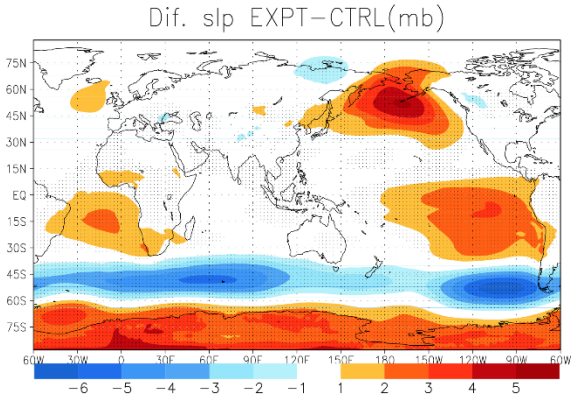

Fig. 2. Diferencia de SLP entre el exp. cosz y la simulación de control. Se refuerzan las altas presiones subtropicales.

Las limitaciones en resolución del modelo hacen que la mejoría de los sesgos sea menor cuanto más cerca de la costa nos encontremos, dado que los efectos orográficos de pequeña escala no están correctamente simulados. Para corregir aún más los sesgos de temperatura en las zonas de upwelling sería necesario utilizar modelos climáticos regionales, con una resolución mucho mayor. En cualquier caso, el objetivo de este trabajo es mostrar cómo incluso un CGCM puede mejorarse, aumentando su utilidad para hacer estudios de las zonas de upwelling.

Los modelos de circulación general tienen importantes limitaciones en lo que se refiere a estudiar procesos tan locales como los afloramientos costeros, pero hemos mostrado que una mejoría general del comportamiento del modelo (reducción del bias global) impacta favorablemente en la representación de los procesos regionales.

AGRADECIMIENTOS

Los autores agradecen la financiación del European Union Seventh Framework Programme (FP7/2007–2013), con el número de beca 603521; también agradecen la financiación del Ministerio de Economía y Competitividad a través del proyecto MULTISCALE CLIMATE VARIABILITY. AGRONOMICAL AND ECONOMIC IMPACTS (MULCLIVAR, ref: CGL2012-38923-C02-01), así como el uso del supercomputador Yellowstone, proporcionado por el Laboratorio de Computación y Sistemas de Información de NCAR, financiado por la National Science Foundation, y de EOLO, el computador de alto rendimiento del Campus de Excelencia Internacional de Moncloa

REFERENCIAS

1 - Ryther JH *(1969)* Photosynthesis and fish production in sea. *Science* 166:72–76.

2 - Wang, C., L. Zhang, S.-K. Lee, L. Wu, and C. R. Mechoso, 2014: A global perspective on CMIP5 climate model biases. *Nat. Climate Change*, 4, 201–205, doi:10.1038/nclimate2118.

3 - Richter, I. *WIREs Clim Change* 2015. doi: 10.1002/wcc.338

4 - Hwang, Y.-T., and D. M. M. Frierson, 2013: Link between the double-intertropical convergence zone problem and cloud biases over the Southern Ocean. *Proc. Natl. Acad. Sci. USA*, 110, 4935–4940.

5 - Mechoso, C. R. *et al.* The seasonal cycle over the tropical Pacific in general circulation models. *Mon. Weath. Rev* 123, 2825–2838 (1995).

6 - Kirtman, B. P., J. Shukla, B. Huang, Z. Zhu, and E. K. Schneider, 1997: Multiseasonal predictions with a coupled tropical ocean– global atmosphere system. *Mon. Wea. Rev.,* 125, 789–808.

7 - Mechoso, C.R. *et al.* Amplification in coupled GCM of the effects of Southern Ocean biases on the Tropics. *To be submitted*.

Agulhas leakage increasing trend: its relation to regime shift in the western boundary of the Tropical Atlantic
El aumento en la fuga de Agulhas: su relación con el cambio de regimen en el margen occidental del Atlántico Tropical

Paola Castellanos[1], Edmo Campos[1], Jaume Piera[2], Olga Sato[1], Maria Assunção Silva Dias[3]

[1] Instituto Oceanografico da Universidade de São Paulo, Brazil
[2] Institut de Ciències del Mar, CSIC, Spain.
[3] Instituto de Astronomia, Geofísica e Ciencias Atmosféricas, Universidade de São Paulo, Brazil

ABSTRACT

The Agulhas System is a complex dynamical structure characterized by the intrusion of Indian Ocean waters into the South Atlantic Ocean by means of filaments and rings shed from the Agulhas Current retroflection. This influx of warmer and saltier Indian Ocean waters into the Atlantic –Agulhas leakage – is now recognized to play an important role in the global thermohaline circulation. Due to the absence of an adequate observing system, studies of the Agulhas system have relied on outputs of ocean models, which revealed a recent increase in the Agulhas leakage. Here we present the results of a 1/12° simulation with the Hybrid Coordinate Ocean Model (HYCOM), which also show an augmentation in Agulhas leakage. This increase in the leakage ought to have an impact on the meridional oceanic volume and heat transports in the Atlantic Ocean. Significant linear trends found in the integrated transport at 20 ºS, 15 ºS, and 5 ºS correlate well with Agulhas leakage. The augmented transport seems to be related to an increase in the latent heat flux observed along the NE Brazil coastline since 2003. Our study shows that the precipitation in the Brazilian coast has been increasing since 2005, with the same regime shift observed for the latent heat flux and the volume transport. This strongly suggests that the increase of the Agulhas transport affects the western boundary system of the Tropical Atlantic Ocean, which is directly related to the increase in the precipitation and latent heat flux along the western coast.

Operational forecasting and statistical products for short term port management: Barcelona, Bilbao and Tarragona harbours

Pablo Cerralbo[1], Manel Grifoll[1], Laura Rafols[1], Agustín S-Arcilla[1], Manuel Espino[1], Marc Mestres[1], Marcos G-Sotillo[2], Enrique-Álvarez Fanjul[2]

[1] Laboratori d'Enginyeria Marítima (LIM). Universitat Politècnica de Catalunya (UPC). Carrer Jordi Girona 1-3, 08034 Barcelona, Spain. E-mail: pablo.cerralbo@upc.edu
[2] Puertos del Estado, Avenida del Partenón 10, 28042, Madrid, Spain.

ABSTRACT

Understanding the physical behavior of coastal areas, such as harbors and estuaries, is important to manage the main problems related to anthropic impacts and resource exploitation activities. The implementation of numerical models in these areas, as well as the analysis of measured data, enables a better understanding and characterization of their main hydrodynamic features. Operational products providing a hydrodynamic forecasting of the area under study with a proper time horizon (e.g., 48–72 h), should allow to elaborate management plans and reduce the risk associated to extreme/hazardous events.

Based on previous work on the design of operational systems for the prediction of currents and sea level in harbors [1][2], we present in this contribution the most recent implementation of the high resolution harbor operational systems developed within the SAMOA project framework.

These systems are fully implemented nowadays for the harbors of Barcelona, Tarragona and Bilbao. We will present the nesting scheme utilized to go from regional systems (IBI-MFC) to local scales, as well as the main results of the corresponding validation. This validation has been performed over an entire year (2014) and utilizing a wide spectrum of meteo-oceanographic data: tide gauges, current-meters, temperature and salinity sensors, as well as data from the new HF Radar in the Ebro Delta. The results reveal high correlations with most of the oceanographic variables, showing a remarkable improvement in sea level and surface currents during some periods compared with IBI-MFC. Finally, the longer-term (statistical) oceanographic description of the harbor is presented, based on a collection of maps for typical meteo-oceanographic situations.

INTRODUCTION

Operational systems (OS) for the prediction of currents in seaports constitute a convenient instrument for risk assessment and environmental harbor management [1], [2]. Additionally, for long term management, a water circulation pattern for the characteristic meteo-oceanographic situations may provide relevant information for a suitable make decision protocols.

In the paper we present the development and implementation of a high-resolution OS in three of the main Spanish harbors, characterized by different hydrodynamic conditions (micro- vs. meso-tidal domain; one mouth vs two mouths, etc.). For each one, a nested suite of numerical models is set up to downscale the regional information (with a horizontal resolution of a few km) to the "coastal" and "harbor" scale (horizontal resolution of 350 and 70 m, respectively). The models are nested into the EU operational system Copernicus (IBI-MFC [3]) and use high-resolution meteorological (provided by AEMET) and tidal products (provided by Puertos del Estado).

NUMERICAL MODEL AND NESTING SCHEME

The three-dimensional hydrodynamic model used in this work is an adapted Regional Ocean Modeling System (ROMS). Numerical aspects are described in detail in [4] and a complete description of the model, documentation and code are available at the ROMS website: http://myroms.org. The forecasting horizon is 3 days, plus 1 day of hindcast (Fig. 1a). The OS consists of two domains, coast and harbor (Fig. 1b), which works sequentially: coastal domains are nested to the more regional solution of IBI-MFC (which provides currents, salinity and temperature) and NIVMAR (meteorological tide).

Numerical assessments for the quality of the solution have been done using oceanographic data from the Puertos del Estado observational networks (REDCOS, REDEXT and REDMAR) for the salinity, temperature, sea level and

currents. Moreover, the data from the HF Radar in the Delta del Ebro has been used to validate the surface currents (Figure 2). These validations have been performed over the entire year 2014 (offline), and using the online operational results.

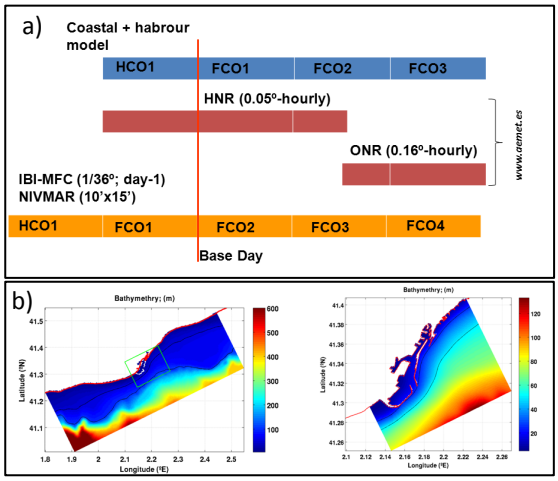

Figure 1. – a) Operational scheme. b) Numerical domain example for the Barcelona implementation.

RESULTS

The requirements of high-resolution, accuracy and robustness pose a tough challenge for conventional current/wave operational modelling tools. The role of boundary (intermediate) conditions in nested models and the extraction of statistical estimators from limited duration time-series are some of the critical points solved before the numerical simulations can be used for harbor exploitation. Comparison data from HF Radar showed good results for the skill assessment of along and across shore currents in the CST-TAR implementation (Fig. 2).

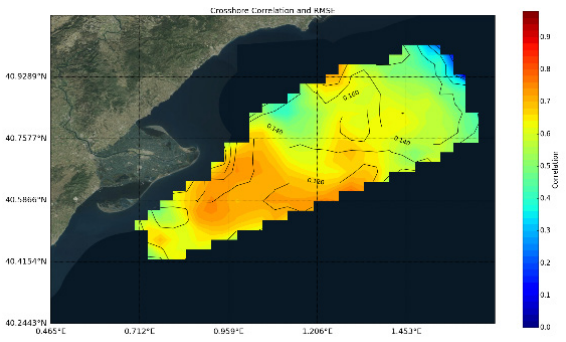

Figure 2. – Correlation coefficient between HF Radar and long-term numerical results during April 2014 for across shore currents.

However, and in spite of their usefulness, the typical forecast horizon (3 to 5 days) of operational forecasts unable them to provide information on the medium and long term behavior of the port system. OS prognosis, for instance, cannot be used to estimate the best period to undertake port development works. To overcome this limitation, OS must be complemented with longer-term (statistical) descriptions of the harbor that supports decision-making at longer timescales (case atlas). For this, typical meteo-oceanographic conditions in the domain, but also atypical conditions that might be of interest to the port authorities, are used to feed "offline" runs of the operational model, and the results are analyzed, processed and graphically presented according to the precise needs of the harbor, which can include hydrodynamic (currents, renewal times, etc.), dispersion (spill trajectories and concentrations) or management (risk indices) parameters. These statistical atlases provide a fast, direct and simple tool to predict off-line the behavior of selected variables relevant to port management decisions under typical meteo-hydrodynamic scenarios, and they should allow planning harbor interventions at a +3 day horizon.

ACKNOWLEDGMENTS

The authors acknowledge the economical funding and support received from the MINECO and FEDER who funded the Plan-Wave (CTM2013-45141-R) project, as well as the collaboration of the harbor authorities of Barcelona, Tarragona, Bilbao and Canarias. We also want to thank the Secretaria d'Universitats i Recerca del Dpt. d'Economia i Coneixement de la Generalitat de Catalunya (Ref 2014SGR1253) who support our research.

REFERENCES

1 - Grifoll, M., Jordà, G., Espino, M., Romo, J., García-Sotillo, M. (2011): A management system for accidental water pollution risk in a harbour: The Barcelona case study, Journal of Marine System, ELSEVIER, vol. 80, pp. 60-73.

2 – Grifoll, M., Jordà, G., Sotillo, M.G., Ferrer, L., Espino, M., Sánchez-Arcilla, A., Álvarez-Fanjul, E., 2012. Water circulation forecasting in Spanish harbours. Sci. Mar. 76, 45–61. doi:10.3989/scimar.03606.18B

3- Sotillo M G, Cailleau S, Lorente P, Levier B, Aznar R, Reffray G, 3, A.-B. a, Chanut J, Benkiran M, Alvarez-Fanjul E, 2015. The MyOcean IBI Ocean Forecast and Reanalysis Systems: Operational products and 1 roadmap to the future Copernicus Service. 2. J. Oper. Oceanogr. 8778. doi:10.1080/1755876X.2015.1014663

4- Shchepetkin, A.F., McWilliams, J.C., 2005. The regional oceanic modeling system (ROMS): a split-explicit, free-surface, topography-following-coordinate oceanic model. Ocean Model. 9, 347–404. doi:10.1016/j.ocemod.2004.08.002

Sistema frente-remolino: ¿subducción o barrera? Caso de estudio en el sistema de surgencia de Chile central

Andrea Corredor-Acosta[1,2], Ángel Rodríguez-Santana[3], Carmen E. Morales[2,4], Samuel Hormazabal[2,5]

[1] Programa de Postgrados en Oceanografía, Universidad de Concepción, Barrio Universitario s/n, Concepción, Chile.
[2] Instituto Milenio de Oceanografía (IMO), Barrio Universitario s/n, Concepción, Chile.
[3] Departamento de Física, Facultad de Ciencias del Mar, Universidad de las Palmas de Gran Canaria, España.
[4] Departamento de Oceanografía, Universidad de Concepción, Barrio Universitario s/n, Concepción, Chile.
[5] Escuela de Ciencias del Mar, Pontificia Universidad Católica de Valparaíso, Avda Altamirano 1480, Valparaíso, Chile.

RESUMEN

Las estructuras físicas de sub- y mesoescala tales como frentes, remolinos y/o filamentos en los sistemas de borde oriental, favorecen el intercambio de propiedades entre la costa y el océano, modifican la pendiente de las isopicnas en la columna de agua y permiten la generación de gradientes laterales de flotabilidad que a su vez podrían facilitar la mezcla vertical mediante la cizalla vertical del flujo baroclino asociado al frente. En este estudio, datos in situ de temperatura, salinidad y densidad obtenidos a lo largo de dos transectas en la zona frontal adyacente al área de surgencia de Chile central (Transecta Norte (TN), 36.50°S, 73.10-74.50°W; Transecta Sur (TS), 36.75°S, 73.30-74.50°W; 3-7 Febrero 2014), fueron usados para calcular la velocidad geostrófica, frecuencia de flotabilidad, cizalla vertical y las variaciones del número de gradiente de Richardson (Ri) en la columna de agua y a lo largo de la sección costa-océano. Los resultados obtenidos permitieron identificar una zona frontal (~73.8°W) intensificado durante el periodo de surgencia, y su límite oceánico se caracterizó por la presencia de un remolino anticiclónico de agua cálida. En términos de la frecuencia Brunt-Väisälä, la inestabilidad de la columna de agua fue mayor en los primeros 50m, acompañada de valores altos de cizalla vertical y en el frente más que en las estaciones adyacentes costa/océano para ambas transectas. Ri <10 fueron observados en la capa superficial sugiriendo zonas donde los procesos de mezcla se pueden intensificar, sin embargo, el gradiente zonal fue mayor en la TS, indicando posibles intrusiones subsuperficiales de agua superficial en la interacción frente-remolino para dicha transecta.

INTRODUCCIÓN

Los frentes han sido definidos como regiones de fuertes contrastes laterales en temperatura y/o salinidad en el océano, caracterizándose además por una curvatura de la picnoclina capaz de generar un gradiente horizontal de densidad en la dirección perpendicular al frente [1]. En los sistemas de borde oriental, paralelo a la costa se ha establecido la presencia del *frente de masas de agua* en donde los gradientes de densidad son debidos a las diferencias en la salinidad, dada la convergencia de dos cuerpos de agua con distintas propiedades [1]. Sin embargo, el flujo de Ekman que se produce hacia afuera de la costa debido a la tensión del viento en estos sistemas de surgencia, conlleva al ascenso de la picnoclina cerca de la costa, provocando un fuerte frente en densidad superficial denominado *frente de surgencia* [2]. Si bien ambos parecen ser rasgos característicos de los sistemas de borde oriental, algunos estudios asocian el gradiente de estratificación alrededor del frente debido a la salinidad, con la subducción de material particulado hacia el lado oceánico, mientras que, otros estudios han mostrado la acumulación y mantenimiento local de material particulado en el frente mismo [2]. No obstante, los frentes de surgencia pueden estar acompañados de remolinos capaces de cambiar los gradientes de flotabilidad alrededor de la zona frontal, facilitando la cizalla vertical, la mezcla diapicna y la subducción de material particulado proveniente de la capa superficial [3,4]. En consecuencia, es posible que el sistema frente-remolino actúe como un sistema acoplado de *frente surgencia - masas de agua*, permitiendo la coexistencia de "acumulación" y "subducción".

MATERIAL Y MÉTODOS

En la zona frontal adyacente al área de surgencia de Chile central durante el periodo del 3-7 Febrero del 2014, datos in situ de temperatura, salinidad, densidad y fluorescencia fueron obtenidos a lo largo de dos transectas perpendiculares a la costa hasta los 300m de profundidad (TN: 36.50°S, 73.10-74.50°W, 15 estaciones y TS:

36.75°S, 73.30-74.50°W, 11 estaciones). Los datos fueron adquiridos con el equipo CTD Sea-Bird SBE 9 y procesados a resolución vertical de 0.5m usando el software Seasoft v.130. A partir de los datos de temperatura, salinidad y densidad se realizaron los cálculos de anomalía geopotencial para obtener las velocidades geostróficas (Velg) en ambas transectas. Se estimaron la frecuencia Brunt-Väisälä al cuadrado (N^2) para cada estación y transecta, la cizalla vertical al cuadrado (S^2) a partir del gradiente vertical de velocidad geostrófico entre las estaciones. Con el propósito de calcular Ri, N^2 fue interpolada en longitud en función de S^2, posteriormente ambas variables fueron suavizadas cada 8m en profundidad y finalmente, Ri fue obtenido dividiendo las series filtradas de N^2 y S^2. Adicionalmente, con el propósito de analizar las diferencias frente vs. costa/océano, 3 estaciones en ambas transectas fueron seleccionadas: estación costera (EC, ~73.6°W), estación frente (EF, ~73.8°W) y estación oceánica (EO, ~74°W).

RESULTADOS Y DISCUSIÓN

Los resultados obtenidos en ambas transectas mostraron gradientes horizontales en temperatura, salinidad y densidad, con una inclinada pendiente de las isolíneas hacia la costa. En la TN y TS la mayor tasa de cambio de dichos gradientes se ubicó en los ~73.8°W, posición del frente en la zona de surgencia costera de Chile central [5]. Sin embargo, los gradientes laterales fueron mayores y más profundos a lo largo de la columna de agua en la TS en comparación con la TN. La velocidad geostrófica en ambas transectas mostró la presencia de un remolino anticiclónico adyacente al frente en su extremo oceánico y un flujo hacia el norte paralelo a la costa, similar a lo encontrado por [5]. En comparación la TS presentó velocidades máximas mayores que la TN por ~10cm/s (Fig. 1).

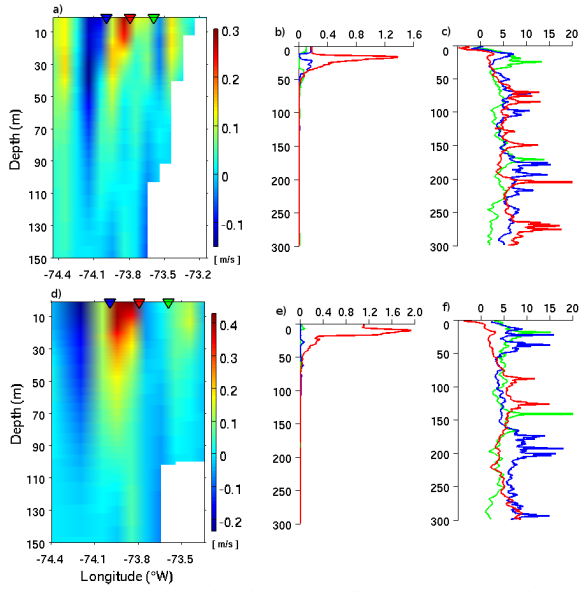

Fig. 1. Sección de velocidad geostrófica en a) TN y d)TS, incluyendo la posición de EC, EF y EO (triángulo verde, rojo y azul, respectivamente). Cizalla vertical y logaritmo del número de Richardson en función de la profundidad en b, c) TN y e, f) TS. La línea verde indica la EC, la línea roja la EF y la línea azul la EO.

N^2 en ambas transectas presentó valores altos en los primeros 50m y mostró mayores inestabilidades en la estratificación en la EF, tanto en la TN como en la TS (datos no mostrados). S^2 y Ri fueron igualmente importantes en la capa superficial, observando altos valores de cizalla en la EF combinados con valores bajos de Ri sugiriendo la tendencia a la mezcla vertical. Cabe resaltar que los valores máximos de S^2 y los valores mínimos de Ri fueron más evidentes en la EF para la TS que para la TN. Adicionalmente, en la TS se ve una amplia diferencia en Ri al comparar la EF con las estaciones adyacente EC y EO (Fig. 1), lo que podría ser producto de una mayor influencia del remolino anticiclónico adyacente en la TS (mayores Velg), facilitando los procesos de mezcla, las intrusiones subsuperficiales de agua superficial y posiblemente la subducción de material particulado hacia el lado oceánico del frente (Fig. 2). En tanto que, la TN podría tener una menor influencia del remolino permitiendo la acumulación de material particulado en el frente. Posteriores análisis son necesarios para dar una mayor y mejor interpretación al sistema frente-remolino en Chile central.

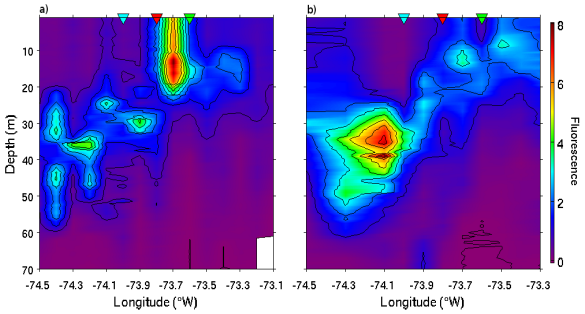

Fig. 2. Sección de fluorescencia en a) TN y b)TS, incluyendo la posición de EC, EF y EO (triángulo verde, rojo y azul, respectivamente).

AGRADECIMIENTOS

Beca Conicyt de Doctorado para extranjeros en Chile. Proyecto Fondecyt 1151299.

REFERENCIAS

1 – Franks P, 1992. Phytoplankton blooms at fronts: Patterns, scales and physical forcing mechanisms. *Rev. Aqu. Sci.,* 6:121-137.

2 – Zhang Y, Bellingham J, Ryan J & Godin M, 2015. Evolution of a physical and biological front from upwelling to relaxation. *Cont. Shelf Res.,* 108: 55-64.

3 – Johnston T, Rudnick D & Pallàs-Sanz E, 2011. Elevated mixing at a front. *J. Geophys. Res.,* 116, C11033.

4 – Omand M, D'Asaro E, Lee C, Perry M, Briggs N, Cetinic I & Mahadevan A, 2015. Eddy-driven subduction exports particulate organic carbon from the spring bloom. *Science.* 348, Issue 6231.

5 – Letelier J, Pizarro O & Nuñez S, 2009. Seasonal variability of coastal upwelling and the upwelling front off central Chile. *J. Geophys. Res.,* 114, C12009.

Plástico en mares y océanos: un problema global solucionable.

Andrés Cózar[1]

[1] Departamento de Biología, Facultad de Cc. del Mar y Ambientales, Universidad de Cádiz, Campus de Excelencia Internacional del Mar (CEIMAR), E-11510 Puerto Real, Spain

RESUMEN

Resulta muy significativo que, con solo unas décadas de uso generalizado de materiales plásticos, el hombre haya inundado con residuos plásticos todos los océanos. La contaminación marina por plásticos es uno de los asuntos que mejor ilustra la capacidad del hombre para modificar la apariencia y composición del planeta. La enormidad de los océanos parecía suficiente para diluir nuestros desechos, pero nos hemos encontrado en poco tiempo con un problema de escala planetaria. El progresivo incremento en la producción global de plástico y nuestra dependencia de este material hacen además pensar que se trata de un problema de difícil solución. Por otra parte, la contaminación marina por plásticos es un asunto que ha conseguido conectar ciencia, medios de comunicación y sociedad como en pocas ocasiones. En las últimas dos décadas, esta comunión se ha reforzado y retroalimentado de tal forma que el número de trabajos de investigación así como el grado de implicación social ha crecido exponencialmente, un movimiento que empieza incluso a influenciar las estrategias del propio sector empresarial del plástico. La contaminación por plástico puede por tanto llegar a convertirse también en un ejemplo de la capacidad del hombre para afrontar y corregir los problemas ambientales que amenazan nuestro planeta. En esta charla, mostraremos una panorámica integral de la problemática de la contaminación marina por plástico, mostrando los avances más recientes y las perspectivas de futuro para su estudio y gestión.

INTRODUCCIÓN

La acumulación de residuos plásticos en mares y océanos es un problema que genera gran preocupación social debido a los numerosos ejemplos de impactos sobre organismos así como las evidencias científicas que demuestran la escala planetaria de esta contaminación. Se han documentado impactos por ingestión y enredamiento en invertebrados, peces, aves, tortugas, y hasta grandes cetáceos [1,2]. Se han encontrado acumulaciones de residuos plásticos en costas, fondos y aguas de casi todas las regiones del planeta [3, 4]. Existe además gran incertidumbre acerca de los posibles efectos de la contaminación marina por plásticos a nivel ecosistémico [4, 5] o incluso en la salud humana [1].

El escenario descrito unido al incremento exponencial en la producción global de plástico hacen pensar que los esfuerzos por combatir esta contaminación han sido infructuosos, y que este es un problema de difícil solución que puede deparar consecuencias a gran escala [6].

RESULTADOS Y DISCUSIÓN

Es sabido que los desechos plásticos marinos se pueden acumular en aguas superficiales e intermedias, costas, fondos, e incluso en la biota. Sin embargo, el único *stock* de plástico que ha podido ser evaluado a escala global es el la capa superficial del océano, gracias al uso extensivo de redes de arrastre superficial para medir concentraciones de plástico flotante. Análisis de amplia escala espacial y temporal para otros reservorios de plástico son todavía difíciles de abordar.

Año tras año se completa el mapa global de residuos plásticos flotantes (Fig. 1). Las zonas de convergencia de cada una de las cinco Giros Subtropicales se han identificado como grandes regiones de acumulación de desechos flotantes. Los modelos de circulación oceánica predicen potenciales de acumulación de plásticos en mares semi-cerrados con alta densidad poblacional, lo que ha sido demostrado recientemente para el caso del Mar Mediterráneo [7]. La posibilidad de acumulación de plástico en las latitudes polares ha sido hasta ahora pasada por alto, aunque una reciente expedición circumpolar ha permitido completar esta parte del mapa global con resultados sorprendentes.

En la dimensión temporal, las series históricas de contaminación por plásticos flotantes, disponibles desde los años 80 para algunas regiones [8, 9], convergen en la conclusión de que no aparecen claras tendencias de incremento en el grado de contaminación durante los últimos años, un resultado que no ha sido explorado en profundidad por la comunidad científica. De hecho, existen grandes incógnitas en relación a cuál ha sido

realmente la evolución histórica de la contaminación marina por plástico y cómo las medidas aplicadas para su gestión han incidido en las tendencias históricas.

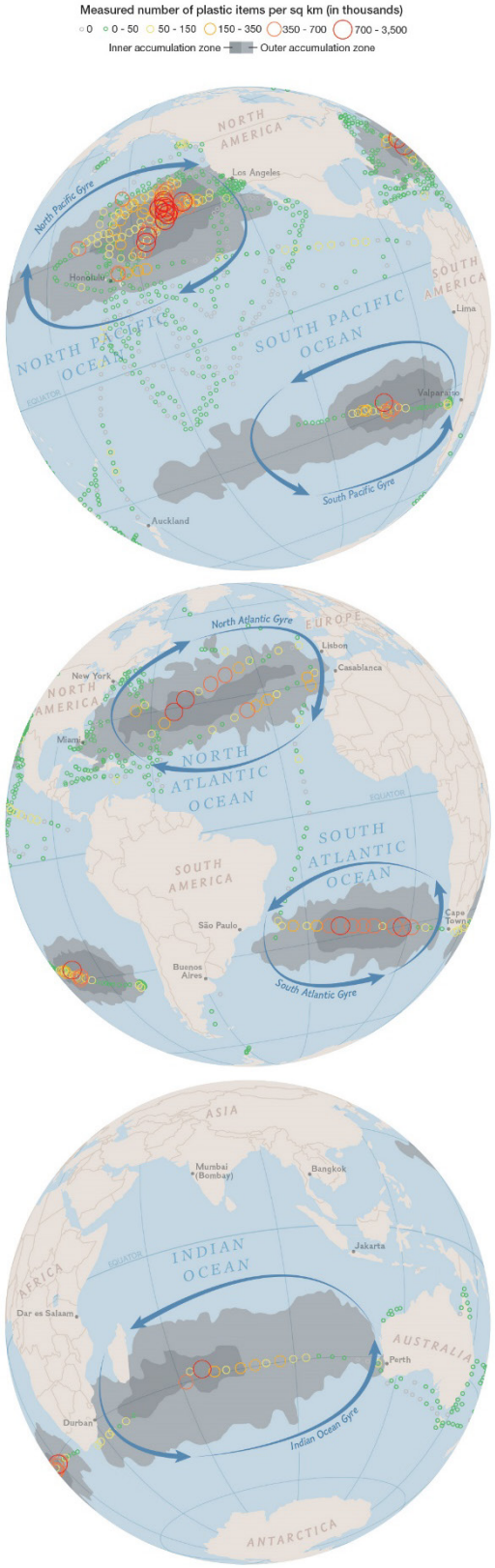

Fig. 1. Primer mapa de contaminación marina por plásticos flotantes (Fuente: National Geographic, Autores: A. Cózar y J. Hawk).

Los desechos plásticos sufren un continuo proceso de fragmentación que hace que se puedan encontrar en el mar desde objetos del orden de metros a partículas de pocas micras. Debido a esta movilidad en la escala de tamaños, las afecciones sobre organismos y ecosistemas pueden llegar a ser muy diversas, actuando a múltiples niveles [1-2, 5]. Especialmente llamativos son los nano-plásticos (en la escala de micras), capaces de ser incorporados en el tejido de sus consumidores [10], lo que plantea una vía potencial de impacto totalmente desconocida.

Estos y otros avances en el conocimiento de la contaminación marina por plásticos han atraído enormemente la atención de medios y ciudadanía a nivel global. Así, numerosas iniciativas sociales se han puesto en marcha para combatir la contaminación marina en los últimos años. La sinergia entre el conocimiento científico y la implicación social crece, existiendo ejemplos de actuaciones preventivas y correctoras a escala regional de enorme éxito. El fenómeno de la contaminación por plástico es un problema inquietante, pero la preocupación y la acción social surgida hacen pensar que esta amenaza global pueda ser solucionable.

AGRADECIMIENTOS

Esta contribución es el resultado de la colaboración de una larga lista de investigadores en distintos proyectos (Malaspina CSD2008-00077, MedSeA FP7-2010-265103; Programa S. de Madariaga PRX14/00743, *Tara Oceans*)

REFERENCIAS

1 - Rochman CM, et al. 2015. Anthropogenic debris in seafood: Plastic debris and fibers from textiles in fish and bivalves sold for human consumption. *Sci. Rep.,* 5:14340.

2 - de Stephanis R, et al. 2013. As main meal for sperm whales: Plastics debris. *Mar Pollut Bull*, 69(1–2):206–214.

3 - Pham CK, et al. 2014. Marine litter distribution and density in European seas, from the shelves to deep basins. PLOS ONE 9(4): e95839.

4 - Cózar A, et al. 2014. Plastic debris in the open ocean. PNAS 2014 111(28): 10239–10244.

5 - Sussarellu R., et al. 2016. Oyster reproduction is affected by exposure to polystyrene microplastics. PNAS 113(9): 2430-2435.

6 - Wilcox, C., et al. 2015. Threat of plastic pollution to seabirds is global, pervasive, and increasing. PNAS 112:11899–11904.

7 - Cózar A, et al. 2015. Plastic accumulation in the Mediterranean Sea. PLOS ONE 10(4): e0121762.

8 - Law KL et al. (2010) Plastic accumulation in the North Atlantic Subtropical Gyre. *Science* 329:1185–1188.

9 - Law KL, et al. (2014) Distribution of surface plastic debris in the eastern pacific ocean from an 11-year data set. *Environ Sci Technol* 48(9):4732–4738.

10 - Avio CM, et al. 2015. Pollutants bioavailability and toxicological risk from microplastics to marine mussels. *Environ Pollut.*, 198:211-22.

Observaciones en la Confluencia de Brasil-Malvinas durante marzo de 2015

Mikhail Emelianov[1], Marc Gasser[1], Jordi Isern-Fontanet[1], Dorleta Orue-Echevarría[1], Jesús Peña-Izquierdo[1], Sergio Ramírez[1], Miquel Rosell-Fieschi[1], Joaquín Salvador[1], Martín Saraceno[2], Daniel Valla[3] & Josep L. Pelegrí[1]

[1] Departament d'Oceanografia Física i Tecnológica, Institut de Ciències del Mar, CSIC, Barcelona
[2] Centro de Investigaciones del Mar y la Atmósfera, UMI/IFAECI, CONICET, Buenos Aires, Argentina
[3] Departamento de Oceanografía, Servicio de Hidrografía Naval, UMI/IFAECI, CONICET, Buenos Aires, Argentina

RESUMEN

La Confluencia de Brasil-Malvinas (CBM), donde confluyen las masas de agua de origen subtropical (Corriente de Brasil) y subantártico (Corriente de Malvinas), juega un papel clave en la transferencia meridional de masa, calor y sal, como parte del ramal de retorno de la cinta transbordadora global en el Océano Atlántico. En marzo de 2015 se realizó a bordo del BIO Hespérides la campaña TIC-MOC, con el fin de caracterizar las condiciones oceanográficas en la región de la CBM. Durante la campaña se hicieron 66 estaciones hidrográficas y se lanzaron 8 flotadores y 9 perfiladores de deriva, en lo que resultó ser un muestreo de alta resolución espacio-temporal de los procesos que se desarrollan en la Confluencia a distintas escalas. Las observaciones revelan la colisión frontal de las dos corrientes, cada una de ellas con altas velocidades, que en superficie pueden exceder 1 m s^{-1}. Este choque crea un complejo sistema frontal, con elevados gradientes horizontales de variables físicas y biogeoquímicas, que está caracterizado por intrusiones termohalinas y remolinos de ambos signos, además de un filamento superficial que se extiende hacia el este con velocidades cercanas a 2 m s^{-1}.

INTRODUCCIÓN

La región de encuentro de las Corrientes de Malvinas y Brasil, denominada la Confluencia de Brasil-Malvinas (CBM) (Fig. 1), constituye uno de los puntos reguladores de la cinta transportadora global oceánica durante su camino de retorno hacia las zonas de formación de aguas profundas en el Océano Atlántico Norte.

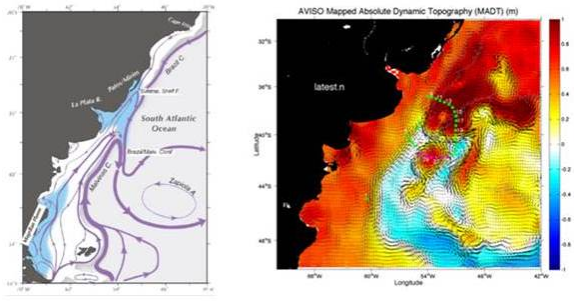

Fig. 1. (Izq.) Esquema del patrón de circulación superficial en la región de la CBM [1]. (Der.) Detalle del campo superficial del nivel del mar (en colores) y los campos de velocidad geostrófica superficial (vectores) en la CBM para el día 20 de marzo de 2015; el área de muestreo durante la campaña TIC-MOC queda delimitada por los puntos verdes, que corresponden a las estaciones del transecto exterior.

La confluencia entre las Corrientes de Brasil y Malvinas se caracteriza por la generación de remolinos de ambos signos y una compleja estructura termohalina, que favorecen el intenso intercambio de masa, calor y sal entre las aguas de origen subtropical y subantártico. Los estudios previos han permitido describir las características termohalinas de las masas de agua [2], revelando una enérgica interacción entre estas aguas a través de los frentes subantártico y subtropical [3]. Otros estudios también han permitido investigar la dinámica de la zona con base en la información satelital de las bandas infrarroja [4] y visible [5], así como por altimetría [6]. La variabilidad estacional e interanual también ha sido examinada usando modelos numéricos [1] así como a partir de observaciones remotas y de instrumentos en la zona [7].

A pesar de todos estos avances, puede decirse que la CBM permanece poco estudiada a nivel regional. En particular, se sabe bastante poco sobre los procesos de mesoescala y pequeña escala que se desarrollan entre las masas de agua subantártica y subtropical, que son los responsables últimos de la transferencia meridional de propiedades. Estas masas colisionan frontalmente con velocidades muy intensas, generando una zona frontal con muy elevados gradientes horizontales en prácticamente todos los parámetros físicos y biogeoquímicos. Se trata, probablemente, del frente a escala regional más intenso (e.g. gradientes transfrontales de hasta 4ºC por kilómetro) y energético (velocidades superficiales a lo largo del frente que alcanzan valores cercanos a los 2 m s^{-1}) en todos los océanos. En este trabajo presentamos los resultados de una campaña realizada en esta región a finales

del verano austral de 2015, centrándonos en la descripción hidrográfica de la región y la caracterización de los procesos dominantes a escala regional, mesoescalar y submesoescalar.

MATERIAL Y MÉTODOS

Los datos de campo fueron obtenidos durante la campaña oceanográfica TIC-MOC, realizada a bordo del BIO Hespérides, con mediciones en la CBM entre el 9 y el 22 de marzo de 2015. Durante la campaña se hizo un seguimiento en tiempo cuasi-real de la región frontal mediante imágenes de satélite de color, temperatura y altimetría, así como por medio de las salidas numéricas diarias del modelo operacional MyOcean, con 1/12° de resolución horizontal (http://marine.copernicus.eu/). Esto permitió la localización precisa del frente de modo que se llevó a cabo un transecto externo que englobó la región frontal, para posteriormente realizar el muestreo con alta resolución en la propia región frontal.

En total se hicieron 66 estaciones hidrográficas, donde se tomaron medidas de conductividad, temperatura, presión, oxígeno disuelto y fluorescencia con resolución vertical de 1 m, además de muestras de agua en hasta 24 profundidades distintas para el posterior análisis de salinidad, oxígeno, nutrientes inorgánicos, materia orgánica disuelta y particulada, y respiración. Las estaciones fueron distribuidas en un transecto exterior y una malla interior como sigue: 22 estaciones en el transecto exterior que engloba la región frontal (con 14 estaciones hasta el fondo oceánico y 8 estaciones hasta 2000 m de profundidad) y otras 44 estaciones en la malla interior que muestrea la propia región frontal (16 estaciones hasta 2000 m y 28 estaciones hasta 400-500 m). Durante toda la campaña se determinaron también las velocidades del agua mediante dos perfiladores acústicos (*Acoustic Doppler Current Profiler*, ADCP), uno midiendo en continuo hasta unos 600 m de profundidad (Ship-ADCP) y el otro en las estaciones hidrográficas (Lowered-ADCP). Además, se midió en continuo la temperatura y salinidad superficial del agua, junto con las variables meteorológicas en superficie.

Como parte de las actividades de la campaña se lanzaron un total de 8 derivadores, con 6 unidades dragadas a 100 m (3 de ellas con sensores de conductividad y temperatura a 100 m) y 2 unidades dragadas a 200 m. También se lanzaron un total de 9 perfiladores, 7 de los cuales pertenecientes a Mercator-Coriolis (MC) como parte del programa Argo y otros 2 del Instituto de Ciencias del Mar (ICM). Los perfiladores MC derivaron a 200 m (2 unidades con ciclos de 5 días), 400 m (3 unidades con ciclos de 10 días) y 1000 m (2 unidades con ciclos de 10 días). Los perfiladores ICM fueron lanzados en la región frontal y realizaron ciclos continuos hasta una profundidad de unos 1000 m durante cerca de una semana, tras lo cual fueron recuperados. En total durante la campaña oceanográfica esto representó unos 50 perfiles adicionales, y otros 60 más para los meses de marzo-abril de 2015.

En este trabajo se caracteriza la distribución espacial de las diversas propiedades medidas durante la campaña TIC-MOC en la CBM, a escalas regional y mesoescalar, además de las estructuras termohalinas en la propia región frontal. Se muestran los campos de temperatura, salinidad y velocidad en el transecto exterior, que ilustran la penetración de aguas cálidas y saladas por el note y frías y relativamente frescas por el sur (fuertemente moduladas por un remolino anticiclónico) para luego escapar mayoritariamente por el este. También se caracterizan las distintas propiedades en la región frontal, donde se aprecian intrusiones laterales intercaladas (*interleaving*), con una serie de inversiones consecutivas de temperatura y de salinidad en la vertical.

AGRADECIMIENTOS

Estamos muy agradecidos a la tripulación del BIO Hespérides, así como al personal técnico de apoyo durante la campaña. Este trabajo ha sido posible gracias a la financiación del Ministerio de Economía y Competitividad del gobierno de España, a través de los proyectos TIC-MOC (CTM2011-28867) y VA-DE-RETRO (CTM2014-56987-P).

REFERENCIAS

1 - Combes V & Matano RP, 2014. A two-way nested simulation of the oceanic circulation in the Southwestern Atlantic. *J. Geophys. Res. Oceans*, 119, 731-756.
2 - Mémery L et al., 2000. The water masses along the western boundary of the south and equatorial Atlantic. *Progr. Oceanogr.*, 47, 69–98.
3 - Jullion L et al., 2010. Circulation and Water Mass Modification in the Brazil–Malvinas Confluence. *J. Phys. Oceanogr.*, 40, 845-864.
4 - Emelianov MV et al., 1990. Some features of the Falkland (Malvinas) current according to sattelite and ship data. In: *Ocean research using satellite information*, IOAN RAS, 61-77 (en ruso)
5 - Barré N et al., 2006. Spatial and temporal scales of the Brazil–Malvinas Current confluence documented by simultaneous MODIS Aqua 1.1-km resolution SST and color images. *Adv. Space Res.*, 37, 770–786.
6 - Saraceno M et al., 2009. Long-term variation in the anticyclonic ocean circulation over the Zapiola Rise as observed by satellite altimetry: Evidence of possible collapses. *Deep-Sea Res.*, 56, 1077–1092.
7 - Goni GJ et al., 2011. Observed low frequency variability of the Brazil Current front. *J. Geophys. Res.*, 116, C10037.

Efecto del aumento del nivel del mar y del oleaje en la línea de costa: aplicación a la playa de Cala Millor (Mediterráneo Occidental)

Alejandra R. Enríquez[1], Marta Marcos[1], Damià Gomis[12], Amaya Álvarez-Ellacuría[3], Alejandro Orfila[1]

[1] IMEDEA (UIB-CSIC)
[2] Departamento de Física, Universitat de les Illes Balears
[3] SOCIB, Sistema de Observación Costero de las Islas Baleares

RESUMEN

El presente trabajo evalúa los impactos en la línea de costa del aumento de nivel del mar y los cambios en el régimen de oleaje. Se propone una metodología que combina los modelos numéricos SWAN y SWASH para propagar el oleaje de aguas profundas hasta la costa. El estudio se aplica a la playa de Cala Millor (Mallorca, Mediterráneo Occidental). Primero el sistema de modelado se valida utilizando observaciones in-situ de un experimento de campo, que incluye sensores de oleaje en aguas someras y video monitorización de la línea de costa. Una vez validada, la metodología se aplica a escenarios climáticos (rcp45 y rcp85) para los cuales se han obtenido previamente las proyecciones de nivel medio del mar y de los cambios en el oleaje. Los resultados preliminares indican un retroceso de la línea de costa con una pérdida de superficie en la playa de aproximadamente un 60%.

INTRODUCCIÓN

El aumento de la concentración de gases de efecto invernadero en la atmósfera como consecuencia de la actividad humana tiene importantes repercusiones en el sistema climático del planeta. Entre las consecuencias del calentamiento global, el aumento paulatino del nivel del mar es una de las potencialmente más dañinas para las regiones costeras. Los océanos absorben más del 90% del calor extra almacenado en la atmósfera [1] con la consiguiente expansión térmica. A ello se suma el aumento de masa de agua por deshielo de las capas polares, glaciares y la menor retención de aguas continentales. Recientemente se ha demostrado que el aumento de nivel del mar global observado en el pasado siglo es el mayor durante al menos 3000 años [2] y que además esto se debe sin lugar a dudas a las emisiones de origen antrópico [3]. La sumersión de las zonas de cotas bajas, la mayor exposición a fenómenos extremos o la intrusión de sal en acuíferos son sólo algunos de los efectos de la subida del nivel del mar con implicaciones ecológicas pero también socio-económicas.

En este trabajo se evalúan los efectos combinados del aumento de nivel del mar proyectado para las próximas décadas y de los cambios en el régimen de oleaje en la playa de Cala Millor, en la isla de Mallorca (Mediterráneo Occidental). El presente trabajo se enmarca en las actividades del proyecto de investigación sobre "Impactos medioambientales y económicos del cambio climático en las costas y puertos españoles (CLIMPACT)" (CGL2014-54246-C2-1-R).

MATERIAL Y MÉTODOS

El estudio se centra en la playa de Cala Millor para la cual se dispone de batimetría y topografía de detalle. Se propone una metodología enfocada en el uso de dos modelos numéricos, SWAN y SWASH con el objetivo de resolver los procesos del oleaje desde aguas indefinidas hasta la disipación de la energía en la playa. El modelo espectral SWAN permite una rápida computación en dominios relativamente grandes manteniendo la exactitud en los parámetros estadísticos del oleaje. Por otro lado, SWASH resuelve la fase de la onda, permitiendo un estudio más exhaustivo del oleaje, sin embargo, se ve restringido a pequeñas áreas de estudio debido a su elevado coste computacional. El acoplamiento de estos dos modelos numéricos permite una alta resolución y exactitud de los resultados, con un menor coste computacional.

En un primer paso, el sistema de modelado se valida en base a datos experimentales obtenidos en la campaña de campo RISKBEACH realizada por SOCIB entre Marzo y Abril de 2014. Durante esta campaña se fondearon tres ADCP (Acoustic Doppler Currentmeter Profiler) costeros situados a 25, 17 y 12 m de profundidad, que proporcionan los parámetros del oleaje necesarios para la validación de los resultados del modelo SWAN. Al mismo tiempo, se dispone de líneas de costa obtenidas mediante fotografías horarias aéreas de la playa, procedentes del sistema de monitorización permanente de SOCIB. El oleaje en aguas profundas para inicializar el modelo se obtiene de la base

de datos de SIMAR- 44, un reanálisis del oleaje que cubre 58 años (desde 1958 hasta la actualidad) realizado por Puertos del Estado.

Una vez validada la metodología se aplica un régimen medio de oleaje sobre dos escenarios climáticos (rcp4.5 y rcp8.5). Las proyecciones del nivel del mar para 2100 son adquiridas de resultados del estado del arte de proyecciones regionales que tienen en cuenta la dinámica y el calentamiento oceánico y el deshielo de hielos terrestres, así como los patrones geográficos que inducen en el geoide éstos últimos. Por otra parte las proyecciones del oleaje se obtienen de modelos climáticos regionales forzados con vientos en superficie provenientes de simulaciones climáticas.

RESULTADOS Y DISCUSIÓN

En la fase de validación la propagación del oleaje en aguas profundas se evalúa gracias a una boya de oleaje direccional situada a una profundidad de 48 metros y perteneciente a Puertos del Estado. Las comparaciones muestran resultados muy satisfactorios en altura significante de ola (Hs), con un error cuadrático medio (RMS) de 0.3 m, así como 2 s en periodo (Tp) y 35º en la dirección de pico (θ_p). El oleaje en aguas someras se valida con los ADCP costeros. En la figura 1 se muestran las series temporales de los parámetros espectrales obtenidos con SWAN frente a los datos observados del ADCP de 12

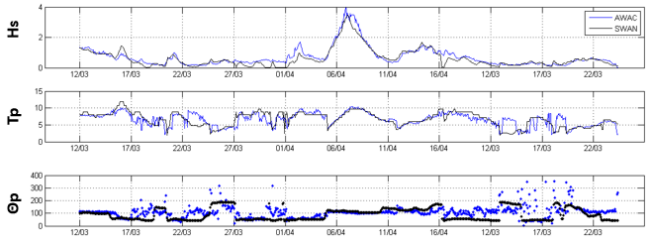

m de profundidad. La comparación entre ambos es satisfactoria.

Fig. 1. Oleaje propagado con SWAN (negro) y observado (azul) para Hs (arriba), Tp (centro) y θ_p (abajo).

En el último paso de la validación, las líneas de costa modeladas con SWASH son comparadas con las líneas de costa del sistema de video. En la figura 2 se muestra un ejemplo correspondiente al día 28 de Marzo y en la Tabla 1 las estadísticas (bias y RMS) correspondientes a 4 casos de estudio.

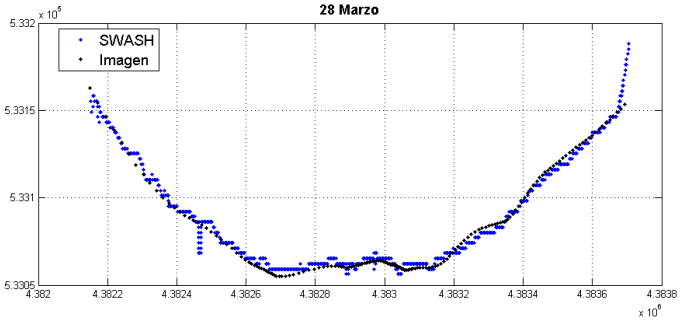

Fig. 2. Línea de costa observada (negro) y propagada mediante SWASH (azul) para un caso de estudio.

Tabla 1. Error cuadrático medio (RMS) y desviación (BIAS) entre líneas de costa observada y modelada. Unidades en m.

Día	RMS	BIAS
27 M	5,679	3,0754
28 M	2,7883	-0,677
1 A	6,6439	-3,2062
2 A	7,38	-8,4505

Una vez validada la metodología, se procede al estudio del cambio en la línea de costa producida por un aumento en el nivel del mar. Los resultados preliminares de retroceso en la costa teniendo en cuenta un aumento del nivel del mar de 98 cm, correspondiente al límite superior del escenario rcp8.5, promediado en el Mediterráneo, frente a la línea de costa actual, se sitúa en aproximadamente un 60%.

AGRADECIMIENTOS

El trabajo se realiza en el marco del proyecto CLIMPACT (CGL2014-54246-C2-1-R) financiado por el MINECO. A.R.E. agradece el contrato FPI (BES-2015-075934). Las observaciones usadas en este estudio han sido cedidas por SOCIB y por Puertos del Estado.

REFERENCIAS

1 – IPCC AR4 (2013)

2 – Kopp et al (2016). Temperature-driven global sea-level variability in the Common Era. *PNAS (113) no. 11. 1434 - 1441*

3 - Slangen, (2016). A. B. A. et al. *Nature Clim. Change* http://dx.doi.org/10.1038/nclimate2991

3 – Andrea Ruju et al (2014). Numerical analysis of run-up oscillations under disspitaive conditions *Coastal Engineering (86) 45 - 56*

4 – P. Veras Guimarães (2015). Numerical simulation of extreme wave runup during storm events in Tramandí Beach, Rio Grande do Sul, Brazil. *Coastal Engineering (95) 171 - 180*

Characterization of the resuspension events in a micro-tidal and shallow bay (Alfacs Bay, NW Mediterranean Sea)

Manuel Espino[1], Manel Grifoll[1], Laura Solà[1], Pablo Cerralbo[1]

[1] Laboratori d'Enginyeria Marítima (LIM). Universitat Politècnica de Catalunya (UPC)

ABSTRACT

Suspended matter near the bed have been recorded through Optical Backscatter Sensors (OBS), jointly with water current and sea-level measurements, in Alfacs Bay (NW Mediterranean Sea). The field campaign covered 2 months during summer 2013, and additional CTD profiles were measured. Alfacs bay (16 km length and 4 km width) is characterized by a micro-tidal environment, relative shallow depth (max. 6.5 m) and freshwater discharges from the drainage channels of the surrounding rice fields. Water currents measurements revealed a relevant influence of the wind forcing and Seiche events at high-frequency hydrodynamics.
OBS voltage gain show an evident relation with energetic hydrodynamic events, which included strong wind (high near-bottom water velocity) and seiche episodes. Two episodes were selected to show the re-suspension mechanisms: E1 and E2. E2 represents a resuspension event due to a ~1 hours Seiche episode consistent with the anti-node position near the geometrical center of the bay, and node position at bay mouth. Spectral analysis applied to OBS showed a clear energetic peak at daily frequency for E1. The periodic traffic vessel seems the mechanism responsible of the resuspension of fine bed sediment for E1. Still most of the OBS signal have been well characterized with physical conditions, some peaks remains unexplained. Preliminar results in wave-current numerical modelling are used to obtain wave and current bottom stresses.

INTRODUCTION

A good comprehension of sediment dynamics in coastal ecosystems is a key topic for coastal administration and management because the presence of suspended sediment in marine waters influences coastal ecosystems and pollution dynamics. As example, suspended sediment may prevent sunlight penetration into the water affecting submerged vegetation and primary production. Moreover, sediments from the continent tend to carry organic and inorganic pollutants into the marine habitat. All these processes are more critic in coastal embayments and harbors where the residence times are much higher.

Different hydrodynamic processes influence the sediment resuspension. In that sense, waves and currents are usually the predominant driving mechanism. Waves are directly related to the wind stress and fetch, whilst water currents could be affected mainly by winds and tides. However, some studies revealed the importance of more local resuspension mechanisms as seiches [1, 2], especially where tides are not noteworthy. Also anthropogenic activities such as fishing trawling, ship propellers and waves generated by vessels may bring additional energy at the water system influencing the resuspension, transport and final deposition of suspended matter in shallow waters [3].

The objective of this study is to identify and describe the main resuspension forcing mechanisms in a shallow micro-tidal semi-enclosed bay in the Mediterranean Sea through the analysis of observational data and modelling tools.

STUDY SITE AND FIELD CAMPAIGNS

Alfacs bay (16 km length and 4 km width) is characterized by a micro-tidal environment, relative shallow depth (max. 6.5 m) and freshwater discharges from the drainage channels of the surrounding rice fields. Suspended matter near the bed have been recorded through Optical Backscatter Sensors (OBS), jointly with water current and sea-level measurements through Acoustic Doppler Current Profiler (ADCP) during 2 months in summer 2013. The numerical model ROMS [4] is utilized to investigate the role of bottom friction induced by waves and currents on the Alfacs Bay resuspension.

RESULTS

Water currents measurements revealed a relevant influence of the wind forcing [5] and Seiche events [6] at high-frequency hydrodynamics.

OBS voltage gain (Figure 1, (top)) show an evident relation with energetic hydrodynamic events, which included strong wind (high near-bottom water velocity) and seiche episodes. Two episodes were selected to show the re-suspension mechanisms: E1 and E2. E2 represents a resuspension event due to a ~1 hours Seiche episode

consistent with the anti-node position near the geometrical center of the bay and node position at bay mouth. Spectral analysis applied to OBS (Figure 1 (bottom)) showed a clear energetic peak at daily frequency for E1. The periodic traffic vessel seems the mechanism responsible of the resuspension of fine bed sediment for E1.

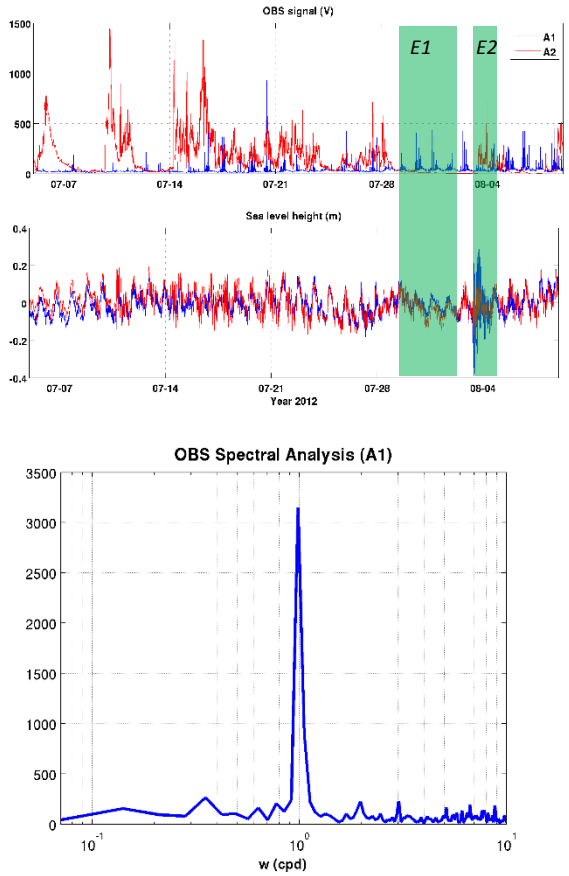

Figure 1. (Top) Time-series for the OBS and sea level height. Green boxes showed the episodes (E1 and E2) selected for the detailed analysis. (Bottom) Spectral analysis for the OBS signal moored at bay mouth.

Still most of the OBS signal have been well characterized with physical conditions, some peaks remains unexplained. Preliminary results in wave-current numerical modelling are used to obtain wave and current bottom stresses (Figure 2) and. maximum current-induced bottom stresses are found in bay mouth.

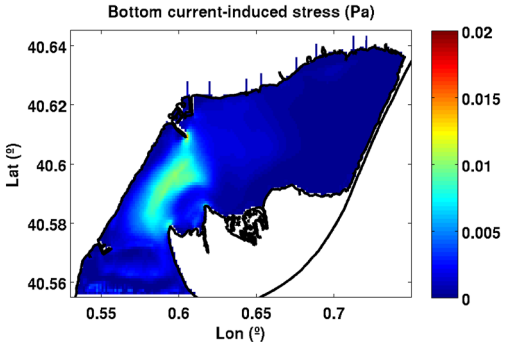

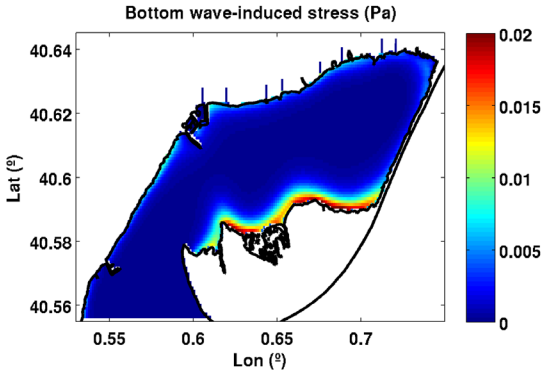

Figure 2. Typical bottom current-induced (top) and wave-induced (bottom) bottom stresses for the summer period. Maximum bottom wave-induced stresses are found in the shoals near the coastline. Maximum current-induced bottom stresses are found in bay mouth.

ACKNOWLEDGMENTS

The campaigns were carried out thanks to the MESTRAL (CTM2011-30489-C02-01). The authors also acknowledge the economical funding and support received from the MINECO and FEDER who founded the Plan-Wave (CTM2013-45141-R) and Rises-AM (contract GA603396, founded by European Community's Seventh Framework programme) projects. We also want to thank to Secretaria d'Universitats i Recerca del Dpt. d'Economia i Coneixement de la Generalitat de Catalunya (Ref 2014SGR1253) who support our research group.

REFERENCES

[1] - Pritchard, D., Hogg, A.J., 2003. Suspended sediment transport under seiches in circular and elliptical basins. Coastal Engineering 49 (1–2), 43–70

[2] - Jordi, a., Basterretxea, G., Casas, B., Anglès, S., Garcés, E., 2008. Seiche-forced resuspension events in a Mediterranean harbour. Cont. Shelf Res. 28, 505–515.

[3] - Garel, E., L. López, M. Collins. Sediment resuspension events induced by the wake wash of deep-draft vessels
Geo-Marine Letters (2008) 28:205-211.

[4] - Haidvogel, D.B. et al., 2008. Ocean forecasting in terrain-following coordinates: Formulation and skill assessment of the Regional Ocean Modeling System. J. Comput. Phys. 227, 3595–3624.

[5] - Cerralbo, P., Grifoll, M., Espino, M., 2015. Hydrodynamic response in a microtidal and shallow bay under energetic wind and seiche episodes. J. Mar. Syst. 149, 1–13.

[6] - Cerralbo, P., Grifoll, M., Valle-Levinson, A., Espino, M., 2014. Tidal transformation and resonance in a short, microtidal Mediterranean estuary (Alfacs Bay in Ebre delta). Estuar. Coast. Shelf Sci. 145, 57–68.

Impacts of Initialization Errors on the AMOC on a Decadal Timescale

Victor Estella-Perez[1,2], Florian Sévellec[2] & Bablu Sinha[2]

[1] University of Southampton, National Oceanography Centre (Southampton, UK)
[2] National Oceanography Centre, Southampton (Southampton, UK)

ABSTRACT

The Atlantic Meridional Overturning Circulation (AMOC) is one of the principal regulators of the climate in the North Atlantic on decadal to multi-decadal time scales. This work aims to look at the impacts of initial errors on the AMOC variability and predictability on this time scale, particularly on the implication of erroneous initialization of the surface salinity field. We performed a set of experiments perturbing the surface salinity field in the North Atlantic (focused in the East Coast of Greenland), and study the response with respect to the intensity of the perturbation (strength). Testing different amplitudes, or extensions of the perturbation, we obtained a similar qualitative AMOC response. An induced Rossby-like feature propagates the anomaly, which remains trapped in the coast of Newfoundland and dissipates. They induce an oscillatory response of the AMOC that varies up to 0.14 Sv per psu of the perturbation distribution's maxima introduced. Current work is focused on investigating the physical mechanisms behind this propagation and on understanding its relation with possible precursors of AMOC variability caused by observed Great Salinity Anomalies [1].

REFERENCES

1 - Belkin, I. M. Propagation of the "Great Salinity Anomaly" of the 1990s around the northern North Atlantic, *Geophysical Research Letters,* 31, 8 (2004), 4–7.

Enhanced Surface Diapycnal Mixing in a Mode Water Anticyclonic Eddy

Sheila Estrada-Allis[1], Borja Aguiar-González[2], Ángel Rodríguez-Santana[1], Pablo Sangrà[1], Antonio Martínez-Marrero[1] & Carmen Gordo[1]

[1] Departamento de Física, Universidad de Las Palmas de Gran Canaria (ULPGC). Canary Islands, Spain.
[2] NIOZ Royal Netherlands Institute for Sea Research, Department of Ocean Systems Sciences and Utrecht University, P.O. Box 59, 1790 AB Den Burg, Texel, the Netherlands

ABSTRACT

A subtropical mode water eddy located southwest of the Canary Islands was surveyed with an interdisciplinary sampling on September 2014. The surface diapycnal mixing is investigated along a meridional transect crossing the eddy intensively sampled with CTD, SADCP and with a microstructure turbulence profiler.
We observe an enhancement of diapycnal mixing at the eddy periphery consistent with an increase of the turbulent kinetic energy dissipation rates. Our analysis reveals that it is driven by three main sources of turbulent kinetic energy, namely nocturnal convection, vertical current shear at the base of the mixed layer and mechanical stirring by wind stress. Due to the characteristic dome shape of the isopycnals at the uppers layers the mixing layer depth, where active mixing occurs, was always deeper than the mixed layer. This results in on the enhancement of diapycnal entrainment and thus diapycnal mixing all along the mode water eddy and in particular at its periphery. The underlying physic mechanism lies in that a positive entrainment zone, creates optimal conditions to enhance turbulent mixing in the pycnocline. Thus, the strong stratification below the mixed layer can be more easily overcome in these regions. This results in erosion of the mixed layer and a subsequent tracer redistribution in upper layers.
It is then hypothesized that the enhancement of diapycnal mixing and entrainment at the eddy periphery, with the corresponding increase of vertical fluxes of nutrient may contribute to the enhancement of primary production in these westward-propagating eddies within the oligotrophic region of the subtropical Northeast Atlantic.

INTRODUCTION

The upper ocean layer is strongly dependent on the air-sea interaction, and the resulting convection and wind-stirring processes at the sea surface [1]. Additionally, it can be sensitive to other processes occurring between the seasonal pycnocline and the stably stratified ocean layer below it, such as local increases of vertical current shear at the base of the mixed layer [2]. Nevertheless, controlling factors remain unknown since upper ocean mixing processes, as the entrainment velocity (w_e), are small-scale related quantities that act as transient turbulent processes.
Entrainment-driven sources depend on the interface (or entrainment zone; Δ_h). This layer is often determined by the difference between the mixed (h_ρ) and the active mixing layer (h_ε), where active mixing occurs. $\Delta_h > 0$ is an indicator for the occurrence of entrainment according to recent observational findings [2]. This is because w_e can only be induced in regions of active mixing, where the turbulence within the pycnocline is strong enough to overcome the effects of stratification.
The upper mixing processes sketched above may be particularly active in mesoscale eddies and their associated submesoscale structures. There is still a lack of observations about the associated enhancement of diapycnal mixing within mesoscale structures with consistent sampling of the microstructure shear. Here a microstructure turbulent profiler was deployed with considerable effort in order to achieve a near-synoptic survey inside a mesoscale eddy.
The goal of this study is to evaluate diapycnal mixing within a typical mode water anticyclonic eddy of the Canary Eddy Corridor (CEC) [3] in the subtropical Northeast Atlantic.

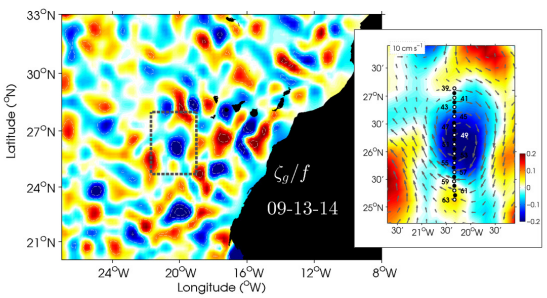

Fig. 1. Map of normalized vorticity (ζ_g/f) and velocity field of the studied eddy as obtained from merged altimeter data of Sea Level Anomalies (SLA), provided by AVISO (http://www.aviso.altimetry.fr/en/home.html). The small box in the left panel delimits the region where the anticyclonic

eddy is found. Hydrographic/ADCP (black dots) and microstructure (white dots) stations are superimposed.
The mesoscale structure was surveyed during the PUMP cruise in September 2014. To our knowledge, this is the first case of high-resolution sampling of the turbulent kinetic energy (TKE) rates (ε_o) with a microstructure profiler within an eddy of the Northeast Atlantic.

DATA AND METHODOLOGY

The PUMP eddy was generated in the lee of the Tenerife island and at the time of the survey it was four months old (Fig. 1).
High resolution turbulent mixing was measured through a microstructure profiler TurboMAP, CTD, and SADCP stations (25 and 24 respectively) were 5 nautical miles apart, whereas TurboMAP stations (13) were 10 nautical miles apart. The transect crossing the eddy (Fig. 1), named Le Tourmalet, was sampled over about 3.5 days.
To assess the relationship between atmospheric forcing and upper ocean turbulence, meteorological data from the aboard meteorological station were used to compute the surface wind stress, net surface buoyancy flux and net surface heat flux.

RESULTS AND DISCUSSION

The eddy is noticeable by a local minimum of the normalized vorticity and a corresponding anticyclonic closed circulation (Fig. 1). In the upper layers the isopycnals have a dome shape, whereas in the deeper layers they have a bowl shape. This is a typical signature of a mode water eddy.

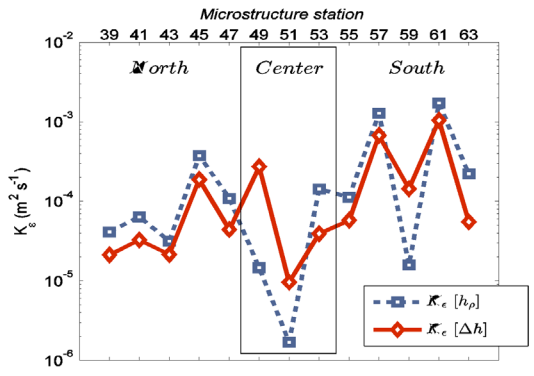

Fig. 2. Depth averaged diapycnal diffusivity coefficients, K_ε (m^2 s^{-1}), in logarithmic scale, where K_ε is integrated at h_ρ (blue), and within Δ_h (red). The dashed box indicates the stations located within the eddy center.

The observed increase of the wind stress at the last stations coincides with an enhancement of ε_o. There is recent interest in the determination of h_ε since may have important implications in the critical depth for phytoplanktonic blooms [4]. When h_ε is deeper than h_ρ, Δ_h becomes positive and turbulent mixing may be large enough to overcome the restoring effects of the stratification in the pycnocline [2].

The results indicate that $\Delta_h > 0$ at each microstructure station, even under weak wind conditions. It also appears to be independent of day/night-time conditions. A plausible explanation may be related to the shallow depth of the mixed layer as a result of a low momentum transfer by relatively low Trade winds and also weak buoyancy flux. Thus, intermittent surface mixing events such as, for example, an instantaneous increase in the wind speed, can easily be extended below the shallow mixed layer leading to positive Δ_h and hence favors turbulent diapycnal transport. The shallowest mixed layers at the eddy periphery are also due to the doming of the isopycnals of a mode water eddy, reducing the depth of the stratified layer so that TKE sources can penetrate up to the pycnocline and erode it more effectively. As a result, an increase of w_e is observed at the eddy periphery suggesting that concentrations of nutrients may be enhanced at these locations, by permitting their exchange between the pycnocline and the euphotic layer.
At surface eddy layers, diapycnal diffusivity (K_ε) decreases at the eddy core (station 51), while it is enhanced at the northern and southern flanks of the eddy, with a maximum in station 61.
Below this first layer, within the entrainment zone, K_ε increases with respect to surface layers of the near core eddy station 49 and the core station 51. This suggests that turbulent diapycnal mixing is linked with the dynamics of mesoscale structures that interact with the implicated TKE sources. The subsequent increase of nutrient distribution due these mixing process may act to enhance the primary production at the periphery of long lived westward propagating anticyclonic eddies in the oligotrophic area of the North Atlantic.

ACKNOWLEDGMENTS

This study was made possible by the project PUMP (PUMP:CTM2012-33355) of Universidad de Las Palmas de Gran Canaria, co-founded by European Union (FEDER) and Ministerio de Economía y Competitividad of Spain.

REFERENCES

1 – Nagai T, Yamazaki H, Nagashima H & Kantha LH, 2005. Field and numerical study of entrainment laws for surface mixed layer. *Deep Sea Res. II*, 52(9): 1109-1132.
2 – Estrada-Allis S, Rodríguez-Santana A, Garabato ACN, García-Weil L, Arcos-Pulido M & Emelianov M, *(Under Review*), Diapycnal entrainment in an Eastern-Boundary upwelling filament.
3 – Sangrà P, Pascual A, Rodríguez-Santana A, Machín F, Mason E, McWilliams JC, Pelegrí JL, Dong C, Rubio A, Arístegui A, Marrero-Díaz A, Hernández-Guerra A, Martínez-Marrero A & Auladell M, 2009. The Canary Eddy Corridor: A major pathway for long-lived eddies in the subtropical North Atlantic. *Deep-Sea Res. I*, 56:2100-2114.
4- Sverdrup HU, 1953. On conditions for the vernal blooming of phytoplankton. *J. Cons. Int. Explor. Mer*, 18(3):287-295.

Mixing and turbulence sources during the summer upwelling season in the Ría de Vigo (NW Spain)

Bieito Fernández Castro[1], Miguel Gilcoto[2], Marina Villamaña[1], Alberto C. Naveira Garabato[3], Paloma Chouciño[1], Rocío Graña[2], Beatriz Mouriño Carballido[1]

[1] Departamento de Ecoloxía e Bioloxía Animal, Universidade de Vigo, 36310, Vigo Spain
[2] Instituto de Investigacións Mariñas, Consejo Superior de Investigaciones Científicas, Eduardo Cabello 6, 36208 Vigo, Spain
[3] National Oceanography Centre, University of Southampton, Southampton, UK

ABSTRACT

High-frequency observations of microstructure turbulence were carried out in the Ría de Vigo in August 2013 during two 25-hours cycles corresponding to spring (CHAOS 1) and neap (CHAOS 2) tides. This presentation describes the variability observed in turbulence levels at different time scales, and investigates the mechanisms driving this variability. Our results revealed enhanced levels of turbulent kinetic energy dissipation and turbulent mixing during CHAOS 1. Within cruise variability was relevant during both periods. In particular, strong bursts of turbulence occurred during the ebb, associated with enhanced vertical shear of tidal currents. The shear enhancement, which was more intense during spring tides, could be related to the interaction between tidal and upwelling driven circulation. Furthermore, the analysis of the potential energy involved in isopycnal displacements supports that internal wave activity was more intense during CHAOS 1, which could contribute to the enhanced levels of mixing observed during this period.

INTRODUCTION

The Ría de Vigo (NW Spain) is a highly dynamic partially mixed estuarine-like coastal environment where the variability of the relevant physical processes (upwelling-downwelling, tides, etc.) occurs at a wide range of temporal scales (i. e. seasonal, fortnightly, weekly, daily or shorter). During spring-summer months (April to September) the NW Iberia is characterized by intense and intermittent upwelling pulses [1]. Although the circulation of the Ría de Vigo is relatively well characterized [2], a description of the different scales involved in the variability of turbulence field is lacking. For both physicists and biologists, ocean turbulence is a relevant mechanism by which energy is dissipated and solutes, including dissolved nutrients, are transported. With the aim of characterizing different scales of variability in turbulence and their driving mechanisms, high-frequency observations of microstructure turbulence were carried out in the Ría de Vigo (NW Spain) in August 2013.

MATERIAL AND METHODS

Two cruises were conducted on board the R/V Mytilus in the outer part of the Ría de Vigo (42.174ºN, 8.890ºW) during spring (20-21 August 2013, CHAOS 1) and neap (27-28 August 2013, CHAOS 2) tides. During each cruise, by using a microstructure turbulence profiler (MSS), an intensive sampling (yo-yo) of measurements of turbulent kinetic energy (TKE) dissipation rates (ε) was carried out covering a complete diurnal tidal cycle (ca. 25 hours). Temperature and salinity values were measured by the CTD sensors incorporated into the MSS profiler, and used to calculate seawater potential density (σ_T) and buoyancy frequency (N^2). Diapycnal diffusivity (K_ρ) was calculated as $K_\rho = 0.2\varepsilon N^{-2}$.

Currents were measured with a vessel-mounted Acoustic Doppler Profiler (vmADCP). Vertical shear (S) was calculated as the vertical derivative of horizontal velocities. Gradient Richardson number (Ri) was calculated as $Ri = N^2/S^2$.

Internal wave potential energy was calculated from the vertical displacements of the isopycnals (η) as $E^{IW} = 0.5N^2<\eta^2>$, where $\eta = (\sigma_T - <\sigma_T>)/\partial_z<\sigma_T>$ [3] and $<\sigma_T>$ is the averaged density profile during the tidal cycle.

RESULTS AND DISCUSSION

Turbulence microstructure measurements indicated that TKE dissipation rates ($<\varepsilon>$) and diapycnal diffusivity ($<K_\rho>$), averaged in the main thermocline (12-32 m) away from boundary influence, were more than 2-fold higher in spring compared to neap tides (Table 1). Both variables showed significant variability along the semi-diurnal tidal cycle, and this variability was more evident during spring compared to neap tides (see Fig. 1 and Table 1). $<\varepsilon>$ varied up to two orders of magnitude during the sampling period in spring tides. Minimum values of ca. 10^{-8} W/Kg occurred

during high tides and then <ε> sharply increased during the ebb reaching ca. 10^{-6} W Kg^{-1} 1-2 hours before low tides (Fig. 1). As the result of this, <ε> and $<K_\rho>$ averaged in a 6-hour window around the low tide, were more than 2-fold higher compared to high tides (Table 1). Although weaker, this pattern was also observed during neap tides.

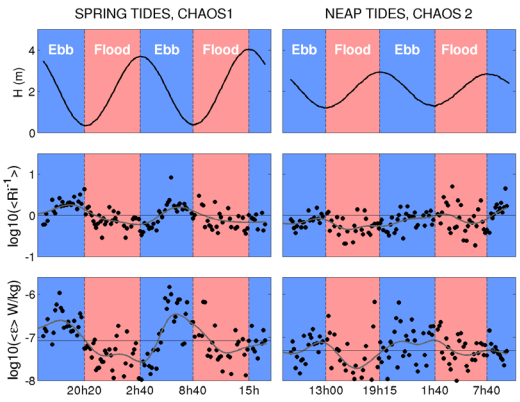

Fig. 1. Time evolution of tidal height (H), and averaged (12 – 32 m) inverse Richardson number ($<Ri^{-1}>$) and TKE dissipation rates (ε) for the 25-hour sampling cycles carried out during spring (CHAOS 1) and neap (CHAOS 2) tides. Grey lines are running averages.

Table 1. Averaged values (±se) of TKE dissipation rates (ε), turbulent diapycnal diffusivity (K_ρ), gradient Richardson number (*Ri*) and internal wave energy (E^{IW}) computed during spring (CHAOS 1) and neap (CHAOS 2) tides. Averages were calculated for the whole tidal cycle (average), and for 6-hous periods centered at low and high tides.

	<ε> 10^{-7}(W/kg)	$<K_\rho>$ 10^{-4} (m^2/s)	<Ri>	$\int E_{IW}$ (J/m^2)
Spring tides (CHAOS 1)				
Average	1.76±0.23	4.09±0.74	5.2±1.0	59
Low	2.26±0.34	6.0±1.3	3.18±0.63	
High	1.22±0.26	2.05±0.42	7.4±2.1	
Neap tides (CHAOS 2)				
Average	0.68±0.07	1.70±0.20	11.2±2.3	44
Low	0.71±0.90	2.03±0.39	8.6±1.7	
High	0.67±0.09	1.55±0.22	12.3±3.2	

The observed enhanced values of TKE dissipation during the ebb were associated with reduced values of *Ri*. During spring tides *Ri* ranged between supercritical and subcritical values along the tidal cycle (Fig. 1). This decrease in *Ri* was caused by a significant increase of shear during the ebb, when the tidal current showed a sheared pattern, with circulation towards the ocean predominantly occurring in the upper 20 m (data not shown). We hypothesize that this pattern was driven by the interaction with positive upwelling circulation, which was active during the sampling period. Enhanced internal wave activity during the more energetic spring tide period could contribute to explain the observed differences, as internal wave energy was ca. 35% higher during this period (Table 1)

It has been proposed that tidal [4], and wind induced positive circulation [5] of surface waters towards the open ocean, can result in a net increase in stratification in estuaries, due to the straining caused along the channel density gradient. Our observations suggest that a different mechanism could be at work during the upwelling season, when freshwater input into the Ría is relatively weak. Sheared ebb tidal current, likely caused by the interaction of the tidal wave with the upwelling circulation, results in a net increase of bulk shear and TKE dissipation, which peaks before the low tide. This mechanism could have important ecological implications in this region. Complementary observations carried out during the CHAOS cruises showed that enhanced nutrient diffusive supply during spring tides could contribute to the continuous dominance of large-sized phytoplankton during the upwelling favorable season (Villamaña et al., this issue) [6].

ACKNOWNLEDGEMENTS

Funding for this study was provided by the Spanish Ministry of Science and Innovation (MINECO) under the research project CTM2012-30680 to B. M.-C.. B. F.-C. thanks the Spanish Government for a FPU grant (AP2010/5594), and a travel grant (EST14/00366) to the National Oceanography Centre, Southampton (UK).

REFERENCES

[1] Fraga, F. (1981). Upwelling off the Galician Coast, Northwest Spain, *Coast. Estuarines Sci.*, vol. 1, no. 1974.

[2] Barton, D., Largier, J.L, Torres, R., Sheridan, M., Trasviña, A., Souza, A., Pazos, Y., Valle-Levinson, A. (2015) Coastal upwelling and downwelling forcing of circulation in a semi-enclosed bay: Ria de Vigo. *Progress in Oceanography*, 134, 173-189.

[3] Waterman, S., Naveira Garabato, A. C., & Polzin, K. L. (2013). Internal Waves and Turbulence in the Antarctic Circumpolar Current. *Journal of Physical Oceanography*, 43(2), 259–282.

[4] Simpson, J. H., Brown, J., Matthews, J., & Allen, G. (1990). Tidal Straining, Density Currents, and Stirring in the Control of Estuarine Stratification. *Estuaries*, 13(2), 125.

[5] Scully, M. E., Friedrichs, C., & Brubaker, J. (2005). Control of Estuarine Stratification and Mixing by Wind-Induced Straining of the Estuarine Density Field. *Estuaries*, 28(3), 321–326.

[6] Villamaña, M., Mouriño-Carballido, B., Marañón E., Cermeño P., Chouciño P., da Silva J.C.B., Díaz P.A., Fernández-Castro B., Gil Coto M., Graña R., Latasa M. Magalhaes J., Otero-Ferrer J.L., Reguera B., Scharek R.. Internal wave activity and its role on mixing, nutrient supply and phytoplankton community structure during spring and neap tides in the Ría de Vigo (NW Iberian Peninsula), *this issue*.

Changes in Arctic freshwater export: a new proxy from 60 years of hydrographic surveys in the Labrador Sea

Cristian Florindo López[1], N. Penny Holliday[2], Sheldon Bacon[2], Yevgeny Aksenov[2] & Eugene Colbourne[3]

[1]OCEAN AND EARTH SCIENCES, UNIVERSITY OF SOUTHAMPTON, UK
[2]NATIONAL OCEANOGRAPHY CENTRE, UNIVERSITY OF SOUTHAMPTON, UK
[3]NORTHWEST ATLANTIC FISHERIES SECTION, ST. JOHNS, CANADA

ABSTRACT

The Arctic Ocean is the most rapidly changing environment in the globe. One of the observed changes is a significant increase in the freshwater storage at the region. It is believed that a large and rapid export of this freshwater into the North Atlantic could potentially affect high-latitude dense water formation, the overturning circulation and climate. However, Arctic freshwater fluxes to the Labrador Sea are poorly known and observational time series are not available beyond the last decade. In this study we use the high-resolution (1/12 degree) NEMO model to provide new insight in the Labrador Shelf dynamics. We demonstrate that the inshore jet on the Labrador Shelf is a continuation of the Hudson Outflow, dynamically and geographically independent from the Labrador Current. We refer to it as the Labrador Coastal Current. It yields the Hudson water inshore and allows us to isolate the Arctic water on the Labrador shelf. We use a 60 year long series of hydrographic observations at the Labrador Shelf to identify the Arctic export signal and define a new multi-decadal proxy of Arctic freshwater export west of Greenland. This allows us to provide insight into the processes linking the Arctic freshwater budget and North Atlantic salinity, and how they relate to the export variability. Here we show a previously unseen time series of Arctic freshwater transport on the Labrador Shelf and how it serves as a proxy for Arctic freshwater export through Davis Strait. We are able to identify decades of enhanced and decreased transport and to relate them to Arctic freshwater storage variability and North Atlantic salinity anomalies.

Técnicas de Sistemas Dinámicos y de Sensores Remotos para la Gestión en Tiempo Real de Derrames de Petróleo en el Mar

V. J. García-Garrido[1], A. Ramos[2], A. M. Mancho[1], J. Coca[2] & S. Wiggins[3]

[1] Instituto de Ciencias Matemáticas, CSIC-UAM-UC3M-UCM, C/ Nicolás Cabrera 15, Campus Cantoblanco UAM, 28049, Madrid, España.
[2] División de Robótica y Oceanografía Computacional, IUSIANI, Universidad de Las Palmas de Gran Canaria, Las Palmas de Gran Canaria, España.
[3] School of Mathematics, University of Bristol, Bristol BS8 1TW, Reino Unido.

RESUMEN

En esta comunicación describiremos como un enfoque interdisciplinar que combina técnicas de la Teoría de Sistemas Dinámicos y de Sensores Remotos por satélite puede contribuir de manera relevante a la gestión efectiva de vertidos de petróleo en el mar y en el desarrollo futuro de planes de contingencia para afrontarlos. Este trabajo se centra en el análisis del hundimiento del barco pesquero Oleg Naydenov, que tuvo lugar en abril de 2015 cerca de la isla de Gran Canaria.

Desde la perspectiva de los Sistemas Dinámicos, hemos analizado el evento utilizando una técnica conocida como Descriptores Lagrangianos [1,2], que tiene la capacidad de detectar las barreras dinámicas que rigen los procesos de transporte y mezcla en el océano. Esta metodología permite evaluar casi en tiempo real el riesgo potencial del punto de hundimiento y la posible llegada del petróleo a la costa. Por otro lado, hemos aplicado herramientas de advección de contornos [3,4] para estudiar la evolución de las manchas de fuel. Los resultados obtenidos reproducen de manera notable los avistamientos de fuel durante el evento.

En este contexto, los métodos de Sensores Remotos contribuyen permitiendo la detección de manchas de fuel a partir de imágenes por satélite, gracias al empleo de los espectros de reflectancia [5]. Esta técnica permite analizar la presencia de fuel en distintas regiones del mar, guiando las labores de monitorización y limpieza de los operativos de tierra/aire durante el evento.

Indudablemente, toda la información obtenida mediante la aplicación conjunta de estas dos disciplinas puede ser de gran utilidad para ayudar a los Servicios de Emergencia en la gestión efectiva de futuras catástrofes.

AGRADECIMIENTOS

Nos gustaría dar las gracias al Comité Regional de Emergencias: Oleg Naydenov 16 Abril – 30 Mayo 2015 y a la Dirección General de Seguridad Marítima (Ministerio de Fomento) por proporcionar los informes técnicos diarios del evento. También a la OceanColor Web por el acceso a los datos MODIS y al sistema COPERNICUS IBI por los datos de corrientes utilizados en este estudio.

La investigación de V. J. García-Garrido y A. M. Mancho está financiada por el proyecto MINECO MTM2014-56392-R y el proyecto Severo Ochoa SEV-2011-0087, la de A. Ramos y J. Coca por MINECO UNLP-13-3E-2664 (2013-2015). y la de S. Wiggins por la ONR No. N00014-01-1-0769.

REFERENCIAS

1 – Madrid JA & Mancho AM, 2009. Distinguished trajectories in time dependent vector fields. *Chaos,* 19.
2 – Mancho AM, Wiggins S, Curbelo J & Mendoza C, 2013. Lagrangian descriptors: A method for revealing phase space structures of general time dependent dynamical systems. *Commun. Nonlinear Sci.*, 18(12):3530-3557.
3 – Dritschel DG, 1989. Contour dynamics and contour surgery: Numerical algorithms for extended, high-resolution modelling of vortex dynamics in two-dimensional, inviscid, incompressible flows. *Comput. Phys. Rep.,* 10(3):77-146.
4 – Mancho AM, Small D, Wiggins S & Ide K, 2003. Computation of stable and unstable manifolds of hyperbolic trajectories in two-dimensional, aperiodically time-dependent vector fields. *Physica D,* 182(3):188-222.

5 – Bulgarelli B & Djavidnia S, 2012. On MODIS retrieval of oil spectra properties in the marine environment. *IEEE Geosci. Remote S.,* 9(3):398-402.

Aplicación de la teoría SQG para la obtención de corrientes de alta resolución en el Mar de Alborán

E. García-Ladona[1], J. Isern-Fontanet[1], J. Jiménez-Madrid[1] & J. Ballabrera-Poy[1]

[1] Institut de Ciències del Mar, ICM-CSIC, Passeig Marítim, 37-49, 08003 Barcelona.

RESUMEN

En la teoría quasigeostrófica de superficie (SGQ) el flujo oceánico puede obtenerse a partir de las perturbaciones del campo de densidad en la superficie. Esta aproximación de la dinámica oceánica abre la puerta para la obtención de un diagnóstico del campo de corrientes superficiales en primera aproximación, e incluso permite propagar la solución al océano interior y reconstruir el campo 3D de velocidades. Asumiendo la aproximación de que el campo de densidad depende en gran medida de la temperatura, y que ésta se observa hoy en día de forma regular mediante diversos satélites operacionales, podemos explotar la teoría SQG para obtener de forma operacional campos de velocidades diagnóstico. Además estos campos son de alta resolución (~1km para captores infrarojos) y en escalas diarias. En este trabajo se presentan resultados preliminares de la aplicación directa de esta técnica para la obtención del campo de velocidades en el caso del Mar de Alborán durante el experimento lagrangiano MEDGIB realizado en Septiembre del 2014. En dicho experimento se lanzaron 35 flotadores de superficie desde el Estrecho de Gibraltar para trazar la entrada de aguas Atlánticas.

El intercambio a través del Estrecho de Gibraltar: la conexión Mediterránea

Jesús García Lafuente[1] Cristina Naranjo[1], Simone Sammartino[1], José Carlos Sánchez-Garrido[1]

[1] Grupo de Oceanografía Física de la Universidad de Málaga (GOFIMA).

RESUMEN

El doble intercambio de aguas que se establece a través del Estrecho de Gibraltar es consecuencia de las pérdidas evaporativas o, más estrictamente, del balance negativo de flotabilidad (hacia la atmósfera) que experimenta el Mediterráneo. Alternativamente, las propiedades fundamentales de las aguas Mediterráneas quedan determinadas por la morfología del Estrecho. Ambos forman por lo tanto un sistema indivisible en el que cualquiera de las dos partes es sensible a las modificaciones que pueda experimentar la otra. Se ejemplifican procesos de ambos tipos, locales en el Estrecho de Gibraltar (básicamente de origen mareal) cuya influencia se extiende a buena parte de la cuenca Mediterránea, y también la respuesta de los flujos intercambiados a variaciones en la circulación de dicha cuenca, con énfasis en la más próxima al Estrecho: el Mar de Alborán.

1.- MARCO FUNDAMENTAL: EL INTERCAMBIO ESTACIONARIO

Empleando un modelo bicapa estacionario, en el que se tiene que verificar que el ritmo de formación de agua Mediterránea Q_M iguale al flujo saliente Q_2, y para la morfología del Estrecho (cuya anchura es inferior al radio interno de deformación por lo que la rotación terrestre no es un término dominante), puede mostrarse que la densidad de equilibrio del Mediterráneo debe exceder a la de las aguas entrantes en una cantidad $\Delta\rho$ dada por

$$\Delta\rho = \left(\frac{A_{MED}}{g\,a}\right)^{2/3} \left(B_0^{2/3}\right) \left(H_{2C}^{-5/3}\right) \qquad (1)$$

y el flujo saliente a través del Estrecho venir dado por

$$Q_2 = \left(\frac{a^2 A_{MED}}{g}\right)^{1/3} \left(B_0^{1/3}\right) \left(H_{2C}^{5/3}\right) \qquad (2)$$

Cada expresión tiene tres términos (paréntesis) diferenciados. Superficie del Mediterráneo (A_{MED}), gravedad g y un factor a que incluye parámetros de la sección transversal del Estrecho en el primero, que reúne aspectos geométricos del sistema. El segundo es el flujo de flotabilidad B_0, conductor de la circulación termohalina del Mediterráneo. El tercero es el espesor de la capa saliente en el umbral del Estrecho (H_{2C}), indeterminado salvo que el intercambio sea el máximo posible, lo que conlleva mínima diferencia de densidad $\Delta\rho$ entre cuencas. Esta situación corresponde a un mínimo de energía potencial del sistema en su conjunto y es el estado de equilibrio esperable. Para la geometría del Estrecho el intercambio máximo requiere un doble control hidráulico en secciones de mínima profundidad (umbral) y mínima anchura, en cuyo caso, H_{2C} sí está determinado [1]. Para valores realistas de todos los parámetros anteriores, $\Delta\rho \sim 0.2$ kg·m^{-3} y Q_2=1.1Sv, en el rango observado. Las estimaciones cambian algo si se retienen los otros términos ignorados en las ecuaciones de movimiento (rotación, fricción). Ambos reducen el intercambio calculado una pequeña fracción [2,3]

Frecuentemente se asume que las variaciones de densidad en Ec.(1) son debidas exclusivamente a las de salinidad (de hecho explican más del 80%) en cuyo caso el término de flotabilidad sólo debe incluir la evaporación y la Ec.(1) establecería proporcionalidad entre ΔS y $E^{2/3}$ [1]. Por otro lado es interesante notar que el exponente de B_0 (o E) en Ec.(1) es el doble que en Ec.(2), lo que indica que $\Delta\rho$ (o ΔS) es más sensible (el doble también) a cambios en B_0 (o E). Por ejemplo, los efectos del cambio climático en el Mediterráneo se percibirán antes en la densidad (salinidad) que en el flujo saliente.

2.- PROCESOS LOCALES CON REPERCUSIÓN EN LA CUENCA: LA INFLUENCIA DE LAS MAREAS

Para variaciones temporales lentas, el modelo estacionario es todavía aplicable [4,5], pero para fluctuaciones mareales ya no sirve, pues las aceleraciones locales son del mismo orden que los términos advectivos. No obstante, si los flujos mareales son pequeños comparados con los valores del intercambio estacionario (forzamiento débil), su efecto promediado en el largo término se cancela y su influencia se limita a distorsionar las variables instantáneas, que se verán modificadas respecto a la solución estacionaria. Pero si el forzamiento es grande (caso del Estrecho donde el flujo mareal llega a ser 5 veces mayor que el intercambio medio), entonces ocurren otros efectos de mayor alcance espacial. Algunos de ellos se enumeran a continuación.

Aumento del intercambio medio

Forzamientos mareales grandes bloquean e invierten transi-toriamente alguna de las capas y son capaces de generar "eddy-fluxes", que surgen de las correlaciones positivas entre corrientes mareales y oscilaciones de la interfaz. Los eddy-fluxes no promedian cero sino que

contribuyen al intercambio neto de largo término incrementándolo en un 8-10%. El fenómeno tiene fuerte dependencia espacial siendo más importante en el umbral principal del Estrecho, donde los eddy-fluxes representan más de un 40% del intercambio [6,8].

Mayor drenaje de aguas profundas

Las intensas corrientes de marea proporcionan un extra de energía que parece ser aprovechada por las aguas profundas para remontar el umbral del Estrecho y verter en el océano Atlántico. Simulaciones efectuadas con y sin forzamiento mareal indican que el drenaje de agua Mediterránea Profunda del Mediterráneo Occidental (WMDW) aumenta en un 30% cuando se incluyen mareas en la simulación [7]. Puede entenderse que es precisamente esta masa de agua la que se ve más favorecida por el incremento de intercambio que producen las mareas.

Mejor precondicionamiento del flujo entrante

La importante interacción topográfica de las corrientes de marea engrosa la capa interfacial al fomentar la mezcla entre las capas superior e inferior. Una consecuencia es el aumento de densidad del flujo entrante, más frío y salino que si no existiesen mareas según las simulaciones [7]. Esta pérdida de flotabilidad inducida por la marea tendría consecuencia en la formación de WMDW en el Golfo de León, que se vería favorecida frente a una situación de no mareas [7,8]. Algunos resultados preliminares indican hasta un incremento de entre el 20 y 30% en el volumen de agua formada debido a este efecto mareal [7]

Mayor fertilización en el Mar de Alborán

Otro efecto de las mareas es el bombeo de nutrientes desde la capa Mediterránea hacia la capa interfacial forzado por la intensa mezcla vinculada al flujo mareal. Parte de ellos son transportados hacia el interior del Mediterráneo, llegan a la capa fótica y contribuyen a la fertilización del Mar de Alborán. De nuevo las simulaciones numéricas indican un incremento de hasta el 40% en la producción primaria de esta cuenca y del 60% en la subcuenca occidental de este Mar debido a las mareas en el Estrecho [9].

3.- PROCESOS EN LA CUENCA CON INFLUENCIA EN EL INTERCAMBIO.

Forzamiento meteorológico

Es un clásico: por ser el Mediterráneo una cuenca semi-cerrada de dimensiones relativamente reducidas frente a los sistemas atmosféricos, el ajuste de su nivel a la presión atmosférica cambiante sobre su cuenca fuerza la aparición de un flujo neto a través del Estrecho (unos 0.08 Sv por cada mb de variación de presión [5]). Ese flujo se comparte al 50% entre el entrante y saliente aproximadamente. Así, una alta presión sobre la cuenca, por ejemplo, reduce el flujo entrante y aumenta el saliente [5].

Formación de WMDW

Como se sabe, es un proceso estacional que ocurre a finales de invierno en la región del Golfo de León que muestra una notable variabilidad interanual. Inviernos duros (los de 2004-05 y 2005-06 son un buen ejemplo) producen una gran cantidad de WMDW que levanta la interfaz que la separa de las aguas superiores, fundamentalmente la Levantina Intermedia (LIW). Este levantamiento tiene eco prácticamente instantáneo en la fracción de aguas que forman el flujo saliente, principalmente LIW y WMDW, incrementando la proporción de esta última, y también el volumen de agua evacuada [10].

El giro de Alborán Occcidental

La trayectoria que siguen las aguas Mediterráneas en el Mar de Alborán en su camino de salida es diferente para la LIW y la WMDW. La primera tiende a hacerlo pegada a la costa española en tanto que la segunda lo hace adosada a la Marroquí. El giro anticiclónico que suele localizarse en la cuenca occidental de Alborán facilita la evacuación de la WMDW, al transferir momento y energía a la vena para remontar el umbral [11]. Sin embargo, el giro no haría lo propio con la LIW, sino más bien lo contrario: la ausencia de giro anticiclónico favorecería la evacuación de LIW y dejaría de favorecer la de WMDW [12].

AGRADECIMIENTOS

Parte de los resultados presentados han sido obtenidos en el marco de los proyectos INGRES (REN03-01618, CTM06-02326, CTM2010-21229) financiados por el Plan Nacional de Investigación.

REFERENCIAS

1- Bryden, H. & Kinder, T. 1991. Steady two-layer exchange through the Strait of Gibraltar *Deep-Sea Res.,* 38, S445-S463

2- Whitehead, J., Leetma, A., & Knox, R. 1974. Rotating hydraulics of strait and sill flows. *Geophys. Fluid Dyn.*, 6, 101-125

3- Bormans, M. & Garrett, C. 1989. The effects of non-rectangular cross section, friction and barotropic fluctuations on the exchange through the Strait of Gibraltar. *J. Phys. Oceanogr.,* 19: 1543-1557.

4- Armi, L. & Farmer, D. 1985. Maximal two-layer exchange through a contraction with barotropic net flow. *J. Fluid Mech.*, 164, 27-51.

5- García-Lafuente, J., Alvarez-Fanjul, E., Vargas, J.M. & Ratsimandresey, W., 2002. Subinertial variability in the flow through the Strait of Gibraltar, *J. Geophys. Res*., 107(C10), 3168.

6- Bryden, H., Candela, J., & Kinder, T., 1994. Exchange through the Strait of Gibraltar. *Prog. Oceanogr.*33, 201-248

7-Naranjo, C., García-Lafuente, J., Sannino, G., Sánchez-Garrido, J.C. 2014. How much do tides affect the circulation of the Mediterranean Sea? From local processes in the Strait of Gibraltar to basin-scale effects. *Prog.Oceanogr.* 127, 108-116.

8- Sannino, G., Carillo, A., Pisacane, G., & Naranjo, C. 2015. On the relevance of tidal forcing in modelling the Mediterranean thermohaline circulation. *Prog. Oceanogr*., 134, 304-329

9- Sánchez-Garrido, J.C., Naranjo, C., Macías, D., García-Lafuente, J., & Oguz, T., 2015. Modelling the impact of tidal flows on the biological productivity of the Alboran Sea. *J. Geophys. Res*., 120, DOI: 10.1002/2015JC010885

10- García-Lafuente, J., Sánchez-Román, A., Díaz del Río, G., Sannino, G., & Sánchez-Garrido, J.C. 2007. Recent observations

of seasonal variability of the Mediterranean outflow in the Strait of Gibraltar, *J. Geophys. Res.,*112, C10005,
11- Naranjo, C., García-Lafuente, J., Sánchez-Garrido, J.C., Sánchez-Román, A., & Delgado- Cabello, J. 2012. The Western Alboran Gyre helps ventilate the Western Mediterranean Deep Water through Gibraltar. *Deep-Sea Res. Part 1*, 63, 157–163.
12- García-Lafuente, J., Naranjo, C., Sammartino, S., Sánchez-Garrido, J.C., 2016. The Mediterranean outflow and its link with the upstream conditions in the Alboran Sea (enviado)

Estuarine Classification of the Ría de Vigo Based on Seasonal Cycles of Stratification and Mixing

Miguel Gilcoto[1], Rocío F. Graña[1], Silvia Piedracoba[2], Pedro Montero[3], Nicolás Villacieros-Robineau[4], Ricardo Torres[5], John L. Largier[6], and Eric D. Barton[1]

[1]Instituto de Investigaciones Marinas, CSIC, Vigo, Spain (migil@iim.csic.es)
[2]Facultad de Ciencias del Mar, Universidad de Vigo, Vigo, Spain
[3]Instituto Tecnolóxico para o Control do Medio Mariño (INTECMAR), Xunta de Galicia, Spain
[4]Laboratoire d'Océanographie et du Climat, Université Pierre et Marie Curie, Paris, France
[5]Plymouth Marine Laboratory, Plymouth, United Kingdom
[6]Bodega Marine Laboratory, University of California Davis, Bodega Bay, California

ABSTRACT

The Ría the Vigo is traditionally classified as a partially mixed estuary. Using a comprehensive database of atmospheric, thermohaline and velocity observations the subtleties to correctly identify the possible circulation regimes of the ría at seasonal scale are exposed. First, the different time series of each direct or derived variable was fit to a seasonal cycle (annual and semiannual periods). Then the stratification and circulation parameters and the mixing and Froude numbers were calculated from those seasonal cycles and depicted in the Hansen-and-Rattray and Geyer-and-MacCready diagrams. We find that it is necessary to account for coastal upwelling effects in order to obtain circulation regimes that represent partially mixed behavior in either diagram.

INTRODUCTION

The Ría de Vigo (northwest Iberian Peninsula) has been traditionally classified as a partially mixed estuary [1, 2]. It has a semidiurnal tidal regime that drives the high-frequency currents, and a residual circulation greatly modulated by the action of coastal upwelling. Beyond the very dynamic and event-driven character of the Ría de Vigo, here, we provide a description of the seasonal evolution of the ría's hydrography and dynamics.

This work has two main goals, i) estimate the seasonal evolution of the stratification and mixing cycles and ii) describe the associated seasonal circulation regimes, in the context of estuarine classification diagrams.

The derived seasonal cycles establish a frame of reference for future studies and analysis. Also, they will serve as starting climatologies for feeding numerical simulations and as baseline for the study of more event-driven processes.

MATERIAL AND METHODS

We have compiled long-term time series of atmospheric data, hydrographic data (CTD profiles), river runoff and ADCP and HF Radar velocity observations that span several years (with non-overlapping periods among them). All these time series were fit to the general expression:

$$y = A_0 + A_1 \cdot \cos(\frac{2\pi}{T_1} + F_1) + A_2 \cdot \cos(\frac{2\pi}{T_2} + F_2)$$

based on annual (T_1) and semiannual (T_2) periods and amplitudes (A_i) and phases (F_i) estimated with a least squares technique for each variable *y*.

Four parameters will be used here, calculated from the seasonal cycles, to identify the estuarine regimes in function of stratification and mixing:

i) The stratification parameter, vertical salinity difference dS over average vertical salinity S_0.

ii) The circulation parameter, surface velocity u_s over river (U_R), or other net vertical, velocity U_f.

iii) The mixing number $M^2 = \frac{C_D \cdot U_M^2}{\omega \cdot N \cdot H^2}$, with C_D the bottom drag coefficient, U_M the amplitude of the velocity responsible for the mixing and which is modulated at frequency ω, N the Brunt-Väisälä frequency and H the depth.

iv) The Froude freshwater number $Fr = \frac{U_{Fr}}{\sqrt{g' \cdot H}}$, with U_{Fr} the net velocity, g' the reduced gravity and H de depth.

RESULTS AND DISCUSSION

As with many estuaries, it is difficult to define the estuarine classification of the Ría de Vigo, even on seasonal scales. This issue is probably more subtle in the ría because of the influence of the coastal upwelling in its residual circulation.

Coastal upwelling modifies the stratification conditions in the ría. During winter the water column is stratified mainly because of runoff from rivers and creeks. Although downwelling events, frequent in this season, may vertically homogenize the ría. In summer, according to the classical stratification-circulation diagram of Hansen and Rattray [3], based on salinity to estimate the stratification parameter, the ría would erroneously be described as a well-mixed estuary (cyan line in Fig. 1). In this season, since the runoff is scarce the vertical gradients of salinity are weak but the stratification could be as strong as in winter because the frequent coastal upwelling events reduce bottom temperatures while the sunny days heat the sea surface. This latter problem can be avoided in the Hansen and Rattray diagram using temperature corrected salinity (blue line in Fig. 1).

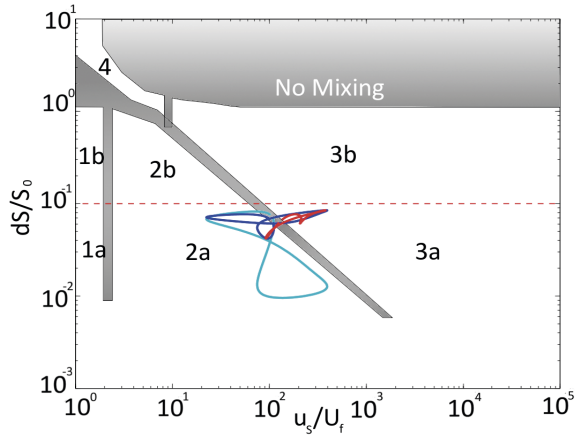

Fig. 1. Seasonal cycle of stratification and circulation in Ría de Vigo portrayed in the Hansen and Rattray [3] diagram. Cyan: circulation parameter obtained with $u_s = U_{HF}$ and $U_f = U_R$ and stratification parameter with standard salinity. Blue: circulation based on U_{HF} and U_R but, since stratification in the Ría de Vigo on summer is also controlled by temperature, a modified stratification parameter was estimated with a temperature corrected salinity $S_T = S - \beta/\alpha \cdot T$, where α is the thermal expansion coefficient and β the salinity contraction coefficient. Red: circulation parameter based only on estimations of gravitational circulation $u_s = U_G$ [4] and stratification with S_T.

However, the upwelling process also affects the circulation parameter. Indeed, if only the gravitational induced residual velocity [4] is included in the calculation of the circulation parameter, excluding the effect of the upwelling, then the range of possible circulation regimes in the ría is reduced (red line in Fig. 1.).

Similar conclusions are drawn from the more recent diagram of Geyer and MacCready [5]. The upwelling process must be taken into account in estimating both the mixing and the Froude numbers. The Ría de Vigo is erroneously defined as a salt-wedge estuary (red line Fig. 2.) when the upwelling is only considered on the Froude number, or as a well-mixed estuary if upwelling only influences the mixing number (brown line Fig. 2.). Therefore, upwelling must be included in both numbers. Doing so, the most probable circulation regimes in the Ría

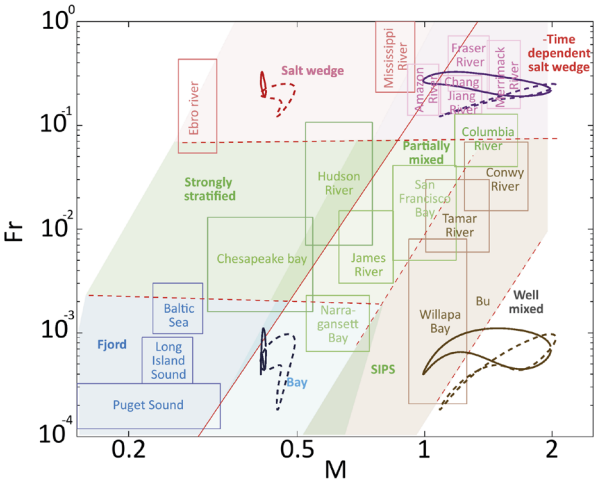

de Vigo are those falling between bay (black line in Fig. 2) and time-dependent salt wedge (magenta line in Fig. 2), i.e the partially mixed estuary, depending on the magnitude of the standard deviation of the Ekman transports on the shelf (σ_{Ek}).

Fig. 2. Seasonal cycles (color l) of Froude (Fr) and mixing (M) numbers overlaid Geyer and MacCready [5] diagram. Solid lines correspond to numbers (N and g' on M and Fr_f, respectively) estimated with density depending only on salinity while dashed lines refer to density depending on salinity and temperature. Black: $M=M_t$ ($U_M=U_t$, $\omega=\omega_t$) for tidal mixing vs. $Fr=Fr_f$ ($U_{Fr}=U_R$) for river runoff. Red: $M=M_t$ for tidal mixing vs. $Fr=Fr_f+Fr_{Ek}$ for combined river runoff and upwelling/downwelling events Fr_{Ek} ($U_{Fr}=\sigma_{Ek}$). Brown: $M=M_t+M_{Ek}$ for combined tidal and upwelling/downwelling events M_{Ek} ($U_M=\sigma_{Ek}$, $\omega = \omega_{Ek}$) mixing vs. $Fr=Fr_f$ for river runoff. Magenta: $M=M_t+M_{Ek}$ for combined tidal and upwelling/downwelling events mixing vs. $Fr=Fr_f+Fr_{Ek}$ for combined river runoff and upwelling/downwelling events.

ACKNOWLEDGEMENTS

Funding has been provided by STRAMIX research project (CTM2012-35155), Spanish Ministry of Economy and Competitiveness.

REFERENCES

1 – Prego R, Fraga F & Ríos AF, 1990. Water interchange between the Ría of Vigo and the coastal shelf. Scientia Marina, 54(1): 95-100.

2 – Nogueira E, Pérez FF & Ríos AF, 1997, Seasonal patterns and long-term trends in an estuarine upwelling ecosystem (Ría de Vigo, NW Spain). *Estuarine, Coastal and Shelf Science*, 44(3):285-300.

3 – Hansen DV & Rattray MJ, 1966. New dimensions in estuary classification. *Limnology and Oceanography*, 11(3):319-326.

4 – Officer CB, 1976. Physical oceanography of estuaries (and associted coastal waters), 465 pp., John Wiley & Sons, New York.
5 – Geyer WR & MacCready P, 2014. The Estuarine Circulation, Annu. Rev. Fluid Mech., 46(1):175-197.

Investigating SWOT capabilities to detect meso and submesoscale eddies in the Western Mediterranean

Laura Gómez Navarro[1, 2, 3], Ananda Pascual Ascaso[3], Baptiste Mourre[2], Evan Mason[3]

[1] Université de la Bretagne Occidentale, France
[2] SOCIB, Balearic Islands Coastal Observing and Forecasting System, Mallorca, Spain
[3] Institut Mediterrani d'Estudis Avançats, IMEDEA (CSIC-UIB), Mallorca, Spain

ABSTRACT

The primary oceanographic objective of the Surface Water Ocean Topography (SWOT) mission, to be launched in 2020, is to characterize the ocean mesoscale and submesoscale circulation determined from ocean surface topography at spatial resolutions of 15 km. SWOT altimeter swaths will provide a perfect observational region around the Balearic Islands. The Spanish waters of the Western Mediterranean, have an unprecedented opportunity to provide an ideal study region for quantification of the dynamic processes, during the 60 days fast phase after launch in which the satellite will provide daily high resolution sea surface height measurements in selected areas of the global ocean. The present study focuses on the Balearic Islands, using ROMS model data as input for the SWOT simulator that generates pseudo SWOT data. The simulator's outputs are then compared with the ROMS input data, available *in situ* measurements and other satellites' altimetric, temperature and chlorophyll data. The aim of this new study, in addition to evaluating the capability of SWOT to detect meso and submesoscale eddies, is to improve the knowledge of the surface circulation around the Balearic Islands.

INTRODUCTION

Understanding the relationship between the physical and biological processes is crucial for predicting the marine ecosystems response to changes in the climate system [1]. Mesoscale and submesoscale features play a major role in the redistribution of properties such as heat, salt and biochemical tracers with a significant impact on the ocean's primary productivity.

Although satellite altimetry has revolutionized our view and understanding of surface ocean circulation during the last two decades (e.g. [2]), leading to major breakthroughs, for e.g., the quantification of Eddy Kinetic Energy [3], or eddy identification and tracking [4], present altimetry fields still lack of enough resolution to cover scales shorter than 200 km, typical of ubiquitous mesoscale and submesoscale features. Instead, it is necessary to rely on new advances and integrated approaches using high-resolution autonomous, *in situ* and remotely sensed observations, modelling, and theoretical advances [5].

The Mediterranean Sea has a direct impact on the Atlantic Ocean circulation due to the exchanges through the Strait of Gibraltar and, subsequently, influencing the great ocean conveyor belt. Further, the Mediterranean Sea is a natural reduced-scale laboratory basin for the examination of processes of global importance, being much more accessible to ocean monitoring due to its size and distance to new coastal observatories. Finally, intense mesoscale and submesoscale variability interacts with the sub-basin and basin scales [6, 7]. Three scales of motion are therefore overlaid, making an amalgam of intricate processes that require high-resolution and comprehensive observations to be fully understood [8]. In this respect, major breakthroughs are expected from the wide-swath Surface Water Ocean Topography (SWOT) altimeter, which will allow first-time observations in the 15-100 km band [9] with a resolution one order of magnitude higher than current altimeters.

This study is a continuation of a previous one we carried out in the Canary Islands region. We used the SWOT simulator with the objective of understanding the future data from SWOT and to make an attempt to detect submesoscale eddies. It allowed to explore a range of optimum parameters for the SWOT simulator, to now carry out more accurate simulations in the Balearic Islands. [10]

The region of interest is expanded to the Balearic Islands, as it coincides with one of the SWOT satellite's swaths during the fast-sampling (calibration/validation) phase. Our study period is 2009-2015, taking advantage of the high-resolution simulation developed at SOCIB in the framework of the Medclic project, which focuses on the study of the mesoscale activity and its interactions with the general circulation in the Western Mediterranean Sea. The aim is to contribute to the nowadays challenge of advancing in resolving small scale variability in the Mediterranean Sea, to know and resolve the interannual variability.

MATERIALS AND METHODS

Given the wealth of realistic model outputs at our disposal the SWOT simulator software package will be exploited to generate SWOT-like outputs for the western Mediterranean (https://swot.jpl.nasa.gov/science/resources/). These data will complement both the existing lower resolution altimetry and the high resolution observational data that we collect, with the aim being to learn how we can use SWOT in understanding variability at meso- and submesoscales.

The SWOT simulator is a recently developed numerical tool that provides statistically reliable SSH outputs of what the satellite should be able to measure. Therefore, the existence of the simulator makes it possible to start optimization of information retrieval protocols/procedures for the processing of future SWOT data. [11].

The Western Mediterranean Operatonal forecasting system (WMOP) is used as inputs for the SWOT simulator. WMOP is a regional configuration of the Regional Oceanic Model System (ROMS) with a spatial coverage from Gibraltar strait to Sardinia Channel and a spatial resolution of 2 km. [12]

In addition, the ongoing SOCIB/IMEDEA projects related with bluefin tuna and jellyfish will provide *in situ* data for comparison and will give a greater significance to the study of this region. Data from other altimetric satellites will be also compared with the pseudo SWOT data.

RESULTS AND DISCUSSION

The SWOT simulator allowed to obtain pseudo SWOT altimetric data at a high spatial resolution, to be able to compare it with other datasets and to start developing algorithms to correctly visualize and analyse the future SWOT data. In fig. 2 the WMOP data interpolated into the SWOT grid (right) and the resulting pseudo SWOT swath show the higher spatial coverage SWOT will provide in comparison with present satellites. Mesoscale structures can also be observed, and experiments focusing on smaller regions like the Mallorca channel will be carried out to try to also identify submesoscale structures.

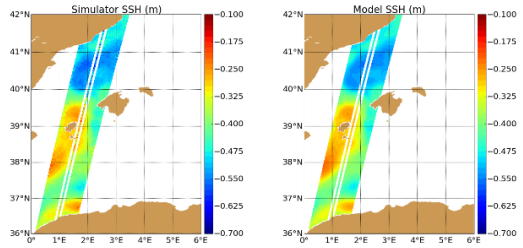

Fig. 2. Pass 182 of cycle 1 of SSH (m) pseudo SWOT (left) and SWOT grid interpolated model data (right) on the 12th of January 2016.

Moreover, in future work interpolation techniques like the dynamic interpolation proposed by [13] could be put into practice to obtain a smoother simulated SSH field.

The SSH and SST ROMS outputs were also analysed to determine the temporal and spatial occurrence of particular eddies. This was then compared with SST, SSH and chlorophyll measurements of other satellites as well as with *in situ* measurements, to confirm the existence of the structures observed in the ROMS output.

We expect that the outcomes of this dataset analysis contribute to better understanding high-resolution sea surface currents. This is important for the characterization of upper ocean dynamics for key geophysical, ecological and environmental processes.

ACKNOWLEDGEMENTS

This study was conducted during a master internship of L. Gómez-Navarro at IMEDEA (CSIC-UIB) funded by SOCIB. It is a contribution to the MULTI-SUB project (Mesoscale and submesoscale vertical exchanges from multi-platform experiments and supporting modeling simulations: anticipating SWOT launch) as part of the SWOT science team.

REFERENCES

1 - McGillicuddy, D. J., Anderson, L. A., Bates, N. R., Bibby, T., Buesseler, K. O., Carlson, C. A., ... & Hansell, D. A., 2007. Eddy/wind interactions stimulate extraordinary mid-ocean plankton blooms. *Science*, 316(5827):1021-1026.

2 - Le Traon, P. Y., 2013. From satellite altimetry to Argo and operational oceanography: three revolutions in oceanography. *Ocean Science*, 9(5):901-915.

3 - Pascual, A., Faugère, Y., Larnicol, G., & Le Traon, P. Y., 2006. Improved description of the ocean mesoscale variability by combining four satellite altimeters. *Geophysical Research Letters*, 33(2).

4 - Chelton, D. B., Gaube, P., Schlax, M. G., Early, J. J., & Samelson, R. M., 2011. The influence of nonlinear mesoscale eddies on near-surface oceanic chlorophyll. *Science*, 334(6054):328-332.

5 - Schiller, A., M. Bell, G. Brassington, P. Brasseur, R. Barciela, … & K. Wilmer-Becker, 2015. Synthesis of new scientific challenges for GODAE OceanView. *Journal of Operational oceanography*, 8(2):259271.

6 - Allen, J. T., D. A. Smeed, J. Tintore., & S. Ruiz, 2001. Mesoscale subduction at the Almeria-Oran front, Part 1: Agesotrophic flow. *J. Mar. Syst*., 30:263–285.

7 - Ruiz, S., A. Pascual, B. Garau, I. Pujol, & J. Tintoré, 2009. Vertical motion in the upper ocean from glider and altimetry data. *Geophys. Res. Lett*., 36.

8 - Ruiz S., Pascual A., Casas B., Poulain P., … & Tintoré J., 2015. Report on operation and data analysis from Multi-Platform Synoptic Intensive Experiment (ALBOREX), 120pp. PERSEUS Project, ISBN: 978-960-9798-13-6.

9 - Fu, L. L., & Ferrari, R., 2008. Observing oceanic submesoscale processes from space. Eos, *Transactions American Geophysical Union*, 89(48):488-488.

10 - Gómez-Navarro, L., Mason, E. & Pascual, A., 2016. Investigating SWOT capabilities to detect submesoscale eddies in the Canary Islands: application of the SWOT simulator. *Submesoscale Processes: Mechanisms, Implications and New Frontiers Colloquium*.

11 - Gaultier, L., Ubelmann, C. & Fu, L. L., 2016. The challenge of using future SWOT data for oceanic field reconstruction. *J. Atmos. Oceanic Technol*., 33:119–126.

12 – Juza M., Mourre B., Renault L., Gómara S. ... & J.Tintoré (2016). SOCIB operational forecasting system and multi-platform validation in the Western Mediterranean Sea. *Journal of Operational Oceanography*.

13 - Ubelmann, C., Klein, P. & Fu, L.L, 2015. Dynamic Interpolation of Sea Surface Height and Potential

Applications for Future High-Resolution Altimetry Mapping. *Journal of Atmospheric and Oceanic Technology*, 32(1):177-184.

Slope currents in the Central Cantabrian Sea from a long-term full-depth resolving mooring line

César González-Pola[1], David Marcote[2] & Ignacio Reguera[1]

[1] Instituto Español de Oceanografía, C.O. de Gijón, Avda. Príncipe de Asturias 70Bis, 33212, Gijón.
[2] Instituto Español de Oceanografía, C.O. de Coruña, Paseo Marítimo Alcalde Francisco Vázquez, 10, 15001, Coruña.

ABSTRACT

A fully equipped mooring line was deployed in summer 2010 in the mid-slope of the central Cantabrian Sea (southern Biscay) to resolve the full-depth vertical structure of the slope currents in the area. The deployment site is located 22 nautical miles north of Peñas Cape, within a relatively flat seafloor patch at 1600 m depth. The mooring line consists of a 75 kHz ADCP at a depth of 300-400 meter to resolve the upper layers and 3 or 4 single point current meters at deeper levels. Within the period August 2010 to January 2016 the mooring has been operating 51 months and not in place for 14 months due to logistics. Main unanswered questions regarding the mid and outer slope circulation in the Cantabrian Sea are related to the progression of the Iberian Poleward Current within the upper 200 meters after turning into a east/west oriented coastline, and the same issue regarding the Mediterranean Water vein, flowing at about 1000 meters. Other issues not well understood are the barotropic vs baroclinic character of the vertical current structure and the possible presence of seasonality. Here we show the available record focusing in the long-term low-passed currents. Prevalence of westwards flow for surface and central waters and the opposite, eastward flows from Mediterranean Water core to the bottom, is the main outcome. IPC advance into the Cantabrian Sea is rarely observed, suggesting that it may progress right at the inner slope closer to the shelf-break.

INTRODUCTION

The Bay of Biscay is a marginal basin of the temperate NE Atlantic, located at the northeastern edge of the subtropical gyre and entering what is known as the intergyre region. It is bounded by the narrow northern Spanish continental shelf and the much wider Armorican continental shelf towards the French side. The Biscay Abyssal Plain reaches 5000 meters depth.

Main circulation patterns at different water levels have been depicted in literature (see [1] for a review). Upper ocean currents over the abyssal plain consist of slow southwards drift with an anticyclonic component. The pattern stands at least to levels of Central Waters. Mesoscale and tides are very important in the region.

Shelf-slope circulation is dominated, like in other eastern boundary current systems, by a geostrophically balanced poleward flow known as the ‘‘Iberian Poleward Current’’ (IPC), which develops mainly in wintertime. The entrance of the IPC in the southern Bay of Biscay (Cantabrian Sea) has been inferred since the late 80s from its hydrographical signature, but mechanisms governing its regional dynamics are not yet fully understood since the main forcing, the along-shore meridional pressure gradient, is locally absent [2]. Tidal rectification has been proposed as a relevant mechanism maintaining the local poleward flows.

Mediterranean water spreading from the Gibraltar Strait into the Atlantic evolves along the Iberian continental slope as a high salinity/temperature vein. After passing Galicia and turning into the Cantabrian Sea it is not clear whether such slope vein continues as a permanent feature. Current-meter records and float drifters available so far appear to depict contrasting circulation patterns. The structure of the slope circulation is thought to be strongly baroclinic and subject to notable seasonality.

Direct measurements of Cantabrian Sea slope currents at mid-depth levels are scarce and very limited in time. With the aim of better understanding the slope circulation, a fully equipped mooring line was devised.

DATA SET

The mooring line was deployed in August 2010 in a location chosen as representative of the mid-outer continental slope within the Central Cantabrian Sea. The site is located 22 nm north of Peñas Cape (Asturias) within a relatively flat seafloor patch, at 1600 m depth. The mooring structure varied slightly in time. First configuration consisted of a 75 kHz ADCP at a depth of about 400 meter to resolve the upper layers, including the structure of the IPC. Below there were 4 single-point current meters (CMs) at 700, 1000, 1250 y 1570 meters (bottom). One CM was

lost after second deployment and the ADCP moved upwards in recent deployments.

Within the period August 2010 to January 2016, 51 full months have been recorded in 7 deployments and 14 months have been lost due to logistics. Fig. 1 shows the available records at different levels. Next recovery is scheduled by October 2016.

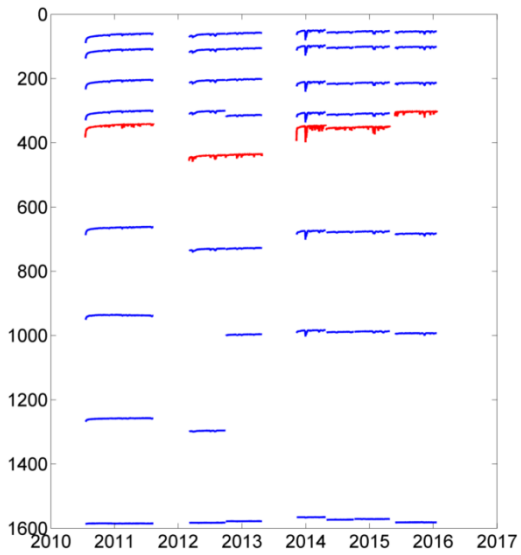

Fig. 1. Available current records at the Peñas mooring shown as pressure vs time. Red line is depth of the ADCP75.

Other mooring lines within the period were deployed in the Avilés Canyon System and over the Biscay Abyssal plain. These shorter records allow a description of the spatial structure of the current field, though this will not be discussed in the present contribution.

RESULTS AND DISCUSSION

Here it is shown the first preliminary analysis of the record, focusing mainly in the long-term average flows. Fig. 2 shows the intensity-frequency roses of the sub-tidal flows (Godin A24A24A25, cut-off period of 30-hours).

Overall, currents have a zonal orientation as it is expected from the alignment of the shelf-slope in the central Cantabrian Sea. Strong current pulses in the upper levels are either westwards or eastwards being the former dominant in frequency. Eastwards currents become less frequent as we progress downwards in the water column to the core of the IPC (100 meters) and below. Therefore it seems that the mooring site lye offshore the main IPC pathway. The existence of the Aviles Canyon upstream and the Peñas Cape headland surely conditions the regional circulation patterns. Inner slope measurements are required to better understand the regional shelf-edge current structure.

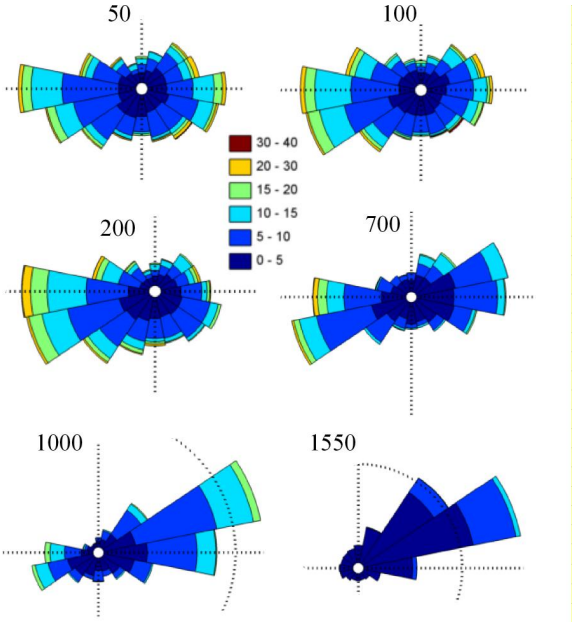

Fig. 2. Current-roses of low-pass filtered currents at the Peñas mooring.

The 700 m depth is the lower limit of Eastern North Atlantic Central Waters, starting the transition towards the MW levels. Dominant currents are also westwards, though sustained periods of eastwards currents are present. Orientation of currents veers to the NE/SW, constrained by the topographical steering. At 1000 m, the core of MW, currents are persistently eastwards with few short-term reversals. This supports the continuity of the MW vein progressing along the continental slope [3]. Near-bottom currents exhibit a very strong tide, up to 50 cm/s and modulated by local neap-spring cycle, contrasting to barotropic character of tide across the water column. Near-bottom residual currents are stable towards the NE (along-slope) without reversals.

ACKNOWLEDGEMENTS

The mooring line was acquired under regional infrastructure project EQUIP09-43, Principado de Asturias, co-funded by FEDER program. We specially acknowledge technicians and the crews of different vessels involved in maintenance and deployment/recovery operations.

REFERENCES

1 - Lavin, A. et.al. The Bay of Biscay. The encountering of the ocean and the shelf. In: *The Seas*, edited by Robinson and Brink, Harvard Press, 2006, p. 933-1001..

2 - Pingree R.D. and B. Le Cann. Structure, strength and seasonality of the slope currents in the Bay of Biscay region. *J.Mar.Biol.Assoc.U.K.* 70 (4):857-885, 1990.

3 - Iorga M.C. and M. S. Lozier. Signatures of the Mediterranean outflow from a North Atlantic climatology II. Diagnostic velocity fields. *J.Geophys.Res.* 104 (C11):26011-26029, 1999.

Glider observations of the Canary Current

Alberto González-Santana[1], Pedro Vélez-Belchí[1], Andrés Cianca[2], Maria Jose Rueda[2], Octavio Llinas[2] and Carlos Barrera[2]

[1] Instituto Español de Oceanografía, Centro Oceanográfico de Canarias
[2] Plataforma Oceánica de Canarias

ABSTRACT

The Canary Islands are immersed in the eastern boundary of the subtropical gyre, in the coastal transition zone of the Canary Current Eastern Boundary Current. They are an ideal place for the study of the variability of the subtropical gyre. With this background, in 2006 the Spanish Institute of Oceanography (IEO) began an observational program around the Canary Islands, know as the *Raprocan* (deep hydrographic section of the Canary Island), in order to establish the scales of variability in the range decadal/subdecadal in the subtropical gyre. *Raprocan* consists in hydrographic cruises in two seasons, with 50 hydrographic stations around the Canary archipelago. The use of Gliders for oceanographic studies has been demonstrated to be an valuable tool to understand the dynamic regimes at the area and it complements studies based in cruise hydrographic data. The large meaningful applications that offer these devices ranges from quantification of heat exchange between atmosphere – ocean, mass transport quantification, water masses identification, primary productivity quantification of the upwelling area and seasonal variability studies, among others. In this context, the Spanish Institute of Oceanography (IEO) and the Canary Islands Oceanic Platform (PLOCAN) developed and join program to set up glider missions to complement Raprocan. Here we describe the program and the first results

INTRODUCTION

The Canary Islands are immersed in the eastern boundary of the subtropical gyre, in the coastal transition zone of the Canary Current Eastern Boundary Current (CanCEBCS). The CanEBCS is a high productive ecosystem with strong socioeconomic impact since it supports a vast and diverse marine population. The high productivity of the CanEBCS is mainly driven by the trade winds that flows alongshore parallel to the northwest Africa coastline. On the other hand, it has been pointed out that the dynamics of the eastern Atlantic as the main driver for the seasonal cycle of the Atlantic meridional overturning circulation (AMOC), specifically Rossby waves excited south of the Canary Islands. All the above, makes the Canary Islands an ideal place for the study of the variability of the subtropical gyre, and therefore in 2006 the Spanish Institute of Oceanography (IEO) began an observational program around the Canary Islands, know as Raprocan (deep hydrographic section of the Canary Island) [1, 2]. In this context, the Spanish Institute of Oceanography (IEO) and the Canary Islands Oceanic Platform (PLOCAN) developed a program to set up glider missions to complement Raprocan. Here we describe the program and its first results.

MATERIAL AND METHODS

The pilot mission partially samples the *Raprocan* section (Figure 1), as a first approach to further expand the mission to the complete northern transect of *Raprocan*, from Africa to La Palma. This pilot glider mission was designed to sample along a triangle between three waypoints, north of the island of Gran Canaria, ESTOC (European Station for Time Series in the Ocean, Canary Islands) and the channel between Fuerteventura and Lanzarote (Fig. 1) . Six missions have been carried out following the same design; in October 2013, February 2014, July 2014, October 2015, December 2015 and March 2016. In all the missions, a slocum G2 glider was navigated remotely via satellite communications. The glider followed a saw-tooth like profile through the water column, completing over 300 profiles between the surface and 1000 m of depth, and covering in each mission a total horizontal distance of approximately 1000 km. The glider collected pressure, temperature, salinity, oxygen, turbidity and Chlorophyll data. GPS location before and after each dive permitted to obtained integrated water velocity.

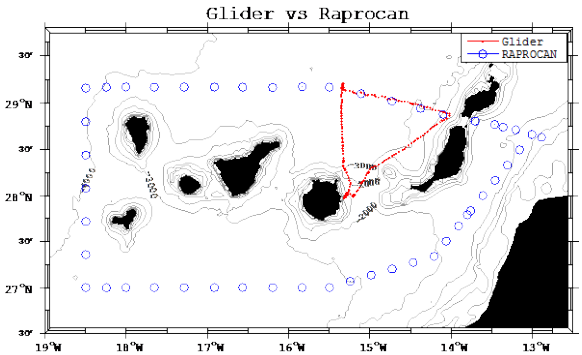

Figure 1. Path (red) of the glider mission compared with the hydrographic stations (blue) carried out in Raprocan.

The high-density sampling of the glider resolved short-scale oscillation in most of the field. These oscillations were dominated by a 24-h and 12-h variability associated with a combination of solar and lunar semi- diurnal internal tides. We used a coseno-lanczos digital filter in the time series to eliminate this high frequency variability since it produced uncertain in water mass transport estimations.

From the filtered time series of temperature and salinity, equivalent vertical profiles were estimated at the mean position of each dive. Mass transport was estimated, using the thermal wind equation, referenced to 1000dbar and absolutely to the GPS–estimated integrated water velocity.

RESULTS AND DISCUSSION

The high-resolution sampling carried out by the glider permit to observe features not observed before in the Canary basin. Among others, the path of the Antartic Intermediate Waters (AAIW) that flows close to the slope of Gran Canaria, as indicated by the relative low salinity waters found at 800 dbar (Fig 2a) and the low oxygen concentration (not shown).

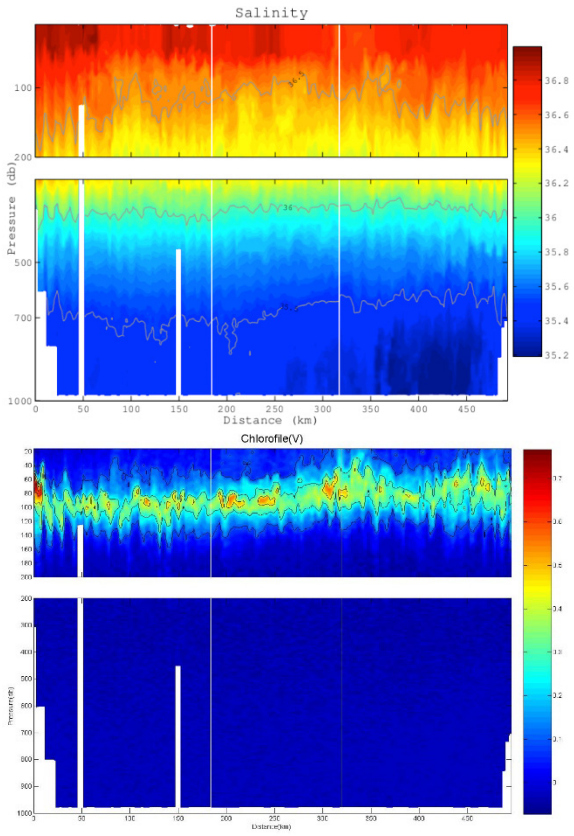

Figure 2. Vertical section of Salinity (a) and Chlorophyll (b). The distance is computed from the deployment position north of Gran Canaria; the first vertical white line corresponds to ESTOC, the second to the west side of the Bocaina channel, between Fuerteventura and Lanzarote, and the section ends in the recovery position, north of Gran Canaria.

Different water masses are delimited by isopycnal bounds. In the west side of the channel between Fuerteventura and Lanzarote there is a maximum in Chlorophyll, possible related with local upwelling associated to the western coast of Lanzarote (Fig.2 b).

During fall 2013, most of the transport of the Canary Current flowed southward between Lanzarote and north of Tenerife, with inverse modeling estimations of 2.9 Sv for the North Atlantic Central Waters (NACW) and the thermocline waters [3]. Using the glider data, referenced to the GPS–estimated integrated water velocity, the transport estimated was 2 Sv in the section between ESTOC, the northern vertices of the sampled triangle, and Lanzarote. The accumulated transport estimated from the glider data for the NACW and the thermocline waters along the closed triangle was 0.2 Sv, indicating that the geostrophic velocities referenced to GPS–estimated integrated water velocity were a proxy for the layer of know-motion.

ACKNOWLEDGMENTS

This study has been performed as part of the RAPROCAN project, from the Instituto Español de Oceanografía (IEO) and the SeVaCan project (CTM2013-48695), from the Ministerio de Economía y Competitividad. Alberto Gonzalez Santana has been funded by a Technical Support Staff contract from the Ministerio de Economía y Competitividad.

REFERENCES

1 – Velez-Belchí P., Hernández-Guerra A., Barrera C., Fraile-Nuez E., Barrera A., Llinas O., Benítez Barrios V., Domínguez F., Alonso-González I., González Dávila M., Santana Casiano M., Hernández Brito J., Presas Navarro C., Arístegui Ruiz J., Comas Rodríguez I., Garijo López J.C., Hernández León S., Pérez Hernández M.D., Rodríguez Santana A., Sosa Trejo D. Monitoring the Oceanic Waters of the Canary Islands: RaProCan. The deep hydrographic section of the Canaries.

2 - Vélez-Belchí, P., González-Carballo, M., Pérez-Hernández, M. D. and Hernández-Guerra, A. 2015. Open ocean temperature and salinity trends in the Canary Current Large Marine Ecosystem. In: Valdés, L. and Déniz-González, I. (eds). Oceanographic and biological features in the Canary Current Large Marine Ecosystem. IOC-UNESCO, Paris. IOC Technical Series, No. 115, pp. 299-308.

3 - Vélez-Belchí, P., Hernández-Guerra, A., Dolores Pérez-Hernández, M., (2016). Seasonal Variability of the Canary Currrent. Ocean Sciences meeting 2016, New Orleans, USA.

Meridional overturning transports at 30°S in the Indian and Pacific Oceans in 2002-2003 and 2009

Alonso Hernández-Guerra & Lynne D. Talley

1 Instituto de Oceanografía y Cambio Global, IOCAG Universidad de Las Palmas de Gran Canaria, ULPGC 35017 Las Palmas, Spain

2 Scripps Institution of Oceanography, UCSD La Jolla CA 92093, USA

ABSTRACT

The meridional circulation and transports at 30°S in the Pacific and Indian Oceans for the years 2002-2003 and 2009 are compared, using GO-SHIP hydrographic section data with an inverse box model and several choices of constraints. Southward heat transport across the combined Indian-Pacific sections, reflecting net heating north of these sections, doubled from -0.7±0.2 PW in 2002-2003 to -1.4±0.1 PW in 2009, with the increase concentrated in the Indian Ocean (~0.6 PW compared with ~0.2 PW in the Pacific), and was insensitive to model choices for the Indonesian Throughflow. Diagnosed net evaporation also more than doubled in the Indian Ocean, from 0.21-0.27 Sv in 2002-2003 to 0.51-0.58 in 2009, with a smaller but significant increase in net evaporation in the Pacific, from 0.06-0.08 Sv to 0.16-0.32 Sv. These increased heat and freshwater exports coincided with Indian Ocean warming, a shift in the Indian's shallow gyre overturning transport to lower densities, and an increase in southward Agulhas Current transport from 75 Sv in 2002 to 92 Sv in 2009. The Indian's deep overturn weakened from about 11 Sv in 2002 to 7 Sv in 2009. In contrast, the Pacific Ocean overturning circulation was nearly unchanged from 2003 to 2009, independent of model within the uncertainties. The East Australian Current transport decreased only slightly, from -52 Sv to -46 Sv.

Reconstruction of ocean currents at scales shorter than 30 km from existing satellite observations

Jordi Isern Fontanet[1], Cristina González Haro[2], Cristina Martín Puig[3] & Antonio Turiel[1]

[1] Institut de Ciències del Mar (CSIC), Barcelona
[2] Télécome Bretagne, Brest, Francia
[3] Laboratory for Satellite Altimetry (NOAA), Washington, USA

ABSTRACT

Along-track altimetric measurements of Sea Surface Heights (SSH) are very well suited to quantify across-track currents. However, the spatial resolution of derived 2D velocities is restricted to scales above 100-150 km and the limited number of altimeters can lead to errors in the location of currents. On the contrary, infrared measurements of Sea Surface Temperature (SST) are well suited to locate flow patterns but it is difficult to extract quantitative estimations of ocean currents. To overcome the previous constrains we have developed a methodology to exploit the synergy between SST and SSH measurements to provide enhanced 2D surface currents. Our approach combines the usage of advanced signal processing techniques, such as wavelet analysis, with dynamical approaches like the Surface Quasi-Geostrophic (SQG) equations. This approach opens the door to retrieve the velocity field associated to structures smaller than 30 km, not accesible through the standard SSH maps. Here we will show some examples of the capabilities of our approach to retrieve the dynamics at such small scales by comparing the reconstruction from existing satellite information with in situ experiments and high resolution satellite data such as SAR mode CryoSat-2 measurements.

Presente y futuro de la modelización climática en el mar Mediterráneo

Gabriel Jordà (1), Josep Llasses (1) y el equipo MedCORDEX

[1] Instituto Mediterráneo de Estudios Avanzados (IMEDEA, UIB-CSIC).

RESUMEN

La modelización regional del clima del mar Mediterráneo ha experimentado un gran avance durante los últimos años. Las simulaciones actuales cubren varias décadas, son de alta resolución espacial (1/8º-1/32º en la horizontal y hasta 75 niveles verticales) y han mejorado significativamente las comparaciones con observaciones. Los datos están accesibles en diversas bases de datos y el número de usuarios de estos datos está aumentado considerablemente. Por lo tanto, es importante ser consciente de las limitaciones y de las fortalezas de éstas simulaciones de cara a sacarles el máximo provecho pero sin caer en la sobreestimación de sus capacidades. En este trabajo se hará una breve revisión del estado actual de la modelización del clima marino y de las líneas futuras. En particular nos basaremos en la experiencia de la iniciativa MedCORDEX, a día de hoy la iniciativa europea más importante a nivel de modelización del clima regional Mediterráneo. MedCORDEX engloba a 23 equipos de 10 países dedicados al desarrollo y análisis de simulaciones climáticas centradas en el Mediterráneo. Fruto del trabajo de los últimos 8 años se ha creado una extensa base de datos que incluye simulaciones atmosféricas, oceánicas y de modelos acoplados atmósfera-océano tanto del clima presente como de proyecciones de futuro. Como ejemplo de los resultados obtenidos se analizarán los resultados del conjunto de simulaciones marinas haciendo especial énfasis en la descripción de los flujos de calor y sal en las fronteras y el interior del Mediterráneo

INTRODUCCIÓN

El Mediterráneo es un mar semi-cerrado unido al océano global principalmente a través del Estrecho de Gibraltar. Más de 150 millones de personas viven a lo largo de sus costas y el Mar es de una importancia capital para la socioeconomía de los países que lo rodean. El Mediterráneo también alberga una gran biodiversidad (8% de las especies marinas conocidas con sólo un 0.8% de la superficie oceánica) y es una cuenca de ecosistemas muy contrastados: desde el interior altamente oligotrófico hasta las zonas totalmente eutrofizadas del Adriático norte.

El clima del Mediterráneo es el resultado de las interacciones lineales y no-lineales de un amplio abanico de procesos físicos. Es uno de los pocos sitios del mundo en el que existe convección profunda y que tiene lugar la formación de masas de agua y la circulación termohalina es muy activa, con celdas cerradas en las cuencas oriental y occidental. Además existe una gran actividad de mesoscala y submesoscala superimpuesta que interacciona con los grandes giros inducidos por el viento.

Una herramienta básica para entender la dinámica de la cuenca son las observaciones. Por desgracia su limitada cobertura espacial y/o temporal convierten a los modelos numéricos en herramientas imprescindibles para poder entender y predecir el clima marino del Mediterráneo. Desde los primeros modelos simplificados en los años 80 hasta los complejos modelos acoplados océano-atmósfera de alta resolución actuales se ha llegado después de un largo y arduo proceso. En este trabajo haremos una breve revisión del estado actual de las simulaciones numéricas climáticas así como de sus limitaciones y fortalezas.

ESTADO ACTUAL

Los modelos del Mediterráneo han experimentado una gran transformación. Desde los primeros modelos simplificados en los años 80 se pasó a los modelos de ecuaciones primitivas en los años 90. Estos consideraban toda la cuenca a una resolución típica de 1/4º y 20 niveles verticales y las simulaciones estaban forzadas por campos climatológicos y duraban unos pocos años (ej. Haines and Wu, 1995, Herbaut et al., 1996). Posteriormente se identificó la importancia de la variabilidad interanual en los forzamientos así como el rol de la alta frecuencia (ej. Castellari et al., 2000). Simulaciones multidecadales permitieron caracterizar la variabilidad de la circulación termohalina así como las correlaciones temporalis entre las masas de agua y sus interacciones.

El aumento de la capacidad computacional ha llevado a un aumento significativo en la resolución espacial de los modelos y de la duración de las simulaciones. Actualmente las simulaciones tienen típicamente resoluciones espaciales de 1/12º , 50-70 niveles verticales, cubren periodos de 50-60 años y son forzadas por campos atmosféricos horarios de alta resolución espacial (10-25km). Esto ha permitido

que se pueden resolver más adecuadamente los procesos de formación de masas de agua, convección intermedia y profunda, la circulación general y el campo mesoscalar.
Pese a estas mejoras cabe remarcar que las simulaciones actuales siguen teniendo capacidad de mejora. Por poner algunos ejemplos se puede mencionar lo siguiente. Se ha descubierto que la representación de los procesos de convección y del transporte de las nuevas masas de agua mejora significativamente cuando la resolución de los modelos se acerca a 1/60º. La interacción de la circulación con la batimetría es clave en la zona del talud y en regiones clave como el Estrecho de Gibraltar, donde los procesos irresolubles por los modelos debe ser parametrizados. También, los forzamientos de los modelos deben ser mejorados. La falta de observaciones en mar abierto limita la fiabilidad de los flujos de calor y agua en la interfase océano-atmósfera. El caudal de los ríos, clave en la representación de procesos de plataforma y costeros, tiene grandes incertezas asociadas. Los flujos a través del Bósforo no están monitorizados por lo que la calidad del forzamiento lateral en esa zona es dudosa.

LA INICIATIVA MEDCORDEX

En la actualidad hay diversas iniciativas que pretenden mejorar la calidad de los modelos climáticos así como generar nuevas simulaciones que puedan ser utilizadas por la comunidad internacional. Entre esas iniciativas, la más importante es el proyecto MedCORDEX (Ruti et al., 2015). Más de 20 equipos de más de 10 países distintos colaboran en MedCORDEX en el desarrollo y análisis de simulaciones regionales del clima Mediterráneo. Esta comunidad de investigadores hace uso de modelos atmosféricos, de océano, de suelo y de ríos así como de modelos acoplados en que dos o más de esos elementos se combinan para ofrecer una representación más completa del sistema climático y de sus interacciones.
Durante los últimos años el equipo de MedCORDEX ha conseguido avances relevantes en el diseño y mejora de los modelos así como en el análisis científico de procesos relevantes (más de 60 artículos publicados en los últimos 5 años). Además, se ha creado una base de datos de simulaciones (www.medcordex.eu) que cuenta actualmente con más de 70 conjuntos de datos. En particular, en la base de datos se pueden encontrar 18 simulaciones del clima marino realizadas por modelos oceánicos forzados y modelos acoplados. Estas simulaciones han sido realizadas por 5 modelos diferentes y en distintas configuraciones, lo cual permite considerar una parte importante de las incertidumbres asociadas a la modelización.

INTERCOMPARACIÓN DE MODELOS

El anteriormente mencionado conjunto de simulaciones de MedCORDEX ha permitido realizar diversos estudios multimodelo sobre nivel del mar, circulación termohalina, convección profunda o balances de calor y sal (número especial de *Climate Dynamics* en proceso de producción). En particular, como ejemplo aquí se mostrarán los resultados de un análisis multimodelo de la transferencia de calor y sal en el Mediterráneo. A partir de un modelo de cajas con 8 compartimentos (Llasses et al., 2016) han caracterizado los flujos de calor y de sal tanto en las fronteras como en el interior del Mediterráneo (Fig. 1). La mayor parte de la circulación de calor tiene lugar en los primeros 600 m. El flujo de calor que entra por Gibraltar en la primera capa (0-150m) aumenta a lo largo de su tránsito en la cuenca oeste debido a los aportes interiores. En al cuenca oriental un 25% se pierde en superficie mientras que el resto pasa a la capa de 150m-600m, donde es redirigido hacia Gibraltar para ser exportado hacia el Atlántico. El flujo hacia capas más profundas es un orden de magnitud menor pero es el responsable de las tendencias de calor y sal observados en capas profundas. Desafortunadamente estos flujos profundos están sujetos a grandes incertidumbres causadas por la configuración de los modelos.

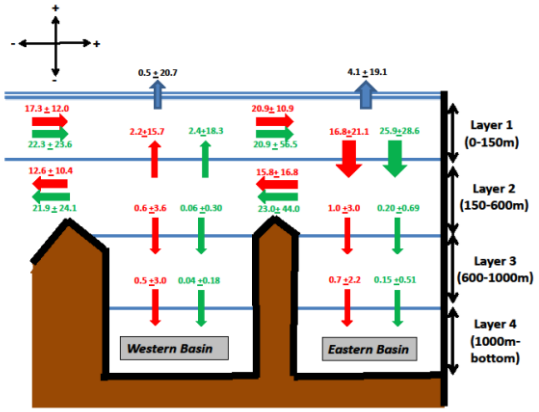

Fig. 1. Esquema de los flujos de calor (rojo, en W/m^2) y sal (verde, en Tn Sal/s) en el Mediterráneo a partir del conjunto de modelos MedCORDEX.

REFERENCIAS

1 - Haines, K., and P. Wu 1995. A modelling study of the thermohaline circulation of the Mediterranean Sea : water formation and dispersal, *Oceanologica Acta*, 18 (4), 401–417.
2 - Herbaut, C., L. Mortier, and M. Crépon 1996. A sensitivity of the general circulation of the western mediterranean sea. part I : the response to density forcing through the straits, J. Phys. Oceanogr., 26 (1).
3 - Castellari, S., N. Pinardi, and K. Leaman 2000. Simulation of the water mass formation processes in the Mediterranean Sea : Influence of the time frequency of the atmospheric forcing, *J. Geophys. Res.*, 105 (C10), 24,157–24,181
4 - Ruti PM, et al. 2015. MED-CORDEX initiative for the Mediterranean Climate studies. *Bull. of the American Meteo. Soc.* doi: BAMS-D-14-00176

5 - Llasses et al., 2016. Heat and salt redistribution within the Mediterranean Sea in the Med-CORDEX model ensemble. *Under review in Climate Dynamics.*

Sea level seasonal cycle along the Gulf of Cadiz continental shelf: the need for higher resolution altimeter products and models

Irene Laiz[1], Begoña Tejedor[1], Jesús Gómez-Enri[1], Alazne Aboitiz[1] & Pilar Villares[1]

[1] Department of Applied Physics, University of Cadiz

ABSTRACT

The spatial distribution of the Gulf of Cadiz (GoC) sea level seasonal cycle has been analyzed using sea level anomalies from gridded multi-mission altimeter data. The forcing mechanisms considered included atmospheric pressure and wind and the steric effect. The atmospheric contribution was evaluated using the VANI2-ERA hindcast, generated with a barotropic version of the HAMSON model. The steric heights were computed from a combination of satellite Sea Surface Temperature (SST) with a very high resolution climatology of temperature and salinity profiles. The oceanographic complexity of the GoC was clearly manifested in the results. While the atmospheric and steric contributions accounted for most of the seasonal cycle offshore, an annual signal of up to 2.5 cm remained along the continental shelves and slope, with the highest values around the Strait of Gibraltar and the North African shelf. Linear correlations between this signal and the along- and across-shore wind stress suggested a baroclinic response of the sea level along the (wide and shallow) eastern shelf not accounted for in the VANI2-ERA residuals. As for the (steep and narrow) western shelf, results showed that the spatial resolution of the HAMSON model might not be enough to accurately represent the barotropic response of the sea level to the wind stress field in that region.

INTRODUCTION

Over the past few years, gridded satellite altimetry products have become a popular tool to analyse the sea level variability at regional scales [1,2,3,4]. Furthermore, an increasing effort is being made in the last decade to develop accurate altimetry sea-level data around the coastal zones, both in terms of along-track [5,6] and gridded [7,8] products. High resolution maps of sea level anomalies have been used to capture coastal and mesoscale processes within the Gulf of Cadiz (GoC) eastern continental shelf linked to heavy river discharges [9].

In terms of the sea level variability forcing agents, the need for higher resolution products has also been raised recently [10].

The aim of this work is to analyse the sea level seasonal cycle along the GoC continental shelf including the contribution of its main forcing agents, namely, atmospheric pressure, wind and the steric effect.

DATA AND METHODS

Weekly maps of sea level anomalies (SLA) were obtained from the AVISO data server for the GoC for the time period 1997-2008 and averaged to obtain monthly means. The SLA are already corrected from the atmospheric pressure and wind effects, among others, using the Dynamic Atmospheric Correction (DAC). In this study, the DAC is added back to the SLA data to obtain the observed sea level anomalies, or *Alt_MSLA*. These *Alt_MSLA* were corrected from the atmospheric contribution (i.e., atmospheric pressure and wind) using monthly means of the VANI2-ERA sea level residuals [11] to produce the adjusted sea level anomalies, or *Alt_ASLA*. The VANI2-ERA hindcast provides an improved barotropic response of sea level to wind stress with respect to other residuals such as the DAC in the GoC [12].

The steric heights were computed as in [12] and were utilized to correct the *Alt_ASLA* data. The resulting data will be designated as Alt_ASLA_{steric} or sea level residuals.

Finally, in order to analyze the observed sea level seasonal cycle and the contribution of the forcing agents considered, a least squares fit to annual and semiannual harmonics was performed to the following variables: *Alt_MSLA*, *Alt_ASLA*, and Alt_ASLA_{steric}.

RESULS AND DISCUSSION

The *Alt_MSLA* showed a marked seasonal cycle along the continental shelf, with higher values of the annual signal at the eastern shelf (~5.5-6.6 cm) and decreasing values at the western one (~4.4-5.6 cm). Moreover, the latter peaked about two weeks later at the end of August, probably related to the summer intensification of the upwelling in that region. The semiannual cycle showed similar values (~2.5 cm) within both shelves. No signal was observed around the Guadalquivir river. Previous studies showed that strong river outflows affect the sea level seasonal cycle

from a neighboring tide gauge, but not from the AVISO data [1,13]. However, more recent studies have showed that high resolution maps of altimeter-derived sea level anomalies can actually capture strong river discharges [9]. When correcting the *Alt_MSLA* with the VANI2-ERA residuals, the amplitude of the semiannual signal decreased to negligible values around both shelfs, confirming its meteorological origin. The annual amplitude was only slightly reduced. It presented higher values near the Strait of Gibraltar that decreased westward, with the minimum values observed over the western shelf, where the peak also occurred later.

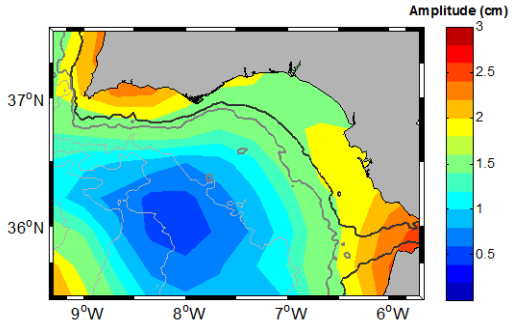

Fig. 1. Amplitude of the sea level residuals annual signal. Black thick line marks the 200 m isobath.

The amplitudes of the Alt_ASLA_{steric} annual signal (Fig. 1) were significantly reduced, with similar values (~2 cm) along the western and eastern shelves. Although these values are comparable to the AVISO errors, they present a clear annual signal that could be linked to the alongshore wind stress seasonal cycle following the meridional migration of the Azores high. Linear correlations between the sea level residuals yearly seasonal cycles and the local alongshore wind stress showed high and significant negative correlations along the eastern shelf (r~-0.4) and even higher along the western shelf (r~[-0.5,-0.6]). In addition, high positive correlations (r~0.5-0.6) were obtained with the across-shore wind stress over the western shelf, which is a region of strong cyclonic wind stress, and might indicate that, although the VANI2-ERA notably improve the barotropic response of sea level to wind stress within the GoC with respect to other hindcasts, they could be underestimating this effect over the western shelf. This shelf is very narrow and hence, an even higher resolution bathymetry should be used in the HAMSON model in order to accurately represent the (barotropic) sea level response to the local wind stress. As for the (much wider) eastern shelf, no correlations were obtained with the across-shore wind stress, indicating that the VANI2-ERA residuals correctly represent the barotropic response to the local wind forcing. The high correlations obtained with the alongshore wind stress suggest a baroclinic response not accounted for in the HAMSON model.

ACKOWLEDGEMENTS

This work has been partially supported by the ALCOVA Project (CTM2012-37839) funded by the Spanish Ministerio de Economía y Competitividad and the European Regional Development Fund (ERDF).

REFERENCES

1 - Laiz I, Tejedor B, Gómez-Enri J, Aboitiz A & Villares P, 2012. Spatial structure of the sea level seasonal cycle within the Gulf of Cadiz, *Rem. Sens. Oc., Sea Ice, Coast. Wat., and Large Wat. Reg.*: 85320S-85320S.

2 - Passaro M, Cipollini P & Benveniste J, 2015. Annual sea level variability of the coastal ocean: The Baltic Sea-North Sea transition zone. *J. Geophys. Res.*, 120(4): 3061-3078.

3 - Saraceno M, Simionato CG & Ruiz-Etcheverry LA, 2014. Sea surface height trend and variability at seasonal and interannual time scales in the Southeastern South American continental shelf between 27°S and 40°S. *Cont. Shelf Res.*, 91:82-94.

4 - Torres RR & Tsimplis MN, 2012. Seasonal sea level cycle in the Caribbean Sea. *J. Geophys. Res.*, 117: C07011.

5 - Vignudelli S, Cipollini P, Roblou L, Lyard F, Gasparini GP, Manzella GMR & Astraldi M, 2005. Improved satellite altimetry in coastal systems: case study of the Corsica Channel (Mediterranean Sea). *Geophys. Res. Lett.*, 32: L07608.

6 - Liu Y, Weisberg RH, Vignudelli S, Roblou L & Merz CR, 2012. Comparison of the X-TRACK altimetry estimated currents with moored ADCP and HF radar observations on the West Florida shelf. *Adv. Space Res.*, 50: 1085–1098.

7 - Dussurget R, Birol F, Morrow R & De Mey P, 2011. Fine resolution altimetry data for a regional application in the Bay of Biscay. *Mar. Geod.* 34(3–4): 447–476.

8 - Escudier R, Bouffard J, Pascual A, Poulain PM & Pujol, MI, 2013. Improvement of coastal and mesoscale observation from space: application to the northwestern Mediterranean Sea. *Geophys. Res.Lett.*, 40: 2148–2153.

9 - Gómez-Enri J, Escudier R, Pascual A & Mañanes R, 2015. Heavy Guadalquivir River discharge detection with satellite altimetry: The case of the eastern continental shelf of the Gulf of Cadiz (Iberian Peninsula). *Advances in Space Res.* 55(6): 1590-1603.

10 - Pascual, A, Marcos M & Gomis D, 2008. Comparing the sea level response to pressure and wind forcing of two barotropic models: Validation with tide gauge and altimetry data. *J. Geophys. Res.*, 113: C07011.

11 - Jordà G, Gomis D & Álvarez-Fanjul E, 2012. The VANI2-ERA hindcast of sea-level residuals: atmospheric forcing of sea-level variability in the Mediterranean Sea (1958-2008). *Sci. Mar.* 76 (S1), 133–146.

12 - Laiz I, Tejedor B, Gómez-Enri J, Aboitiz A & Villares P, 2016 . Contributions to the sea level seasonal cycle within the Gulf of Cadiz (Southwestern Iberian Peninsula). *J. Mar. Sys.*, 159: 55-66.

13 - Gómez-Enri J, Aboitiz A, Tejedor B, Villares & P, 2012. Seasonal and interannual variability in the Gulf of Cadiz: Validation of gridded altimeter products. *Est., Coast. and Shelf Sci.* 96: 114-121.

Ocean Observing Systems

Alicia Lavín Montero

[1] Centro Oceanográfico de Santander. Instituto Español de Oceanografía

ABSTRACT

Observation of the ocean has been traditionally a mission of oceanographers during precedent decades, systematic observations has been produced in the second part of the XX Century and in the later period a large number of automatic systems have been developed. Sea level measurements were performed first time in Spain by the Geographic Instituto in Alicante in 1874.

The Word Ocean Circulation Experiment (WOCE) makes unprecedented in-situ and satellite observations of the global ocean between 1990 and 1998 and to observe poorly-understood but important physical processes. Data from fixed platforms, drifters, profiling floats and oceanographic information were transmitted by satellite reached on real time the data and modelling Centres. Numerical model provide continuous forecast of future conditions of the Sea for as far ahead as possible, and the basis for forecast the climate change. Argo floats were the great success of the beginning of the XXI Century and a record was performed a few years late with 3000 Argo floats functioning around the ocean. This allows, for the first time, continuous monitoring of the temperature, salinity, and velocity of the upper ocean.

Gliders, high frequency radar, recopesca fishing ships, shelf moorings and floats as well as animal-borne systems complete the new observing systems. Global, regional or local modelling and new products from marine observation and modelling form the modern Operational Oceanography. Together with a strong effort on science and technology, exchange, quality and data management, validation and coordination. They support a wide range of applications including environment protection, marine spatial planning, fisheries, health, transport, climate change, sustainable development, civil protection and tourism.

The Intergovernmental Oceanographic Commission (IOC, UNESCO) supervise the Global Ocean Observing System. In this context a pan-European ocean observing network EuroGOOS was funded in 1994, and is organized in 5 Regional Associations that included the Atlantic (IBIROOS) and Mediterranean Spanish waters (MONGOOS). Spanish members of EuroGOOS are Puertos del Estado and IEO, IBIROOS (IEO, MeteoGalicia, PdE, Intecmar, AZTI, Basque Government), and MONGOOS (CSIC, IEO, PdE, SOCIB, LIM/UPC).

On the use of box models to explain the main features of Mediterranean marine climate projections

Josep Llasses[1], Gabriel Jordà[1] & Damià Gomis[1]

[1] IMEDEA (Universitat de les Illes Balears – CSIC), Mallorca, Spain

ABSTRACT

Box models can be an alternative to numerical models when it comes to understand the basic functioning of the climate system. Here they are used, first, to study the sensitivity of the Mediterranean basin to the surface and lateral (Gibraltar) heat and freshwater/salt fluxes. We show that if the forcing fluxes change at the rates projected by climate models, the Mediterranean Sea will drift towards new hydrographic states at a lower rate than the forcing. We also investigate the fate of the salinity of the basin in terms of the evolution of the freshwater deficit and of the incoming Atlantic waters. However, the evolution also depends on how the heat and salt exchanged with the atmosphere and the Atlantic Ocean are redistributed within the basin, which in turn depends on several physical processes that are often accounted for differently by numerical models. In the second part of this study the redistribution of heat and salt is investigated from an ensemble of 16 models. Combining the surface and lateral forcings with the changes in the heat and salt content of each layer it is possible to infer the transfer of heat and salt between layers. We have done it for each model and computed both the ensemble mean values and the spread. For some of the inter-layer heat and salt fluxes the spread of the values if of the same order than the ensemble mean, which explains why different models produce different climate projections.

INTRODUCTION

Numerical models are a powerful tool for process-oriented studies in the ocean. At climate scale, the complexity of the models and the length of the runs (from decades to centuries) greatly increase the computational cost of the simulations, Regional Climate Models (RCMs) dealing with the Mediterranean Sea have an additional handicap: they need a high spatial resolution in order to represent crucial processes such as deep water formation or the fluxes through Gibraltar. This makes that sensitivity studies or studies aimed to investigate the differences between the projections can hardly be undertaken in a reasonable time. A simple alternative to carry out such studies is the use of box models. Here we do it for two, related studies.

In a first step we investigate the sensitivity of the future evolution of the Mediterranean basin with respect to the evolution of the heat, salt and freshwater exchanged with the atmosphere and the Atlantic Ocean. Regarding the salinity, for instance, most RCMs project an increase due to the increasing freshwater deficit, but some models show that salinity could decrease if the future incoming Atlantic waters are fresher than at present. The box model can help to bound the Atlantic salinity below which it would compensate the increase of the freshwater deficit.

In a second step we study the heat and salt redistribution within the Mediterranean Sea. The motivation for doing this is that the evolution of the basin not only depends on the external forcing, but also on how the heat and salt exchanged with the atmosphere and the Atlantic Ocean are redistributed within the basin. In turn, this depends on several physical processes that are accounted for differently by numerical models, which could therefore explain the differences between climate projections.

MATERIAL AND METHODS

For the first study we use the surface heat and freshwater fluxes from NEMOMED8, a state-of-the-art RCM. Here we consider the Mediterranean Sea as a single 3-layer basin: the first layer (0-150m) exchanges freshwater and heat with the atmosphere, and heat and salt with the Atlantic Ocean; the second layer (150-600m) is only connected with the Atlantic Ocean; the deepest layer (600m-bottom) is isolated from both the atmosphere and the open ocean. Three processes allow the exchange of heat and salt between layers: turbulent mixing (between layers 1 and 2 and between layers 2 and 3), intermediate water formation (between layers 1 and 2) and deep water formation (between layers 1 and 3). These processes are simulated in such a way that the box model correctly reproduces the temperature and salinity of the three layers when these are forced with the surface and Gibraltar heat and salt fluxes observed during the XX century. For the XXI century we can make the surface and Gibraltar fluxes to evolve in time under different scenarios, obtaining for each of them the evolution of the temperature and salinity at each layer.

For the second study we use an ensemble of 16 model simulations: 14 from the Med-CORDEX ensemble (available from www.medcordex.eu), a global reanalysis and a regional reanalysis. In this case we dispose 4 layers (layer 3 of the previous model is divided into two layers: 600-1000m and 1000m-bottom) for each of the two Mediterranean sub-basins, which results in an 8-compartment box model. Of the budget equations set for every layer (which relate the fluxes through all boundaries with the changes in the heat and salt content of the layers) we know the surface fluxes, the fluxes through Gibraltar and Sicily, and the evolution of the heat and salt contents of the layers. The only missing components are the vertical fluxes between layers, which can therefore be inferred from the equation system. Doing it for each model we can produce ensemble mean values and the ensemble spread. And correlating the fluxes with parameters representing different physical processes we can attempt to explain the inter-model differences in terms of how physical processes are accounted for in different numerical models.

RESULTS

From the first study we learn that if during the XXI century the forcing fluxes change at the rates projected by state-of-the-art climate models, the Mediterranean Sea will drift towards new hydrographic states at a lower rate than the forcing itself. That is, the basin will not be at any time in the equilibrium state corresponding to the forcing. If after several decades of increase the forcing fluxes would reach a stable level, it would take decades/centuries until the upper/lower layers reach the new equilibrium state.

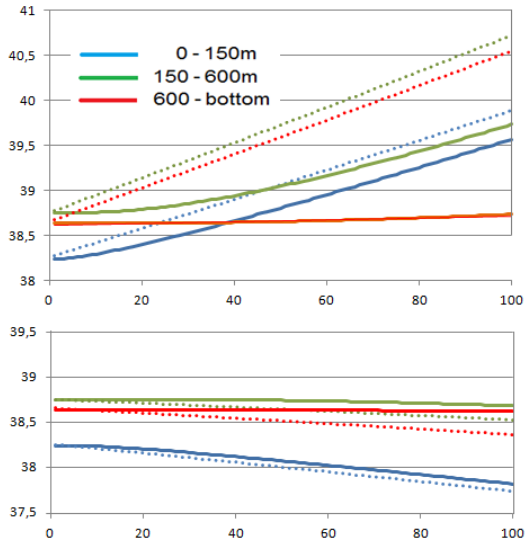

Fig. 1. Evolution (2000-2100) of Mediterranean salinity assuming that: i) the salinity of the incoming Atlantic water is 36.5 along the whole century (upper plot); ii) the Atlantic salinity evolves from 36.5 in 2000 to 35.0 in 2100 (lower plot). In both cases the freshwater deficit of the basin has been set to increase from 63 cm/yr in 2000 to 92 cm/yr in 2100. The dashed lines are the (never reached) equilibrium states corresponding to the forcing at each time.

A second result is that the expected increase in the freshwater deficit (from the ~63 cm/yr of 1970-2000 to the ~92 cm/yr projected for 2070-2100 under scenario A2) would result in a marked salinity increase, provided that the incoming Atlantic waters have the same salinity that at present (~36.5). However, if the Atlantic salinity decreases below ~35.5 by the end of this century (e.g. due to the spread of fresh waters from ice melting at high latitudes), then the salinity of the basin would decrease (Fig. 1).

From the second study, a major result is the plot that summarizes the ensemble mean and the ensemble spread of the fluxes exchanged with the atmosphere, with the Atlantic Ocean and between layers (Fig. 2). Concerning the inter-later fluxes, the model spread is larger than the ensemble average for the mean heat and salt transfers at all depths due to discrepancies in the vertical gradients of temperature and salinity. The seasonal and interannual variations show less spread than the mean values. Most models are correlated in terms of the interannual variations of heat transfer between the first and second layer; the reason is that surface heat fluxes, which are well correlated among models, explain most of the variability of that layer. Conversely, the salt transfer between the first and second layers is less similar among models. For the deeper layers some models show a good agreement among them, while others behave differently from all the others. The spread in the trends of the fluxes is very large for both, heat and salt.

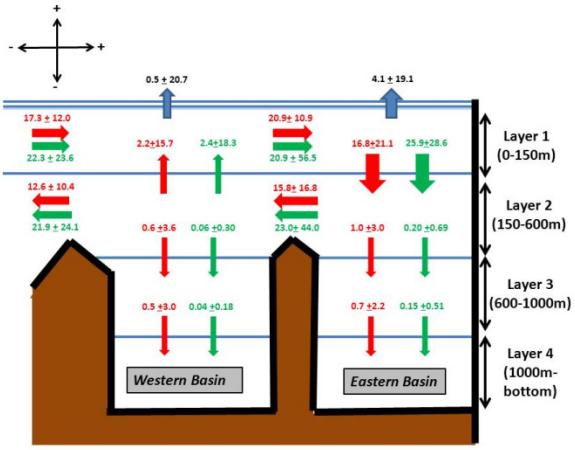

Fig. 2. Ensemble mean value and ensemble spread for the heat and salt fluxes of the 8-compartment box model of the Mediterranean Sea. They have all been computed for the period 1980-2000. Heat fluxes are in red (units are W/m^2), while salt fluxes are in green (units are 10^6kgS/s).

ACKNOWLEDGMENTS

This is a contribution to the HyMeX and Med-CORDEX programs through the CLIMPACT (CGL2014-54246-C2-1-R) and CLIFISH (CTM2015-66400-C3-2-R) projects funded by MINECO. G. Jordà acknowledges a Ramón y

Cajal contract (RYC-2013-14714) funded by MINECO and the government of the Balearic Islands. We also acknowledge the contributions of F. Adloff, D. Macías, A. Harzallah, T. Arsouze, N. Akthar, L. Li, A. Elizalde and G Sannino to the paper outgoing from this work.

Wind-induced surface circulation in the Ebro Delta shelf: evidences from HF radar data and IBI forecasting system estimations

Pablo Lorente[1], Silvia Piedracoba[2], Javier Soto-Navarro[1], Marcos G. Sotillo[1] & Enrique Álvarez-Fanjul[1]

[1] Puertos del Estado, Madrid.
[2] Dpto. de Física Aplicada - Facultad de Ciencias - Universidad de Vigo, Pontevedra.

ABSTRACT

Quality-controlled remotely-sensed surface current observations from a High Frequency radar (HFR) network deployed in the Ebro River Delta (NW Mediterranean) were combined with outputs from IBI operational ocean forecasting system in order to comprehensively portray the ocean state and its variability during 2014. The EOF analysis confirmed that the modeled surface current field evolved both in space and time according to three significantly dominant modes of variability which accounted for the 49.2% of the total variance, in close agreement with the results obtained for HFR (46.1%). The response of the subtidal surface current field to prevailing wind regime in the study area was examined in terms of induced circulation structures and immediacy of reaction by performing a conditional averaging approach and a time-lagged vector correlation analysis, respectively. The wind-current interaction was maximized when the former blew toward SE or NE. This data-model synergistic approach has demonstrated to be valid to describe the complex coastal circulation in the Ebro Delta shelf despite the observed model drawbacks in terms of reduced energy content in surface currents and some inaccuracies in the wind-driven low frequency response. Notwithstanding, IBI has proved to be a consistent large-scale "father" system, able to resolve the background mesoscale shelf circulation, reproduce monthly patterns faithfully in terms of mean and variance and thus be able to provide coherent open boundary conditions to nested fine-resolution coastal models implemented within the frame of SAMOA (Sistema de Apoyo Meteorológico y Oceanográfico de la Autoridad Portuaria) project.

INTRODUCTION

The Ebro River Delta is one the largest and most biodiverse aquatic ecosystem in the western Mediterranean Sea (Fig. 1-a). A 13.5 MHz CODAR SeaSonde High Frequency radar (HFR) was deployed in December 2013 to monitor coastal waters and support marine domain awareness. HFR-derived observations have been combined with IBI model outputs (Fig. 1-b) since this integrated approach can provide a comprehensive characterization of the highly dynamic coastal circulation and gain from the complementary nature of both systems.

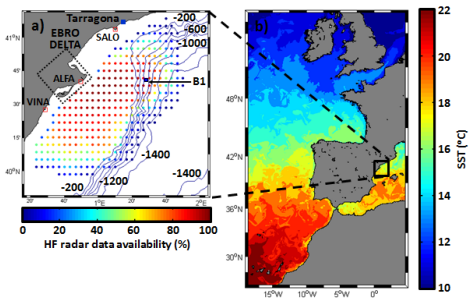

Fig. 1. (a) HFR deployed at the Ebro Delta. Colored dots denote the temporal coverage (%) of HFR current total vectors for 2014. Isobath depths are labeled every 200 m. Locations of Tarragona buoy (B1) and Tarragona harbour are marked with blue solid squares. (b) Example of an hourly sea surface temperature map predicted by IBI.

The main objective of this work is twofold. Firstly, to verify IBI capabilities in reproducing the prevailing circulation features derived from HFR observations and previously reported in [1], namely: the predominant density-driven southwestward (SW) flow, the Ebro River impulsive-type freshwater discharge or the coastal clockwise eddy confined south of Ebro Delta mouth. Lastly, to investigate the relative contribution of local wind as one of the main forcing mechanisms typically associated with estuarine–ocean exchange and its importance as a predominant driving agent in Ebro Delta shelf.

The ultimate goal is to evaluate the potential of IBI as a consistent parent forecast system able to propagate the large-scale dynamics into a coastal fine-resolution OOFS through coherent open boundary conditions. A downscaling approach is currently being implemented to operationally monitor the circulation in Port of Tarragona and the Ebro Delta area, and capture small-scale coastal interactions, which are not always properly represented in coarser resolution OOFSs. This initiative has been launched within the frame of SAMOA (Sistema de Apoyo Meteorológico y Oceanográfico de la Autoridad Portuaria)

project, co-funded by Puertos del Estado (PdE) and 18 Spanish Port Authorities and aimed at putting in place an integrated suite of high-resolution meteorological and coastal hydrodynamic models in order to produce refined port-scale forecasts and increase the efficiency of marine operations in ports and harbours.

DATA & METHODOLOGY

Monthly averaged maps of Eulerian surface currents and Eddy kinetic energy (EKE) have been calculated for HFR and IBI to explore the prevalent circulation patterns during 2014. In addition, a complex Empirical Orthogonal Function (EOF) decomposition has been used to explore the driving forces and spatiotemporal scales behind the variability of sea surface currents. The representative spatial patterns (or EOF modes) and their corresponding temporal coefficients or principal components (PCs, which describe the evolution of the modes) are determined by using the singular value decomposition of the covariance matrix. EOF analysis has been applied to HFR and IBI current velocity datasets using the raw (unfiltered) hourly time series for the entire year 2014. Main spatial modes obtained have been interpreted in terms of physical processes related to the detected spatially coherent structures.

Complementarily, the flow response has been investigated by comparing the PCs associated with IBI and HFR with the PCs of hourly local wind registered at B1 buoy during May-October 2014. The correlation coefficient has been also calculated for the winds in all directions to determine the angle for which the relationship is maximized. Finally, the association between wind and flow variability has been studied for wind data and sub-surface currents measured at B1 and surface velocity estimations provided by HFR and IBI at the nearest grid point. To this purpose, a time-lagged complex correlation analysis has been used to explore the current response for a 24-hour interval.

RESULTS AND DISCUSSION

The sequence of monthly averaged current maps reveals the resemblance between HFR data and IBI modeled currents in terms of main circulation features in the study-area, in spite of some discrepancies found in October. During the spring, the SW shelf-slope jet and the Ebro River impulsive-type freshwater outflow are clearly evidenced, although higher velocities are detected for HFR. Equally, the confinement of a coastal anticyclonic eddy in the south of Ebro Delta can also be observed in radar and modeled data. With regards to the variability of the flow, monthly-averaged maps of EKE exhibit similar spatial distribution along 2014.

The EOF analysis confirmed that the surface current field evolved in space and time according to three dominant modes of variability, which accounted for the 46.1% (49.2%) of the total variance in the case of HFR (IBI). A year-round overall prevailing SW shelf-slope jet is described by the first mode, which basically captures the North Current pathway. EOF-1 represents the 21.6% and 26% of the total variance for HFR and IBI, respectively. The other two HFR (IBI) modes are superimposed onto EOF-1, accounting for the 15.3% (17.2%) and 4.7% (6%) of the variance, respectively. The second mode captures the cross-shelf circulation, with a well-defined offshore-directed flow perpendicular to EOF-1. The third mode adds some heterogeneity to the basic uniform patterns represented by the first two modes, since it introduces curvature to the current field.

Linear correlation coefficients have been computed between the principal components (PCs) related to the two main EOF modes of variability of local wind at B1 and the first two PCs associated with both modeled and radar-derived currents. Although the first two HFR EOF modes have been found to be significantly influenced by local wind, only the IBI PC1 appeared to be correlated with the wind forcing.

Moreover, the flow response is examined by comparing the principal components of HFR and IBI with the wind projected onto each propagation direction in order to infer the angle for which the correlation coefficient reaches a peak. The wind-current interaction was maximized when the former blew toward SE (NE) in the case of PC1 (PC2) – i.e., when the main flow moves SW (SE)-, suggesting the existence of an Ekman-like response of the surface circulation by shifting to the right of local wind.

Complementarily, the time-lagged vector correlation analysis shows the prompt current response to wind forcing. The correlation peak is observed between 0-hour and 3-hour time lag, and is followed by the decay in correlation amplitude, steeper in the case of HFR.

Since IBI seemed not to properly reproduce the observed circulation patterns related to along-shore winds, data-model discrepancies have been in part attributed to the existence of both a wind speed overestimation and also a phase mismatch between the modeled and observed inertial signal. Some of the limitations detected in IBI performance have also been hypothesized to be partially related to the spatiotemporal resolution of the wind field used as forcing mechanism of the surface circulation. This issue has been recently addressed during the pre-operational implementation of the SAMOA fine-scale coastal forecasting system, which is nested to IBI and forced with a higher resolution atmospheric model, based on HIRLAM and provided by AEMET. Likewise, some IBI system shortcomings could also be attributable to the large-scale offshore circulation in the entire Mediterranean basin not included in the present numerical configuration

ACKNOWLEDGMENT

The authors gratefully acknowledge Qualitas Remos Company for their useful suggestions.

REFERENCES

1 - Lorente P, Piedracoba S, Soto-Navarro J & Alvarez-Fanjul E, 2015. Evaluating the surface circulation in Ebro Delta (NE Spain) with quality controlled High-Frequency radar measurements. *Ocean Science*, Vol. 11, pp. 921-935

Multi-parameter ocean model skill assessment: from regional (CMEMS IBI) to coastal scales

Pablo Lorente[1], Marcos G. Sotillo[1], Arancha Amo-Balandrón[1], Roland Aznar[1], Álvaro Pascual[1] & Enrique Álvarez-Fanjul[1]

[1] Puertos del Estado, Madrid.

ABSTRACT

This work showcases the multi-parameter skill assessment of IBI operational ocean forecasting system using a variety of observational networks, encompassing both in situ (moorings and tide-gauges) and remote-sensing instruments (satellite and High-Frequency radar). IBI performance is routinely monitored by means of NARVAL (North Atlantic Regional VALidation) web-based tool. In particular, class-1 and class-2 metrics are computed in concert to quantitatively evaluate the quality of hourly IBI 'best estimate' surface fields. NARVAL also allows the intercomparison of different model solutions in overlapping areas and quantify the added value of downscaling approaches in coastal areas. According to the skill metrics obtained, IBI has proven to be a robust model solution, able to act as a consistent large-scale "father" system in future downscaling approaches by providing coherent open boundary conditions to nested high-resolution coastal models.

INTRODUCTION

Operational ocean forecasting systems (OOFSs) are nowadays used as predictive tools assist high-stakes decision-making related to marine safety, water quality and mitigation of hazards in the coastal environment. In addition, a combined use of multi-platform observing systems provides a supportive framework to enhance the permanent monitoring of coastal areas, essential from diverse socioeconomic and societal concerns.

In this context, a synergistic approach based on the integration of numerical models and observational networks has positively proved its usefulness to comprehensively characterize the highly dynamic coastal circulation and the related complex interactions. In the present work, particular attention is focused on the benefits of using a broad mix of instrumental networks for the rigorous multi-parameter skill assessment of IBI (Iberia-Biscay-Ireland) regional circulation model [1], a NEMO-based operational application implemented within the frame of MyOcean projects and the Copernicus Marine Environment Monitoring Service (CMEMS).

The validation against independent measurements constitutes a core activity in oceanographic operational centers since it aids:

i) To infer the relative strengths and weaknesses in the modeling of several key physical processes and to deepen the understanding of discrepancies in model predictions.

ii) To compare different versions of the same OOFS and evaluate potential improvements and degradations before a new version is transitioned into operational status.

iii) To compare coarse resolution 'father' and nested high-resolution 'son' systems to quantify the added value of downscaling.

iv) To perform intercomparison exercises between different model solutions in the overlapping areas at diverse timescales.

The development of skill assessment software packages and dedicated web applications is a relatively novel theme in operational oceanography. In particular, the quality of IBI forecast products is assessed by means of NARVAL (North Atlantic Regional VALidation) web-based tool, which has been previously described in detail in [1]. This tool has been implemented to routinely monitor IBI performance and to objectively evaluate model's veracity and prognostic capabilities. Both real-time validation and regular-scheduled delayed-mode validation are performed using a wealth of independent observational sources as reference benchmark. Product quality indicators and skill metrics are automatically computed not only averaged over the entire IBI domain but also over specific sub-regions of particular interest from a user perspective in order to infer IBI accuracy and the spatiotemporal uncertainty levels.

The main goal of this work is twofold. Firstly, to quantitatively assess the skill of IBI OOFS performance for a range of physical parameters (SST, SSC and SSH, respectively) This work mainly concentrates on class-1 and class-2 metrics which aid to determine the consistency and quality of the hourly mean IBI best estimates fields (i.e, hindcast).

DATA & METHODOLOGY

A variety of multi-platform observatories encompassing both in situ (moorings and tide-gauges) and remote-sensing instruments (satellite and four High-Frequency radars) are available to adequately sample IBI study domain in near real-time.

Class-1 diagnostics gathers 2-D daily fields bilinearly interpolated into a common ore refined horizontal grid for the same geographic location (Fig. 1). Some traditional statistical variables such as the model mean error, scalar root mean squared error (RMSE) and correlations, complex correlations and Taylor diagrams have been computed.

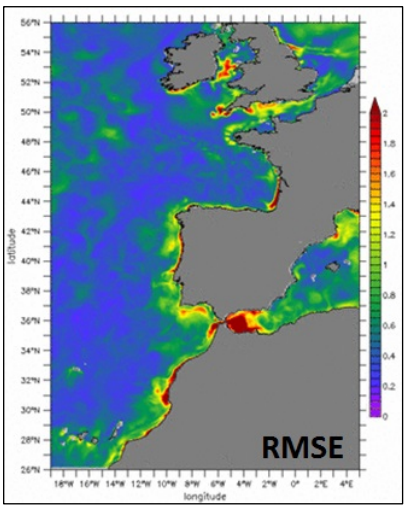

Fig. 1. Example of class-1 validation of sea surface temperature predicted by IBI against OSTIA L4 satellite-derived product for summer 2015.

NARVAL has been also implemented to carry out direct comparison of model outputs with quality-controlled time series of in-situ observations at specific locations (i.e., class-2 metrics). To this aim, the skill assessment software ingests daily model forecasts, extracts the time series on the four grid points closest to the in-situ sensor and performs a bilinear interpolation over its exact location. Both modeled and observed datasets are inserted into a relational database for a long-term storage and subsequently retrieved and visualized through an intuitive georeferenced web interface thanks to a calendar-based access. This interactive approach allows computing a variety of class-2 metrics to validate IBI system products in coastal areas (Fig. 2).

RESULTS AND DISCUSSION

According to the skill metrics obtained and assuming there are inherent constraints that restrict the data-model approach (i.e., sensor limitations, instrumental noise, differences in depth sampling, small-scale energetic processes unresolved by the model, etc.), IBI has proven to be a robust OOFS.

IBI can act as a consistent large-scale "father" system by providing coherent open boundary conditions (in terms of faithful representation of the background mesoscale shelf circulation) to nested high-resolution coastal models. A downscaling approach is currently being adopted to implement finer-solution OOFSs in order to produce high-quality port-scale forecasts. This initiative is carried out under the umbrella of SAMOA (Sistema de Apoyo Meteorológico y Oceanográfico de la Autoridad Portuaria) project, aimed at implementing a fully integrated monitoring service to increase safety and efficiency of marine operations in the Spanish ports and harbours.

Complementarily, this new web module of NARVAL allows judging the strengths and weaknesses of different OOFSs by means of a rigorous intercomparison between a global (Global system) and regional (IBI) configurations, dynamically embedded in the former.

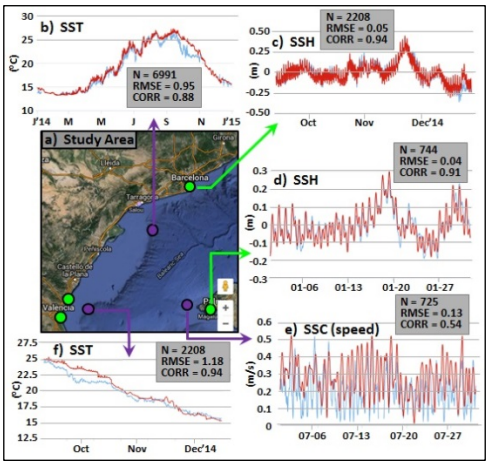

Fig. 2. (a) Study-area (NW Mediterranean), where three buoys (purple dots) and four tide-gauges (green dots) can be found. (b-f) Examples of the multi-parameter validation of IBI performance (red lines) against in situ observations (blue line) on a different time basis. Class-2 metrics gathered in grey boxes. N denotes the number of available observations.

Since data assimilation provides the integrative framework for maximizing the joint utility of observations and OOFSs, an ocean data assimilation scheme has been scheduled to be incorporated in future operational versions of IBI. By April 2018, satellite products (SST and SSH) and CORA (Coriolis Ocean database ReAnalysis) datasets (including ARGO, gliders, etc) are expected to be routinely assimilated in order to enhance IBI predictive skills.

Finally, noticeable efforts are in progress to define meaningful skill metrics, required on both scientific and policy-making fronts, to quantitatively assess the quality of OOFS products and to synthesize different aspects of system performance together (target diagrams, cost functions, etc.).

REFERENCES

1 -Sotillo MG, Cailleau S, Lorente P, Levier B, Aznar R, Reffray G, Amo-Baladrón A, Alvarez-Fanjul E, 2015. The MyOcean IBI Ocean Forecast and Reanalysis Systems: Operational products and roadmap to the future Copernicus Service. *Journal of Operational Oceanography*. Vol. 8, Issue 1: 1-18.

Caracterización de la Corriente de Gravedad de Bransfield (Antártida) a partir de distribuciones de temperatura superficial del mar

Ángeles Marrero-Díaz[13], Carolina Salinas-Núñez[2] & Pablo Sangrà[23]

[1] Universidad de Las Palmas de Gran Canaria, Departamento de Física, Las Palmas de Gran Canaria, Spain
[2] Universidad de Las Palmas de Gran Canaria, Instituto Universitario de Oceanografía y Cambio Global, Las Palmas de Gran Canaria, Spain
[3] Universidad de Las Palmas de Gran Canaria, Facultad de Ciencias del Mar, Las Palmas de Gran Canaria, Spain

RESUMEN

Debido a la enorme dificultad logística para realizar campañas oceanográficas en la zona durante el invierno antártico, la circulación en el Estrecho de Bransfield sólo ha podido ser estudiada a partir de datos obtenidos a finales de primavera y durante el verano antártico. La posibilidad de combinar datos de diferentes sensores satelitales, han permitido obtener productos de SST a la largo de todo el año, con una resolución espacial de 9km. En este trabajo se han utilizado estos datos para dar la primera caracterización de la distribución de la SST en el Estrecho de Bransfield y alrededor de las Islas Shetland del Sur (SSI), pudiendo establecer dos periodos climáticos de 4 meses de duración: el cálido, altamente variable; y el frío, totalmente homogéneo superficialmente; y dos periodos de transición, de dos meses cada uno. Por otro lado, la realización de este trabajo ha permitido reforzar la hipótesis de la Corriente de Bransfield es una corriente de gravedad de descarga que aparece a finales de diciembre cuando el agua procedente del mar de Bellinghausen puede acceder al Estrecho de Bransfield como una corriente de gravedad superficial que circula apoyada sobre el talud sur de las SSI, para continuar rodeando el archipiélago y circular por la plataforma y talud norte de SSI en lo que trabajos recientes han denominado Corriente de Gravedad de Bransfield (Bransfield Gravity Current). La posibilidad de monitorizar la SST a lo largo del año ha permitido establecer que la Corriente de Bransfield desaparece a finales del verano antártico.

Near-inertial waves trapping and deep mixing in an open ocean anticyclonic eddy

Antonio Martínez-Marrero[1], Pablo Sangrà[1], Sheila N. Estrada-Allis[2], Ángel Rodríguez-Santana[2], Borja Aguiar-González[5], Ángeles Marrero-Díaz[2], Eric D. Barton[4], Enric Pallàs-Sanz[3], Bàrbara Barceló-Llull[1], Carmen Gordo[1], Diana Grisolía[1], Luis Cana[1]

[1] Instituto de Oceanografía y Cambio Global, IOCAG, Universidad de Las Palmas de Gran Canaria, Gran Canaria, Spain
[2] Departamento de Física, Universidad de Las Palmas de Gran Canaria, ULPGC, Gran Canaria, Spain
[3] Departamento de Oceanografía Física, CICESE, Ensenada, México
[4] Instituto de Investigaciones Marinas, CSIC, Vigo, Spain
[5] Royal Netherlands Institute for Sea Research, NIOZ, Department of Ocean Systems Sciences and Utrecht University, Den Burg, Texel, the Netherlands

ABSTRACT

Ocean velocity structure inside an open ocean anticyclonic eddy is studied using SADCP, CTD, microstructure profiler and drifter data obtained during the PUMP survey carried out in September 2014. The presence of trapped near-inertial waves (NIW's) characterized by vertical wavelengths of around 250 m and upward phase velocities, are found at the base of the eddy, from 400 to at least 720 m depth. The low values of the Richardson number produced by the shear associated to these trapped waves, and the high turbulent kinetic dissipation rates obtained at the upper bound of the trapped NIW's layer indicate the production of deep turbulent vertical mixing. Wavelet analysis of Lagrangian velocities obtained from two drifters dragged below the mixed layer at 100 and 150 m depth, evidence red-shifted changes of the effective Coriolis frequency produced by variations of the angular velocity of the eddy as predicted by the theory. The near–inertial energy showed by the wavelet spectrogram at the moment of the survey is low compared with the energy observed during the subsequent months in which the drifters were inside the eddy. Both results suggest that the trapped waves and the induced deep mixing might have occurred continuously during the westward propagation of the eddy. Our findings indicate that trapping of NIW's in open ocean eddies could be important for understanding the diapycnal mixing in the ocean interior and ultimately, the pathways of the meridional overturning circulation.

Interactions between the upper ocean and the lower atmosphere in the Brazil-Malvinas Confluence region

Marta Masdeu[1], Josep L. Pelegrí[1] & Pablo Sangrà[2]

[1] Departament d'Oceanografia Física i Tecnológica, Institut de Ciències del Mar, CSIC, Barcelona
[2] Departamento de Física Aplicada, Universidad de Las Palmas de Gran Canaria, Las Palmas de Gran Canaria

ABSTRACT

Recent studies have shown that sea surface temperature (SST) and surface wind speed (SWS) are directly related at ocean mesoscales (10-100 km). Here we examine this relationship in the Brazil-Malvinas Confluence region, where we find one of the most intense regional-scale SST gradients in the world's oceans. We analyze SST and SWS collected in situ during an oceanographic cruise done in March 2015. Data is processed to emphasize the variability of SST and SWS associated with oceanic fronts, both at regional and mesoscalar scales, taking into account the latitudinal SST gradients, the passage of atmospheric synoptic disturbances, and the diurnal variability of SWS. We observe that SST has an influence on SWS – a temperature raise of 1ºC involves a wind-speed increase of 0.36 m s^{-1}, with a correlation coefficient of 0.43 and a 95% confidence level – a relationship that is corroborated using wind data from the European Copernicus Project. Finally, we assess the influence of SST on the lower atmosphere through the changes in sensible and latent heat fluxes across the front. The results point at the existence of significant coupling between the upper ocean and the lower atmosphere.

INTRODUCTION

Ocean and atmosphere have different synoptic scales: in the atmosphere these are ~1000 km and a few days but in the ocean they are ~100 km and weeks. This means that we usually think on the atmosphere as influencing the ocean's variability only at short time and long spatial scales, but playing little or no role at spatially short scales. However, this argument ignores the possibility of feedback mechanisms. Indeed, recent work [1, 2] has pointed at the potential importance of these feedback mechanisms, in such a way that changes in the sea surface temperature (SST) would affect the structure of the lower atmosphere and alter the surface wind speed (SWS), hence potentially affecting back to the upper ocean. Our study seeks to explore precisely this interaction in a region where the oceanic system exhibits an intense and well defined surface front: Brazil-Malvinas Confluence (BMC) region.

The BMC is the encountering region between the Malvinas Current (MC), a northward branch of the Antarctic Circumpolar Current, and the Brazil Current (BC), a southward western boundary current of the South Atlantic subtropical gyre. The thermal contrast between these two currents, or surface front, makes the BMC as an ideal area to study the short-space coupling between the upper ocean and lower atmosphere: the surface waters of the MC are cold (<7ºC during the austral summer), much more than the warm waters (>26°C) of the surface BC [3]. In particular, we expect that this thermal front (some 15ºC in about 30 km) will drive substantial spatial variations in ocean-atmosphere heat exchange [1, 3, 4, 5]. Hence, our objective is double: first, to take advantage of such a unique setting in order to determine the existence of significant SST-SWS relationships and, second, to compute the heat fluxes between ocean and atmosphere that could drive the changes of the lower atmosphere and hence the intensity of the SWS.

MATERIAL AND METHODS

The research vessel BIO Hesperides carried out the TIC-MOC cruise from 5 to 30 March 2015, departing from Ushuaia (Argentina) and arriving at Salvador de Bahia (Brazil). The BMC was sampled from 12 to 22 March, crossing the surface front 11 times.

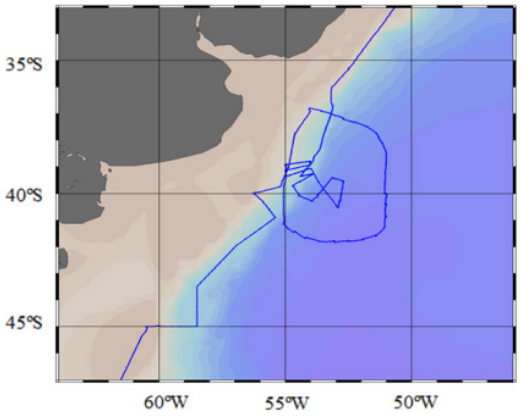

Fig. 1. Trajectory by BIO Hesperides, from SW to NE.

The study area is located between 36ºS-43ºS and 51ºW-57ºW, approximately southeast of Rio de la Plata, outside of the continental shelf and continental slope. The cruise included an initial outer transect followed by an inner mesh (Fig. 1). For our calculations we use the SST data as obtained from the ship's thermosalinograph and the meteorological data as determined by the ship's met-station (at a reference level of 10 m above sea level).

We process the data in order to reduce all those factors that may influence the SST and SWS values at other scales different from the frontal scales: the SST changes because of the ship's motion from high to low latitudes, and the SWS varies as a result of both the passage of frontal systems and the diurnal wind cycle. With this purpose, we follow two steps. First, we search for a low-frequency polynomial filter that removes the synoptic and long-term variations. A key aspect of this calculation is to select the correct polynomial order, such that it properly represents the variability related to atmospheric processes but does not follow the abrupt SST and SWS changes associated with ocean front; from the correlation between the original and adjusted series, we choose a polynomial of order 6 for the SWS and of order 3 for the SST as the best options. The residual time series is then obtained by subtracting the original series to the polynomial adjustment. Second, we average three days of the residual time series prior to arriving to the confluence region so as to produce a daily cycle. We then consider this cycle as characteristic for the entire BMC region, and subtract it to the residual time series in order to produce a new residual time series.

The sensible heat flux (SHF) and latent heat flux (LHF) are calculated from standard bulk formulae [6]. These expressions depend on the SST as well as on variables determined with the ship's meteorological station (wind speed, air density, specific and saturation specific humidity, air temperature, mean surface wind speed.

RESULTS AND DISCUSION

We focus our analysis on the 17-19 March, when the vessel sampled the frontal region with major intensity. During this time period, the residual SWS and SST time series display similar patterns, with coincident SST and SWS minima (Fig. 2). The Pearson correlation coefficient between both variables is 0.428 (calculated with a confidence level of 95%); a Pearson correlation coefficient between 0.3 and 0.5 reflects the existence of a moderate relationship [7].

We conclude that the large contrasts in SST between the subtropical and subantarctic waters lead to substantially different heat fluxes from the ocean to the atmosphere, increasing over the warmer waters. This affects the stability of the marine atmospheric boundary layer (the greater the fluxes the larger the vertical mixing) and therefore produces an increase in SWS.

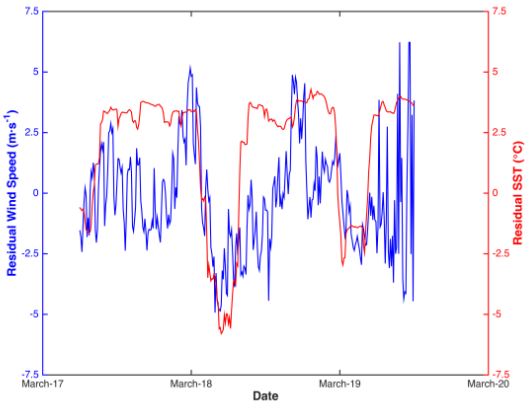

Fig. 2 . Residual SST time series (ºC, red line) and residual SWS (m s^{-1}, blue line) over the frontal region.

AKNOWLEDGMENTS

We are very grateful to the crew, technicians and scientists in the R/V Hesperides, whom made possible the gathering of the data set used in this communication. This research has been supported by the Ministerio de Economía y Competitividad of the Spanish Government through projects TIC-MOC (CTM2011-28867) and VA-DE-RETRO (CTM2014-56987-P).

REFERENCES

1 - Xie SP, 2004. Satellite observations of cool ocean–atmosphere interaction. *Bull. Amer. Meteorol. Soc*., 85, 195–208.

2 - Chelton DB & Xie SP, 2010. Coupled ocean-atmosphere interaction at oceanic mesoscales. *Oceanogr*., 23, 52–69.

3 - Saraceno M, Provost C, Piola AR, Bava J & Gagliardini A, 2004. Brazil-Malvinas frontal system as seen from 9 years of advanced very high resolution radiometer data. *J. Geophys. R*es., 109, C05027.

4 - Chelton DB, Schlax MG, Freilich MH & Milliff RF, 2004. Satellite radar measurements reveal short-scale features in the wind stress field over the world ocean. *Sci*., 303, 978–983.

5 - O'Neill LW, Chelton DB & Esbensen SK., 2012. Covariability of surface wind and stress responses to sea surface temperature fronts. *J. Clim*., 25, 5916–5942.

6 - Fairall CW, Bradley EF, Rogers DP, Edson JB, Young GS, 1996. Bulk parametrization of aie-sea fluxes for Tropical Ocean-Global Atmosphere Coupled-Ocean Atmosphere Response Experiment. *J. Geophys. Res.,* 101, 3747-3764.

7 - Cohen J, 1988. *Statistical Power Analysis for the Behavioral Sciences* (2nd ed.). Lawrence Erlbaum, New Jersey, 567 pp.

Monitoring the hydrological characteristics of the Mediterranean Outflow. A decade of θ-S data in the bottom layer of the Espartel Sill, Strait of Gibraltar

Cristina Naranjo[1], Jesús García Lafuente[1], Simone Sammartino[1], José Carlos Sánchez Garrido[1] and Ricardo Sánchez Leal[2]

[1] Grupo de Oceanografía Física de la Universidad de Málaga. Departamento de Física Aplicada II. Campus de Excelencia Internacional del Mar, CEIMAR.
[2] Instituto Oceanográfico Español, Centro Oceanográfico de Cádiz, Campus de Excelencia Internacional del Mar, CEIMAR.

ABSTRACT

A long time series of temperature and salinity have been collected near the seafloor of the Strait of Gibraltar since 2004 until now. Data show a continuous positive temperature trend of the Mediterranean outflow, 0.0055ºC/yr, coinciding with the order of magnitude of the trend reported by other authors in the western basin. With respect to salinity, data show also a positive trend, $1x10^{-4}$psu/yr, nevertheless this trend is one order of magnitude smaller than the one reported for the western basin. Therefore the contribution of the Mediterranean outflow to the global circulation is now warmer and saltier than a decade before.

INTRODUCTION

The Mediterranean outflow is being monitored at the western exit of the Strait of Gibraltar since 2004. The monitoring station is located in the Espartel Sill, 35º 51.709' N and 5º 58.217' W (Fig. 1), and has been maintained by the Oceanography Group of the University of Málaga, the Spanish Institute of Oceanography (IEO) and the Science Marine Institute of Andalucía (ICMAN). The mooring line collects data of temperature and salinity near the seafloor, therefore measuring the densest outflowing water. Several works have dealt with the long term temperature and salinity trend in different basins of the Mediterranean Sea [1, 2, 3, 4, 5], and they all agree that the Mediterranean has been getting warmer and saltier in the last 40 years. Nevertheless no long term estimation has been presented yet in the Strait of Gibraltar. The present work analyzes an 11 year long temperature and salinity series in the Espartel Sill (Fig. 1), the last constriction the Mediterranean outflow found in its way toward the Atlantic Ocean.

MATERIAL AND METHODS

As mentioned above, the mooring line is located at the Espartel Sill (Fig. 1) at a mean depth of 362±4.6 meters, it is a short line with a total length of about 20 meters. The line consists of an up-looking Acoustic Doppler Current Profiler (ADCP) located about 17 meters above the seafloor, two SAMI sensors measuring the CO_2 and pH, a single point current meter and a CT probe (SBE37), the last four placed about 14 meters above the seafloor (352±6 meters depth). To the aim of this work only the temperature and salinity data collected by the CT probe, whose sampling interval is 30 minutes, will be analyzed.

The data cover the period September 2004 until March 2016, with a gap between March 2011 and August 2012. At the moment the mooring line continues deployed at the Espartel Sill collecting data, so that these series are becoming longer.

The CT has been regularly calibrated and the data corrected taking into account each calibration. This is a mandatory step before analyze the data, as the long term trends we are looking for are similar to the drift of the temperature and conductivity sensors of the CT. In the present case the mean drift of the temperature sensor was $O(10^{-3})$ ºC/yr and $O(10^{-3})$psu/yr for the conductivity sensor. The data presented in this work have been corrected until March 2014, the rest of the data are going to be revised as soon as the calibration of the CT is ready.

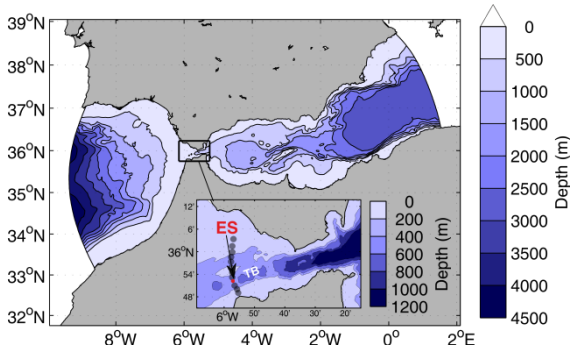

Fig. 1. Location of the monitoring station in the Strait of Gibraltar. The inset shows the detail of the Strait of Gibraltar highlighting with a red point the position of the mooring line in the Espartel Sill (ES). Grey dots mark the

CTD section and TB indicates the position of the Tanger Basin.

Several repetitions of the Espartel CTD section have been made coinciding with the maintaining campaign when it was possible (grey circles in Fig.1). Since the CT position has slightly changed (±6m), the cast that correspond with the monitoring point has been analyzed (red point in Fig.1). We found that there were not significant changes in temperature or salinity in the depth range in which the CT was placed along this period.

RESULTS AND DISCUSSION

Positive significant trends have been detected for both potential temperature and salinity of the Mediterranean outflow. The temperature trend for the whole period is 0.0055ºC/yr, with the same order of magnitude that the one estimated by other authors (Table 1), and the same reported by [3] for the period 1995-2005 in the Ligurian Sea. The above indicates that the temperature of the deep Mediterranean water has experienced a continuous increase of 0.005ºC/yr since 1995 up to now. Furthermore, data suggests that this trend has been intensified in the last five years by one order of magnitude, reaching 0.022ºC/yr (Fig. 2). Since the monitoring station continues moored at this moment collecting data, this issue will be further investigated in the near future.

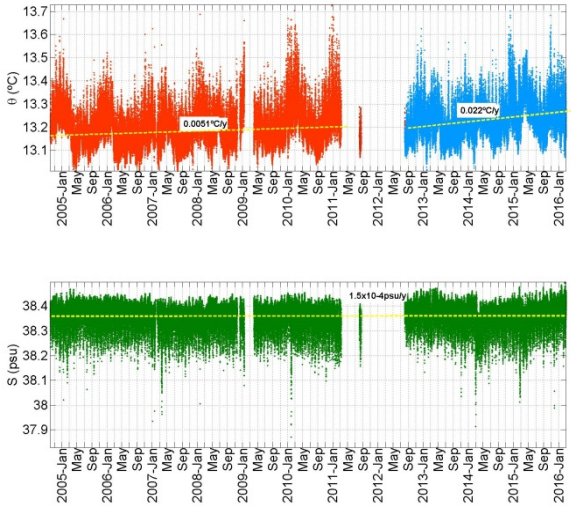

Fig. 2. Upper panel shows the potential temperature measured at a mean depth of 352 meters at the Espartel Sill (Fig.1). Colors indicate the different periods, red for the 2004-2011 period and blue for the 2012-2016 period. The dashed yellow line indicates the trend of each subset, both being significant at 99% of confidence. The trend of the whole period is 0.0055ºC/yr (not shown). The bottom panel shows the practical salinity for the whole period, the yellow line and the text above it indicating the salinity trend.

On the other hand the practical salinity shows a positive trend of 1.5×10^{-4} psu/yr, which is one order of magnitude smaller than the trend found for the Mediterranean according to several authors (Table 1). This lower salinity trend is a consequence of the erosion of the salinity signal, due to the great mixing the Mediterranean water undergoes in the Tangier basin (TB in Fig.1) [6], where it mixes with the fresher North Atlantic Central Water (NACW).

Table 1. Estimations of the temperature and salinity trends in different places of the Western Mediterranean Sea.

Author	θ trend (ºC/yr)	S trend (psu/yr)	Period of time	Area in the Mediterranean
[1]	0.0035	0.0010	[1995-1997]	Algero-Provençal basin (200-2700m)
[2]	0.0035	0.0010	[1959-1997]	Balearic Sea
[3]	0.005	0.0022	[1995-2005]	Ligurian Sea (2000m)
[4]	0.012	0.0043	[1995-2004]	Ligurian Sea (400-2000m)
[5]	0.004	0.0015	[1961-2008]	Entrance to the Alboran Sea (below 200m)

In view of the above the data presented in this work show that the contribution of the Mediterranean to the Atlantic Ocean is now warmer and slightly saltier than a decade before. However, following other authors, density does not show a trend in the western Mediterranean, while the data at Espartel Sill suggest a small negative trend $O(10^{-3})$, likely related with the erosion of the salinity signal when it mixes with NACW. Using a subsampling of the maximum salinity every 15 days we select the saltiest samples, getting a salinity trend of $O(10^{-3})$, closer to that reported in other works.

ACKNOWLEDGEMENTS

This work was funded by the Spanish Ministry of Economy Competitiveness under the three Research Projects INGRES (REN2003_01608 ,CTM2006_02326 and CTM2010-21229).

REFERENCES

1 – Bethoux, J.P., et al., 1998. Warming and freshwater budget change in the Mediterranean since the 1940s, their possible relation to the greenhouse effect. Geophys. Res. Let., 25:1023-1026.

2 - López-Jurado, J.-L., et al., 2005, Observation of an abrupt disruption of the long-term warming trend at the Balearic Sea, western Mediterranean Sea, in summer 2005, Geophys. Res. Lett., 32, L24606, doi:10.1029/2005GL024430.

3 - Marty, J. C. and Chiavérini, J.: Hydrological changes in the Ligurian Sea (NW Mediterranean, DYFAMED site) during 1995–2007 and biogeochemical consequences, 2010. Biogeosciences, 7, 2117-2128, doi:10.5194/bg-7-2117-2010.

4 - Grignon, L., et al., 2010. Importance of the variability of hydrographic preconditioning for deep convection in the Gulf of Lion, NW Mediterranean, Ocean Sci., 6, 573-586, doi:10.5194/os-6-573-2010.

5 - Borghini, M., et al., 2014. The Mediterranean is becoming saltier, Ocean Sci., 10, 693-700, doi:10.5194/os-10-693-2014.

6 - García-Lafuente J., et al., 2011. The very first transformation of the Mediterranean outflow in the Strait of Gibraltar. J. Geophys. Res., C07010, 116, doi: 10.1029/2011JC006967.

The role of submesoscale turbulence in regulating the annual cycle of the upper-ocean mixed layer

Alberto Naveira Garabato[1], Christian Buckingham[1], Xiaolong Yu[1], Natasha Lucas[2], Adrian Martin[3], Thomas Rippeth[2], Liam Brannigan[4], George Nurser[3] & David Marshall[5]

[1] Ocean and Earth Science, National Oceanography Centre, University of Southampton, Southampton, U.K.
[2] School of Ocean Sciences, Bangor University, Bangor, U.K.
[3] National Oceanography Centre, Southampton, U.K.
[4] Department of Meteorology, Stockholm University, Stockholm, Sweden
[5] Department of Physics, University of Oxford, Oxford, U.K.

ABSTRACT

The role of submesoscale turbulence in regulating the annual cycle of the upper-ocean mixed layer is investigated through the analysis of a 1-year-long record of hydrographic and velocity measurements, collected by a cluster of 9 moorings, 2 gliders and a meteorological buoy deployed in 2012 – 2013 in the Northeast Atlantic under the auspices of the U.K. OSMOSIS experiment. The mooring cluster consisted of two nested arrays with horizontal spacings of ~1.5 km and ~15 km that provided resolution of submesoscale and mesoscale flows, respectively, and included point measurements of the rate of turbulent kinetic energy dissipation using high-frequency ADCPs. The measurements reveal that the experimental area is riddled with submesoscale turbulence throughout the year, despite hosting modest mean and mesoscale eddy flows. Submesoscale turbulence exhibits a significant annual cycle, with intensified (reduced) submesoscale activity in winter (summer). A major proportion of the upper-ocean de-stratification and turbulent kinetic energy dissipation in the autumn and winter is associated with symmetric instabilities triggered by winds blowing down submesoscale density fronts, rather than the gravitational instabilities that control the mixed layer's seasonality in ocean general circulation models. Upper-ocean re-stratification is also regulated primarily by submesoscale turbulence, and is commonly associated with persistent frontogenesis induced by the mesoscale eddy field. Our findings demonstrate that parameterisation of the de-stratification and re-stratification effects of submesoscale turbulence is essential to the realistic representation of the annual cycle of the mixed layer in climate-scale ocean models.

Enhanced retrieval of the geophysical signature of SMOS SSS maps

Estrella Olmedo[1], Justino Martínez[1], Antonio Turiel[1], Joaquim Ballabrera[1]& Marcos Portabella[1]

[1] Departamento de Oceanografía Física y Tecnológica. Instituto de Ciencias del Mar. Passeig Marítim de la Barceloneta, 37-49. 08003 Barcelona.

ABSTRACT

The Soil Moisture and Ocean Salinity (SMOS) mission has provided a unique remote sensing platform capability for observing key variables of the hydrological cycle, such as the Sea Surface Salinity (SSS). However, due to some limitations related to the instrument interferometric concept and its challenging data processing, SMOS SSS maps still display significant artifacts and biases, especially close to the coast due to the presence of Radio Frequency Interferences (RFI) and Land-sea contamination (LSC). A new methodology for filtering salinity retrievals and correcting for spatial biases is introduced and validated here.

INTRODUCTION

The Soil Moisture and Ocean Salinity (SMOS) mission is an innovative Earth Observation satellite launched in November 2009 to remotely sense soil moisture (SM) over land and sea surface salinity (SSS) over the oceans.

The SMOS single payload is the Microwave Imaging Radiometer using Aperture Synthesis (MIRAS), a L-band 2D synthetic aperture radiometer with multi-angular and full polarization capabilities. This completely new Earth observation instrument concept has entailed a technological challenge for which the development of dedicated calibration and image reconstruction algorithms have been required.

SMOS L1 and L2 SM/OS products, provided by the European Space Agency (ESA) are freely available at https://earth.esa.int/web/guest/data-access/browse-data-products?selectedTags=smos. On the other hand, SMOS L3/L4 products provided by the SMOS Barcelona Expert Centre (SMOS-BEC) are freely available in http://cp34-bec.cmima.csic.es.

The L2 OS product provided by ESA has an overall good quality over open ocean. There are however significant issues, the most relevant of them are land-sea contamination (LSC), latitudinal bias and the seasonal bias. In this paper a new SSS retrieval algorithm aimsing to correct some of those issues, is presented.

MATERIAL Y METHODS

The new algorithm is based in the non-Bayersian approach. This approach differs with the standard one in that we do not assume any model either for the marginal or the joint distribution of the errors. Therefore, the statistics of the retrievals is analysed a posteriori, classified according to the orbital and geographical parameters that are known to influence the systematic biases. The classes allow to define SMOS-based annual climatologies and from them, with the appropirate filtering, SMOS-based anonalies. The final SSS product of absolute salinity is constructed by adding an annual climatology provided by the World Ocean Atlas.

By construction, L3 products (regularly gridded) are derived. Our reference product witll be a global map at 0.25º of spatial resolution and defined over a 9-day map.

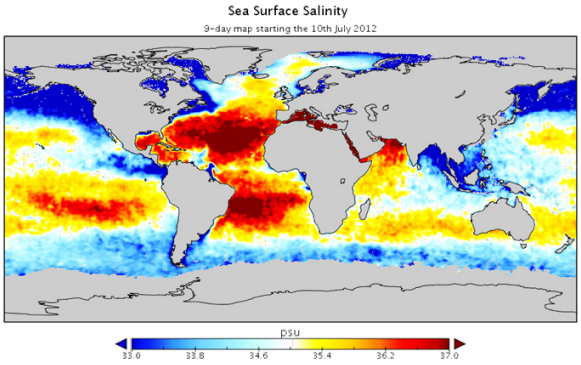

Fig. 1. Example L3 non-Bayesian SSS map

RESULTS AND DISCUSSION

The introduction of this methodology removes LSC and also improves the overall quality of the signal with respect to the standard product.

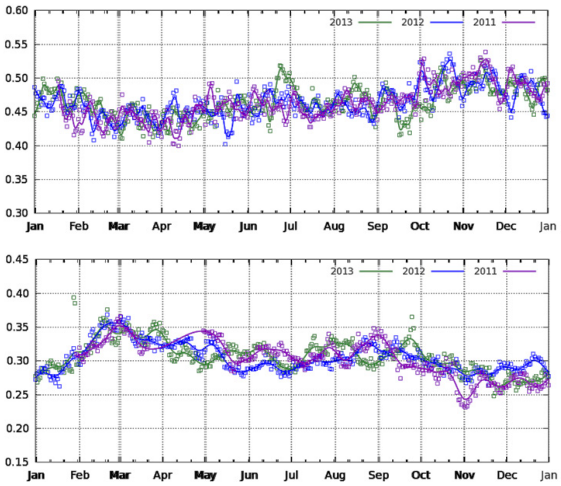

Fig. 2. Time evolution (for years 2011, 2012 and 2013) of the standard deviation of the difference of SMOS L3 maps (9-day, 0.25º resolution) with Argo close-to-surface SSS values. Top panel: Current ESA official version (v620); Bottom panel: non-Bayesian.

ACKNOWLEDGMENTS

This work has been funded by the Spanish Ministry of Economy through the National R+D Plan by means of Promises project ESP2015-67549-C3 and previous grants.

Mass transports in the Brazil Malvinas Confluence from an inverse box model

Dorleta Orúe-Echevarría[1], Francisco Machín[2] & Josep L. Pelegrí[1]

[1] Departament d'Oceanografia Física i Tecnológica, Institut de Ciències del Mar, CSIC
[2] Departamento de Física Aplicada, Universidad de Las Palmas de Gran Canaria, Las Palmas de Gran Canaria

ABSTRACT

The Brazil Current (BC) and the Malvinas Current (MC) meet at the Brazil-Malvinas Confluence (BMC) region. This encounter is characterized by a complex mesoscale structure, with numerous eddies, filaments and thermohaline intrusions that lead to meridional exchange of mass, heat and salt between both currents. Therefore, the BMC is the site where the subtropical gyre and the ACC exchange key properties, thus playing a fundamental role in the Earth's climate. During March 2015, the R/V Hespérides carried out the TIC-MOC cruise in the BMC with the objective of sampling the BMC with high resolution. Here we use 28 hydrographic stations from this cruise that, together with the South American coast, constitute a closed ocean volume with sides about 400 km, and build an inverse box model to quantify the mass exchange through its contour. We find that mass enters the region predominantly from the north, carried by the BC, and leave through the eastern section; most of the flow from the south also leaves the region through the southern boundary. The results are consistent with the velocity field as measured during the cruise.

INTRODUCTION

The Brazil Current (BC) is the western boundary current of the South Atlantic subtropical gyre, transporting warm and saline waters southward. The Malvinas Current (MC), a branch of the Antarctic Circumpolar Current (ACC), transports cold and fresher water of subantarctic origin to the north, along the east coast of South America. The Brazil and Malvinas currents meet in the Southwest Atlantic, in what is known as the Brazil Malvinas Confluence (BMC) [1], a key site where the subtropical and Antarctic Circumpolar Current exchange water masses, heat and freshwater [3].

The encountering of the southward warm and salty waters with the northward cold and fresher waters becomes one of the most intense open-ocean frontal system in the world, with high horizontal gradients in temperature, salinity and biogeochemical properties, such as temperature gradients of up to 4 ºC km^{-1} [2]. This frontal system is characterized by numerous mesoscale eddies, filaments and a complex vertical and horizontal thermohaline structure [4].

In March 2015 an oceanographic cruise was carried out in the area, providing for novel data that can be used to describe the three-dimensional structure of the BMC, as well as for determining the exchange of properties in the region. Here we will apply an inverse box model to part of these data, in order to quantify the transport of mass and other properties in the BMC.

METHODOLOGY

During TIC-MOC cruise, carried out by the R/V Hespérides in March 2015, a total of 66 stations where done in the BMC area. In particular, a perimeter around the confluence area was completed with 28 stations at intervals of about 45 km and down to at least 2000 m (Fig. 1).

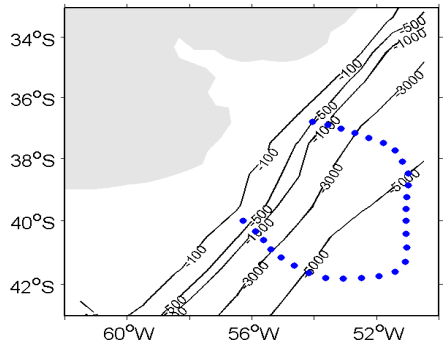

Fig. 1. Location of hydrographic stations in the perimeter section englobing the BMC area; contour lines show the bathymetric contours in meters.

All stations include temperature, salinity, pressure, dissolved oxygen, fluorescence, turbidity and transmittance measurements, taken with a CTD SBE911plus. Water velocities were measured underway with the Ship-ADCP Ocean Surveyor; in addition, vertical velocity profiles were

obtained at each station with a Lowered-ADCP, installed on the carousel water sampler.
For our analysis, we use an inverse box model that assumes the ocean to be hydrostatic and in geostrophic balance but allows the exchange of properties between adjacent layers [5, 6]. The model outputs are the geostrophic velocity field normal to the vertical section englobing the study area, as well as the mean vertical diffusivities between layers within this region. These values may then be used to calculate the corresponding horizontal and vertical transports of heat and other properties [5].

The volume used for our calculations is delimited by the south american coast to the west and by a total of 28 stations in the deep ocean around the BMC sampled during the TIC-MOC cruise (Fig. 1). The netural density layer 27.82 kg m^{-3} is set as the no-motion reference level, used to integrate the thermal wind equation. Over the slope, the reference level for any pair of stations is set to be the shallowest among them. We divide the water column into seven neutral-density layers, with the deepest one being motionless, which separate different water masses [Table 1]. These levels are chosen on the basis of previuos works for the Atlantic Ocean [5].

Table 1. Neutral density (kg m^{-3}) layers used in the inverse box model.

Layer	y^n (kg m^{-3})
1	sea surface-26.2
2	26.2-26.8
3	26.8-27.3
4	27.3-27.5
5	27.5-27.72
6	27.72-27.82
7	>27.82

RESULTS

We find that most of the water transport enters the closed box through the north and departs east across the eastern margin, predominantly in the surface layers (Fig. 2). Specifically, about 27 Sv enter from the north and depart eastward in the upper three layers (neutral densities between 26.8 and 27.3 kg m^{-3}). In particular, in the uppermost layer (typically less than 100 m thick) the transport is about 8 Sv, related to the presence of very swift currents (with peak values of 1.2 m s^{-1} associated to an eastward filament at the confluence of both currents). In contrast, in the southern section, the net mass transport is close to zero for all layers. This is caused by a 180° turn of the MC, so that water incorporated to the box through the southern margin is rapidly exported south, out of the box.

Our velocity fields are consistent with the velocity values measured with both ADCP instruments during the TIC-MOC cruise. In particular, the velocities reflect the complex mesoscalar structures observed in the BMC.

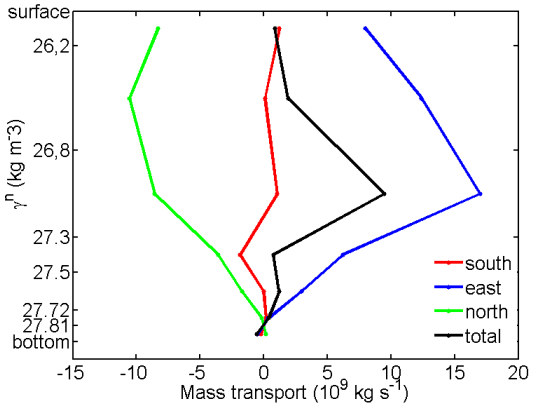

Fig. 2. Mass transport by layers for each section and the net transport in the box.

ACKNOWLEDMENTS

We are very grateful to the crew, technicians and scientists in the R/V Hespérides, whom made possible the gathering of the data set used in this communication.
This research has been supported by the Ministerio de Economía y Competitividad of the Spanish Government through projects TIC-MOC (CTM2011-28867) and VA-DE-RETRO (CTM2014-56987-P). Dorleta Orue-Echeverría has been funded through a FPU contract of the Ministerio de Educación y Ciencia.

REFERENCES

1- Gordon AL & Greengrove CL, 1986. Geostrophic circulation on the Brazil-Falkland Confluence. Deep-Sea Res., 33,573-585.
2- Garzoli SL & Garraffo Z, 1989. Transports, frontal motions and eddies at the Brazil-Malvinas Currents Confluence. Deep-Sea Res.,36,681-703.
3- Jullion L, Heywood KJ, Naveira Garabato AC & Stevens DP, 2010. Circulation and Water Mass Modification in the Brazil-Malvinas Confluence. J. Phys.Oceanogr.,40,845-864.
4- Provost C, Garçon V & Medina Falcon L, 1999. Hydrographic conditions in the surface layers over the slope-open ocean transition area near the Brazil-Malvinas Confluence during austral summer 1990. Cont. Shelf. Res., 16,215-235.
5- Ganachaud A , 2003. Large-scale mass transports, water mass formation, and diffusivities estimated from World Ocean Circulation Experiment (WOCE) hydrographic data. J. Geophys.Res., 108, 3213.
6- Machín F, Hernández-Guerra A, & Pelegrí JL, 2006. Mass fluxes in the Canary Basin. Prog. Oceanogr. 70,416-447.

Idealized box models as effective tools to understand the glacial-interglacial response of the ocean-atmosphere coupled system

Dorleta Orúe-Echevarría, Josep L. Pelegrí, Antonio García-Olivares[1]

[1] Departament d'Oceanografia Física I Tecnológica, Institut de Ciències del Mar, CSIC.

ABSTRACT

The Earth's climate is the outcome of numerous feedback energetic mechanisms. Paleoclimatic data tell us that the Earth has shifted between glacial and interglacial periods during the last 3 Myr, alternating between different temperature and atmospheric-CO_2 states. Variations in key global processes are responsible for these transitions: CO_2 atmospheric concentration, incoming solar radiation, meridional overturning circulation and albedo. Here we propose two simple box-models in order to analyze the effect of these processes on the heat content of the atmosphere and the upper-ocean during the last 450 kyr. The simplest model has only three boxes: atmosphere, upper-ocean and deep-ocean. The atmosphere and upper-ocean are allowed to exchange heat while the upper and deep oceans are connected through the meridional overturning circulation (MOC); it allows assessing the effects of cloud cover, greenhouse gases and MOC on climate but presents several important limitations, e.g. in the absence of a cooling mechanism, the deep ocean would warm up in times scales of order 10 kyr. Hence, we move to a more realistic five-box model, distinguishing now between high- and low-latitude atmospheric and upper-ocean compartments. This model, which adequately reproduces current estimates of preindustrial temperatures and heat fluxes, is used to estimate how these variables changed during glacial periods. Most important, the model helps us assess the relevance of the different physical processes on the Earth's climate, such as the latitudinal exchange within the ocean and atmospheric compartments, the intensity of the MOC and the reflecting power of albedo at high latitudes.

INTRODUCTION

Different processes have been suggested as responsible for past climate transitions, the most important being changes in (1) incoming solar radiation, (2) greenhouse gases (GHG), (3) the meridional overturning circulation (MOC), (4) and the planetary albedo. Variations in solar radiation during the last 5 Myr have represented very small changes in global annual mean insolation, yet they have driven major climate changes [1]. The glacial-interglacial periods are also characterized by changes in the concentration of GHGs, particularly CO_2, with low/high concentrations during glacial/interglacial periods [2]. Because of the role the MOC plays both on heat transport from low to high latitudes [3] and on the carbon cycle [4], it is an essential element determining the climatic state of equilibrium [5]. Finally, the increase in the extension of sea ice during glacial periods affects the albedo and hence the amount of solar radiation that is incorporated into the ocean, thus playing a principal role on the climate of the Earth [6].

Here we propose a simple time-dependent coupled ocean-atmosphere model to analyze changes in the heat content of the atmosphere and the upper-ocean for the last 450 kyr and the sensitivity of the atmosphere-ocean system to changes in albedo, cloud cover, thermohaline circulation and atmospheric and oceanic heat transports.

METHODOLOGY

We start with a three-box model that includes single atmospheric and upper-ocean compartments, the latter holding both the surface and permanent thermocline layers, and one deep-ocean box. The first two boxes are connected through turbulent heat fluxes (latent and sensible heat) and both ocean compartments through the MOC. In this model we assume that warm waters go back to the deep ocean where they are effectively cooled down. Secondly, we set a five-box model, which distinguishes between low- and high-latitude atmospheric and upper-ocean compartments, and retains one single deep-ocean compartment. In this simple approach, deep-ocean waters return to the sea surface at low-latitudes, where they capture heat, and follow to the high-latitude ocean where they release this heat before sinking back to the deep ocean.

We set a constant deep-ocean and investigate the time evolution of the well-mixed and interdependent atmospheric and upper-ocean compartments (Fig. 1). The independent variable is time and the dependent variables

are temperature (T), short- and long-wave radiation (S, Lw), and latent- and sensible-heat fluxes (LH, SH); the parameters are low-high latitude ocean and atmosphere exchange coefficients (K) and the MOC intensity (Q), plus other parameters setting the ocean-atmosphere exchange coefficient, the effect of greenhouse gases, cloud cover, relative humidity, and the atmospheric and oceanic albedo. The $S(t)$ term comes from known astronomical forcing [7] and the greenhouse effect $G(t)$ is set as a function of the paleoclimatic CO_2 record [8]. In these variables and parameters, the a, o and d subindexes respectively stand for the atmosphere, upper-ocean and deep ocean variables, and the l and h subindexes respectively stand for the low- and high-latitude boxes. The three-box model is much simpler as there is no low-high latitude heat exchange.

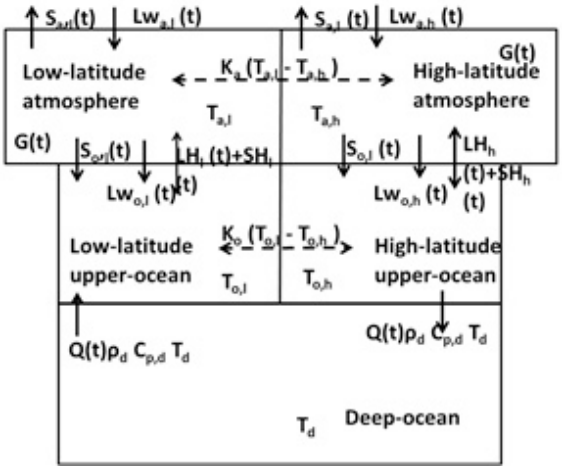

Figure 1. Five-box model compartments and fluxes.

We run several cases in order to determine the effect on climate, as assessed through the temperatures of the atmospheric and upper-ocean compartments, caused by changes in the following properties: cloud cover, water vapour, high-latitude ocean albedo, meridional atmospheric and oceanic heat fluxes, latent and sensible heat fluxes, and MOC strength.

RESULTS AND DISCUSSION

Changes in the annual mean solar radiation and in the GHGs only lead to small variations in the energy balance of the system, which are not enough to reproduce the observed climatic transitions. The principal processes leading to latitudinal heat redistribution during interglacial periods are the atmospheric and, to a lesser degree, the upper-ocean fluxes.

During glacial periods, the weakening and even collapse of the MOC tends to reduce the poleward heat transport. However, the latitudinal fluxes are intensified as the temperature difference between the low- and high-latitude compartments is enhanced. The main control of high-latitude cooling is the change in surface albedo due to the presence of ice.

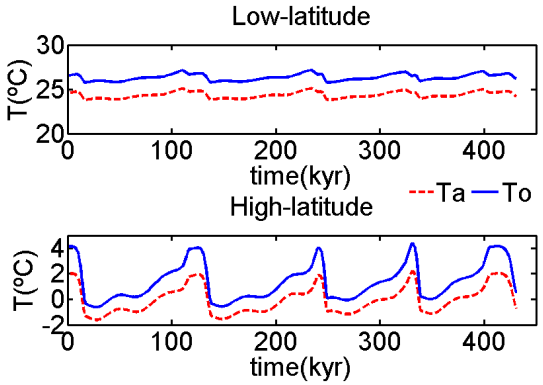

Figure 2. Example of atmospheric (red) and upper-ocean (blue) temperatures during the last 450 kyr as obtained from the three-box model.

Despite its simplicity, our model turns out to be an excellent tool to explore the glacial-interglacial response of the Earth's climate to changes in those parameters that control the different feedback mechanisms between the several major oceanic and atmospheric compartments.

ACKNOWLEDGEMENTS

This research has been supported by the Ministerio de Economía y Competitividad of the Spanish Government through project VA-DE-RETRO (CTM2014-56987-P). Dorleta Orúe-Echeverría has been funded through a FPU contract of the Ministerio de Educación y Ciencia.

REFERENCES

1 – Hays JD, Imbrie K & Shackleton NJ, 1976. Variations in the Earth's orbit: Pacemaker if the Ice Ages. Science 197 (4270):1121-1132.

2 – Petit JR, Jouzel J, Raynaud D, Barkov NI, Barnola JM, Basile I, Benda M, Chappellez J, Davis M, Delaygue G, Delmotte M, Kotlyakov VM, Legrand M, LipenkovVY, Lorius L, Pépin L, Ritz C, Saltzman E & Stievenard M, 1999.Climate and atmospheric history of the past 420,000 years from the Vostok ice core, Antarctica. Nature 399: 429-436.

3 – Kuhlbrodt T, Griesel A, Montoya M, Levermann A, Hofmann M & Rahmstorf S, 2007. On the driving processes of the Atlantic meridional overturning circulation. Rev. Geophys., 45, RG2001.

4 – Siegenthaler U & Wenk TH, 1984. Rapid atmospheric CO2 variations and ocean circulation. Nature, 308:624-626.

5 – Rahmstorf S, 2002. Ocean circulation and climate during the past 120,000 years. Nature 419: 207-214.

6 – Gildor H & Tziperman E, 2003. Sea-ice switches and abrupt climate change. Phil. Trans. A Math. Phys. Eng. Sci. 361(1810): 1935-1942.

7 – Berger A & Loutre MF, 1991. Insolation values for the climate of the last 10 million years. Quat. Sci. Rev., 10: 297-317.

8 – Hogg AMC, 2008. Glacial cycles and carbon dioxide: A conceptual model. Geophys. Res. Lett., 35.

The benefits of unstructured grids for wave modelling in semi-enclosed domains. Application to the Western Mediterranean Sea

Elena Pallares[1], Agustín Sánchez-Arcilla[1], Jaime Lopez, Manuel Espino[1]

[1] Universitat Politècnica de Catalunya, LIM, Barcelona, Spain (elena.pallares@upc.edu / agustin.arcilla@up.edu)

ABSTRACT

Traditionally, the methodology to improve the resolution of wave forecasting near the coast consists of a downscaling process with a system of nested domains, each with a smaller resolution and covering a smaller area than the previous one, where the required boundary conditions are provided by the coarser mesh. An alternative to this methodology consists in using an unstructured grid. Generating a simple unstructured grid for wave modeling is not a difficult process, just the contour of the study domain and a mesh generator are needed. Nevertheless, special attention should be payed to the grid design in order to optimize the triangles size and its distribution in the study area. With this purpose two different criteria to design an unstructured grid efficiently are presented, reducing the cell size only when necessary. Once the unstructured grids are designed for two different domains covering the Western Mediterranean Sea and the Balear Sea respectively, wave simulations are carried out for a one year period. The code used for wave modelling is SWAN v.40.91A, for which also the numerical settings require attention. The results are validated with buoy measurements near the coast and satellite data offshore. The results show good agreement between the modelled and the measurements, mainly near the coast, with an important reduction of the computational time required.

INTRODUCTION

The main advantage of using an unstructured grid for wave modelling is that it allows working with a single grid with different resolutions at each sub-domain, thus improving the resolution in coastal areas, and therefore the nesting is not needed. Another advantage is that the unstructured grid is able to reproduce the sharp coastline and around islands more accurately than regular meshes [1]. Finally, unstructured grids allow indirectly what is known as two-way nesting, where information is transferred not only from the coarser to the finer domain but also in the other direction – a process especially interesting in situations with inland winds, such as the case of the Mistral on the Mediterranean coast.

Nevertheless, special attention should be payed to the grid design in order to optimize the triangles size and its distribution in the study area. With this purpose, two size criteria are designed: the first one considers the distance to the coast, where more accuracy is required, and high resolution winds are provided while the second criterion considers the effect of the bottom on the waves, including the depth, the bathymetric gradient, and the level of bottom influence (in terms of a classification into deep/intermediate /shallow waters). Both criteria try to infer/predict where gradients in the wave field are likely to occur.

Once the unstructured grids are designed, sensitivity test are performed to study the effects of using different spatial resolutions in the wind field for the entire domain. The code used for wave modelling is SWAN [2], for which also the numerical settings require attention [1,3].

The SWAN model has previously been used to simulate the wave field with unstructured girds [4] and it is prepared to work with both types of grids, nested regular systems and unstructured grids, using exactly the same physics. [1] presents and validates the numerical scheme adapted for unstructured grids, consisting of a vertex-based, fully implicit, finite-differences method that requires several sweeps through the grid.

However, in previous works the unstructured grids for wave simulation have been mainly applied to small domains nested to regional or global grids [1,4]. In the present study an unstructured grid for a semi enclosed domain such the Western Mediterranean sea is designed and compared with a regional unstructured grid nested to a coarser model.

The results of the different simulations are validated with buoy measurements located near the Catalan coast and satellite data for the Western Mediterranean Sea.

METHODOLOGY

The main data necessary to generate an unstructured grid are the bathymetry and the coast line (also used as the contour of the domain). For the present study the bathymetry has been obtained from GEBCO (General Bathymetric Chart of the Oceans, www.gebco.net) with a grid resolution of 30 arc-second (0.0083º), and the coast

line has been extracted from the National Geographycal Data Center (www.ngdc.noaa. gov/mgg/shoreline).
In order to test the designed unstructured grids simulations with the SWAN wave model are carried out for a period of one year, corresponding to the 2013. For the present study the wind fields have been provided by the Spanish Meteorological Agency (AEMet, www.aemet.es) and include a coarser wind field that provides the wind conditions 10 m above the sea level, with a spatial resolution of 0.16 degrees for the entire Western Mediterranean Sea, and a better resolution wind field that covers only the Catalan coast area, with a spatial resolution of 0.05 degrees.

There are plenty of mesh generators able to create an unstructured grid from a closed contour, just considering the length of the boundary segments and some size proportion between neighbour triangles. However, in some of the grid generators a sizing function can be also introduced to control varying levels of mesh resolution within the domain.
The grid generator used in the present study is the MESH2D – Automatic Mesh Generation for Matlab, a toolbox for 2D meshing in which a function size can be included together with a maximum grid size and the maximum size proportion between neighbour cells.
Two size functions are defined and used in the present study to improve the unstructured grid design (Fig.1). The idea is to refine the mesh only where this procedure can improve the wave simulations results, so a balance can be stablished between grid resolution and computational time required to solve the simulation. The first criteria considers the distance to the coast, where more accuracy is required, high resolution winds are provided and buoy measurements are available. The second criteria applied considers the effect of the bottom on the wave propagation, including the water depth, the bathymetric gradient and the level of bottom influence (in terms of classification into deep/intermediate/shallow waters).

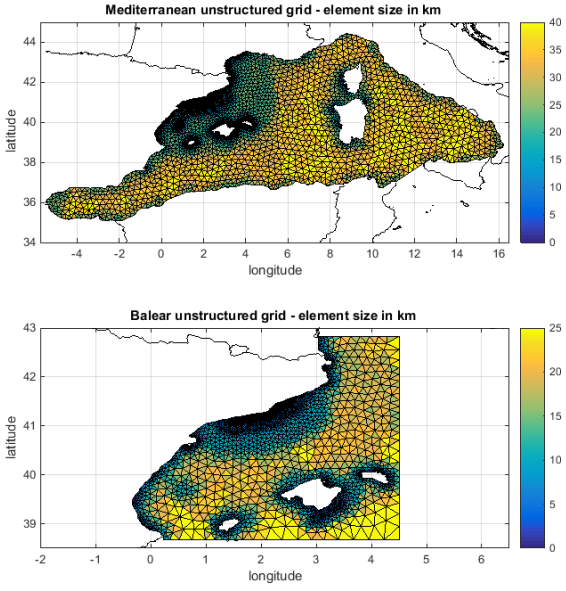

Fig. 1. Unstructured grids designed using the proposed size criteria for the Western Mediterranean Sea (top) and the Balear Sea (bottom). The colours represent the grid size in km.

RESULTS AND DISCUSSION

The validation of the unstructured grids is performed in two different ways. The model results are validated with buoy measurements near the coast, obtaining RMSE around 0.22 m for the significant wave height, with a bias around 10 cm and correlation coefficients between 0.83 and 0.93 depending on the location, values very similar to the ones obtained from regular grids. Also good results are obtained when validating the mean wave period and the mean wave direction. The second validation is performed in open waters, comparing the model results with the altimeter significant wave height measurements, with very good results. In conclusion, the SWAN model using well designed unstructured grids provide good wave simulations, and can be a good alternative to the regular grids.

Until now the comparison has been focused on the accuracy and quality of the results. However, there is another key point to account for in the comparison: the computational time required to obtain the results. The results show a reduction of time of about 66% from the traditional way of providing a high-resolution wave forecast (the nested grids) to the regional unstructured grid proposed in the present study.

ACKNOWLEDGEMENTS

The authors want to acknowledge the Spanish meteorological agency (Agencia Estatal de Meteorologia, AEMET, Ministerio de Agricutura, Alimentación y Medio Ambiente) for providing the wind fields for the present study, and the Secretaria d'Universitats i Recerca del Dpt. d'Economia i Coneixement de la Generalitat de Catalunya (Ref 2014SGR1253). The work has been performed in the framework of the Spanish national project PLANWAVE (ref. CTM2013-45141-R) from the MINECO and FEDER.

REFERENCES

1 - Zijlema, M., 2010. Computation of wind-wave spectra in coastal waters with SWAN on unstructured grids. Coastal Engineering, 57, 267-277
2 - Booij, M., Ris, R., Holthuijsen, L., 1999. A third-generation wave model for coastal regions, Part I: Model description and validation. Journal of Geophysical Research, 104, 7649-7666.
3 - Dietrich, J., Zijlema, M., Allier, P., Holthuijsen, L., Booij, N., Meixner, J., Profit, J., Dawson, C., Bender, C., Naimaster, A., Smith, J., Westerink, J., 2013. Limiter for spectral propagation velocities in SWAN. Ocean Modelling, 70, 85-102.

4 - Hsu, T., Ou, S., Liau, J., 2005. Hindcasting nearshore wind waves using a FEM code for SWAN. Coastal Engineering, 52, 177-195.

Spiciness and potential-density anomalies as useful variables to assess the contribution of diapycnal and isopycnal processes to water mixing

Josep L. Pelegrí[1] & Marc Gasser[1]

[1] Departament d'Oceanografia Física i Tecnològica, Institut de Ciències del Mar, CSIC, Barcelona

ABSTRACT

Temperature-salinity (T-S) diagrams are widely used to spot the temperature (T) and salinity (S) relations at different places and times. They also help visualize how water masses with different T and S values mix up as they propagate away from the formation regions. Potential density (ρ_θ) is typically included in these diagrams to emphasize the vertical stability of a given hydrographic cast or to illustrate how two water masses remain at different density levels. Alternatively, we may introduce a new variable that sets a surrogate orthonormal space, with ρ_θ on one axis and spiciness (π) on the other (Flament, 2002; but see Veronis, 1972, and Jackett and McDougall, 1985). Here we discuss how the ρ_θ and π anomalies in this space may be interpreted as latent diapycnal and epipycnal mixing, or mixing yet feasible to take place, between two water masses. We illustrate these concepts with casts that sample the Mediterranean Outflow (MO) running under the North Atlantic Central Waters (NACW) stratum in the eastern Gulf of Cádiz (Fig. 1).

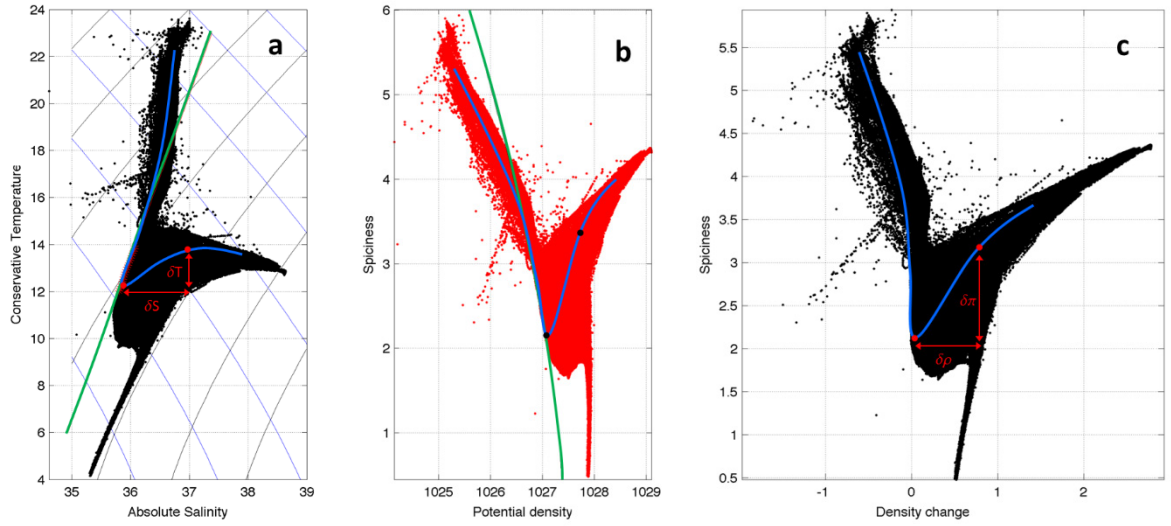

Fig. 1. Data points (black dots) for the MO region in the Gulf of Cadiz; the blue line illustrates one individual cast sampling the MO core in the eastern Gulf and the green line shows the T-S relation for NACW. (a) Isopycnals (black thin lines) and isospicy (blue thin lines) contours in a classic T-S space (with units of °C and g kg^{-1}). (b) Data points in the ρ_θ-π space (both with units of kg m^{-3}). (c) As for (b) but with vertical changes in density referenced to the NACW potential-density values; the change in spiciness for any vertical profile is calculated as the spiciness at any point minus the minimum spiciness value for that profile, which corresponds to the deepest NACW level on top of the MOW. The changes in potential density $\delta\rho_\theta$ and spiciness $\delta\pi$ can respectively be interpreted in terms of latent diapycnal and epipycnal mixing.

ACKNOWLEDGEMENTS

This research has been supported by the Ministerio de Economía y Competitividad of the Spanish Government through project VA-DE-RETRO (CTM2014-56987-P).

REFERENCES

1 - Veronis G, 1972. *J. Mar. Res*., 30, 227-255.
2 - Jackett DR & McDougall TJ, 1985. *Deep-Sea Res*., 32, 1195-1207.
3 - Flament P, 2002. *Progr. Oceanogr*., 54, 493-501.

Characterizing the recurrent dipolar vorticity structures in the outer Ría de Vigo (NW Spain) using HF radar

Silvia Piedracoba [1], Gabriel Rosón[1] & Ramiro Varela[1]

[1] Dpto. de Física Aplicada - Facultad de Ciencias - Universidad de Vigo, Pontevedra

ABSTRACT

Two high-frequency radars (HFR) were operating in the Ría de Vigo (NW Spain) during one year between September 2012 and August 2013 to diagnose surface circulation. An analysis of low-pass current and its relative vorticity revealed two opposite vorticity structures in the coverage area. Simultaneously, wind stress and its curl, calculated in the HFR coverage area, were assessed to establish the main mechanisms promoting the formation of these two structures. Examining vorticity at specific grid points representing both vorticity structures reveals a greater correlation between vorticity and the y-component of wind stress at the Cíes meteorological station (R=0.52-0.80) than correlation between the vorticity and the wind stress curl (R=0.50-0.62).

Once wind forcing has been reported as the main factor responsible for generating these dipolar vorticity structures at subtidal frequencies, these structures, which life span ranges from 2 to 8 days, can be shown to develop from two different wind sources: 1) counter-clockwise (CCW) and clockwise (CW) relative vorticity in the northern and southern outer ría respectively, mainly evolving during the transition from upwelling to downwelling; and 2) clockwise and counter-clockwise vorticity in the northern and southern outer ría respectively, mainly originated during moderate to intense upwelling events. The existence of these double vorticity structures is key to understanding the mechanisms of transport between the Ría and the shelf, and they also could help explain the retention of plankton or pollutants inside some regions of the ría.

INTRODUCTION

The Ría de Vigo is a V–shaped coastal inlet located in the NW Iberian Peninsula, connected with the adjacent shelf. Upwelling, downwelling, and the transitions between them are well-known short timescale events (2–4 days) affecting residual circulation, since ría behaves as an extension of the shelf with a two–layered residual circulation pattern that is positive under upwelling and negative under downwelling conditions. The changes observed in the hydrography of the ría, as well as the outputs from inverse [1] and numerical models [2], indicated that shelf winds drive a two-layered circulation pattern in the inner and middle ría. This forcing interacts with the circulation of the outer ría to produce a 3D residual circulation pattern in that region. However, despite efforts to elucidate the dynamics of the Ría, precise current measurements are still scarce and limited by restricted spatial and temporal coverage. The high-frequency data provides a detailed description of the circulation of the ría [3], coupled with the stratification and water mass exchange in the Ría. However, the use of (HFR for mapping sea surface currents permits tracking certain structures at the surface that cannot be detected otherwise. The University of Vigo installed a HFR system (~46 MHz) in 2010 that enables tracking studies with high spatial and temporal resolution. In this study, we used HFR data to assess the subtidal surface circulation in the outer part of the Ría. This work provides a first view of two structures with opposite relative vorticities. The main objective of this work is to evaluate the forcing conditions that promote the development of these dual opposite relative vorticity structures, assess its importance and deliver a first approximation of the life span of these structures.

DATA & METHODOLOGY

Surface currents of the outer third of the Ría were obtained using HFR data derived from two short range SeaSonde CODAR radar antennas installed at Toralla Island (TORA) and Point Subrido (SUBR) (Fig. 1). The system provides radial vectors every 30 minutes in a coverage area of 75 km^2, with a distance between grid points of ~375 m and 5º azimuthal resolutions from the two remote sites. Total currents were calculated by combining all radial currents of less than 80 cm/s within 1 km of a grid point.

Zonal and meridional wind stress components were calculated at the meteorological stations of Cíes and Borneira. In order to compare the response of HFR-derived currents and the coastal wind forcing, a Butterworth filter with a cut-off period of 32 h was applied to the time series of currents and winds to eliminate the variability at tidal and higher frequencies. Once the low pass wind stress was

obtained, wind stress curl was computed by finite differences between Cíes and Borneira.

The currents over the study area were then used for calculating relative vorticity, in each node of the grid, by finite differences between contiguous nodes using a time step of 0.5 h. Averages and skewness of vorticity for all grid points were calculated using all daily-average vorticity maps for the full year covered by this study. Simultaneously, grid points of extreme vorticities (>1.5 10^{-4} s^{-1} or <-1.5 10^{-4} s^{-1}) were selected so as to identify zones representing CCW (cyclonic) and CW (anticyclonic) rotation. The vorticity analysis calculated at these grid points will then be used in the subsequent statistical analyses.

The relationship between coastal wind forcing and current was assessed by performing complex correlation. We also established scalar correlations between vorticity and x- and y-components of Cíes and Borneira wind stress, and also between vorticity and wind stress curl.

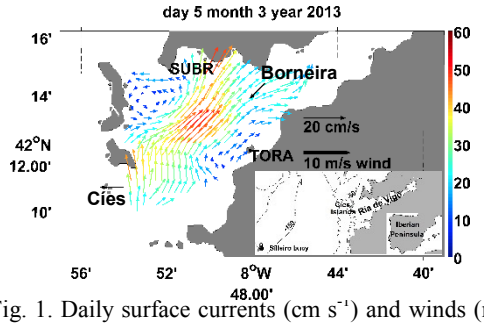

Fig. 1. Daily surface currents (cm s^{-1}) and winds (m s^{-1}) at the beginning of an extreme relative vorticity event in the outer Ría de Vigo (5th March 2013).

RESULTS AND DISCUSSION

This is the first time these structures have been observed at such a high spatial and temporal resolution, in a manner that their subtidal nature can be confirmed [4]. Here, we demonstrate that the presence of the positive vorticity structure in the northern outer region is linked to the negative vorticity structure in the southern outer region at the surface layer under downwelling/relaxation conditions (Figs. 1 and 2); on the other hand, the opposite vorticity structure (negative in the northern and positive in the southern ría) develops under moderate or intense upwelling conditions. The largest vorticity range is observed during downwelling events. These dual vorticity structures are more related to prevalent wind forcing (R=0.52-0.80) than to curl wind stress (R=0.50-0.62), revealing that these complex flow patterns are produced by an interaction between wind-driven shelf flows and the ría topography.

We also found the differences in the intensity of these two types of vorticity structures to be related to the upwelling/downwelling coastal jet. These structures can last between 2 and 8 days. Occasionally, and under downwelling conditions, a transient CCW eddy may also develop in the northern region of the outer ría with a life span of around 1 day.

The vorticity skewness calculated in the outer region of the ría shows that the study year is biased toward a CCW/CW dipole structure in the northern/southern outer region, coinciding with prevalent southerly wind conditions; the study year is therefore coherent with the general trend of weaker upwelling that has been observed in the last 40 years. Further studies should be conducted to examine the seasonal and interannual variability of the vorticity structures characterized by cyclonic and anticyclonic vorticity in the northern and southern regions of the outer ría, since these structures can signal more relaxation-downwelling events at the expense of upwelling events.

The analysis of the frequency, intensity and life span of these vorticity structures for each year will allow us to highlight when a northern CCW gyre develops and persists more than 1 day, condition from which effect on retention of plankton or pollutants in the ría could be assessed.

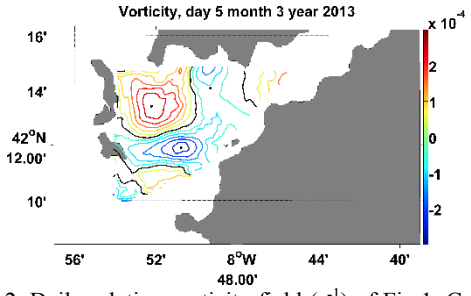

Fig. 2. Daily relative vorticity field (s^{-1}) of Fig.1. Contours are given every *f*/2, being *f* the planetary vorticity ($1 \cdot 10^{-4}$ s^{-1}).

ACKNOWLEDGEMENTS

Financial support for this study was provided by the TRALARA Project (EM2012/080, Xunta de Galicia) and the MORADA Project (BTE CGL2010-16177).

REFERENCES

1 - Gilcoto, M., Pardo, P.C., Álvarez- Salgado, X.A. and Pérez, F.F. 2007. Exchange fluxes between the Ría de Vigo and the shelf: A bidirectional flow forced by remote wind. J. Geophys. Res 112: doi: 10.1029/2005JC003140.

2 - Souto, C., M. Gilcoto, L. Fariña-Busto, and Pérez, F. F. 2003. Modelling the residual circulation of a coastal embayment affected by wind driven upwelling: Circulation of the Ria de Vigo (NW Spain), J. Geophys. Res., 108(C11), 3340.

3 - Barton, E.D., Largier, J. L., Torres , R. Sheridan, M., Trasviña, A., Souza , A., Pazos, Y. 2015. Coastal upwelling and downwelling forcing of circulation in a semi enclosed bay: Ria de Vigo. Prog. Oceanogr. 134, 173-189.

4 - Piedracoba, S., Rosón, G, Varela, R. 2016. Origin and development of recurrent dipolar vorticity structures in the outer Ría de Vigo (NW Spain). Cont. Shelf Res.,118, 143-153.

Ten-year evolution of the (New) Western Mediterranean Deep Water

Safo Piñeiro[1], Rosa Balbín[1], Cesar González-Pola[2], Pedro Vélez-Belchí[7], José Luís López-Jurado[1], Alberto Aparício-González[1], Juan Jiménez[1], Ángel Martínez[3], Cristina Naranjo[4], Catalina Pasqual[1], Pere Puig[5], Jordi Salat[5] & Manolo Vargas-Yáñez[6]

[1] Instituto Español de Oceanografía, Centro Oceanográfico de Baleares, Palma de Mallorca, Spain
[2] Instituto Español de Oceanografía, Centro Oceanográfico de Gijón, Gijón Spain
[3] Agencia Estatal de Meteorología, Madrid, Spain
[4] Universidad de Málaga, Málaga, Spain
[5] Instituto de Ciencias del Mar, Consejo Superior de Investigaciones Científicas, Barcelona, Spain
[6] Instituto Español de Oceanografía, Centro Oceanográfico de Málaga, Málaga, Spain
[7] Instituto Español de Oceanografía, Centro Oceanográfico de Canarias, Santa Cruz de Tenerife, Spain

ABSTRACT

Temporal evolution of the Western Mediterranean Transition (WMT) was analysed using θ-S data from two deep stations seasonally sampled in the NE of Minorca and off Cape Palos since 2003 and 2007 respectively. Increasing trends in S and θ of the order of 10^{-3} year^{-1} and $5 \cdot 10^{-3}$ ºC year^{-1} were shown, higher than values previously reported for the 1900-2008 period. To clarify the processes and changes induced by the WMT a deep mooring off Minorca (≈2500 m depth) has been installed in the framework of the RADMED and ATHAPOC projects.

INTRODUCTION

The dense Western Mediterranean Deep Water (WMDW) is formed during winter in the northern part of the Western Mediterranean (WMED), off the Gulf of Lions by open sea convection [1]. WMDW spreads over the whole WMED and eventually contributes to the characteristics of the Mediterranean Outflow Water (MOW) [2].

During winter 2004-2005 a major production of anomalous deep water occurred [3, 4, 5] and in summer 2005 an abrupt switch in WMDW characteristics was reported, involving a complex thermohaline structure [3]. This new situation, named Western Mediterranean Transition (WMT) [6], which implied the contribution of different water masses, created a hook-shaped θ-S profile in the deep waters by the appearance of more saline and warmer new deep water beneath the old WMDW and a cascading-origin fresher and cooler water at bottom [7] (Fig.1). Since it was detected, WMT signal has been tracked up to now.

Along the Mediterranean coast, areas where differences in the large-scale hydrographic conditions are expected have been seasonally monitored through the RADMED programme [8]. RADMED deep stations provide a description of the water column, including intermediate and deep water masses and their anomalies along the time. They also allow for the study of some seasonal phenomena such as intermediate and deep waters formation and transport.

In addition, to study the new WMDW and to offer a comprehensive view of the internal processes occurring in the water column in relation to the changes induced by the WMT, a deep mooring equipped with five current meters, eight CTDs, eight thermistors and two sediment traps has been installed at the Menorca station, in the frame of the RADMED programme and the ATHAPOC project. ATHAPOC main objective is the study of the new WMDW.

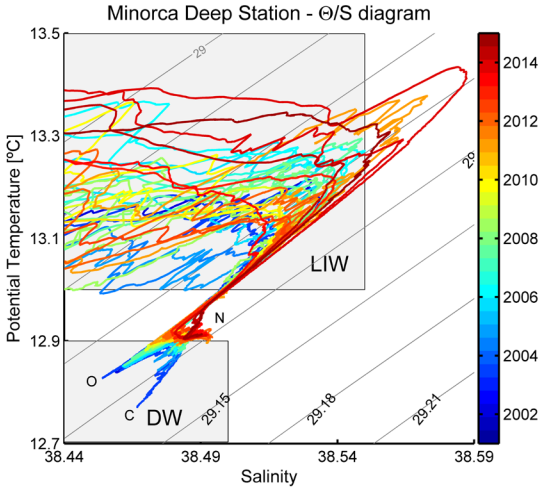

Fig.1. θ-S diagram temporal evolution in the Minorca deep station (2002-2014). Shaded areas show local values of the different water masses. O, N and C refer to Old WMDW, New WMDW and Cascading-origin water respectively.

MATERIALS AND METHODOLOGY

Historical CTD cast data from Cape Palos (00º 45.45 W, 37º 22.27 N, 2400 m depth, sampled since 2007) and Minorca stations (04º 34.96 E, 40º 10.00 N, 2540 m depth, sampled since 2003) sampled during RADMED surveys are used to characterise the new WMDW temporal evolution. Data from these surveys are part of the IBAMar database [9]. The interface between new and old WMDW has been defined as the salinity minimum below 700 m, well beneath the LIW core. Mean S, θ and potential density anomaly (σ_0) below the interface to the bottom has been calculated to compare their temporal evolution with the mean values below 700 m to the bottom.

RESULTS AND DISCUSSION

Figure 2 shows a striking uplift of the old WMDW after winter 2004/2005 and the appearance of the interface at about 1000 meters above the bottom, due to the large input of the denser new deep water. Afterwards, it remains oscillating between 1000 and 1500 dbar with a slightly depth-losing trend.

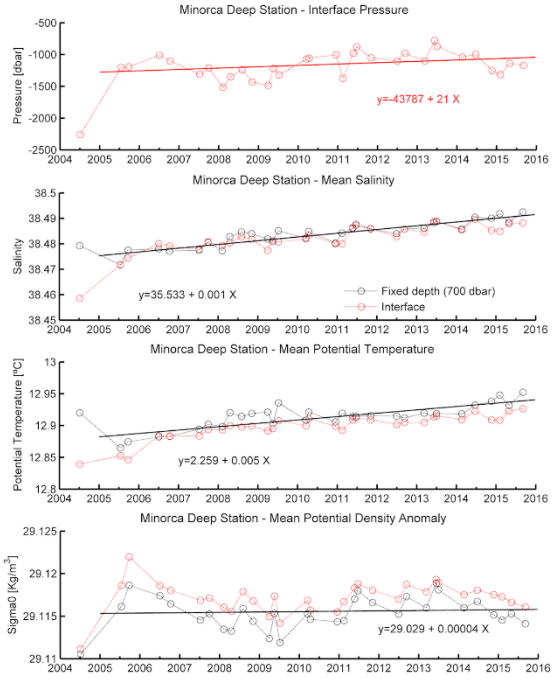

Fig.2. Temporal evolution of interface depth, mean S, θ and potential density anomaly from WMDW to bottom (red dots) and from 700 dbar to bottom (black dots). Lines indicate linear trends of mean values from 700 dbar to bottom, calculated from 2005 to 2015.

Similar trends have been observed at Cape Palos site (not shown) with a seasonal oscillation of the interface depth from 2007 to 2011, probably a dynamic feature due to a combined effect of seasonal forcing with the proximity of the continental slope.

Both stations show an increasing trend in S and θ of the order of 10^{-3} year^{-1} and $5 \cdot 10^{-3}$ ºC year^{-1} respectively along the analysed period, an order of magnitude higher than values previously reported for the 1900-2008 period [10]. Same temperature trend is found in the Strait of Gibraltar for the MOW (C. Naranjo, personal communication).

Data from the ATHAPOC mooring off Minorca together with historical RADMED data will serve to clarify the relative contribution of new WMDW formation and the diffusive evolution of the θ-S profiles.

ACKNOWLEDGMENTS

This work is supported by the RADMED project, funded by the Instituto Español de Oceanografía, and the ATHAPOC project (Ref. CTM2014-54374-R), funded by the Spanish Ministry of Economy and Competiveness.

REFERENCES

1 – MEDOC Group, 1970. Observation of formation of deep water in the Mediterranean Sea. *Nature*, 227, pp.1037–1040.

2 - Tomczak, M. & Godfrey, J.S., 2003. Regional Oceanography: an Introduction, Daya Publishing House.

3 - López-Jurado, J.L., González-Pola, C. & Vélez-Belchi, P., 2005. Observation of an abrupt disruption of the long-term warming trend at the Balearic Sea, western Mediterranean Sea, in summer 2005. *Geophys Res Lett*, 32(24), 1–4.

4 - Schroeder, K. et al., 2006. Deep and intermediate water in the western Mediterranean under the influence of the Eastern Mediterranean Transient. *Geophys Res Lett*, 33(21), 2–7.

5 - Font, J. et al., 2007. Sequence of hydrographic changes in NW Mediterranean deep water due to the exceptional winter of 2005. *Sci Mar*, 71(2), 339–346.

6 - Briand, F. ed., 2009. Dynamics of Mediterranean deep waters. In CIESM Workshop Monographs. Malta: CIESM, p. 132.

7 - Puig, P. et al., 2013. Thick bottom nepheloid layers in the western Mediterranean generated by deep dense shelf water cascading. *Prog Oceanogr*, 111, pp. 1–23.

8 - López-Jurado, J.L. et al., 2015. The RADMED monitoring programme as a tool for MSFD implementation: towards an ecosystem-based approach. *Ocean Sci*, 11, pp. 897–908.

9 - Aparicio-González, A. et al., 2014. IBAMar Database: 4 decades sampling on the Western Mediterranean Sea. *Data Science Journal*, 13, pp.172–191.

10 - Vargas-Yáñez, M. et al., 2009. Warming and salting in the western Mediterranean during the second half of the 20th century: inconsistencies, unknowns and the effect of data processing. *Sci Mar*, 73(1), pp. 7–28.

The science of ocean predictions and operational oceanography: the new science paradigm

Nadia Pinardi[1], Francesco Trotta[1], Giovanni Coppini[2], Emanuela Clementi[3], Claudia Fratianni[3] and Ivan Federico[2]

[1] Department of Physics and Astronomy, Alma Mater Studiorum University of Bologna, Bologna (IT)
[2] Centro EuroMediterraneo sui Cambiamenti Climatici, Ocean Predictions and Applications, Lecce (IT)
[3] Istituto Nazionale di Geofisica e Vulcanologia, Bologna section, Bologna (IT)

ABSTRACT

The science of ocean predictions has started in the eighties and it has rapidly advanced thereafter due to satellite sea level data availability and increasingly accurate numerical ocean models. The last ten years have seen great advances in this new sector of oceanography: numerical ocean models that resolve the mesoscales were implemented from the global ocean to the regional seas (scales of few km), data assimilation schemes capable to assimilate frequent ocean profiles and satellite data were developed, coupling between eulerian hydrodynamics and surface waves was started to better resolve the surface currents and nesting of unstructured ocean models allows to forecast properly the coastal, tidal and baroclinic currents at the resolution of few hundred meters. The predictability limit for ocean short term forecasts is of the order of several days, depending on the ocean variable and the accuracy of the atmospheric forcing forecast.
The possibility to produce analyses and forecasts at the ocean mesoscales is underpinning our new capacity to understand ocean dynamics and investigate the climate variability of the ocean: ocean forecasting models in fact are also used to produce reanalyses that allow an accurate reconstruction of the mean and eddy components of the flow field and their relationship, describe wáter mass formation processes and study the ocean dynamics at unprecedented resolution and accuracy. On the other hand, the access to open data from the operational services and in particular the Copernicus Marine Enrvironment Monitoring Service (http://marine.copernicus.eu/), allows to develop new ocean applications for the blue economy that were unthinkable few years ago, among others, accurate search and rescue decision support systems, oil spill forecasting and hazard mapping, efficient ship routing and good environmental status marine indicators.

Tidal and wind influences on circulation in the southern mouth of the Ría de Vigo (NW Iberian Peninsula)

Safo Piñeiro[1], Miguel Gil Coto[2], Francisco de la Granda[2], Nicolás Villacieros-Robineau[3], Fernando Alonso-Pérez[2], Rocío Graña[2], Silvia Piedracoba[4], Ricardo Torres[5], John L. Largier[6] & Eric Desmond Barton[2]

[1] Centro Oceanográfico de Baleares, Instituto Español de Oceanografía, Palma de Mallorca, Spain
[2] Instituto de Investigaciones Marinas, Consejo Superior de Investigaciones Científicas, Vigo, Spain
[3] Laboratoire d'Océanographie et du Climat, Université Pierre et Marie Curie, Paris, France
[4] Universidad de Vigo, Vigo, Spain
[5] Plymouth Marine Laboratory, Plymouth, United Kingdom
[6] Bodega Marine Laboratory, University of California Davis, Bodega Bay, California, United States of America

ABSTRACT

Tidal and wind influences on the velocity field in the Ría de Vigo were assessed using atmospheric data from two meteorological stations located at Bouzas port and on an oceanic buoy off Silleiro Cape along with oceanic data from an ADCP moored in the Ría for a 72-day period. A two-layer circulation pattern was observed. Near-surface and near-bottom currents are primarily influenced by wind (especially remote winds), separated by an intermediate layer dominated by tidal variability. At subtidal frequencies, residual currents are well correlated with wind variability. Remote wind forcing exhibited a markedly high correlation with surface layer currents, indicating the major role played by wind in the long-term upwelling-modulated circulation of the Ría.

INTRODUCTION

The Ría de Vigo is the southernmost of the Rías Baixas, which define the northern boundary of the Eastern Atlantic Upwelling System [1]. Its waters are in free exchange with the adjacent inner shelf by two mouths separated by a landform: the Cíes Islands. Coastal upwelling/downwelling events in the region are triggered by seasonal variations of the dominant wind component [2]. The drag of the ocean surface in response to Ekman transport caused by the action of wind on the shelf and the forcing due to the local wind generates a two-layer circulation pattern within the Ría de Vigo, positive during upwelling events and negative during downwelling events. Despite this marked seasonality, short time scale variations in the wind pattern produce upwelling/downwelling and transitions events with typical 2-6 days response periods [2,3].

Although the variability in the velocity field in the Ría can be largely explained by tidal influences, ultimately it is the residual circulation (i.e., at subtidal frequencies), that determines the net exchange with the continental shelf. Therefore, it is important to determine to what extent currents are explained by the wind (either remote or local) and how that modulates upwelling and estuarine circulation in the Ría.

The aim of this study is to contribute to the understanding of tidal and local/remote wind influences on the circulation of the Ría. To achieve that, current velocity and pressure data obtained by an ADCP (Acoustic Doppler Current Profiler) moored at the southern mouth of the Ría were analysed along with meteorological data recorded by a station installed in the port of Bouzas and an oceanic buoy located off Silleiro Cape (south of the Ría de Vigo).

MATERIAL AND METHODOLOGY

Velocity, pressure and temperature data were obtained using an Acoustic Doppler Current Profiler (ADCP) moored for 72 days (20/06/2013-02/09/2013) at the southern mouth of the Ría de Vigo (8º45.604'W, 42º14.463'N; 41.6 m depth). Speed and direction of local and remote winds were measured by a meteorological station installed on the Bouzas terminal of the Port of Vigo (8º45.4167'W, 42º 13.967'N) and by an ocean buoy from 'Puertos del Estado' (http://www.puertos.es) located off Silleiro Cape (9.43ºW, 42.12ºN) respectively.

ADCP data were used to calculate the free surface height. Atmospheric pressure effect was corrected using the Bouzas' station data. Finally, harmonic constituents data, pure tidal signal and harmonic fit residues were obtained computing a tidal harmonic analysis using MATLAB toolbox T_TIDE [4].

To assess the influence of each constituent over the water column, a layer by layer (70 layers, 0.5 m width) harmonic analysis to horizontal velocities was computed and determination coefficient (R^2) for each layer harmonic fit was obtained. Equally, tidal ellipses of the four main major constituents (greatest amplitude) were determined at three significant depths of the water column (not shown).

Finally, vectorial cross-correlation [5] between current and wind (local and the remote) horizontal velocity time series were estimated, first including the full-frequency spectrum of both series and later with tidal frequencies filtered out after applying a A24/25/25 filter [6]. These correlations allow for obtaining the percentage of current variance explained by wind variance (R^2) in the water column and the angle at which these time-series best correlate along the vertical profile.

RESULTS AND DISCUSSION

Harmonic analysis of the sea level signal shows a clear semidiurnal tide of mesotidal range [6]. Most energetic constituents were M_2, N_2 and S_2. Along with this, harmonic analysis of the velocity field throughout the water column revealed amplitude variations of the tidal constituents (Fig.1). Influences of M_2, N_2 and S_2 become evident over the entire depth of the southern mouth of the Ría; likewise, only a diurnal constituent, K_1, presented a more or less homogeneous influence. For those major constituents, the absence of changes in amplitude with depth indicates the barotropic behavior of the tidal currents.

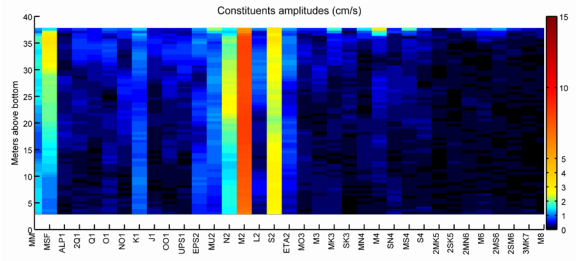

Fig.1. Harmonic constituents amplitudes throughout the water column

Vertical distribution of R^2 for the tidal fit (Fig.2a) shows the existence of a surface layer of less tidal influence and affected by other processes such as local wind, waves, river discharge and Ekman transport induced by remote shelf winds. There is also a central layer where tidal currents dominate the circulation and a bottom layer with less tidal dominance (greater than in the surface layer) and influenced by other processes (mainly friction with the bottom). This two-layer circulation (almost three-layer) observed at tidal time scales, fits the residual bidirectional circulation (mainly) induced by the coastal upwelling, but also by the local wind and the river, widely described in the literature.

Local (not shown) and remote wind correlation with full-spectrum currents velocities revealed a similar inverse distribution in accordance to that for the tidal fit, with greater influence at surface and bottom (Fig.2a). Even though both local and remote wind R^2 profiles had similar shapes, the latter presented higher values.

When tidal frequencies are removed from the signals, the best R^2 values appear. Although R^2 profiles preserve the previous shape, remote wind correlates better with residual velocities and it is in perfect accordance with the R^2 distribution for the tidal fit (Fig.2a), evidencing the vital

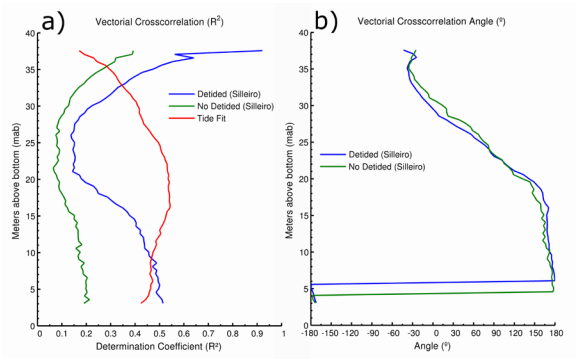

Fig.2. a) R^2 for the tidal fit and between remote wind and current velocities (both detided and no detided). b) Cross-correlation angle beween remote wind and currents (both detided and no detided)

role played by remote wind in the hydrodynamics of the Ría.

Regarding the vectorial correlation angle between remote wind and residual velocities, in the surface layer the best correlation is with a 30° angle of the current relative to the wind, counterclockwise. As is the case with local wind (not shown), this angle increases with the depth clockwise until 180º, showing again the two-layer circulation in the Ría. This two-layer structure differs in its circulation pattern (positive and negative) in response to the wind field characteristics (especially remote winds) and hence to the incidence of upwelling/downwelling events.

ACKNOWLEDGEMENTS

This work was supported by the STRAMIX Project (CTM2012-35155), funded by the Spanish Ministry of Economy and Competitiveness.

REFERENCES

1 – Arístegui, J. et al., 2009. Sub-regional ecosystem variability in the Canary Current upwelling. *Prog Oceanogr*, 83 (1-4), pp. 33–48.

2 - Piedracoba, S. et al., 2005. Short-timescale thermohaline variability and residual circulation in the central segment of the coastal upwelling system of the Ría de Vigo (northwest Spain) during four contrasting periods. *J Geophys Res*, 110 (C3), p.C03018.

3 - Pardo, P.C., Gilcoto, M. & Pérez, F.F., 2001. Short-time scale coupling between termohaline and meteorological forcing in the Ría de Pontevedra. *Sci Mar* 65, supplement, pp. 229–240.

4 - Pawlowicz, R., Beardsley, B. & Lentz, S., 2002. Classical tidal harmonic analysis including error estimates in MATLAB using T_TIDE. *Computers & Geosciences*, 28 (8), pp. 929–937.

5 - Kundu, P.K., 1976. Ekman Veering Observed near the Ocean Bottom. *J Phys Oceanogr*, 6 (2), pp. 238–242.

6 - Godin, G., 1972. The analysis of tides, Liverpool: University of Toronto Press.

Study of the local circulation induced by a wind jet at the northern margin of the Ebre Shelf

Laura Ràfols[1,2], Manel Grifoll[1], Manuel Espino[1], Abdel Sairouní[2] & Manel Bravo[2]

[1] LIM-UPC (Laboratori d'Enginyeria Marítima, Universitat Politècnica de Catalunya - BarcelonaTech)
[2] SMC (Servei Meteorològic de Catalunya)

ABSTRACT

The dynamical response to cross-shelf wind jets at the northern margin of the Ebre Shelf is analysed. The study area is located at the NW of the Mediterranean Sea and is characterized by the prevalence of NW winds (offshore). This wind component is channelled through the Ebre valley and is intensified when reaches the sea, resulting in a wind jet. This contribution show the surface and deep water circulation during the wind jet events, as well as the density vertical structure of the water column and the principal mechanism that governs the water circulation. Results from a numerical model, previously verified with data from buoys and a HF radar, are used. The results show a surface circulation induced by the wind in the same direction as the wind and a circulation in the opposite direction in deeper layers. This leads an upwelling region near the coastline consistent with a decrease of the sea level height. Comparing wind-jet response for different water stratification in the vertical, the results indicate that the water column is less mixed when the stratification is higher but, in all cases, the two-layer flow behaviour is observed. Finally, the momentum balance exhibits, in general, a balance between the frictional terms and the pressure gradient in shallower region and a geostrophic balance in deeper areas of the domain.

INTRODUCTION

Regions with low-level coastal wind jets induced by orographic effects are areas with a complex dynamic in terms of water circulation response, spatial and temporal wind variability and wave height variations.

An observational study carried out in the northern Margin of the Ebre shelf [1] revealed a seasonal response of the water column due to offshore winds. They highlighted the presence of cold water at the surface but did not discern between an upwelling process or a cooling effect due to mixing. Also, the scarcity of their measurements does not allow to extrapolate their results in the whole region since the shelf response at cross-shelf winds is highly dependent of the water depth.

The main goal of this study is to describe the water circulation induced by a wind jet at the northern margin of the Ebre Shelf. The aim of this work is to investigate the wind jet response in terms of water circulation and density vertical structure. Additionally, the influence of the stratification and the main mechanism that governs the circulation are also analysed.

To conduct the analysis, a numerical model has been implemented in the region and run for a period of 7 months (from the first of March until the first of October 2014).

DATA AND METHODOLOGY

The numerical model used in this study is the Regional Ocean Modeling System (ROMS). It is a split-explicit, free-surface, terrain-following, primitive equations oceanic model that solves the 3D Reynolds-averaged Navier-Stokes equations using the hydrostatic and Boussinesq assumptions [2]. As initial and boundary conditions, data from IBI-MFC (Iberian Biscay Irish - Monitoring and Forecasting Centre) products are used. And outputs from the Weather Research and Forecasting (WRF, [3]) model implemented at high resolution (3 km) at the Catalan Service of Meteorology are used for the atmospheric forcings. The domain (see Fig. 1) has a spatial resolution of 350 m in both horizontal directions and 20 sigma levels in the vertical.

Data from the Puertos del Estado (http://www.puertos.es) network for oceanographic and coastal meteorological measurements (owned by the Spanish Government) are used in order to validate the numerical outputs. In particular, data from a tide gauge (located at Tarragona harbour), two buoys (moored at 688 m and 15 m) and a High Frequency radar (see Fig. 1). From HF radar data, only points with more than 50% of data availability are used to ensure data quality.

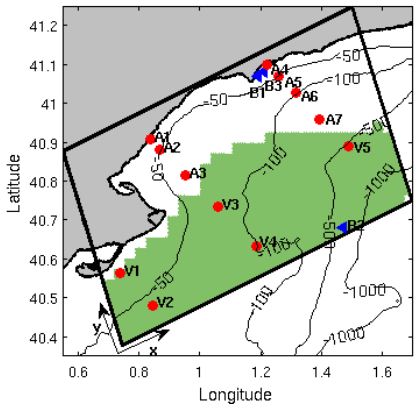

Fig 1. Numerical model domain (black rectangle), HF radar validation area (in green), tide gauge and buoy locations (blue triangles) and validation/analysis points (red dots).

RESULTS

The results from the numerical model simulations exhibit a good agreement with the observational data at the continental shelf (depths less than 200 m). Fig. 2 shows the Skill Score for the along-shelf and across-self direction. The agreement of the numerical model outputs decreases at deeper areas, highly influenced by the boundary conditions. Since the aim of this work is to study the wind jet response at the continental shelf (shallow waters), the poor quality of the results at the lower right corner of the domain (deep waters) is despicable.

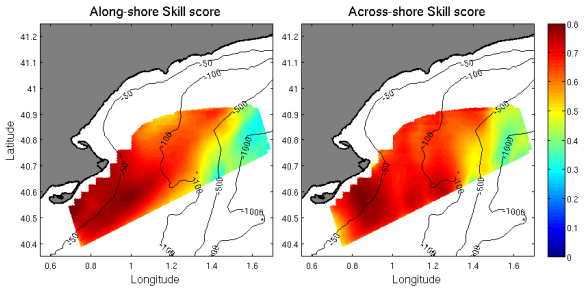

Fig 2. Surface currents model skill score comparing the numerical model results and the HF radar data in the along-shelf (left) and cross-shelf (right) direction.

Analysing the wind data for the studied period, nine wind-jet events were identified. One of these events is selected to carry out a detailed analysis of the evolution of the dynamics caused by offshore winds. An integral analysis, using the evolution of the buoyancy frequency, is carried out for the other identified events showing the common response in the water column density structure evolution.

During the wind jet episodes, the across-shelf surface currents are controlled by the wind flowing in the offshore direction. At deeper layers, the circulation is onshore with intensities much smaller than the surface ones. In consequence, a two-layer flow is observed with an upwelling zone near the coastline. As for the along-shelf currents, they undergo a shift from north-eastward to south-westward. This shifting is probably caused by along-shelf adjustment of the barotropic pressure gradient caused by the spatially-varying wind forcing. Besides, a sea level set-down is observed during the wind jet.

In the analysis of the buoyancy frequency, it is observed that, during colder months (less stratified), the water column is well-mixed after the wind jet event. In contrast, during warmer months (more stratified), the wind-driven mixing is reduced and, in general, just a deepening of the pycnocline is observed after the wind jet. Nevertheless, in all cases, the across-shelf vertical structure exhibits a two-layer flow structure.

Finally, during the wind jet event, the momentum balance analysis presents a balance between frictional terms and the pressure gradient at shallow areas. When the water depth increases the Coriolis force becomes more important, relegating the frictional terms to a second order, thus the balance tends to turn into a geostrophic balance.

ACKNOWLEDGEMENTS

The development of this research is funded by the “Doctorat Industrial 2013” PhD Program of the Catalan Government. The first author thanks the UPC (Universitat Politècnica de Catalunya) and the SMC (Servei Meteorològic de Catalunya) for their support. The authors also acknowledge Puertos del Estado for the set of data provided.

REFERENCES

1 - Grifoll M, Aretxabaleta AL & Espino M, 2015. Shelf response to intense offshore wind. *J. Geoph. Res.*, 120:6564-6580.

2 - Shchepetkin AF & McWilliams JC, 2005. The regional oceanic modeling system (ROMS): a split-explicit, free-surface, topography-following coordinate oceanic model. *Ocean Model.*, 9:347-404.

3 – Skamarock WC, Klemp JB, Duhdia J, Gill DO, Barker DM, Duda MG, Huang X, Wang W & Powers JG, 2008. *A description of the Advanced Research WRF, Version 3*. NCAR Technical Note.

Modelado de la salida de agua mediterránea por el Estrecho de Gibraltar

Sergio Ramírez Garrido[1], Álvaro Peliz[2], Antonio García Olivares[1] & Josep L. Pelegrí[1]

[1] Departament d'Oceanografia Física i Tecnológica, Institut de Ciències del Mar, CSIC, Barcelona
[2] Departament of Geophysics and Energy, University of Lisbon, Lisbon

RESUMEN

El objetivo del estudio es validar un modelo regional tridimensional que simula la salida de agua mediterránea desde el Estrecho de Gibraltar hacia el Golfo de Cádiz en la época actual. Este modelo está únicamente forzado por la diferencia de densidad existente entre dos aguas tipo idealizadas: agua Atlántica y Mediterránea. La densidad de cada tipo de agua está definida por los correspondientes perfiles de temperatura y salinidad. Mediante la diferente carga hidráulica en el Estrecho, se estudia el ajuste en profundidad del agua mediterránea en su salida desde el Estrecho de Gibraltar hacia la cuenca Atlántica.

INTRODUCCIÓN

Existen modelos realistas que simulan la salida de agua mediterránea desde el Estrecho de Gibraltar hacia el Golfo de Cádiz (*Mediterranean Outflow Water*, MOW), incorporando la complejidad física que resulta de la batimetría, mareas y forzamiento atmosférico [1]. Sin embargo, no existe un estudio que la modelice mediante un forzamiento simple idealizado, basado en la diferencia de densidad existente entre el agua Atlántica y Mediterránea. Dicho análisis ayudaría no solo a entender los mecanismos y vías de penetración de la MOW en el Golfo de Cádiz, sino también a comprender cómo ha variado la trayectoria de la MOW en el pasado y como puede modificarse en un futuro como consecuencia de los cambios en la estructura de la columna de agua, producto del cambio climático.

MATERIAL Y MÉTODOS

El modelo numérico utilizado es el Regional Ocean Modeling System, ROMS (http://www.myroms.org/). ROMS es un modelo de superficie libre, ajustado al terreno, que resuelve las ecuaciones primitivas del océano, muy utilizado por la comunidad científica para una amplia gama de aplicaciones, incluidas las previsiones sobre la evolución futura del clima del planeta en relación con distintos escenarios futuros.

El dominio comprende desde el Golfo de Cádiz hasta el Mar de Alborán, con un malla de 486 □ 205 puntos y 32 niveles de profundidad, obteniendo una resolución horizontal de 2 km. Las masas de agua mediterránea y atlántica se definen mediante perfiles verticales analíticos de temperatura y salinidad, que a su vez definen los perfiles de densidad. De este modo se establecen las condiciones iniciales de partida, que también se utilizan para reponer los valores originales de estas masas de agua en las fronteras. No se aplica ningún forzamiento atmosférico, ni ciclo de mareas, ni se contempla la variabilidad estacional.

Los perfiles de temperatura y salinidad se definen mediante funciones analíticas que simula adecuadamente la estructura invernal de la columna de agua; la expresión para la temperatura sería la siguiente:

$$T = T_f - T_s \tanh\left(\frac{H}{nz}\right)$$

donde T_f y T_s respectivamente representan la temperatura de fondo y superficie, H es la profundidad total de la columna de agua, z es la coordenada vertical y n es un único parámetro capaz de hacer variar el gradiente de densidad con la profundidad y así definir la profundidad de ajuste de la MOW en el Golfo de Cádiz. Cuanto mayor es el valor de n más abrupto es el cambio de la temperatura con la profundidad (Fig. 1).

Puesto que el modelo no incluye mareas, se utiliza un procedimiento alternativo para reproducir el efecto de las mareas sobre la mezcla. Se define una zona de intensificación de la mezcla, con un punto máximo que corresponde a la mayor velocidad de salida de la MOW y una función que representa un decaimiento en la mezcla a medida que nos alejamos de este punto. Para conservar masa, se utiliza una función que redistribuye la masa en función del caudal neto de entrada/salida a través del estrecho, que actualmente es de 0.05 Sv; de este modo se ajusta el transporte para ambas cuencas de modo independiente. Esto simula una evaporación uniforme en la cuenca mediterránea.

En los límites del dominio se define una capa de amortiguación (*sponge*) y se ajusta cada cierto tiempo a una climatología especificada en las fronteras del dominio (*nudging*). De este modo se consigue reponer los valores de

temperatura y salinidad en las fronteras de ambas cuencas. En la cuenca Mediterránea se define un canal infinito que replica la batimetría existente en el Cabo de Palos, con un aumento progresivo de la viscosidad y difusividad en dirección Este.

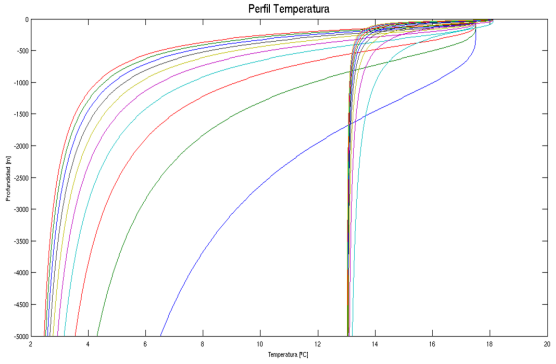

Fig. 1. Perfiles de temperatura, salinidad y densidad para diferentes valores de *n*; los perfiles atlánticos se encuentran a la izquierda y los mediterráneos a la derecha.

En el caso de la velocidad, al partir de un estado en reposo, se utiliza un fichero de climatología específico. Para ello, se efectúa una primera ejecución del modelo con la batimetría que simula el canal y los perfiles de T y S deseados, con unas condiciones de frontera radiadas para los campos de velocidades barotrópicos y baroclínicos. En el momento en que la Corriente de Argelia alcanza la frontera este del dominio, tras 15 días de simulación, se paraliza la ejecución. El fichero climatológico se forma con los valores promediados de los dos últimos días.

RESULTADOS Y DISCUSIÓN

El método propuesto consigue reproducir el patrón de circulación superficial y en profundidad para el Mar de Alborán, destacando los dos giros anticiclónicos que condicionan la entrada de agua atlántica y sitúan el agua mediterránea a mayor profundidad.

Tras un período inicial de spin up de aproximadamente un año se puede considerar que el modelo se ha estabilizado. Es a partir de este período de spin up que se ejecuta de nuevo el modelo por otro período de 4 años y se efectúa el estudio de sensibilidad para cada valor de *n*. Finalmente se hace el análisis de la profundidad a la cual se sitúa el máximo salino para las distintas condiciones de estratificación en ambas cuencas (Fig 2).

Para valores de *n* menores a 3 la densidad del agua Atlántica no alcanza un valor lo suficientemente elevado como para sustentar la lengua salina a las profundidades que se observan en la actualidad, haciendo que la MOW se sitúa a profundidades ligeramente superiores al oeste de Cabo San Vicente (9ºO). En contraste, para valores de *n* mayores a 6 el agua Mediterránea adquiere una densidad tan elevada, cercana a 1029 kg/m^3, que la lengua salina sigue siempre a lo largo del fondo oceánico. Para *n* igual a 3 y 4 la MOW se ajusta a las profundidades observadas en la actualidad [2, 3, 4]

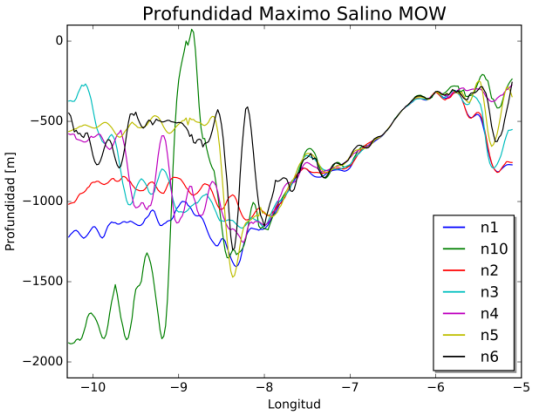

Fig. 2. Profundidad a la que se sitúa la MOW para diferentes valores de *n*.

El modelo desarrollado, forzado con condiciones analíticas muy idealizadas, reproduce correctamente la salida del agua mediterránea a lo largo de toda la cuenca del Golfo de Cádiz. Más aún, el modelo demuestra ser una herramienta sencilla y potencialmente muy útil para determinar los cambios paleoclimáticos de la MOW en el Golfo de Cádiz, así como los posibles cambios futuros como resultado de las modificaciones que están actualmente experimentando tanto las aguas atlánticas como mediterráneas, producto del calentamiento global.

AGRADECIMIENTOS

Este trabajo ha sido financiado por el Ministerio de Economía y Competitividad del gobierno de España a través de los proyectos TIC-MOC (CTM2011-28867) y VA-DE-RETRO (CTM2014-56987-P). Durante la realización de este trabajo, Sergio Ramírez Garrido ha tenido un contrato FPI del Ministerio de Economía y Competitividad vinculado al proyecto TIC-MOC (CTM2011-28867).

REFERENCIAS

1 – Peliz A, Dubert J, Marchesiello P & Teles-Machado A, 2007. Surface circulation in the Gulf of Cadiz: Model and mean flow structure. *J. Geophys. Res*., 112, C11015.

2 – Papadakis MP, Chasignet RC & Hallberg RW, 2003, Numerical simulations of the Mediterranean Sea outflow: impact of the entrainment parameterization in an isopycnic coordinate ocean model. *Ocean Model*., 5, 325-356.

3 – Ambar I & Howe MR, 1979. Observations of the Mediterranean outflow—1: mixing in the Mediterranean outflow. *Deep-Sea Res*., 26A, 535–554.

4 – Baringer MO & Price JF, 1997. Mixing and spreading of the Mediterranean outflow. *J. Phys. Oceanogr*., 27, 1654-1677.

Lagrangian path planning for the first Autonomous Underwater Vehicles in transoceanic missions: The new boundaries of operational oceanography

A.G. Ramos[(1)], V.J García-Garrido [(2)], S. Glenn[(3)], J. Kohut[(3)], O. Schofield[(3)], D.K. Aragon[(3)], N. Strandskov[(3)], A.M. Mancho[(2)], S. Wiggins[(4)], J. Coca[(1)].

(1). División de Robótica y Oceanografía computacional (ROC-SIANI). Integrated Marine Technology Service (SITMA. Facultad de Ciencias del Mar. Campus de Tafira, 35017-Las Palmas de GC. Spain. antonio.ramos@ulpgc.es
(2). Instituto de Ciencias Matemáticas, CSIC-UAM-UC3M-UCM, C/ Nicols Cabrera 15, Campus Cantoblanco UAM, 28049, Madrid, Spain.
(3). Coastal Ocean Observation Lab (COOL). Institute of Marine Sciences. Rutgers University, New Brunswick, USA.
(4). School of Mathematics, University of Bristol, Bristol BS8 1TW, United Kingdom.

ABSTRACT

Unmanned Underwater Vehicles (UUVs) are used in Oceanography due to their relative low cost and wide range of capabilities. Gliders change their buoyancy in order to dive and climb, describing a vertical saw tooth route. These displacements produce an effective although low horizontal speed which makes the glider strongly sensitive to the ocean dynamics. In order to control the glider path its heading is adapted by using information obtained from verified 4D current data sets. In particular from these data, Lagrangian descriptors have supplied potentially useful paths for piloting the RU-29 *Challenger* glider in the first South Atlantic Circumnavigation crossing flight (760 days-sea, 17400 km) held from 16th January 2013 to 31st March 2016). A description of the Challenger glider mission is found at **http://challenger.marine.rutgers.edu/** .

Invariant manifolds of hyperbolic trajectories were obtained from the *real time* 4D current fields (1º/12) forecast (+5 days) provided by the european marine forecasting system COPERNICUS in the South Atlantic domain during the last quarter of the mission (1500km far from S Africa). Manifolds outputs were then compared with the *ground true* paths and the *ground currents* provided by RU29 when it surfaced (every 14 hours). Preliminary results reported by the glider at its arrival at Cape Town (end of March, 2016), showed that the strong Agulhas current/mixing dynamics, was not captured by any of the 5 current models (Copernicus, Hycom, Oscar, NRTOFS, Glory) used for the comparison. Prior to this stage however (December 2015-mid March 2016) the manifolds obtained from the COPERNICUS current fields showed a high percentage of confident good routes that were confirmed by the ground true flying paths reported by the glider nearing the South African ZEE border (10th March 2016). The preliminary combination of the glider data with the invariant manifolds suggests a potentially useful tool for glider path planning for future long range transoceanic glider missions (Indian Ocean 2017-).

Keywords: South Atlantic Crossing. Autonomous Underwater Vehicles (AUVs). Path planning. Lagrangian Descriptors. Hyperbolic Trajectories. Decision Support.

Escenarios de circulación meridional global a partir de un modelo estuarino idealizado

Josep-Miquel Roca Sans[1] & Josep L. Pelegrí[1]

[1] Departament d'Oceanografia Física I Tecnológica, Institut de Ciències del Mar, CSIC

RESUMEN

Un modelo oceánico de cajas, al que se imponen condiciones de conservación de energía interna, de salinidad y de masa, permite establecer (a) en que escenarios se forma agua de mayor densidad en la alta latitud norte, en lo que denominamos situación de estuario inverso o negativo (flujo en sentido norte-sur por el fondo oceánico), y (b) en que otros escenarios dicha formación se produce en las latitudes tropicales, en lo que sería un estuario directo o positivo. Se contrastan los escenarios resultantes a la vista de las condiciones del océano actual.

INTRODUCCIÓN

En el Mar Mediterráneo, probablemente el más estudiado en la oceanografía física [1, 2, 3], hay evaporación neta de agua marina que es compensada por la entrada de agua superficial atlántica. A su vez, la evaporación neta del Mar Mediterráneo, y la conjunción de otros fenómenos atmosféricos en algunas zonas concretas, como vientos fuertes, secos y muy fríos durante el invierno, generan aguas de mayor densidad que la entrante, que se ubican cerca del fondo. Esta masa de mayor densidad termina saliendo parcialmente al océano vecino, estabilizando así el diferencial de salinidad. Se trata de lo que podríamos denominar un estuario inverso o negativo.

En el Atlántico Norte se produce una situación que puede considerarse análoga, como si se tratase de un estuario inverso o negativo de dimensiones globales. En esta parte del océano se da una situación de evaporación neta [1, 3, 4, 5], así como una climatología que produce la formación de aguas de gran densidad en sus latitudes más altas, aguas que se precipitan al fondo del océano formando el agua atlántica de fondo (NADW, North Atlantic Deep Water). Por otra parte, se produce un retorno o circulación hacia el norte de aguas más cálidas, tanto superficiales como termoclinas, procedentes de latitudes tropicales, cerrándose de esta forma el ciclo que se produciría en un estuario negativo.

METODOLOGIA Y DESARROLLO

De forma similar a otros estudios, se establece un modelo de dos cajas [6, 7, 8] (norte y sur), con una de ellas representando las aguas de latitudes tropicales y la otra las aguas localizadas a altas latitudes del Atlántico Norte. Cada una de estas cajas experimenta flujos opuestos de agua, en direcciones norte-sur y sur-norte (Fig. 1), con valores de temperatura T, salinidad S, densidad ρ, velocidad u y transporte U, tanto en la termoclina permanente (índice 1) como en las aguas de fondo (índice 2). En la caja de latitud norte se define un balance hídrico negativo $wb<0$, es decir con evaporación neta, y en la caja de latitud inferior con balance hídrico positivo $wb>0$, equivalente a precipitación neta [4].

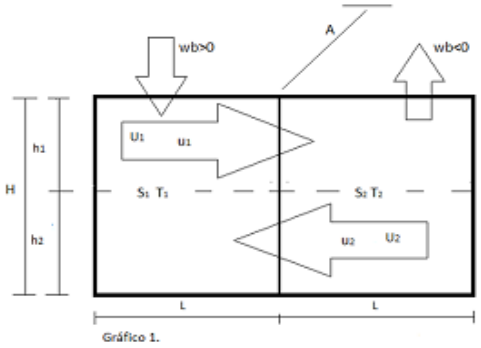

Fig. 1. Esquema del modelo de dos cajas.

Para cada una de las cajas, se hace un análisis de conservación de energía interna, masa y salinidad:

a) La variación en energía interna es el resultado de la ganancia (perdida) de la energía interna por advección de (hacia) la otra caja más (menos) la ganancia (perdida) de calor latente por precipitación (evaporación) neta.
b) La variación en sal se da por la entrada (salida) de masas de agua de diferente salinidad
c) La variación en masa resulta de la suma de masa entrante (saliente) de la referida caja más el efecto de la precipitación (evaporación) neta en la misma.

Las ecuaciones adimensionales que rigen los balances de energía, masa y sal son las siguientes:

a) Energía interna:

$$\rho_1 \frac{dT_1}{dt} = -\rho_1 U_1 T_1 + \rho_2 U_2 T_2 + wb$$

$$\rho_2 \frac{dT_2}{dt} = \rho_1 U_1 T_1 - \rho_2 U_2 T_2 - wb$$

b) Salinidad:

$$\rho_1 \frac{dS_1}{dt} = -\rho_1 U_1 S_1 + \rho_2 U_2 S_2$$

$$\rho_2 \frac{dS_2}{dt} = \rho_1 U_1 S_1 - \rho_2 U_2 S_2$$

c) Masa:

$$\frac{d\rho_1}{dt} = -\rho_1 U_1 + \rho_2 U_2 + wb$$

$$\frac{d\rho_2}{dt} = \rho_1 U_1 - \rho_2 U_2 - wb$$

Cuyas soluciones son:

$$T_1 = K_1 + \frac{K_3}{U_1 + U_2} e^{-(U_1 + U_2)}$$

$$T_2 = K_2 + \frac{K_4}{U_1 + U_2} e^{-(U_1 + U_2)}$$

$$S_1 = C_1 + \frac{C_3}{U_1 + U_2} e^{-(U_1 + U_2)}$$

$$S_2 = C_2 + \frac{C_4}{U_1 + U_2} e^{-(U_1 + U_2)}$$

Las constantes de integración (K_1, K_2, K_3, K_4) y (C_1, C_2, C_3, C_4) se obtienen a partir de las condiciones iniciales de temperatura, (T_1^i, T_2^i), salinidad, (S_1^i, S_2^i) y densidad , (ρ_1^i, ρ_2^i).

RESULTADOS Y DISCUSIÓN

Trasladando los resultados de esas ecuaciones a un estado estacionario, para $t \to \infty$, se tienen cuatro escenarios en los cambios de temperatura y salinidad se traducen en aumento o disminución de densidad (Fig. 2). Estos escenarios pueden explicarse como sigue:

- Cuadrante I: a altas latitudes *S* aumenta y T disminuye, ocasionando que aumenta la densidad y se forma agua de fondo, mientras que a bajas latitudes *S* disminuye y *T* aumenta, por tanto disminuyendo la densidad. Esta es la situación actual de circulación en el hemisferio norte atlántico.
- Cuadrante II: la situación es la inversa a la del cuadrante I, en la que el agua de mayor densidad se formaría en el océano tropical.
- Cuadrantes III y IV: en una misma zona geográfica se produce aumento/descenso de *S* y aumento/descenso de *T*. Por tanto, para conocer la evolución de la densidad, es necesario conocer los valores iniciales de ambas variables.

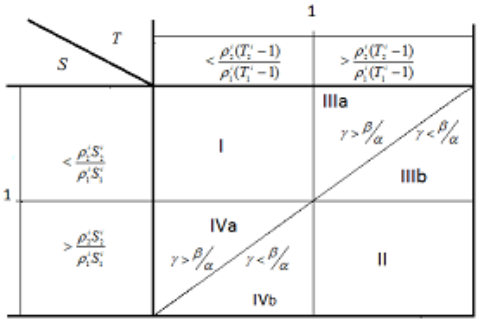

Fig. 2. Escenarios de los cambios de salinidad y temperatura.

La incertidumbre de los cuadrantes III y IV puede resolverse usando una expresión lineal de la ecuación de estado $\rho = 1 - \alpha(T_1 - t_0) + \beta(S - S_0)$, que conduce a:

$$\gamma \equiv \frac{-\rho_1^i (T_1^i - 1) + \rho_2^i (T_2^i - 1)}{-\rho_1^i S_1^i + \rho_2^i S_2^i} > 1 < \frac{\beta}{\alpha}$$

Inicializando el modelo con las condiciones actuales oceánicas, (S_1^i, S_2^i) y (T_1^i, T_2^i), se deduce que el esquema actual de (circulación oceánica ↔ evaporación ↔ circulación atmosférica ↔ precipitación) mantiene y consolida la situación actual del Atlántico Norte como estuario negativo. Para que dicho estuario cambie de signo, dado que la temperatura oceánica en altas latitudes es inferior a la de las aguas tropicales, la salinidad en altas latitudes debería descender radicalmente.

AGRADECIMIENTOS

JLP agradece el apoyo recibido por parte del Ministerio de Economía y Competitividad del gobierno de España a través del proyecto VA-DE-RETRO (CTM2014-56987-P).

REFERENCIAS.

1 - Birchfield GE, 1989. A coupled ocean-atmosphere climate model. *Clim. Dyn*., 4, 57-71.

2 - Knudsen M, 1900. *Ein Hydrographischer Lehrsatz*. *Annal. Hydrograph. Marit. Meteorol*., 28, 316–32.

3 – Talley LD, et al., 2011. *Descriptive Physical Oceanography*. Elsevier, 250 pp.

4 - Randall D, 2012. *Atmosphere, Clouds and Climate*. Princeton Primers in Climate, 167 pp.

5 - Schmitt RW et al., 1989. Evaporation minus precipitation and density fluxes for the North Atlantic. *J. Phys. Oceanography.*, 19, 1208-1221.

6 - Huang, R.X.and Guan,Y.P., 2008. Stommel's box model of thermohaline circulation revisited. *J. Phys. Oceanogr*., 38, 909-017.

7 - Huang RX, et al., 1992. Multiple equilibrium states in combined thermal and saline circulation. *J. Phys. Oceanogr.*, 22, 231-246.

8 - Stommel, H.,1961. Thermohaline convection with two stable regimes of flow. *Tellus*, 13, 224-230.

The Contribution of Double Diffusion versus Shear-Driven Turbulent to Diapycnal Mixing in the Cape Ghir Upwelling Region

Ángel Rodríguez-Santana[1], Mireya Arcos-Pulido[1], Sheila Estrada-Allis[1], M. Emelianov[2]

[1] Departamento de Física, Universidad de Las Palmas de Gran Canaria (ULPGC). Canary Islands, Spain (angel.santana@ulpgc.es)
[2] Instituto de Ciencias del Mar, CSIC, Barcelona, Spain (mikhail@icm.csic.es),

ABSTRACT

One oceanographic survey was carried out within a project multidisciplinary (PROMECA) from 18 to 29 October 2010 in the Canary Basin. During three days, conductivity–temperature-depth (CTD), expandable bathytermograph temperature (XBT), microstructure turbulence (free-fall turbulence profiler) and acoustic Doppler current profiler (ADCP) data were collected in several stations in the Cape Ghir upwelling region. The results show how the vertical distribution of the dissipation rate of the turbulent kinetic energy, ε, and of the dissipation rates of thermal variance, χ, are modified by the filaments present in the region. These oceanographic structures intensify the vertical shear of the flow and modify the vertical gradients of temperature and salinity, thus influencing the sources of mixing processes associated (Kelvin-Helmholtz instabilities and double diffusion). The ε values range between 10^{-7} and 10^{-10} W/kg in the first 500 m of the water column with maximum values near the surface or associated to the filaments. By examining vertical distributions of density ratio, R_ρ, and gradient Richardson number, Ri, together with ε and χ, we found zones of the water column where dominates salt fingers or shear-driven turbulence. Applying an analysis based on the intermittency factor with a model based on the dissipation ratio, we estimate the net turbulence diffusivities when processes of double diffusion and shear-driven turbulence are present in the same region.

The Canary Deep Poleward Undercurrent

Eusebio Romero-García[1], Pedro Vélez-Belchí[2], Ricardo Sánchez-Leal[3] & Alonso Hérnadez-Guerra[1]

[1] Instituto de Oceanografía y Cambio Global - Universidad de Las Palmas de Gran Canaria.
[2] Instituto Español de Oceanografía, Centro Oceanográfico de Canarias.
[3] Instituto Español de Oceanografía, Centro Oceanográfico de Cádiz.

ABSTRACT

Poleward undercurrents are well known features in Eastern Boundary systems. In the California Current Eastern Boundary upwelling system (CalCEBS) the California poleward undercurrent has been widely reported, and it has been demonstrated that it transports nutrients from the equator waters to the northern limit of the subtropical gyre. However, in the Canary Current Eastern Boundary upwelling system (CanCEBS), the Canary deep poleward undercurrent (CdPU) has not been properly characterized. In this study, we use trajectories of Argo floats and model simulations to properly characterize the CdPU, including its seasonal variability, and the driving mechanism. The Argo observations show that the CdPU flows from 26ºN, near cape Bojador, to approximately 45ºN, near cape Finisterre in the northwest Spanish's coast. The CdPU flows deeper than the CalUC, and its mean depth varies with latitude, from near surface at 20ºN to 900 m at 44ºN. The CdPU shows a marked seasonal variability, with it maximum strength in fall, and the minimum in spring.

INTRODUCTION

In the California Current Eastern Boundary upwelling system (CalCEBS) the California poleward undercurrent (CalUC) has been widely reported [1], as well as its importance in maintain the high productivity of the California Current system [2]. However, in the case of the CanCEBS there are just few, and sparse, observations of the poleward undercurrent [3,4]. Most of these are short-term mooring records, or drifter trajectories of the surface or upper-slope flow. In spite that the CalUC and CdPU are similar and comparable, there are some differences between both currents that suggest slightly different forcing mechanisms. For instance, it was observed than the core of the CdPU is deeper (~800 dbar) than the core of the CalUC (~500 dbar) [1,4]

In this study we have used different data sets from the Argo network, and model simulations to characterize the CdPU.

MATERIAL AND METHODS

We have taken advantage of the Argo data set, since most of the Argo floats have its parking depth at 1000 dbar. From the YoMaHa database of Argo velocities at the parking depth, we have selected those trajectories with a poleward component in the slope of the northwest African coast or the California coast. Once the Argo floats were identified, the full set of measurements for each float, including the measured pressure at the parking depth were used to verify the actual trajectory of the float. From a total of 157 floats in the CanCEBS region, bounded by 25-5ºW and 20-45ºN, 20 floats described a poleward flow, while in the CalCEBS not a single float described a poleward trajectory of a total of 123 floats analysed.

To complement the direct observations from the Argo network, model simulations from the Ocean General Circulation Model for the Earth Simulator (OFES) were used. The simulations were done by JAMSTET, based on MOM3, in a global domain with a horizontal resolution of 0.1 degree and 54 vertical levels. Two different wind forcings were used, QuikSCAT (QS) and NCEP winds [5]. We have used monthly data in the period January 1999 to December 2006 in both regions.

RESULTS AND DISCUSSION

For the CanCEBS, the Argo floats trajectories show an overall continue poleward flow from cape Bojador (26ºN) to the northwest Spanish's coast (44ºN) (Fig. 1), with continues trajectories from the Canary Islands to Cape Ghir, from Cape Ghir to Cape Saint Vincent and from Cape Saint Vincent to Cape Finisterre. The mean velocity of the estimated current at the parking depth was ~4 cm/s, and a water mass analysis (not shown) at the parking depth indicates that there was a gradient from Antarctic intermediate Waters at 25ºN to Mediterranean Waters at 44ºN, although the CdPU was not associated with a particular water mass.. The CdPU is a persist and continuous current with a core at ~1000 dbar, as demonstrated by the fact that after surfacing every 10 days, and spending 15 hours ascending and in the surface, 20 floats returned to the CdPU.

In the CalCEBS any of the Argo floats trajectories showed poleward flow, indicating that, at least, the core of the CalUC and the CdPU are at different depth. The model simulations forced with QS winds confirm this. This simulation show that the core of the CalUC was at ~500dbar, while it was at ~800dbar for the CdPU

For the CanCEBS, the model simulations forced by the QS winds show an overall agreement with the observation, and

therefore may be used to understand the forcing mechanism and variability of the CdPU.

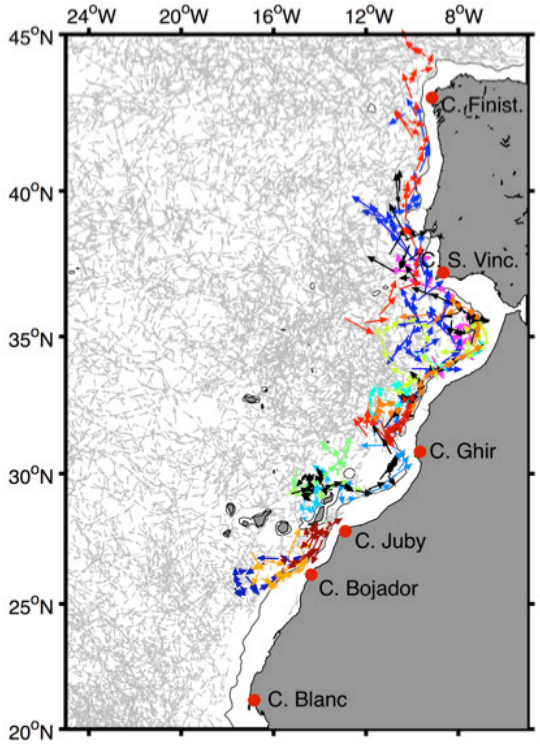

Fig. 1. Selected Argo floats trajectories. The different coloured arrows represent individual selected trajectories, while grey arrows represent the trajectories of all Argo floats in the area. The parking depth of the floats was 1000 dbar. For reference, the 1000m isobaths is presented as a black line.

At 800 dbar, the mean velocity form the QS-model simulations (Fig. 2) shows that there is not poleward flow south of 25ºN, coincident with the area where no Argo floats where found with poleward trajectories, since the core is shallower at lower latitudes. At 30ºN there is also a region without any trajectory (Fig. 1) that is probably associated to the mesoscale activity in the area of the cape Ghir filament and the meandering of the poleward flow in the simulation, possibly due to the step topography. The model simulation shows a strong seasonal variability for the CdPU. It appears between spring to winter, with its maximum during fall. During winter, the poleward flow decrease and it reverses in the coast of the Iberian Peninsula (37-44ºN), to practically disappear in spring.

In the simulations, the CalUC is flow continuously from San Diego (USA) to Vancouver Island (Canada), but it seasonal cycle is less intense that the CdPU.

Overall, the forcing that produces the poleward is the north south pressure gradient that causes an eastward flow to develop, which balances the northward pressure force by centrifugal acceleration. Near the coast, within a distance comparable to the Rossby radius of deformation, the eastward flow is blocked by the coastal boundary, and accelerates northward. Diagnosis of the north-south pressure gradients will allow us to understand the different seasonal cycle of the CdPU and the CalUC.

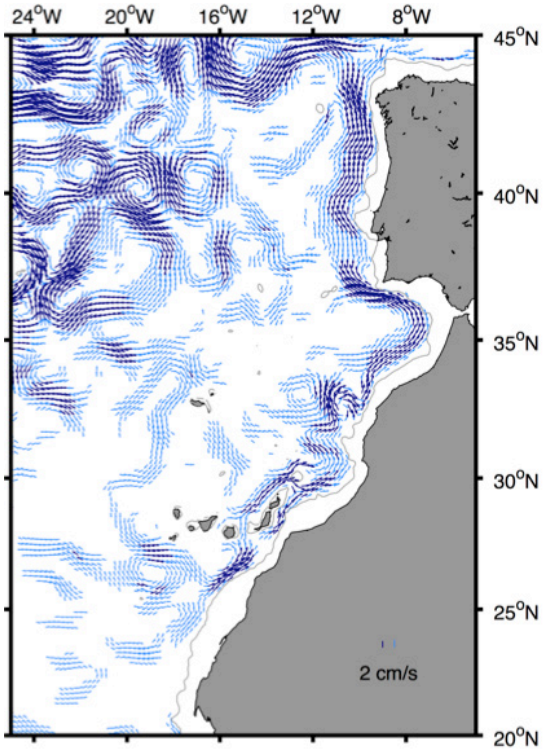

Fig. 2. Autumn (September October November) mean OFES-QuikSCAT velocity at 800m depth (time averaged 1999-2006). Light blue (dark blue) vectors represent currents between 1-2 cm/s (>2 cm/s). The scale of the two vectors is shown into the figure. For reference, the 1000m isobaths are represented as grey line.

ACKNOWLEDGMENTS

This study has been performed as part RAPROCAN Project from the Instituto Español de Oceanografía, and as part of the SeVaCan project (CTM2013-48695), funded by the Ministerio de Economía y Competitividad

REFERENCES

1 - Collins CA, Ivanov LM, Melnichenko OV & Garfield N, 2004. California Undercurrent variability and eddy transport estimated from RAFOS float observations. *J. Geophys. Res.*, 109(C5), C05028, doi:10.1029/96GL02138.

2 - Thomson RE & Krassovski MV, 2010. Poleward reach of the California Undercurrent extension. *J. Geophys. Res.*, 115(C9), doi:10.1029/2010JC006280.

3 - Vélez-Belchí P, Hernández-Guerra A, González-Pola C & Machín F, 2012. The Canary deep poleward undercurrent. AGU Fall meeting 2012.

4 - Barton ED, 1989. The poleward undercurrent on the eastern boundary of the subtropical North Atlantic, in Poleward flows along Eastern Ocean Boundaries, vol. 34, edited by Neshyba S and Smith RL, pp. 82-95, Coastal and Estuarine Studies, Springer-Verlag, New York.

5 - Masumoto Y, Sasaki H, Kagimoto T, Komori N, Ishida A, Sasai Y, Miyama T, Motoi T, Mitsudera H, Takahashi K, Sakuma H & Yamagata T, 2004. A fifty-year eddy-resolving simulation of the world ocean—Preliminary

outcomes of OFES (OGCM for the Earth Simulator). *J. Earth Simulator*, 1, 35–56.

An Argo-inferred Lagrangian view of the South Atlantic Ocean at 1000 dbar

Miquel Rosell-Fieschi[1], Jerôme Gourrion[2] & Josep Lluís Pelegrí[1]

[1] Departament d'Oceanografia Física i Tecnológica, Institut de Ciències del Mar, CSIC
[2] Centre National de la Recherche Scientifique, Division Technique de l'Institut de Sciences de l'Univers, Plouzané, France

ABSTRACT

Maps of velocity vectors and streamlines, calculated after integration from some reference contour, can be very useful to illustrate the gross characteristics of the changing velocities. Nevertheless, they are only snapshots of the velocity field that cannot be used to directly infer exchange between different oceanic regions. In order to do so, we must use of a Lagrangian approach, where we actually track water parcels as they move under the influence of the spatially and temporally changing velocity fields. Here we present a simple model that integrates monthly velocity fields in time, either forward or backward, in order to track the origin or fate of water parcels. In our case, the velocity fields are inferred from the positions of Argo floats. We illustrate the model by examining the recirculation of intermediate waters in the southern South Atlantic Ocean. The model allows us tracking whether and how the water parcels at these intermediate depths recirculate zonally or drift meridionally. In this application, we carefully explore the important role of the Brazil-Malvinas Confluence and the Agulhas Leakage. We estimate that most of the intermediate waters recirculate across the ocean in time periods between about 10 and over 20 years, eventually meeting at the Brazil-Malvinas Confluence region. Our results show no water transfer from the Indian Ocean, i.e. they show no Agulhas Leakage, although this may be an artefact caused by the absence of rings in the mean fields. A remarkable feature is the presence of a meridionally pulsating behaviour in the transoceanic trajectories, best visible in an accompanying video.

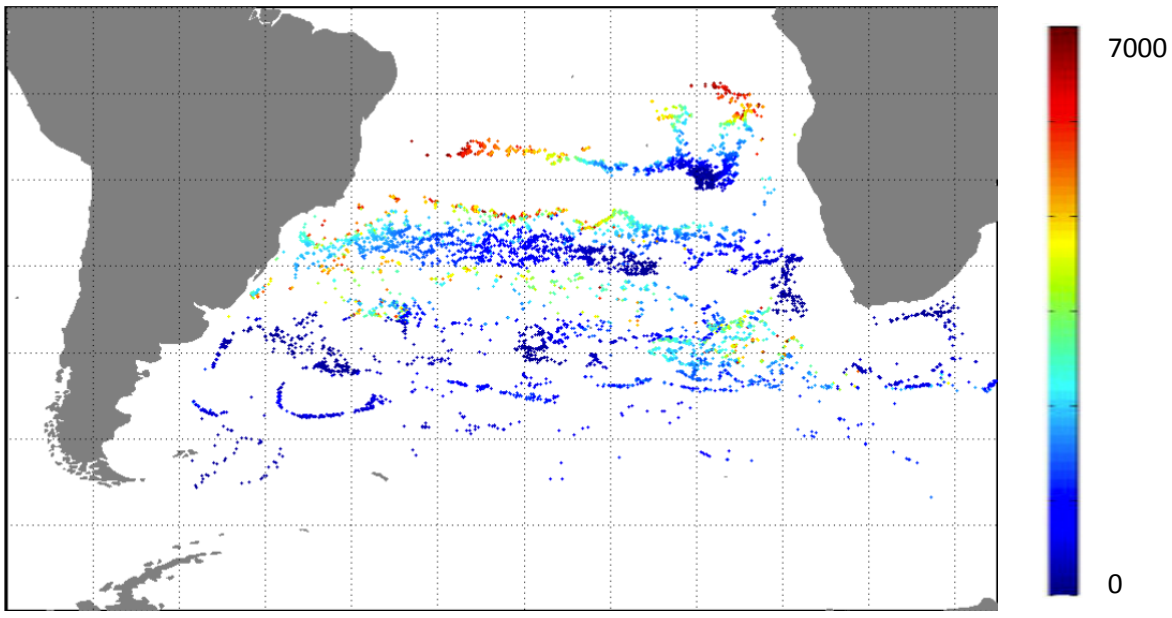

Fig.1. Last frame of a 20 year simulation for the velocities at 1000 dbar. Floats have been released continuously from seven (lat,lon) points: (-20,0); (-30,-5); (-34,30); (-38,-50); (-40,-42); (-40,-20); (-55,-60). The particles are randomly released in a 2º box centered on the specified points. The colorbar indicates the time after release for each float in days.

ACKNOWLEDGEMENTS
This research has been supported by the Ministerio de Economía y Competitividad of the Spanish Government through project VA-DE-RETRO (CTM2014-56987-P).

Global ocean oscillation as seen from Argo-inferred surface velocities

Miquel Rosell-Fieschi[1], Jerôme Gourrion[2] & Josep Lluís Pelegrí[1]

[1] Departament d'Oceanografia Física i Tecnológica, Institut de Ciències del Mar, CSIC
[2] Centre National de la Recherche Scientifique, Division Technique de l'Institut de Sciences de l'Univers, Plouzané, France

ABSTRACT

Since 2007, in the world's oceans there are over 3000 Argo floats that transmit position data typically once every 10 days. This represents some 100.000 positions yearly that lead to an equivalent number of velocity vectors. This massive amount of velocity data allows us constructing monthly-mean fields with spatial resolution of the order of 1º in latitude-longitude. Here we present, for the first time, the monthly sea-surface velocity fields for all oceans, unravelling the spatial distribution of the seasonally evolving fields. The velocity fields are predominantly zonal except for the western boundary subtropical regions. Further, these zonal fields change spatially following the evolution of the Intertropical Convergence Zone and the accompanying low- and high-pressure centres in both hemispheres. The resulting patterns appear as a transoceanic meridional seasonal pulse, typically propagating from south to north and from east to west. This work illustrates the potential of the Argo-inferred velocity data for an improved description of the surface currents at regional and, most remarkably, global scales.

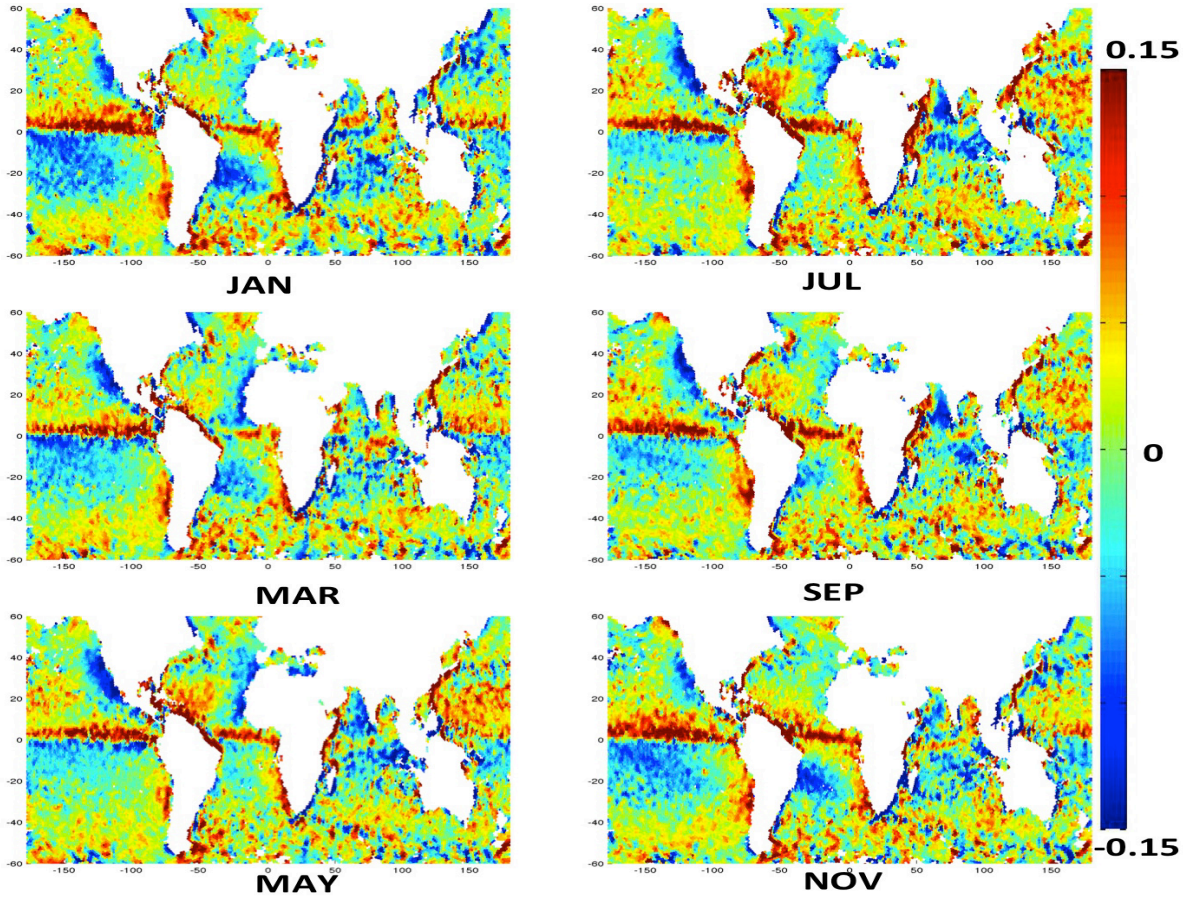

Fig. 1. Meridional velocity fields (90-day averaged), centred on the specified months.

ACKNOWLEDGEMENTS

This research has been supported by the Ministerio de Economía y Competitividad of the Spanish Government through project VA-DE-RETRO (CTM2014-56987-P).

HF radar insight into rapidly evolving mesoscale structures in the SE Bay of Biscay

Anna Rubio[1], Ainhoa Caballero[1], Lohitzune Solabarrieta[2], Luis Ferrer[1] & Julien Mader[1]

[1] AZTI-Marine Research, Herrera Kaia, Portualdea z/g, 20110 Pasaia, Spain (arubio@azti.es)
[2] DeustoTech Energy, Unibertsitate etorbidea, 24, Bilbo, Spain

ABSTRACT

Two HF radar stations are working operationally in the south-eastern Bay of Biscay since 2009, and providing hourly surface currents with 5 km radial and 5º angular resolutions, in a 150 km mean coverage. The historical 7-year quality-controlled HF radar data time series allows the study of the surface circulation in the area linked to different ocean processes. A description, from a Lagrangian point of view, of the surface signature of a rapidly evolving mesoscale structure is provided here. Additional satellite and wind data are used to complete HF radar information and to investigate the generation process of this structure. The presence of mesoscale structures in the study area is recurrent and it is expected to have a significant impact in the coastal ocean transports.

INTRODUCTION

The primary surface circulation pattern in the SE Bay of Biscay (hereinafter SE BoB) presents a marked seasonal variability [1]. A key component of this variability is the slope Iberian Poleward Current (IPC). In winter, the IPC flows eastward along the Spanish coast and northward along the French coast, affecting the upper water column (up to 300 m). This IPC is associated with warm surface waters [2]. In summer, the flow is reversed and three times weaker than in winter [3]. Overlaid to the density-driven slope circulation, wind-induced currents are the main drivers of the surface ocean circulation in the area (e.g., [4]). At shorter time-scales, the variability is dominated by inertial oscillations and tides. From HF radar data, inertial oscillations have been observed to be seasonally modulated and intensified in summer, within the central part of the study area [3,5]. In addition to these processes, mesoscale eddies in the SE BoB are generated most frequently during winter by the interaction of the IPC with the abrupt bathymetry [6]. Mesoscale coherent structures have also been observed within the HF radar footprint area (e.g., [7]). The SE BoB is an area where relevant human activities linked to marine resources are concentrated. This area represents a particular challenge for the accurate monitoring and forecast of 4D transports. In this context, the main objective of this work is to investigate the characteristics of the mesoscale structures observed in the area using the HF radar and to analyze their potential impact on the coastal ocean transport patterns.

DATA AND METHODS

A main component of the SE BoB Operational Oceanography observational network is, since 2009, a 2 long-range HF radar system, owned by the Directorate of Emergency Attention and Meteorology of the Basque Government Security Department. The radar antennas emit at a central frequency of 4.5 MHz and a 40 kHz bandwidth. The range coverage of radial data is 150 km, with 5 km radial resolution. HF radar validation exercises with this system have been previously done by several authors with suitable results [3,5]. The received signal (every 20 minutes), an averaged Doppler backscatter spectrum, is processed to obtain radial currents using the MUSIC algorithm. These radial currents are converted to total fields using the HFR_Progs MATLAB package least mean square algorithm (spatial interpolation radius of 10 km). The radial currents are processed as well to generate Open Mode Analysis (OMA, see [8]) gap-filled total derived currents. Then, to simulate trajectories using HF current fields we used a new version (adapted to 2D fields) of the Lagrangian particle-tracking model previously used by [9]. To describe mesoscale patterns, Lagrangian residual currents (LRC) were calculated following a methodology similar to that described in [7] and using an integration time of 3 days to filter out high-frequency processes. Additional AVHRR and MODIS-Aqua data from NERC Earth Observation Data Acquisition and Analysis Service (NEODAAS) and hourly winds from MeteoGalicia (WRF model) were also analyzed.

PRELIMINARY RESULTS AND DISCUSSION

The visual inspection of low-pass filtered HF radar data suggests the recurrent presence of cyclonic and anticyclonic structures in the study area. One example of these structures is shown in Fig. 1. This dipole was observed during several days at the end of 2011 and beginning of 2012. Its generation seems to be linked to a

strong wind-induced coastal jet. At the end of 2011, the wind stopped and the jet relaxation generated an anticyclonic structure over the shelf, which migrated offshore and westward. At the east of this structure, a cyclone developed forming the dipole. The presence of the dipole in the HF radar data was discontinuous, because strong winds caused intense surface currents, which masked the surface signature of this structure. When these strong winds stopped, the structure was visible again and could be observed until the surface signal of the cyclone disappeared. The anticyclonic signature was observed during some additional days, at the beginning of 2012, until it drifted to the west, out of the HF radar footprint area.

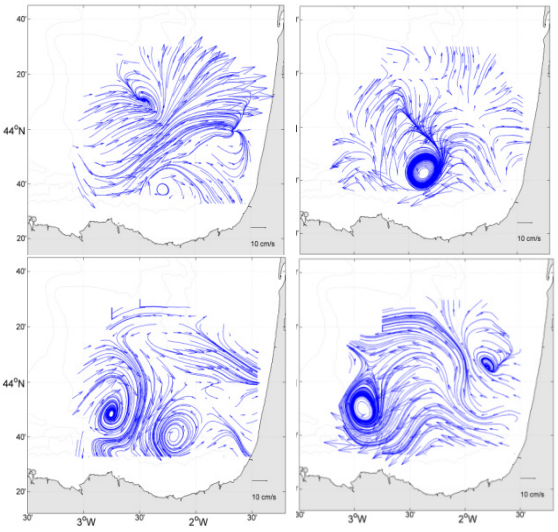

Fig. 1. Sequence of LRC fields showing the generation (upper panels: 23-26/12/2011) and decay (lower right panel: 10/01/2012) of a mesoscale dipole (lower left panel: 29/12/2011) observed in the HF radar footprint area.

A careful determination of the eddy cores using non-divergent low-pass HF OMA currents is shown in Fig. 2. The origin, signal and effect of this structure were also analyzed using available model winds (not shown) and satellite information (see Fig. 2, right panel).

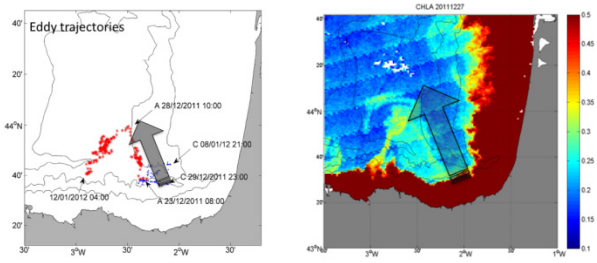

Fig. 2. Eddy center tracking (left panel: anticyclone in red, cyclone in blue) and satellite image showing eddy-induced offshore transport of coastal Chl-a rich waters (right panel).

Further work (and observations) are needed to characterize the 3D structures of the mesoscale eddies observed in the area and to investigate their role on cross-shelf transports. Besides, additional work on the observability and possibilities for automated tracking of these structures in the HF radar fields is needed. Finally, it is worth noting that the 3D characterization of these coastal mesoscale structures is a key point toward a better assessment and improvement of coastal models and, thus, toward more accurate coastal transports forecasts.

ACKNOWLEDGMENTS

The authors thank the Directorate of Emergency Attention and Meteorology of the Basque Government for sustaining the coastal observing network. This study was supported by the Spanish Ministry of Science and Innovation (National R&D&I Plan, MESOANCHOA project) and the H2020 JERICO_NEXT project.

REFERENCES

1 - Charria G, Lazure P, Le Cann B, Serpette A, Reverdin G, Louazel S, Batifoulier F, Dumas F, Pichon A & Morel Y, 2013. Surface layer circulation derived from Lagrangian drifters in the Bay of Biscay. *J. Mar. Syst*., 109-110: S60-S76.

2 - Le Cann B & Serpette A, 2009. Intense warm and saline upper ocean inflow in the southern Bay of Biscay in autumn-winter 2006-2007. *Cont. Shelf. Res*., 29 (8): 1014-1025.

3 - Solabarrieta L, Rubio A, Castanedo S, Medina R, Fontán A, González M, Fernández V, Charria G & Hernández C, 2014. Surface water circulation patterns in the southeastern Bay of Biscay: New evidences from HF radar data. *Cont. Shelf. Res.*, 74: 60-76.

4 - Solabarrieta L, Rubio A, Cárdenas M, Castanedo S, Esnaola G, Méndez FJ, Medina R & Ferrer L, 2015. Probabilistic relationships between wind and surface water circulation patterns in the SE Bay of Biscay. *Ocean Dyn*., 65 (9): 1289-1303.

5 - Rubio A, Reverdin G, Fontán A, González M & Mader J, 2011. Mapping near-inertial variability in the SE Bay of Biscay from HF radar data and two offshore moored buoys. *Geophys. Res. Lett.,* 38 (19): L19607.

6 - Caballero A, Rubio A, Ruiz S, Le Cann B, Testor P, Mader J & Hernández C, 2016. South-Eastern Bay of Biscay eddy-induced anomalies and their effect on Chlorophyll distribution. *J. Mar. Syst.* (in press).

7 - Rubio A, Solabarrieta L, González M, Mader J, Castanedo S, Medina R, Charria G & Aranda JA, 2013. Surface circulation and Lagrangian transport in the SE Bay of Biscay from HF radar data. *OCEANS - Bergen, 2013 MTS/IEEE*, doi: 10.1109/OCEANS-Bergen.2013.6608039.

8 - Kaplan DM & Lekien F, 2007. Spatial interpolation and filtering of surface current data based on open-boundary modal analysis. *J. Geophys. Res.,* 112 (C12007), doi:10.1029/2006JC003984.

9 - Ferrer L, Fontán A, Mader J, Chust G, González M, Valencia V, Uriarte Ad & Collins MB, 2009. Low-salinity plumes in the oceanic region of the Basque Country. *Cont. Shel. Res*., 29 (8): 970-984.

Ocean frontogenesis and submesoscale processes: Observational and numerical evidence in the eastern Alboran Sea

Simón Ruiz[1], Ananda Pascual[1], Amala Mahadevan[2], Mariona Claret[3], Antonio Olita[4], Charles Troupin[5], Arthur Capet[6], Pierre Poulain[6], Baptiste Mourre[5], Antonio Tovar-Sánchez[1] & Joaquín Tintoré[1,5]

[1]Instituto Mediterráneo de Estudios Avanzados, IMEDEA(CSIC-UIB), Esporles, Spain
[2]Woodshole Oceanographic Institution (WHOI), Woodshole, Massachusets, US
[3]McGill University, Montréal, Canada
[4]CNR, Oristano, Sardinia, Italy
[5]Balearic Islands Coastal Observing and Forecasting System (SOCIB), Palma de Mallorca, Balearic Islands, Spain
[6]OGS, Trieste, Italy

ABSTRACT

An intensive multi-platform and multidisciplinary experiment was completed in May 2014 as a part of PERSEUS EU funded project, lead by CSIC and with strong involvement of SOCIB, OGS, CNR, WHOI and McGill U. This unique process-oriented experiment in the Eastern Alboran sea (ALBOREX), conducted during 8 days, included 25 drifters, 2 gliders, 3 Argo floats, one ship and 50 scientists. The experiment was designed to capture the intense but transient vertical motion associated with mesoscale and submesoscale features, in order to fill gaps in our knowledge connecting physical process to ecosystem response. High-resolution (0.4 - 1 km) observations from autonomous underwater gliders revealed lateral density gradients of the order of 1 kg/m^3 in 10 km and significant vertical excursions of chlorophyll and oxygen at both sides of the front. We quantify frontogenetic terms to assess the intensification/relaxation of buoyancy forcing which can be responsible of large vertical displacements in a scenario of strong confluence of (fresh) Atlantic Water and the resident (more saline) Mediterranean Water. Our results suggest that frontogenesis mechanism induces vertical velocities higher than 100 m/day in the eastern Alboran front, driving the tongues of chlorophyll and oxygen captured by ocean gliders. These findings, based on observations, are consistent with numerical simulations from a Process Ocean Model Study.

INTRODUCTION

Vertical motion associated with mesoscale and submesoscale features plays a major role in the exchanges of properties between the surface and the ocean interior [1]. Modelling studies of frontal regions suggest that vertical exchange is enhanced at density fronts [2,3]. Significant uncertainty still exists, however, in our understanding of the net effect of mesoscale and submesoscale variability on biochemical tracer redistribution and the consequent marine ecosystem response. In order to monitor and establish the vertical exchanges associated with fine-scale structures, multi-sensor synoptic observations need to be collected [4] [5]. In situ systems, including R/V (CTD, water samples, ADCP), gliders and drifters have to be coordinated with satellite data to provide a full description of the physical and biogeochemical variability. The observational approach must be integrated with numerical simulations both realistic and process oriented studies.

In the Western Mediterranean, the transition region between the Alboran Sea and the Algerian sub-basin to the east is characterized by strong fronts (mostly governed by salinity) and mesoscale anticyclonic eddies. In this study, we present the results of ALBOREX, a multi-platform and multi-disciplinary experiment as part of PERSEUS EU funded project in the Eastern Alboran Sea. The final goal was to monitor and establish the vertical exchanges associated with mesoscale and submesoscale (e.g fronts, meanders, eddies and filaments) and their contribution to upper-ocean interior exchanges. We address this question using the new observational technology and innovative sampling strategies that provide novel insights on the coupling between submesoscale physics and biogeochemical processes.

DATA AND METHODS

A synoptic multi-sensor experiment was designed and conducted onboard SOCIB coastal vessel between 25 and 31 May 2014 in the eastern Alboran Sea (Western Mediterranean). In situ systems, including gliders, drifters and Argo floats were coordinated with satellite data and modeling simulations to provide a full description of the physical and biochemical variability. Two high-resolution grids were sampled with the ship (area covered 40 km x 40 km, See Figure 1). At each station one CTD cast and water samples for Chl and nutrients analysis were collected. Additional ADCP data was registered in continuous mode. Two gliders crossed an intense front. Details of the sampling for each of the platforms are given in [6].

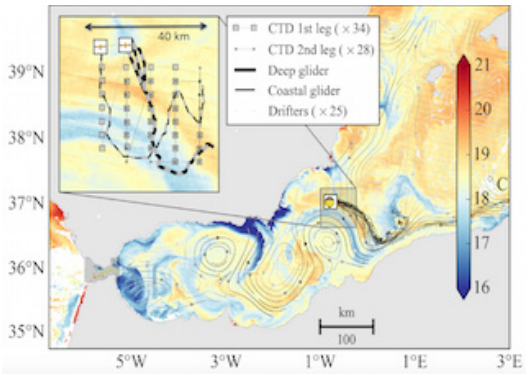

Fig. 1. SST (Modis-Aqua) for 29 May 2014 with CTD cats, glider and drifter tracks during Alborex experiment. The isolines correspond to Absolute Dynamic Topography from gridded altimeter fields (CMEMS-SLTAC).

RESULTS AND DISCUSSION

[1]

During the Alborex experiment the thermosalinograph measured differences in salinity of about 1.5 in less than 5 km [6]. The drifters followed coherently an anticyclonic gyre. Near real time data from ADCP showed consistent patterns with currents up to 1m/s in the southern part of the sampled domain. Gliders were able to sample at high-resolution the frontal zone. The coastal glider was configured to collect hydrographic and biogeochemical data at about 0.5 km while resolution of data from the deep glider was of about 1 km along track. Figure 2 shows the chlrophyll concentration from the deep glider. Small scales (less than 10 km width) filaments subducting are observed in different parts of the sampled area.

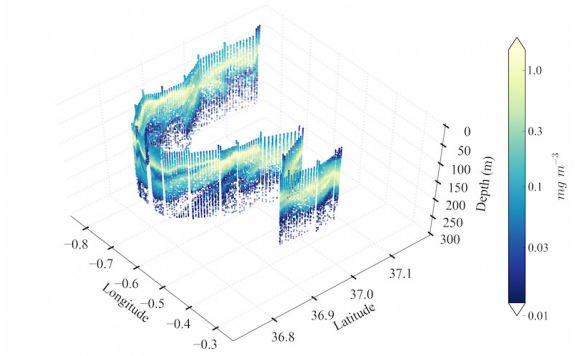

Fig 2. Chlorophyll concentration (mg/m^3) from deep glider.

The quasi-geostrophic theory can partially explain vertical exchanges at the mesoscale [6], however at smaller scales (submesocale), with Rossby number 1, other mechanisms play an important role and need to be investigated in detail. Our results suggest that frontogenesis mechanism induces vertical velocities higher than 100 m/day in the eastern Alboran front, driving the tongues of chlorophyll and oxygen captured by ocean gliders.

This intensive multi-platform and multidisciplinary experiment is an example of the new integrated and quasi real time approach to ocean observation thanks to joint and collaborative efforts of scientists and technicians from diverse international institutions. The Alboran Sea is indeed an ideal test site for studying 3D meso and submesoscale processes, with intense fronts impacting biogeochemistry. Future studies will have to expand the observing capabilities with new high-resolution interdisciplinary experiments integrating diverse multi-platform approaches with numerical models.

ACKNOWLEDGEMENTS

The Alborex experiment was conducted in the framework of PERSEUS EU-funded project (Grant agreement no: 287600) with substantial support from SOCIB. Glider operations were partially funded by JERICO FP7 projects. We would like to thank all the crew on board R/V SOCIB for their efficient collaboration during the Alborex experiment.

REFERENCES

1 - Klein P. and Lapeyre, G.: The oceanic vertical pump induced by mesoscale eddies. Annual Review of Marine Science, 1, 351-375, (2009).

2 - Lévy, M., Klein, P., and Treguier, A. M.: Impact of sub-mesoscale physics on production and subduction of phytoplankton in an oligotrophic regime, Journal of Marine Research, 59, 535-565, 2001.

[2]

[3] 3 - Mahadevan, A., A. Tandon, An analysis of mechanisms for submesoscale vertical motion at ocean fronts. Ocean Model. 14, 241 (2006).

[4]

4 - Ruiz, S., A. Pascual, B. Garau, M.-I. . Pujol, and J. Tintoré, Vertical motion in the upper ocean from glider and altimetry data, Geophys. Res. Lett., 36, L14607, doi:10.1029/2009GL038569, (2009).

5 - Pascual, A.; Bouffard, J.; Ruiz, S.; Buongiorno Nardelli, B.; Vidal-Vijande, E.; Escudier, R.; Sayol, J.M.; Orfila, A.; Recent improvements in mesoscale characterization of the western Mediterranean Sea: synergy between satellite altimetry and other observational approaches. Scientia Marina, Vol. 77, Pg. 19-36 (2013).

6 - Ruiz, S., A. Pascual, B. Casas, P. Poulain, A. Olita, C. Troupin, M. Torner, J.T. Allen, A. Tovar, B. Mourre, A. Massanet, M. Palmer, F. Margirier, P. Balaguer, C. Castilla, M. Claret, A. Mahadevan, J. Tintoré. Report on operation and data analysis from Multi-platform synoptic intensive experiment (ALBOREX), D3.8 Policy-oriented marine Environmental Research in the Southern European Seas, 120pp, ISBN: 978-960-9798-13-6, (2015).

Analysis of the high frequency dynamics of the bottom boundary layer in the Strait of Gibraltar by ADCP single-ping measurements

Simone Sammartino[1], Jesús García Lafuente[1], Cristina Naranjo[1], José Carlos Sánchez Garrido[1], Ricardo Sanchez Leal[2]

[1] Physical Oceanography Group, University of Málaga, Campus de Teatinos s/n, 29017, Málaga, Spain
[2] Spanish Institute of Oceanography, Cadiz Oceanography Center, Muelle de Levante (Puerto Pesquero), 11006, Cádiz, Spain

ABSTRACT

A series of single-ping Acoustic Doppler Current Profiler (ADCP) measurements carried out in the Strait of Gibraltar allowed for a preliminary assessment of turbulence parameters of the Outflowing Mediterranean Water, and its tidal variability. The variance method has been applied to single-ping ensemble measurements of the radial velocity, after a careful analysis of the accuracy associated to the fluctuation magnitude estimated by the instrument. Maxima of Reynolds' stress τ and dissipation coefficient ϵ are observed during flood tide in the bottom boundary layer, when the westward Mediterranean flow is strong and the derived turbulence is highest. A diurnal modulation is also observed, more marked in spring tides. The application of a logarithmic law to the near-bottom layer also confirms the magnitudes of τ and ϵ observed with the variance method and gives some hints of the presence of a double velocity maximum in this layer.

INTRODUCTION

Since 2004, the Physical Oceanography Group of the University of Málaga has been holding a monitoring station located at the western exit of the Strait of Gibraltar, with the aim of gathering data of the thermohaline properties of the Mediterranean Outflowing Water (MOW) and its dynamics. The station is constituted by a mooring line whose principal element is an up-looking RDI 75 kHz Acoustic Doppler Current Profiler (ADCP) embedded in a sub-surface buoy, deployed ~20m above the bottom, capable of obtaining profiles of the three-dimensional current along the whole water column. Although the principal aim of the project was to assess the long-term variability of the MOW dynamics, recently, the configuration of the instrument has been slightly modified to integrate a parallel study of the high frequency variability of the outflow. The present contribution describes the first results of this operation.

EXPERIMENTAL SETUP

Typically, the ADCP collects current profiles individually (pings) and then averages them over a fixed time interval (ensembles), with the aim to improve the statistical significance of the measure. In this experiment, however, we set the instrument to collect every individual ping (with a sampling interval of 36 seconds), treating them as single-ping ensembles, and applying all the post-sampling processing steps prescribed for the latter. The profiles have a vertical resolution of 8m and span from ~35m above the sea bottom to ~50m from the surface. This means that the frequencies that can be investigated are not purely turbulence, but involve also the internal waves dynamics.

THEORETICAL FRAMEWORK

The turbulent energy balance equation accounts for the different terms that contribute to the production and dissipation of turbulence in a fluid:

$$\frac{\partial E}{\partial t} = -\rho_0 \langle u'w' \rangle \frac{\partial U}{\partial z} - g\langle w\rho' \rangle - \rho_0 \epsilon \qquad (1)$$

The rate of variation of turbulent energy, the term on the lhs of equation (1), is the net sum of the production (P) of turbulent kinetic energy (TKE) by the advection of eddies characterized by the (Reynolds') stress $\langle u'w' \rangle$ by means of the mean sheared current U, the buoyancy flux characterized by the density fluctuations ρ', and the rate of loss of turbulent kinetic energy into heat through viscosity, characterized by the dissipation coefficient ϵ [2]. Here the prime symbol represents the instantaneous fluctuation of a quantity around its mean, as defined within a fixed time interval, and ρ_0 is a mean density. In a steady state, when TE can be assumed to be constant, in conditions of no convection, where the buoyancy fluxes are negligible, and in presence of vertical velocity shear, the balance can be simplified as:

$$\epsilon = -\langle uw \rangle \frac{\partial U}{\partial z} \qquad (2)$$

where the production of turbulent energy, ascribed to the mean shear flow as source of turbulent motion, is compensated by its dissipation through viscosity. These conditions are reasonably satisfied in the bottom boundary layer (BBL) where the stratification is weak and the velocity shear is usually high. In this

framework, the ADCP measurements allow to estimate the vertical shear ($\partial U/\partial z$) directly and the Reynolds' stress, $\langle u'w' \rangle$ and $\langle u'w' \rangle$, indirectly (the variance method).

THE VARIANCE METHOD

The variance method [3] consists in estimating the Reynolds' stress by means of the ADCP radial velocity fluctuations with respect to some time averages:

$$\langle u'w' \rangle = \frac{\overline{U_1'^2} - \overline{U_2'^2}}{4 \sin\theta \cos\theta}; \quad \langle v'w' \rangle = \frac{\overline{U_3'^2} - \overline{U_4'^2}}{4 \sin\theta \cos\theta} \qquad (3)$$

where θ is the slant angle of the ADCP, U_j is the radial velocity along the j-th transducer, and $U_j'^2$ stands for the variance of the fluctuations of this velocity. Notice that in case of tethered ADCP, as it is our case, equations (3) get much more complicated by the inclusion of the tilt angles.

ADCP NOISE

By using single-ping records we pay for the relative low precision of the instrument (ADCP noise). In order to employ these measurements to assess the current variability, we have to account for this noise. To this aim, a series of a-posteriori ensemble averages, with varying pings-per-ensemble (ppe) value, have been simulated, and an asymptotic behavior of the ensemble standard deviation around 15 ppe (~10 minutes) has been observed. We hence established the time interval of 10 minutes as the width of the average window to compute the current fluctuations. Then, we simulated a series of synthetic random variables and we sampled them with an accuracy corresponding to the ADCP noise defined for our system (~15 cm s^{-1}), and so we estimated our capability of obtaining reliable measurements of the real current fluctuations. The highest accuracy is achieved during flood tides, when the Mediterranean westward current is strongest on the BBL, and the relative overestimation of the ensemble standard deviation by ADCP noise is less than 10%.

RESULTS AND DISCUSSION

The series of Reynolds' stress obtained by applying the variance method to the radial velocities computed on the ADCP records corrected by tilt angles, shows a marked semidiurnal periodicity, with maxima of ~2 Pa occurring in flood tide, according with the highest westward current in the BBL (Fig. 1a).

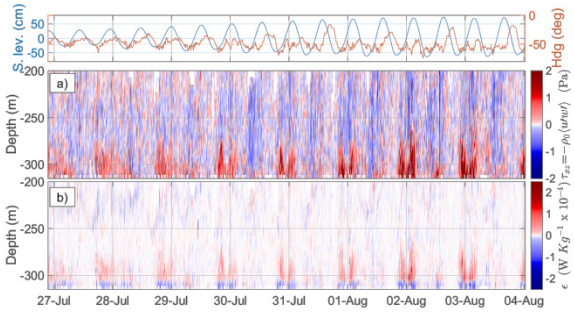

Fig. 1. Fragment of the series of Reynolds' stress $\langle u'w' \rangle$ (panel a), and dissipation coefficient ϵ (panel b). The top panel shows the sea level and the low-passed series of the ADCP heading.

A strong modulation at diurnal timescale is also observed, stronger in spring tide. The corresponding ϵ values (Fig. 1b), estimated as in (2), show peaks of $O(10^{-4})$ W Kg^{-1}. Both results are coherent with previous estimates by [4] and [5].

From the same assumption of (2), we can define the logarithmic law that describes the vanishing behavior of the velocity toward the bottom:

$$U(z) = u_*/k \, ln(z/z_0) \qquad (4)$$

where u_* is the friction velocity, k is the Von Kármán constant (0.41), and z is the distance from the sea bottom. Based on (4) we can obtain estimations of τ and ϵ, assuming $\tau = \rho_0 u_*^2$ and $\epsilon = u_*^3/kz$, respectively [2].

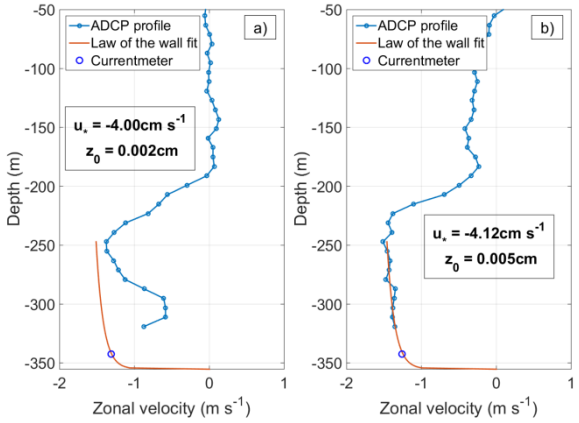

Fig. 2. Two examples of zonal velocity profiles with the near-bottom layer fitted by the law of the wall, in presence (a) and absence (b) of the double maximum.

With a friction velocity u_* of ~4 cm s^{-1}, we derived estimates of τ of ~2 Pa and ϵ of $O(10^{-3})$ W Kg^{-1}, in a good agreement with results from the previous approach. A stable and permanent double maximum structure of the very near-bottom layer is also observed, likely related to some topographic interaction of the flow upstream (Fig. 2).

ACKNOWLEDGEMENTS

This work was funded by the Spanish Ministry of Economy and Competitiveness under the three Research Projects INGRES (REN2003_01608, CTM2006_02326 and CTM 2010-21229).

REFERENCES

1 - Sammartino, S. et al., 2015, J. Geophys. Res.
2 - Thorpe, S. A., 2007. Cambridge University Press.
3 - Lohrmann, A. et al. 1990, J. Atmos. Oceanic Technol.
4 - Johnson, G.C., 1994, J. Phys. Oceanogr.
5 - Price, J.F. et al., 1993, Science.

Circulation and water renewal patterns of the Bay of Algeciras: a combined observational and modeling study

Jose C. Sánchez Garrido[1], Simone Sammartino[1], Cristina Naranjo[1], Jesús García Lafuente[1], Francisco de los Santos[2] & Enrique Álvarez Fanjul[3]

[1] Grupo de Oceanografía Física, Universidad de Málaga.
[2] Autoridad Portuaria de la Bahía de Algeciras, Algeciras, Cádiz.
[3] Área del Medio Físico, Puertos del Estado, Madrid.

ABSTRACT

The circulatory system of the Bay of Algeciras (BA) and its subtidal variability is investigated with the results of a high-resolution primitive equation model. Prior to the analysis, model results were satisfactorily validated with a set of *in situ* observations collected in different locations of the BA. It is shown that the mean near-surface circulation of the Bay consists of an anticyclonic cell fed by a surface coastal current originating from the Northwestern Sector of the Alboran Sea. Several modes of variability of this mean pattern have been identified and linked to lateral and surface boundary forcing exerted by the flow through the adjacent Strait of Gibraltar and the local wind stress. Favorable scenarios and physical forcing for a rapid flushing of the Bay are also identified.

INTRODUCCIÓN

The Bay of Algeciras is in the Northeastern end of the Strait of Gibraltar within one of the busiest marine routes on Earth (Fig. 1). Its relative mild oceanic conditions make of it a natural harbor by its own and it is therefore not surprising that it holds one of the major ports of the Mediterranean (Port of Algeciras). The Bay also holds the port of Gibraltar and numerous industrial plants distributed all along its shoreline, which make of it a marine environment subject to heavy anthropogenic pressure. Marine pollution and the potential risk of oil spills motivate a better understanding of its physical environment. This contribution summarizes the results of a study of its circulatory system, water renewal patterns and driven mechanisms.

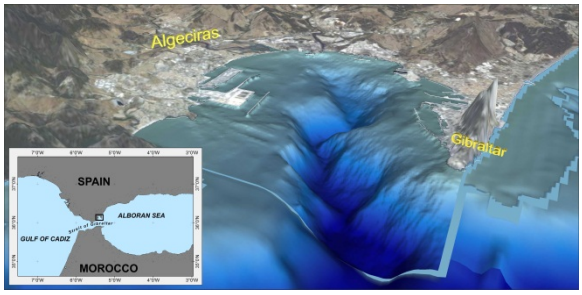

Fig. 1. Location and bathymetry of the Bay of Algeciras.

After the companion work of [1] that focused on the tidal dynamics of the Bay, here attention is paid to its low (sub-tidal) frequency circulation, largely driven by meteorological forcing.

METHODS

The Massachusetts institute of Technology general circulation model [2] was employed to simulate the circulation of the BA during spring and autumn 2011. The model is currently part of the SAMPA operational service provided by Puertos del Estado and its configuration is described in details in [1, 3]. The model domain covers the Gulf of Cadiz and the Alboran Sea and was discretized with a curvilinear stretched grid with enhanced resolution within the Strait of Gibraltar. In the Bay itself horizontal resolution is approximately 300 m and there are 23 vertical levels unevenly distributed throughout the water column, with smaller cell sizes towards the ocean surface. The model is laterally forced with temperature, salinity and barolinic velocities extracted from the MyOcean IBI ocean forecast system [4]. Tidal and subtidal (storm surge) [5] barotropic flows are likewise introduced through the lateral boundaries. At the surface the model is driven by atmospheric forcing fields provided by AEMET.

Two field campaigns were carried out in order to validate the model results. Altogether three mooring stations were deployed in the BA, all of them equipped with an upward-looking ADCP embedded within the mooring buoy located 10 m above the sea floor. A conductivity/temperature sensor was also installed in the mooring line just below the buoy.

Given that our interest here was on sub-tidal time scales tidal variability was removed from the original model time series by applying a Gaussian filter.

Numerical experiments with passive tracers (dye) were conducted for the computation of the flushing times of the BA and with the aim to identify favorable/unfavorable

scenarios for its ventilation. Dye was released every 5 days at the very surface, the Atlantic layer (defined by salinity S <37.5) and the Mediterranean layer (S>37.5), and its evolution was tracked for one week.

RESULTS AND DISCUSSIONS

The BA has a prevailing anti-cyclonic surface circulation with a branch of surface water entering through the mid-western half of its mouth and a second one exiting through its eastern side, as reflected in Fig. 2a,b. The incoming branch is a coastal current flowing westward and therefore with opposite direction to the jet of Atlantic water entering the Mediterranean through the Strait of Gibraltar, and originates from the Northwestern region of the Alboran Sea. This region is a quasi-permanent upwelling spot that features nutrient-rich waters, a fact that could explain the presence of high chlorophyll concentrations frequently detected in the BA in ocean color images. On to the hand, Mediterranean water follows a preferred cyclonic pathway (z>100 m, Fig. 2b).

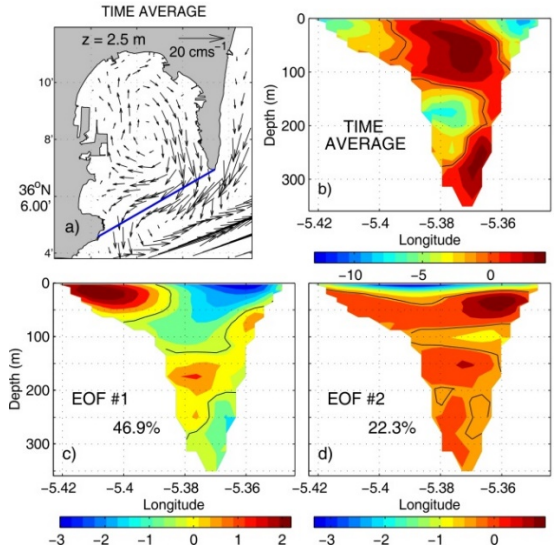

Fig. 1 a) Mean surface velocity of the BA as simulated by the numerical model. b) Mean velocity across the mouth of the Bay (see blue line in panel a). The velocity component is perpendicular to the cross section with positive values pointing to the head of the Bay. Units are in cm/s. Black solid lines correspond to the zero velocity contours. c) First EOF derived from the cross-mouth velocities. Tidal fluctuations were filtered out from the original time series prior to the principal component analysis. The percentage of the total variance accounted for the EOF is labeled. d) Same as c) for the second EOF.

Secondary circulation patterns have been identified by performing a Principal Component Analysis of the velocity component perpendicular to the mouth of the Bay. The first empirical orthogonal function EOF #1 has a marked zonal structure within the Atlantic layer (approximately the first 100 m of the water column; Fig. 2c) and therefore can intensify or weaken, even revert, the anti-cyclonic vorticity of the mean circulation, depending upon the sign of the associated Principal Component (PC #1). The latter correlates well (r=0.69) with meridional fluctuations of the Atlantic jet at sub-tidal time scales, in such a way that the vorticity of the surface circulation of the BA turns to cyclonic only when the meridional excursion of the jet is as far north as to collide with the southern tip of the Rock of Gibraltar. The second mode of variability EOF #2 consists of a vertical overturning cell in the Atlantic layer (Fig. 2d) and is fundamentally due to wind forcing. This statement follows from the high cross-correlation coefficient (r=0.78) between PC #2 and the zonal wind stress over the Bay. Consistently with Ekman dynamics westerly winds drive coastal upwelling at the head of the BA and moves surface waters offshore, while the opposite applies during easterly winds.

The derived modes of variability indicate several ways in which the BA can exchange water with the adjacent Strait of Gibraltar. A marked horizontal structure of the flow, as exhibited by the mean flow and by the EOF #1 in the Atlantic layer, does not seem very favorable for a rapid flushing of the Bay because of the likely recirculation of water parcels: particles exiting the BA along one side of its mouth likely return through the opposite side. A much efficient flushing seems to be associated to the wind-driven circulation (EOF #2), particularly during westerly winds, or to the dispersal of water particles driven by tidal flows which, as recognized by [3], account for most of the velocity variability. Experiments conducted with passive tracers confirm the second possibility highlighting the fundamental role of tides in the flushing of the BA and therefore also in the maintenance of good levels of water quality.

ACKNOWLEDGEMENTS

J.S.G was ssuported by a Juan de la Cierva Postdoctoral Grant (JCI-2012-13451) from Ministerio de Economía y Competitividad. Finantial support from the same Ministry through the research Project ENCIBA (CTM2013-40886-P) is thankfully acknowledged. Partial support has been provided by Junta de Andalucía through the research project MOCBASE (RNM1540).

REFERENCES

1- Sammartino et al. 2014. A numerical model analysis of the tidal flows in the Bay of Algeciras, Strait of Gibraltar, *Continental Shelf Research*, 72, 34-46.

2- Marshall J., et al. 1997. "A finite-volume, incompressible Navier Stokes model for studies of the ocean on parallel computers". *J. Geograph. Res.,* 102 (C3): 5753–5766.

3- Sánchez-Garrido et al. 2013. What does cause the collapse of the Western Alboran Gyre? Results of an operational ocean model, *Prog. Oceanogr., 116, 142-153.*

4- García Sotillo et al. 2015. The MyOcean IBI Ocean Forecast and Reanalysis Systems: operational products and

roadmap to the future Copernicus Service, *Journal of Operational Oceanography*, 8 (1), 63-79.
5- Álvarez Fanjul et al. 2001. Nivmar: a storm surge forecasting model for Spanish Waters, *Scientia Marina*, 65, 145-154.

Ondas internas en el outflow de agua mediterránea en el Golfo de Cádiz

Ricardo F. Sánchez Leal[1], María Jesús Bellanco[1], David Roque[2], Andreas Thurnherr[3], Simone Sammartino[4], Francisco Javier Hernández Molina[5], Jesús García Lafuente[4], César González-Pola[6], Luis Miguel Fernández Salas[1], Miguel Bruno[7], Alfredo Izquierdo[7], Fernando Ramos[1]

[1] Instituto Español de Oceanografía, C.O. Cádiz
[2] ICMAN, CSIC
[3] LDEO
[4] UMA
[5] RHUL
[6] Instituto Español de Oceanografía, C.O. Gijón
[7] Universidad de Cádiz

RESUMEN

En este trabajo se presentan resultados de una serie de 52 de perfiles de CTD-O_2 y LADCP tomados cada 15 minutos en el segmento inferior de la columna de agua en el canal superior de la MOW en el Golfo de Cádiz durante la campaña STOCA 201509. Estas observaciones muestran una variabilidad de tipo semidiurno asociada a la marea interna. La propagación de estas perturbaciones tiene un efecto importante en la modulación de las velocidades máximas de la vena mediterránea, tanto en la componente longitudinal como en la transversal. Asociado al paso de la marea interna se deducen velocidades verticales superiores a los 0.2 m/s en la base de la interfase MOW-NACW que se desatan bruscamente al inicio de la marea llenante y que están relacionadas con el incremento en un orden de magnitud de la disipación obtenida a partir de la VKE. Concluímos que estas perturbaciones tienen un efecto relevante en el flujo diapicno de sal y calor incluso lejos de los puntos clásicos de mezcla localizados en el estrecho de Gibraltar.

INTRODUCCIÓN

La salida de las aguas mediterráneas a través del estrecho de Gibraltar (*Mediterranean outflow*, MO) es uno de los fenómenos de mayor relevancia en la cuenca atlántica. Su aporte de sal es determinante para la formación de aguas profundas en las zonas subpolares y la estimulación de la cinta transportadora oceánica [1]. Inicialmente como una corriente de densidad pegada al fondo marino, estas aguas experimentan mezcla con las aguas circundantes para formar la denominada MOW. En las primeras decenas de km, la mezcla es muy intensa e involucra a la capa de agua suprayacente (agua central del Atlántico norte, NACW), sobre la termoclina estacional [2, 3]. La producción, características y propiedades de la MOW muestran una elevada dependencia espacial y temporal en función de la fase de marea y el relieve submarino [4].

Bajo la termoclina los procesos de mezcla diapicna se deben a la rotura de ondas internas de todo tipo, mezcla por la rugosidad del fondo y disipación mesoescalar [5]. El salto de densidades entre la NACW y la MOW a la salida del Estrecho de Gibraltar favorece la propagación de ondas internas. Existen evidencias de la generación de turbulencia por rotura de éstas así como por cizalladura con el *stress* con fondo y entre el flujo bicapa [4, 6].

El estudio de estas ondas internas en el Golfo de Cádiz se ha centrado en el Estrecho de Gibraltar y el cañón de Portimao [7] o los promontorios portugueses [8]. La interacción de la marea barotrópica con la topografía entre el Banco de Gorringe y el Espolón de San Vicente [9] es clave en generación de trenes de ondas de marea interna que se propagan fontalmente hacia la plataforma y contribuyen a la intensificación de la mezcla diapicna dentro de la vena de MOW y en su interfase con la NACW [10].

Con el objetivo de mostrar el efecto de la propagación de ondas internas sobre la vena de agua mediterránea, en septiembre de 2015 se llevaron a cabo observaciones repetidas en el canal por el que fluye el núcleo superior de la vena de agua mediterránea en el Golfo de Cádiz. Estos resultados se presentan en el presente trabajo.

MATERIAL Y MÉTODOS

Durante 13.15 h entre el 17 – 18 de septiembre de 2015 en el curso de la campaña STOCA201509 en el Golfo de Cádiz a bordo del B/O Ángeles Alvariño se tomaron una serie de observaciones en el segmento inferior de la columna de agua en el canal superior de la MOW (36º 16.12' N 6º 47.60' W, Fig. 1) compuesta por 52 perfiles verticales de CTD-O_2-LADCP así como velocidades absolutas a partir del SADCP del buque. La localización fue coincidente con una de las inmersiones del ARGOS ROV durante la campaña MOWER [11]. Los perfiles se realizaron con un sistema SBE911+ equipado con sensores y un LADCP TRDI WHS

de 300 kHz. El procesado de perfiles hidrográficos y SADCP se procesaron según técnicas estándar [12]. Las observaciones se tomaron a barco parado en DP (dynamic positioning; deriva máxima de 13 m sobre el punto). También se registraron intensidades de eco con la ecosonda multifrecuencia del buque, modelo EK60 (frecuencias de 12, 38, 70, 120, 200 y 333 kHz; ver Fig. 2).

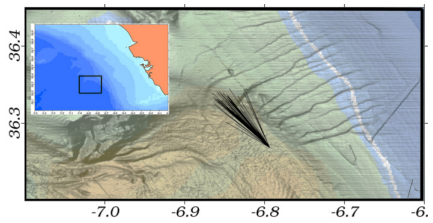

Fig. 1. Relieve marino (sombras grises) y velocidades de corriente cerca del fondo (*sticks* negros). Los tonos anaranjados, verdes y azulados indican la salinidad media sobre el fondo; la isolínea blanca marca 36.25, envolvente de la vena de agua mediterránea.

RESULTADOS Y DISCUSIÓN

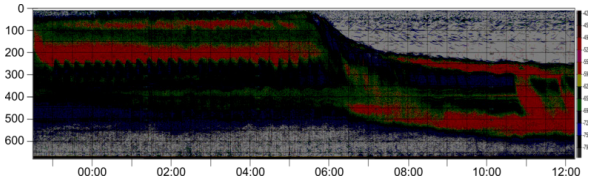

Fig. 2. Registro de la EK60 (18 kHz). Sobre las migraciones verticales del micronecton se observan ondulaciones de alta frecuencia que corresponden con el paso de ondas internas. El eje inferior indica la hora UTC (17 – 18 septiembre de 2015).

La ecosonda muestra la presencia de oscilaciones de alta frecuencia sobre un patrón de marcado carácter semidiurno compatible con la marea interna (Figs. 2-3). Los perfiles de CTD muestran la mayor variabilidad en las zonas de máxima estratificación (Fig. 3) que impone la presencia de la vena de agua mediterránea en la subcapa cercana al fondo así como una pluma de flotabilidad que, anclada en el talud, se extiende *offshore* como un máximo de salinidad. Durante la serie se observa la modulación de la velocidad longitudinal, que varía de los 0.4 – 0.6 m/s, mientras que la velocidad transversal (de media aproximadamente nula) muestra inversiones de signo.

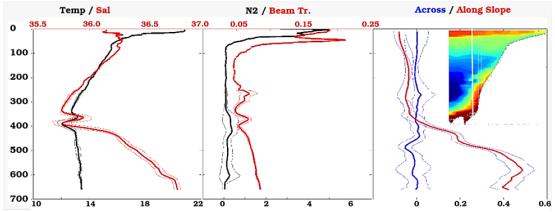

Fig. 3. Perfiles medios y desviación estándar de temperatura / salinidad (dcha), N^2 / transmisividad (ctro) y velocidad transversal y longitudinal (dcha). El recuadro indica la sección transversal de salinidad.

Asociado al paso de la marea interna se deducen velocidades verticales superiores a los 0.2 m/s en la base de la interfase MOW-NACW que se desatan bruscamente al inicio de la marea llenante y que están relacionadas con el incremento en un orden de magnitud de la disipación de Vertical Kinetic Energy (VKE, [13]) (Fig. 4). Concluímos que estas perturbaciones tienen un efecto relevante en el flujo diapicno de sal y calor incluso lejos de los puntos clásicos de mezcla localizados en el estrecho de Gibraltar.

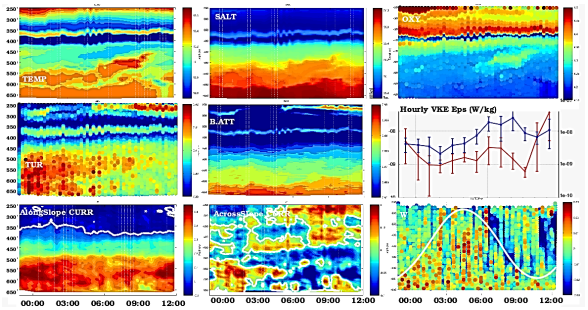

Fig. 4. Serie de obsevaciones. De izqda.- dcha. y de arriba a abajo: temperatura, salinidad, O_2, turbidez, transmisividad, disipación de EKE, velocidad transversal, longitudinal y vertical (LADCP). Sobre este último panel se indica la curva de la marea astronómica en Cádiz.

AGRADECIMIENTOS

Al Capitán y tripulación del B/O Ángeles Alvariño. Esta es una contribución a los proyectos INGRES3 (CTM2010-21229-02), STOCA (IEO2009) y DILEMA (CTM2014-59244-C3).

REFERENCIAS

1 – Mauritzen, C. et al., 2001. *Deep-Sea Res.*, 48, 347–381.
2 – Price, J. F. et al., 1993. *Science* 259, 1277-1282.
3 - Bormans, M. et al., 1986. *Oceanologica Acta*, 9, 403-414.
4 – Nash, J. D. et al., 2012. *Geophys. Res. Lett*. 39, L18611
5 – MacKinnon, J. et al., 2013. In, Siedler, G. et al. (eds.) Ocean Circulation and Climate: A 21st Century Perspective. 2nd Ed. Oxford, GB, Academic Press, 159-184.
6 – G. C. Johnson, et al., 1994, *J. Phys. Oceanogr*. 24, 2084-2092
7 – Bruno, M. et al., 2006. *Deep-Sea Res. II*. 53 (11), 1219-1240
8 – Magalhaes J. et al., 2010. 3rd International Workshop SEASAR 2010
9 – Izquierdo. A. 2011. MPIFM Joint Seminars.
10 – Alvarado-Bustos, R., 2011. PhD Univ. Liverpool
11 – Hernández-Molina, J. Pers comm.
12 – Hood, E.M. et al.. 2010. IOCCP R. No 14, ICPO 134.
13 – Thurnherr, A.M. et a., 2015.Geophys. Res. Lett. 42, 7639–7647

Mid-2000s North Atlantic shift. Heat budget and circulation changes[1]

R. Somavilla[1], C. González-Pola[1], U. Schauer[2] & G. Budéus[2]

[1] C.O de Gijón. Instituto Español de Oceanografía.
[2] Alfred Wegener Institute für Polar und Mereesforschung

ABSTRACT

Prior to the 2000s, the North Atlantic was the basin showing the greatest warming. However, since the mid-2000s during the so-called global warming hiatus, large amounts of heat were transferred in this basin from upper to deeper levels while the dominance in terms of atmospheric heat capture moved into the Indo-Pacific. Here, we show that a large transformation of modal waters in the eastern North Atlantic (ENA) played a crucial role in such contrasting behavior. First, strong winter mixing in 2005 transformed ENA modal waters into a much saltier, warmer, and denser variety, transferring upper ocean heat and salt gained slowly over time to deeper layers. The new denser waters also altered the zonal dynamic height gradient reversing the southward regional flow and enhancing the access of saltier southern waters to higher latitudes. Then, the excess salinity in nothern regions favored additional heat injection through deep convection events in later years.

INTRODUCTION

More than 90% of the increasing radiative forcing imbalance is reflected as global ocean warming. In the view of that, the deceleration of the upper ocean heat storage since the mid-2000s has instigated an active search for the 'missing heat' in the deep ocean. The enhanced downward heat transfer necessary for this vertical heat redistribution has been proposed to be related to the hiatus in global warming, although the hiatus started earlier and lasted for the 15 years period 1998-2013. Two natural mechanisms have

been proposed to explain the deceleration of the rise in global mean surface temperature and the efficient transfer of heat to the deep ocean: (I) the intensification of zonal winds ausing La Niña-like conditions in the tropical Pacific and (II) decadal variations in the strength of deep convection and currents the North Atlantic. Regarding the first mechanism, modeling simulations show that La Niña surface cooling in the eastern and central tropical Pacific can decrease the rate of increase in atmospheric temperature and induce an anomalous heat flux into the ocean. Associated to this anomalous heat flux into the ocean, subsurface heat uptake in the western tropical Pacific and Indian oceans occurs mostly above 300 m, thus not largely involving transfer of heat into the deep ocean. Regarding the second mechanism, vertical heat inventories of the North Atlantic show notable heat transfer from the upper (0-300 m) to intermediate (300-700 m) and deep (>700 m) layers since the mid-2000s. However, the heat redistribution in the North Atlantic since the mid-2000s as a whole has apparently occurred without extra heat uptake from the atmosphere.

Overall, during the past decade, different basins have played contrasting roles on the Earth's atmosphere-ocean heat budget distribution. In particular, the North Atlantic would not have contributed notably as in previous decades to atmospheric heat uptake, in contrast to that observed in the

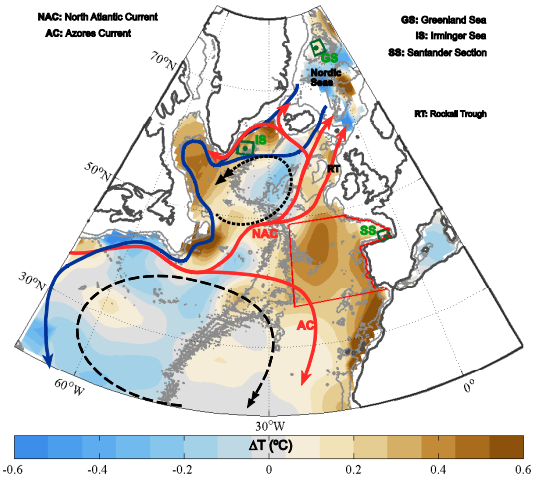

tropical Pacific and Southern oceans, but to the quick transfer of heat accumulated during the previous decades in the upper layers to the deep ocean. Here, we examine the mechanism

Fig. 1. Warming pattern in the North Atlantic at mid-depth. Temperature difference (ΔT in color, ºC) in the 300-700 m layer between the 2007-2012 and the 1997-2002 periods (i.e. an average is performed in each time range). Brown colors indicate warming. Arrows represent (in red) warm and salty upper water currents, (in dark blue) cold and fresh deep water currents, (in black, dotted) the subpolar gyre, and (in black, dashed) the subtropical gyre. Deep convection sites in the Irminger and Greenland seas as well as the position of the Santander standard section in the Bay of Biscay are marked by green squares. mlENA considered as the oceanic area including the mode water formation area of the ENACW and the oceanic waters of the Bay of Biscay and surrounding the Iberian Peninsula to North

Africa as in *Somavilla et al.* [2009], is bounded by a red box.

responsible for the quick transfer of ocean heat from upper to deeper layers in the North Atlantic focusing on the role of ENA modal waters.

DATA SETS

High-quality hydrographic data with global coverage are required for providing observational evidence to the mid-2000s shift in the North Atlantic. These data are obtained from regularly observed hydrographic sections, which are affected by gaps in coverage both in time and space. To overcome this issue we combined standard hydrographic observations (salinity and temperature profiles) at oceanographic sections regularly maintained in the Bay of Biscay and the Greenland Sea (see Fig. 1) with other data sets that offer more global coverage such as Argo floats, global gridded ocean reanalysis (ECMWF Ocean Reanalysis System 4, ORAS4) and objective analysis (Met Office Hadley Centre monthly objective analysis, EN4; and World Ocean Database 2001, WOA01).

RESULTS AND DISCUSSION

Since the mid-2000s, in contrast to the enhanced ocean heat uptake observed in other ocean basins, the North Atlantic deep ocean heat content has significantly increased without apparently intervening ocean heat uptake from the atmosphere. Deep convection in the subpolar North Atlantic under high salinity conditions might account for the quick transfer of heat to the deep ocean. Recent high salinity conditions in the North Atlantic have been proposed to be caused by a strengthening of the Atlantic Meridional Overturning Circulation (AMOC). Agreeing that high salinity in deep convection regions favors heat transfer to the deep ocean two objections can be drawn from this overall view. First, available observational records do not show a strengthening of the AMOC, but suggests a sustained weakening. Second, deep convection in the subpolar North Atlantic is restricted to the Labrador and Irminger seas (see Fig. 1), but far from these prominent deep ocean ventilation sites, ocean observations show the largest deep ocean heat uptake at mid-latitudes in the Eastern North Atlantic (Fig. 1).

We suggest that a sequence of connected strong mixing induced heat injection events originating from this region triggered large transfer of heat from upper to deeper ocean layers, implying a deceleration or halt of the North Atlantic heat uptake from the atmosphere. The first part of the North Atlantic's transformation occurred when the waters of the eastern North Atlantic mixed in the winter of 2005. The induced deep convective mixing resulted in homogeneization of properties of the water column from the surface to density levels at depth ranges of 350-500 m. This mixing of (warmer and saltier) upper water and (colder and fresher) modal waters made the upper waters colder (−0.4◦C), creating a denser (+0.1kgm−3), warmer (+0.23◦C), and more saline (+0.015) type of Eastern North Atlantic Central Water (ENACW). Most of the enhanced warming observed at intermediate depths at ml-ENA shown in Fig. 1 (+0.33ºC gained between 1997 and 2012) is explained by the increase in the modal waters during the winter of 2005 (+0.23ºC). The estimated overall heat content increase in the region accounts for 44% of the total heat content increase at intermediate depths in the North Atlantic (36º to 65ºN) from 1997 to 2012.

Mixing the waters and increasing densities altered the ocean circulation patterns and aided a reverse of the southward circulation of saltier waters from the eastern side of the temperate Atlantic (Fig. 2) with far reaching consequences; the northward flow of saltier waters into the subpolar North Atlantic and Nordic Seas favoured additional heat injection through deep convection events in later years. Thus, we agree that existing high salinity conditions in the late 2000s in areas of deep convection have aided heat transfer to the deep ocean, but the suggestion that an increase of the AMOC is behind such salinity increase is not supported by observations. A greater influence of the saltier ENACW and broadened passage for both ENACW and western subtropical waters towards the north appears to be a more plausible explanation. Anomalous atmospheric patterns such as the one behind this shift are not unique of the last decade,

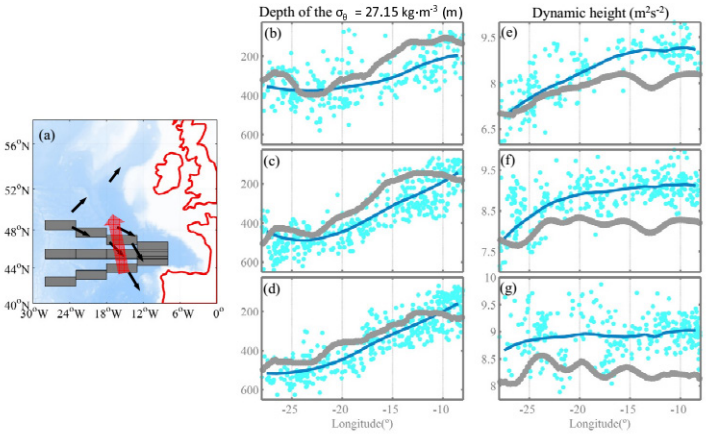

although they may have been exacerbated under global warming.

Figure 3. Flow reversal in ENACW. (a) Map of the North East Atlantic showing the location of the NW-SE, W-E and SW-NE sections across the ENACW formation area where data shown in panels (b-g) are taken. (b), (c) and (d) Location of the $\sigma\theta$ = 27.15 at the NW-SE, E-W, and SW-NE sections marked in (a) based on WOA01 climatological data (grey) and available Argo floats in the corresponding section between 2005 and 2010 (cyan). The blue line indicates the mean filtered value of all the Argo floats each 2º of longitude. (e), (f) and (g) Idem for the dynamic height between 300 and 1500 meters. Black arrows in (a) indicate the climatological southward flow west of the Bay of Biscay based on *Pollard et al.* [1996], and the red arrow the reversed flow after 2005.

REFERENCES

A complete list of references can be found in:

1- Somavilla, R. et al., 2016. Mid-2000s North Atlantic shift. Heat budget and circulation changes. Geophys. Res. Lett., 43, 2059–2068, doi:10.1002/2015GL067254

2- Sullivan, C., 2016. The North Atlantic Ocean's Missing Heat Is Found in Its Depths. EOS Research Spotlight. *Eos, 97,* doi: 10.1029/2016EO047009.

How is the surface Atlantic water inflow through the Gibraltar Strait forecasted? A lagrangian validation of operational oceanographic services in the Alboran Sea and the Western Mediterranean

M.G. Sotillo[1], A. Amo-Baladrón[1], E. Garcia-Ladona[2], A. Orfila[3], P. Rodríguez-Rubio[4], D. Conti[3], J.A. Jiménez-Madrid[2], F. J. de-los-Santos[4], E. Alvarez-Fanjul[1]

[1] Puertos del Estado. 28041 Madrid, Spain
[2].ICM-CSIC. 08003 Barcelona, Spain
[3].IMEDEA-CSIC. 07190 Esporles, Spain
[4].Autoridad Portuaria Bahía de Algeciras. 11207 Algeciras, Spain

ABSTRACT

An exhaustive validation of operational ocean forecast products available in the Gibraltar Strait and the Alboran Sea is presented. The skill of two ocean model solutions (i.e. the regional CMEMS IBI and the local PdE SAMPA ones) in reproducing the complex surface dynamics in the above areas is evaluated. To this aim, in-situ measurements from 35 drifter buoys (the MEDESS-GIB database) are used as observational reference. A Lagrangian separation distance and a skill score have been applied to evaluate the performance of the modeling systems in reproducing the observed trajectories. Furthermore, the SST validation with in-situ data is carried out by means of validating the model solutions with L3 satellite SST products. The IBI products are evaluated in an extended domain, beyond the Alboran Sea, covering western Mediterranean waters. This analysis reveals some strengths of the regional solution (i.e. realistic values of the Atlantic Jet in the Strait, realistic simulation of the Algerian Current), together with some shortcomings (the major one related to the simulated geographical position and intensity of the Alboran Gyres, particularly the western one). On the other hand, the SAMPA system shows a more accurate model performance and it realistically reproduces the observed surface circulation in the area. The results reflect the effectiveness of the dynamical downscaling performed through the SAMPA system with respect to the regional IBI solution (in which SAMPA is nested), providing an objective measure of the potential added values introduced by the SAMPA downscaling solution in the Alboran Sea.

INTRODUCTION

The Gibraltar Strait is the natural connection between the Mediterranean Basin and the Atlantic Ocean and a hot spot of the world ocean, from geostrategic and scientific standpoints. The area is characterized by a very intense maritime traffic (with an estimated 100,000 ships per year) together with a noticeable port activity. All these activities together with an intense human migration entail high number of search and rescue operations in the area. It is also a high risk area in terms of oil spill events. These facts emphasise the necessity for having efficient operational oceanographic services to monitor and forecast these waters. A diagram presenting the Alboran Sea surface circulation is shown in Fig. 1 (Upper panel). The surface Atlantic water inflow through the Strait and its further flow eastward in the Alboran Sea determine the surface circulation in the area, which is characterized by very strong current regimes and complex dynamics. Dynamical downscaling from basin-scale model solution into coastal and shelf areas through nested regional model applications is nowadays a very common, but scientifically challenging approach that needs to be verified.

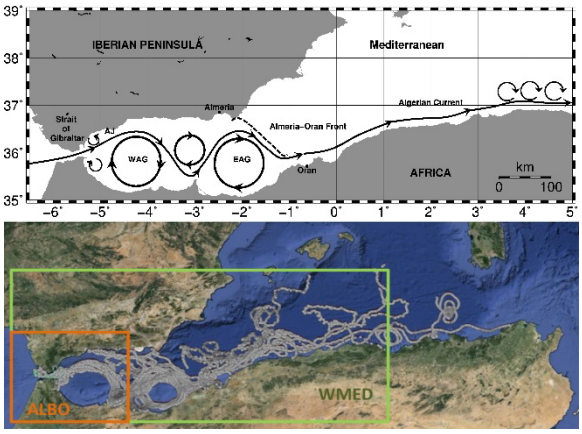

Fig. 1 Upper Panel: Scheme of surface circulation in the Alboran Sea and the Algerian Basin. Features such as the Atlantic Jet, Western and Eastern Alboran Gyres and the Algerian Current are depicted. Lower Panel: Trajectories of the MEDESS-GIB drifter buoys and geographical domains where model validation is performed.

The common Lagrangian validation framework, proposed, is useful to assess the skill of two model systems in

simulating the surface dynamics of the area, and also provides interesting information to quantify the potential added value of the downscaled solution with respect to its parent solution (the regional one).

DATA AND METHODOLOGY

Two different surface ocean model solutions available operationally in the Gibraltar area are validated using the MEDESS-GIB data (Sotillo et al. 2016 [1]) as the observational reference. Scientific validation of modelled surface temperatures and currents delivered by the "regional" CMEMS IBI and the "local" PdE SAMPA Ocean Forecast Services has been performed for the Strait of Gibraltar and the Alboran Sea (see validation domains in Fig. 1), using different metrics and skill scores.

The Copernicus Marine Environment Monitoring Service IBI-MFC (CMEMS Monitoring & Forecasting Centre; http://marine.copernicus.eu/) provides daily ocean model estimates and forecasts for the IBI (Iberia-Biscay-Ireland) region since 2011. The operational IBI Ocean Forecast Service is based on a NEMO model application that includes high frequency processes required to characterize regional scale marine features (further information in Sotillo et al. 2015 [2]).

On the other hand, Puertos del Estado (PdE) operationally provides from 2012 a local high resolution ocean forecast service for the Strait of Gibraltar and its surroundings (Gulf of Cadiz and Alboran Sea). The SAMPA model application was developed by the University of Malaga in collaboration with PdE and it is based on the MITGCM model. The model domain centered in the Gibraltar Strait is covered with a variable horizontal resolution (maximum resolution around 400-500 m in the Strait). The SAMPA model is nested into the Copernicus IBI-MFC forecast solution. SAMPA products are made available to any user through the PdE user interfaces. Further details on the SAMPA model configuration are provided in Sanchez-Garrido et al., 2013 [3].

RESULTS AND DISCUSSION

The present contribution show results from the exhaustive validation of two different model solutions provided by the two ocean forecast services described. Example of some lagrangian metrics for IBI and the SAMPA SST validation are shown in Fig. 2. The analysis reveals some strengths of the regional solution (i.e. realistic values of the Atlantic Jet in the Strait, realistic simulation of the Algerian Current), together with some shortcomings (the major one related to the simulated geographical position and intensity of the Alboran Gyres, particularly the western one). On the other hand, the SAMPA system shows a more accurate model performance and it realistically reproduces the observed surface circulation in the area. The results reflect the effectiveness of the dynamical downscaling performed through the SAMPA system with respect to the regional IBI solution (in which SAMPA is nested), providing an objective measure of the potential added values introduced by the SAMPA downscaling solution in the Alboran Sea.

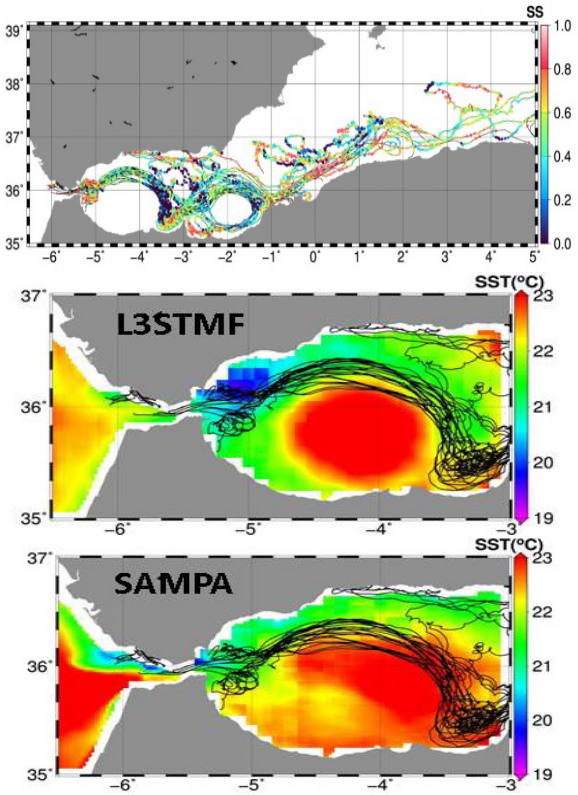

Figure 7 Example of IBI & SAMPA validation metrics Upper panel: IBI normalized skill scores (based on Lagrangian separation distance) computed at observed MEDESS-GIB drifter locations used to initialize model virtual trajectories. 0 the poorest model quality, 1 the best agreement between model and observed trajectories. L3STMF satellite and model (SAMPA) SST averages shown in intermediate and lower panels (MEDESS-GIB buoy tracks depicted in each panel).

REFERENCES

1 - Sotillo MG, E. Garcia-Ladona, A. Orfila, P. Rodríguez-Rubio, J. C. Maraver, D. Conti, E. Padorno, J.A. Jiménez, E. Capó, F. Pérez, J.M. Sayol, F. J. de los Santos, A. Amo, A. Rietz, C. Troupin, J. Tintore, E. Álvarez-Fanjul. (2016). The MEDESS-GIB database: Tracking the Atlantic water inflow. *Earth Syst. Sci. Data*, 8, 141–149, 2016 doi:10.5194/essd-8-141-2016

2 - Sotillo MG, S Cailleau, P Lorente, B Levier, R Aznar, G Reffray, A Amo-Baladrón, J Chanut, M Benkiran & E Alvarez-Fanjul (2015): The MyOcean IBI Ocean Forecast and Reanalysis Systems: operational products and roadmap to the future Copernicus Service, *Journal of Operational Oceanography*,DOI:10.1080/1755876X.2015.1014663

3- Sánchez-Garrido,JC, García-Lafuente, J, Alvarez-Fanjul, E, Sotillo, MG, de los Santos, FJ, 2013. What does cause the collapse of the Western Alboran Gyre? Results of an operational ocean model, *Progress in Oceanography*, 116,142-53 http://dx.doi.org/10.1016/j.pocean.2013.07.002

Can scatterometer winds improve the quality and resolution of the current NWP-based ocean forcing?

Ana Trindade[1,2], Marcos Portabella[1,2], Ad Stoffelen[3], Wenming Lin[1,2], Jos de Kloe[3], Joaquim Ballabrera-Poy[1,2], and Antonio Turiel[1,2]

[1]Institut de Ciències del Mar (ICM-CSIC), Barcelona, Spain
[2]SMOS Barcelona Expert Centre (BEC), Barcelona, Spain
[3]Royal Netherlands Meteorological Institute (KNMI), de Bilt, The Netherlands

ABSTRACT

High resolution satellite derived sea surface wind data, such as those from scatterometers, are increasingly required for operational monitoring and forecasting of the ocean. However, the time and space coverage of these datasets is unsuitable for, among others, high-resolution ocean model forcing.

Recent attempts of combining scatterometer data and numerical weather prediction (NWP) outputs, i.e., blended ocean forcing products, allows for an increased temporal resolution (e.g., daily) but generally only resolves NWP spatial scales of ~200 km. Therefore, information on the wind-current interaction, the diurnal wind cycle and the wind variability in moist convection areas is lost in such products. Moreover, known systematic NWP model (parameterization) errors are in fact propagated at times and locations where no scatterometer winds are available. The alternative, direct forcing from NWP results in even more extensive physical drawbacks. We propose to maintain the increased temporal coverage in a gridded wind and stress product (ERA*), but also to maintain the most beneficial physical qualities of the scatterometer winds, i.e., 25-km spatial resolution, wind-current interaction, variability due to moist convection, etc., and, at the same time correct the large-scale NWP parameterization and dynamical errors. Additionally, we correct these winds for the effects of atmospheric stability and mass density, using stress equivalent 10 m winds, U10S.

In fact, collocations of scatterometer and global NWP winds show these physical differences, where the local mean and variability of these differences are rather constant in time and thus could be added to the ERA-interim time record in order to better represent physical interaction processes and avoid NWP model errors. Correction of the wind vector biases and wind vector variability is expected to affect ocean forcing. Information on the scatterometer wind sampling error is provided by these collocations.

The new ERA* gridded ocean forcing product is validated against continuous 10-min buoy wind datasets (RAMA,TRITON/TAO, PIRATA and NDBC) and against scatterometer data, namely the Ku-band OceanSat-2 (OSCAT) 25 km product. Preliminary results for the year 2012 will be presented at the time of the conference. Future work will focus on assessing the impact of the ERA* product in both global and regional ocean models.

Detection of drogue loss events from drifter positioning data

I. Vallès[1], J. L. Pelegri[1], J. Salvador[1], J. Font[1] & E. Roget[2]

[1] Departament de Oceanografia Física i Tecnològica, Institut de Ciències del Mar, CSIC, Barcelona
[2] Departament de Física, Universitat de Girona

ABSTRACT

Satellite-tracked drifting buoys are useful for sampling sea-surface currents. Standard drifting buoys have drogues centred at a depth of 15 m, a fundamental element that guarantees that the direct wind force on the buoy is much smaller than the drag on the anchor. When a drifter loses its drogue, it no longer becomes a good tracker of the surface currents, hence the relevance of identifying when this happens. Here we propose a spectral-based approach to analyse drifter velocity data so as to detect when a drifter loses its drogue without the need of concurrent wind data. The method, applied to data obtained during the SPURS 2013 cruise, shows a substantial increase in the band-passed velocity energy at the time the drifter loses its drogue, as deduced with an independent method that considers the temporal change of the correlation between wind and positioning data. The results are very promising, pointing at a new method that can detect drogue loss from a relatively simple analysis of positioning data.

INTRODUCTION

Some studies have related the existence of anomalous patterns in drifter velocity, which were supposed to remain dragged, to the actual loss of the drogue. Such difficulties in proper detection of drogue loss may affect greatly the quality of the Global Drifter Program (GDP) data set (Grodsky et al. 2011; Rio et al. 2011). In order to solve this problem, recent techniques have been added to the quality control of the GDP global data (Rio 2012; Lumpkin et al. 2013). These techniques are based on the analysis of the correlation between wind and drifter velocities: when this correlation increases abruptly and remains large it is likely that the drifter has lost its drogue. The application of this method actually removed around 50% of the velocity measurements from the GDP global data, improving its quality considerably. However the joint analysis of wind and drifters trajectory may present difficulties for obtaining accurate results in weak-wind areas, such as centres of subtropical gyres, because of the low-resolution of the wind data products. Further, the method is of no immediate application as it requires the availability of simultaneous sea-surface wind data. These aspects point at the convenience of developing an independent method that may be used for the real-time detection of drogue-loss events using sole drifter positioning data.

Here we propose a double approach to detect when a single drifter losses its drogue. One advantage of this approach is that it allows identifying drogue loss events solely from the analysis of drifter buoy positioning data, not requiring external data such as wind and altimetry data products. These methodologies will be applied to a group of 9 drifters deployed in the centre of the North Atlantic Subtropical Gyre in spring of 2013, as part of the SPURS experiment.

DATA AND METHODS

a) Drifter data

The ICM-SPURS drifters were designed following the requirements of the Surface Velocity Program (SVP). The main requirement is that the drag area has to be large enough such as to reduce the wind slippage to only 0.1% for winds up to 10-m/s. Drifter positions time series (latitude and longitude) are in WGS84 coordinates, obtained via the Argos positioning system. The positions were interpolated to six-hour intervals using an ordinary kriging technique.

b) Wind data

Surface 10-m wind module and direction are obtained from the Global Mean Wind Field produced by CERSAT (http://cersat.ifremer.fr/). The wind velocity values are linearly interpolated at the drifter locations.

c) Filtered velocity

We apply several filters to the drifter-inferred velocities, as follows: high-pass motions correspond to periods shorter than 1.5 times the inertial period, band-pass motions have periods between 1.5 times the inertial period and 10 days, and low-pass motions have periods longer than 10 days. After applying these filters, we end up with three velocity time series that can be analysed for energy content.

d) Wavelet analysis

We use the continuous wavelet transform (CWT) in order to assess the time evolution of the spectral decomposition of

the velocity field (Torrence and Compo, 1998). The CWT analysis is carried out to three time series (low, band and high) of drifter velocities.

Further, we define the cross-wavelet transform (XWT) between surface currents and winds as $W^{uw} = W^{u} W^{wi}$, where W^{u} and W^{w} respectively are the CWT of the drifter velocity and wind time series, and i denotes the complex conjugate. The local cross wavelet power spectrum is given by $|W^{uw}|$ and the complex argument, $\arg(W^{uw})$, is the local relative phase between the two time series in time frequency space (Grinsted et al., 2004).

RESULTS AND DISCUSSION

The hypothesis underlying our analysis is that, after losing its drogue, a drifter will closely respond to the variations in wind intensity. Since most of the energy of the wind lies at time scales of a few days – the synoptic-wind time scale – we expect the band-pass velocity time series will display major changes in behaviour, to be reflected both in the CWT and XWT time series.

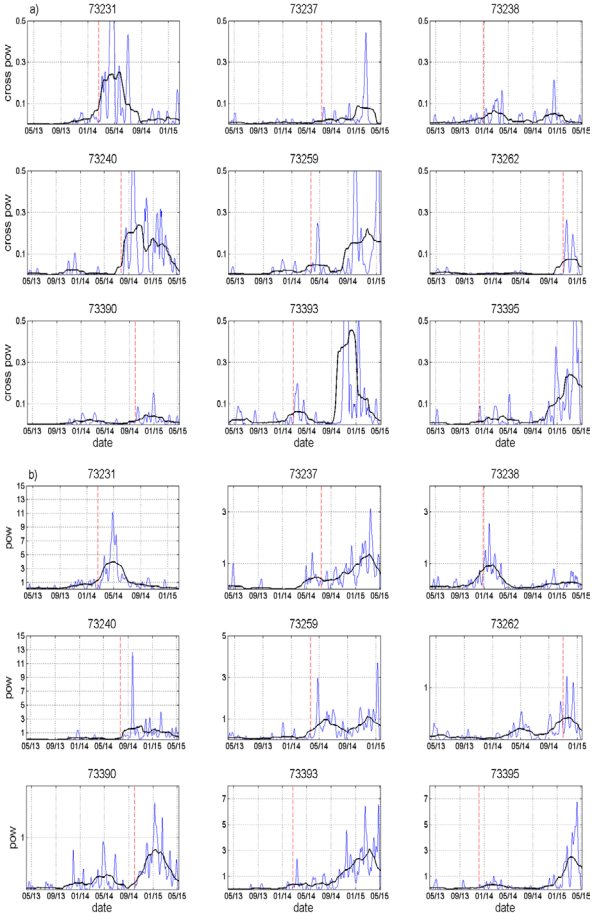

Fig. 1. Normalized (in %) (top panels) cross-wavelet and (bottom panels) continuous wavelet transforms for nine ICM-SPURS buoys in the band-passed frequency (1.5 times the inertial frequency to 10 days). The blue and black lines respectively show the 10- and 100-day moving average values; the vertical-dashed red line indicates the drogue-loss event.

The XWT is our reference time series and we will explore under what circumstances the CWT behaves analogously. For the XWT, we only consider the energy that is phase-locked (values close to zero) as given by the complex argument of W^{uw}. To determine the time when the drifter loses its drogue, we use the following joint criterion: (a) the XWT energy increases over 50% its previous background value, (b) during a sufficiently long time period, with (c) a correlation between both time series remaining always above 0.1%.

When applied to all nine drifters, the band-passed XWT and CWT display similar patterns (Fig. 1). This corroborates the existence of a direct relation between the fluctuations of local winds and the non-drogue drifter velocities at sub-inertial periods until 10 days, confirming that (at least for subtropical latitudes) a major response of the drifters to the wind is located in the synoptic wind frequency. Our results point at the CWT analysis as a useful tool to detect drogue-loss events, not requiring the use of concurrent wind or altimetry data.

ACKNOWLEDGEMENTS

This research has been supported by the Ministerio de Economía y Competitividad of the Spanish Government through project VA-DE-RETRO (CTM2014-56987-P). Ignasi Vallès has been funded through a FPI contract of the Ministerio de Competitividad y Economía. The drifter data was obtained following deployments during the SPURS cruise, in the frame of the MIDAS-6 (AYA2010-22062-C05-01) project, financed by the Ministerio de Economía y Competitividad of the Spanish Government. We are also grateful to Aslak Grinsted for providing the wavelet and cross wavelet MATLAB tool-kit.

REFERENCES

1 – Grinsted A, Moore JC & and Jevrejeva S, 2004. Application of the cross wavelet transform and wavelet coherence to geophysical time series. *Nonlinear Proc. Geophys.*, 11, 561-566.

2 – Grodsky SA, Lumpkin R & Carton JA, 2011. Spurious trends in global surface drifter currents. *Geophys. Res. Lett.*, 38, L160606.

3 – Lumpkin R, Grodsky SA, Centurioni L, Rio MH, Carton JA & Lee D, 2013. Removing spurious low-frequency variability in drifter velocities. *J. Atmos. Oceanic Tech.*, 30, 353-360.

4 – Rio MH, 2012. Use of altimeter and wind data to detect the anomalous loss of SVP-type drifter's drogue. *J. Atmos. Oceanic Tech.*, 29, 1663-1674.

5 – Rio MH, Guinehut S & Larnicol G, 2011. New CNES-CLS09 global mean dynamic topography computed from the combination of GRACE data, altimetry and in situ measurements. *J. Geophys. Res.*, 116, C07018.

6 – Torrence C & Compo GP, 1998. A practical guide to wavelet analysis. *Bull. Amer. Meteorol. Soc*., 79, 61-78.

The AMOC and the seasonal cycle of the Canary Current

Pedro Vélez-Belchí[1], Alonso Hernández-Guerra[2] and Maria Dolores Pérez-Hernández[3]

[1] Instituto de Oceanografía y Cambio Global, Universidad de Las Palmas de Gran Canaria.
[2] Instituto Español de Oceanografía, Centro Oceanográfico de Canarias.
[3] Woods Hole Oceanographic Institution

ABSTRACT

Due to the important role of the eastern Atlantic in the Atlantic Meridional Overturning Circulation (AMOC), in this study we describe the seasonal cycle of the Canary Current system using hydrographic data from two cruises carried out in a box around the Canary Islands, the region where the eastern component of the RAPID array is placed. CTD, VMADCP and LADCP data were combined with inverse modelling in order to determine absolute geostrophic transports in the Canary Islands region in fall and spring. During spring, the overall transport of Canary Current (CC) and the transport in the Lanzarote Passage (LP) were southward. In the Lanzarote Passage (LP), between the Canary Islands and Africa, the transported was 0.6±0.20 Sv southward, while the Canary Current transported 1.0±0.40 Sv in the oceanic waters of the Canary Islands Archipelago. During fall, in the LP the transport was 2.8±0.4Sv northward, while the CC transported 2.9±0.60 Sv southward in the oceanic waters of the Canary Islands Archipelago. The amplitude of the seasonal cycle of the geostrophic transport obtained was quite similar to the seasonal cycle of the Eastern Atlantic contribution to the AMOC, as measured by the RAPID array. To understand the relationship between the seasonal cycle found in the CC and in the LP, and the amplitude of the seasonal cycle of the AMOC transport associated with Rossby waves, a sensitivity study of the Rossby wave model is included.

INTRODUCTION

The Atlantic meridional overturning circulation (AMOC) is recognized as an important component of the climate system, contributing to the relatively mild climate of northwest Europe. Due to its importance, the strength of the AMOC is continually monitored along 26ºN with several moorings located east of the Bahamas, in the Middle Atlantic Ridge and south of the Canary islands, known as the RAPID array. The measurements of the RAPID array show a 6 Sv seasonal cycle for the AMOC, and recent studies [1,2] have pointed out the dynamics of the eastern Atlantic as the main driver for this seasonal cycle, specifically, Rossby waves excited south of the Canary Islands [1].

MATERIAL AND METHODS

Two cruises were conducted in fall 2013 and spring 2014, with 53 (fall 2013) and 51 (spring 2014) hydrographic stations (Fig. 1). The station separation was about 30 km in the oceanic waters and 5-10 km for the coastal and shelf stations. A SeaBird 911+ CTD probe was used together with a 300/150khz Lowered Acoustic Doppler Current Profiler (LADCP). The mass transport was estimated in 13 neutral density layers, the thermocline waters correspond to the first two layers, the NACW are located on the next two layers, the intermediate water masses on the next three and the deep and bottom water masses in the denser layers.
Mass transports were initially estimated using geostrophic velocities obtained with a level of no-motion located at γ^n=27.975 kg m^{-3} (roughly 1950 m) for the oceanic waters, in the interface between the North Atlantic Central Waters (NACW) and the Mediterranean Waters (MW). For the stations in shallower waters the level of no-motion was at γ^n=27.380 kg m^{-3} (roughly 750 m), in the interface between the MW and the Antarctic Intermediate Waters (AAIW). The initial geostrophic velocities were corrected using the LADCP velocities. To reduce the large mass transports imbalances an inverse model [3] was applied to the volume enclosed by the hydrographic stations, and the African coast in the case of the fall survey.

RESULTS AND DISCUSSION

Hydrographic data, a long-term mooring and satellite altimetry-based sea level data show that the Canary Current, in the oceanic waters west of Lanzarote, has a seasonal cycle with amplitude of 1.9 Sv for the NACW and thermocline waters. Between Lanzarote and the African coast, in the Lanzarote Passage, there is a seasonal cycle of 3.4 Sv for the NACW and thermocline waters, that reach 4.0 Sv if the intermediate waters are included (Fig. 1).
This seasonality in the Canary Island region can be attributed to different mechanisms for the surface layer: the recirculation cell found in the eastern part of the Canary Basin and south of Cape Ghir; a cell that might be consequence of the termohaline anomaly created by the giant upwelling filament of Cape Ghir, which usually develops during the late summer; the upwelling current, that shows a seasonal variability due to the seasonal change of the wind-driven upwelling in the Lanzarote Passage.

In contrast, the reverse in the flow of the intermediate waters in the Lanzarote Passage, can be attribute to water column stretching forced by the seasonal cycle of the winds in the eastern subtropical Atlantic [2,4].

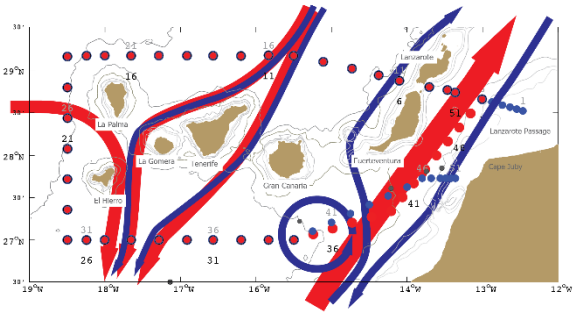

Figure 1. Map of the study area, showing the main topographic and geographical features referred in the text. The 200 m, 500 m, 1000 m and 2000 m isobaths are indicated with gray lines. The blue circles are the stations sampled in the spring 2014 cruise, while the red circles are the hydrographic stations that were sampled in the fall 2013 cruise. The thick red (fall 2013) and blue (spring 2014) lines correspond to the sketch of the thermocline and NACW transports. The grey circles denote the eastern Atlantic moorings of the Rapid array.

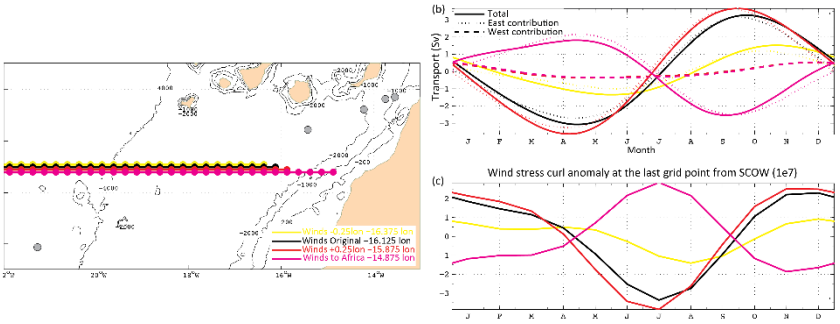

Figure 2. (a) Geographical extension of the SCOW wind stress curl anomaly used. The black line denotes the same winds used by [1]; the yellow line indicates the same winds used by [1] but without the last data point (0.25º in longiude further west); the red line indicates the same winds used but with one more data point (0.25º in longitude further east);the magenta line denotes all the available SCOW data points at 26.5ºN, to the African coast, this is 5 more data points that in [1]. The grey circles indicate the positions of the eastern Atlantic componente of the Rapid moorings. (b) Anomaly of basin-wide mid-ocean geostrophic transport for the first two baroclinic modes of a forced Rossby wave model as in [1], using the SCOW seasonal wind stress curl anomaly climatology. The thick lines show the total geostrophic transport, and the contributions from the variability the eastern boundary (western boundary) correspond to the dotted (dashed) lines. The color codes for the forced winds are the same as in (a). (c) wind stress curl anomaly seasonal cycle at the last data point at 26.5ºN. The color codes for the forced winds are the same as in (a).

Since [1] attributed the decrease in the southward flow in the eastern Atlantic to wind-forced Rossby waves, we carried out a sensitive study to test if the geographical extension of the SCOW wind stress curl (WSC) anomaly used in the wind-forced Rossby wave model has any impact in the magnitude of the seasonal cycle of the anomaly of basin-wide mid-ocean geostrophic transport (Fig. 2). The simulations show a high sensitivity to the SCOW WSC, with a reverse in the sign of the amplitude of the seasonal cycle if one grid point (25 km) was added, or substracted. The phase speed of the Rossby waves did not have any impact in the results when SCOW WSC was used. The uplift (depress) of the density surfaces in the spring (fall) cannot explain the seasonal variability found in the Canary Islands region. The high sensitivity of the wind-forced Rossby wave model to the geographical extension of the SCOW winds is due to the inconsistency between the geostrophic approach, used to estimate the basin-wide transport, and the high spatial resolution of the SCOW winds, smaller than the characteristic Rossby radius of deformation in the area. A smoothed version of the SCOW WSC or the NCEP winds, do not show this high sensitivity of the wind-forced Rossby wave mode to the geographic extension of the WSC.

ACKNOWLEDGMENTS

This study has been carried out as part of the SeVaCan project (CTM2013-48695), from the Ministerio de Economía y Competitividad.

REFERENCES

1 - Kanzow, T. et al. (2010), Seasonal Variability of the Atlantic Meridional Overturning Circulation at 26.5°N, J. Climate, 23(21), 5678–5698, doi:10.1175/2010JCLI3389.1.

Machín, F., and J. L. Pelegrí (2009), Northward Penetration of Antarctic Intermediate Water off Northwest Africa, J. Phys. Ocean., 39(3), 512–535, doi:10.1175/2008JPO3825.1.

2 - Perez-Hernandez, M. D., G. D. McCarthy, P. Vélez-Belchí, D. A. Smeed, E. Fraile-Nuez, and A. Hernández-Guerra (2015), The Canary Basin contribution to the seasonal cycle of the Atlantic Meridional Overturning Circulation at 26°N, J. Geophys. Res, 120(11), 7237–7252, doi:10.1002/2015JC010969.

3 - Hernández-Guerra, A., E. Fraile-Nuez, F. López-Laatzen, A. Martínez, G. Parrilla, and P. Vélez-Belchí (2005), Canary Current and North Equatorial Current from an inverse box model, J. Geophys. Res., 110(C12), doi:10.1029/2005JC003032.

4 - Machín, F., and J. L. Pelegrí (2009), Northward Penetration of Antarctic Intermediate Water off Northwest Africa, J. Phys. Ocean, 39(3), 512–535, doi:10.1175/2008JPO3825.1.

Universitat d'Alacant
Universidad de Alicante

UNIVERSIDAD DE LAS PALMAS
DE GRAN CANARIA

UCA
Universidad
de Cádiz

UNIVERSITAT DE
BARCELONA

Universidad
Católica
de Valencia
San Vicente Mártir

UNIVERSIDADE
DE VIGO